CLIMATE SCIENCE ADVANCES TO ADDRESS 21st CENTURY WEATHER AND CLIMATE EXTREMES

EDITED BY: Chris C. Funk, Andrew Hoell and Dann Mitchell
PUBLISHED IN: Frontiers in Climate

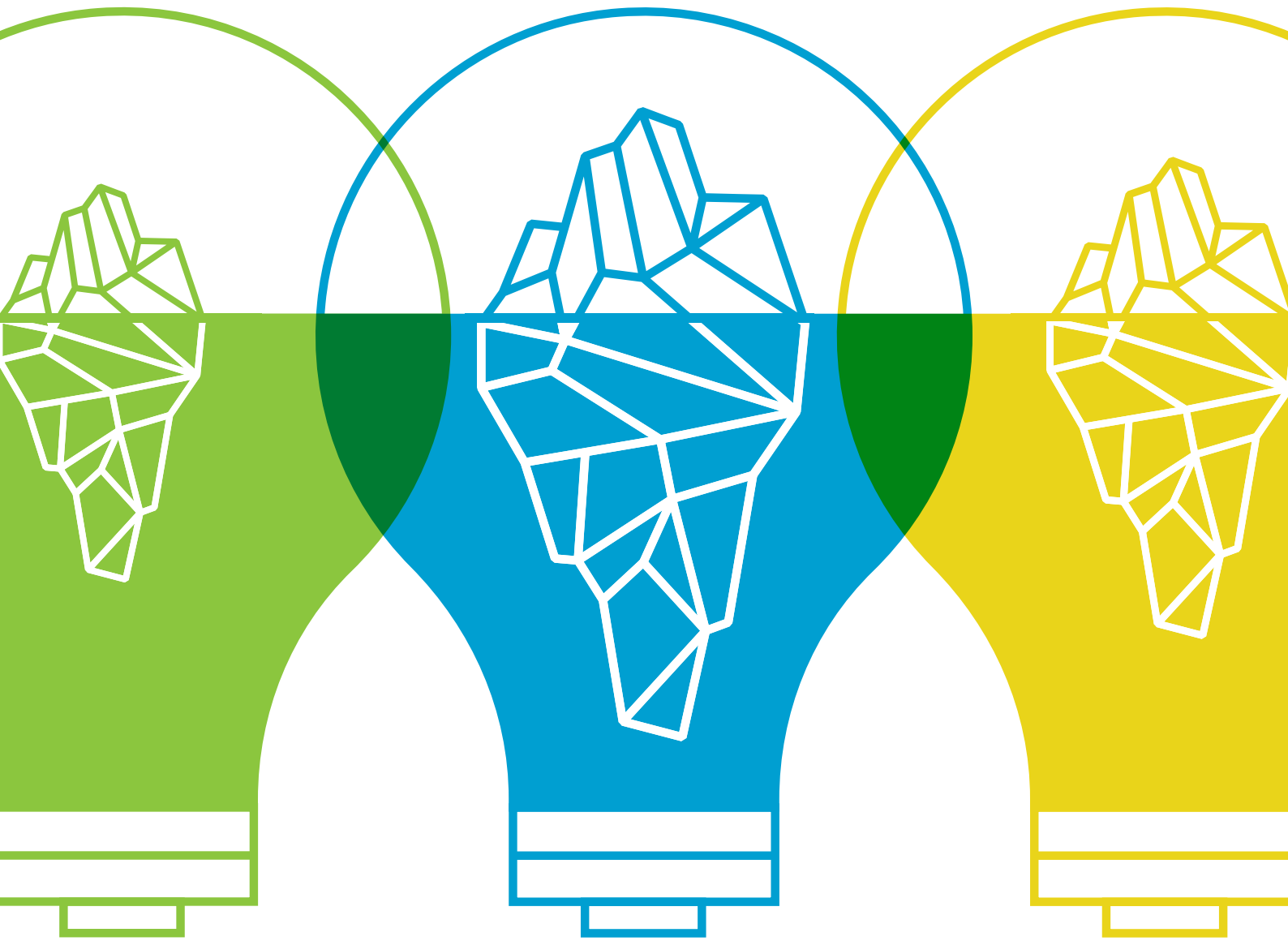

frontiers Research Topics

frontiers

ISSN 1664-8714
ISBN 978-2-88971-219-9
DOI 10.3389/978-2-88971-219-9

About Frontiers

Frontiers is more than just an open-access publisher of scholarly articles: it is a pioneering approach to the world of academia, radically improving the way scholarly research is managed. The grand vision of Frontiers is a world where all people have an equal opportunity to seek, share and generate knowledge. Frontiers provides immediate and permanent online open access to all its publications, but this alone is not enough to realize our grand goals.

Frontiers Journal Series

The Frontiers Journal Series is a multi-tier and interdisciplinary set of open-access, online journals, promising a paradigm shift from the current review, selection and dissemination processes in academic publishing. All Frontiers journals are driven by researchers for researchers; therefore, they constitute a service to the scholarly community. At the same time, the Frontiers Journal Series operates on a revolutionary invention, the tiered publishing system, initially addressing specific communities of scholars, and gradually climbing up to broader public understanding, thus serving the interests of the lay society, too.

Dedication to Quality

Each Frontiers article is a landmark of the highest quality, thanks to genuinely collaborative interactions between authors and review editors, who include some of the world's best academicians. Research must be certified by peers before entering a stream of knowledge that may eventually reach the public - and shape society; therefore, Frontiers only applies the most rigorous and unbiased reviews.
Frontiers revolutionizes research publishing by freely delivering the most outstanding research, evaluated with no bias from both the academic and social point of view. By applying the most advanced information technologies, Frontiers is catapulting scholarly publishing into a new generation.

What are Frontiers Research Topics?

Frontiers Research Topics are very popular trademarks of the Frontiers Journals Series: they are collections of at least ten articles, all centered on a particular subject. With their unique mix of varied contributions from Original Research to Review Articles, Frontiers Research Topics unify the most influential researchers, the latest key findings and historical advances in a hot research area! Find out more on how to host your own Frontiers Research Topic or contribute to one as an author by contacting the Frontiers Editorial Office: frontiersin.org/about/contact

CLIMATE SCIENCE ADVANCES TO ADDRESS 21st CENTURY WEATHER AND CLIMATE EXTREMES

Topic Editors:
Chris C. Funk, University of California Santa Barbara, United States
Andrew Hoell, Earth System Research Laboratory (NOAA), United States
Dann Mitchell, University of Bristol, United Kingdom

Citation: Funk, C. C., Hoell, A., Mitchell, D., eds. (2021). Climate Science Advances to Address 21st Century Weather and Climate Extremes.
Lausanne: Frontiers Media SA. doi: 10.3389/978-2-88971-219-9

Table of Contents

frontiers in Climate

EDITORIAL
published: 22 June 2021
doi: 10.3389/fclim.2021.680291

Editorial: Climate Science Advances to Address 21st Century Weather and Climate Extremes

Chris Funk[1]*, *Andrew Hoell*[2] *and Daniel Mitchell*[3]

[1] Department of Geography, Climate Hazards Center, University of California, Santa Barbara, Santa Barbara, CA, United States, [2] NOAA Physical Sciences Laboratory, Boulder, CO, United States, [3] Cabot Institute for the Environment, University of Bristol, Bristol, United Kingdom

Keywords: climate, climate change, climate extremes, climate service, early warning, weather extremes

The Editorial on the Research Topic

Climate Science Advances to Address 21st Century Weather and Climate Extremes

AN OVERVIEW OF THIS ISSUE

The science surrounding weather and climate extremes, and their relationship with climate change, is rapidly expanding, feeding into improved climate services. As co-editors of "*Climate Science Advances to Address 21st Century Weather and Climate Extremes*," we are proud to share with you these excellent articles that provide valuable advances to our discipline, and come from researchers all over the world. The papers led by Lindsay Johnson and Phuong-Loan Nguyen address, respectively, the development of adequate data resources needed to support drought early warning and the study of precipitation extremes. Johnson et al. *"explore the use of updated drought monitoring tools to analyze data and develop a more holistic drought climatology applicable for New Mexico."* Nguyen et al. *"use a new high-resolution validation dataset to assess the consistency of the representation of annual daily precipitation maxima over land in 13 observational datasets."* Focusing on four cities in Ethiopia, Dessu et al. describe how the rapid expansion of built-up areas and sharp declines in green-space may be increasing climatic risk. Harvey et al. examines ways in which climate information was mobilized for use under Future Climate for Africa, and their findings "*revealed the central role of co-production principles in engaging potential users of climate information, regardless of the knowledge mobilization approach being used.*" Finally, the study by Trainer et al., explored "*trends in nearshore domoic acid along the US west coast in recent years, including the recent establishment of a new seed bed of highly-toxic Pseudo-nitzschia*," and described "*how early warning systems are a useful tool to mitigate the human and environmental health and economic impacts associated with harmful algal blooms.*" All of these articles advance the science of climate services in a warming world, moving us toward a greater capacity to manage future climate risk.

OPEN ACCESS

Edited and reviewed by:
Matthew Collins,
University of Exeter, United Kingdom

***Correspondence:**
Chris Funk
chris@geog.ucsb.edu

Specialty section:
This article was submitted to Climate Services, a section of the journal Frontiers in Climate

Received: *14 March 2021*
Accepted: *14 May 2021*
Published: *22 June 2021*

Citation:
Funk C, Hoell A and Mitchell D (2021) Editorial: Climate Science Advances to Address 21st Century Weather and Climate Extremes. Front. Clim. 3:680291. doi: 10.3389/fclim.2021.680291

As discussed in Sarah Harrison's excellent article in WIRED[1], studies like "*trends in nearshore domoic acid*" can help motivate and inform effective early warning systems, fostering unique partnerships between scientists and community members.

HOW CONCEPTUAL MODELS CAN INFORM CLIMATE SERVICES

Climate attribution and climate diagnostic studies highlight the mechanisms driving extreme events, and elucidate their potential to increase in intensity and frequency as the Earth warms. This research can, and should, inform the development of 21st century climate services. But while the nuts and bolts of climate science are essential, climate services are also fundamentally cultural; they support distributed non-local communities of practice that act, adapt, mitigate, plan, and respond in coherent ways that allow us to better cope with climate and weather risk. These important sub-cultures typically span many academic disciplines and sectors of society. Spanning these gaps is challenging, and it is therefore useful to consider our work from the lens of cultural anthropology.

Cultural anthropologists study how people who share a common cultural system organize and shape the physical and social world around them, and are in turn shaped by those ideas, behaviors, and physical environments. According to one seminal cultural anthropologist, Clifford Geertz, culture is "*a system of inherited conceptions expressed in symbolic forms by means of which men communicate, perpetuate, and develop their knowledge about and attitudes toward life*" (The Interpretation of Cultures," Geertz, 1973). In Interpretation of Cultures Geertz introduces the idea that cultures behave coherently by effectively combining "models of the world" and "models for the world." Models "of" the world resemble our numerical models; they attempt to imitate or simulate the world-as-it-is. Models "for" the world, however, imply specific and coherent actions, actions informed by our models "of" the world. So, according to Geertz, the study of hydraulics might help us design a dam. Because human behavior is driven by extrinsic symbolic structures (not just our genes), that it is precisely the interaction of these two distinct types of models that makes human culture possible.

But what is exciting, and challenging, is that today we can no longer afford to rely on "*inherited conceptions*." In the face of climate change, more and more scientists are realizing that they need to actively participate in culture "fabrication." In addition to algorithms, numerical models, datasets and simulations, we can help co-create coherent systems for early action. But an important component such systems is clear thinking, the development of crisp conceptual models. To be truly successful climate services need to combine accurate and representative models "of" the world with appropriate and localized models "for" intervention. Stepping back from the science, this editorial briefly discusses the important aspect of how these pieces can fit together when disparate "communities of practice"—like the oceanographers, health experts and local tribal leaders discussed in Sarah's story (see text footnote 1), work together.

The provision of freely available climate services is a very exciting prospect, a force for good that can help counter two growing threats—climate change and increasing economic disparity. While climate services will not reverse inequality, they can help the communities most vulnerable to extremes. Enhanced early warning systems are one of the most cost-effective approaches[2] to increasing resilience. Climate information can leap across continents, improving decision-making, early warning systems, and outcomes almost anywhere. As these systems evolve, we will be better together, faster, and more effectively, if we pay attention to the conceptual models that undergird our shared activities.

Climate Services are unique, challenging, exciting, and empowering, precisely because they connect and span many intellectual domains (**Figure 1**). These connections can transform data into wise actions. While the origins of the Data-Information-Knowledge-Wisdom hierarchy is uncertain, it may have originated (Wallace, 2007) in T. S. Eliot's poem "Choruses from the Rock" (Eliot, 1934):

> *Where is the Life we have lost in living?*
> *Where is the wisdom we have lost in knowledge?*
> *Where is the knowledge we have lost in information?*

Effective climate services typically involve contributions from overlapping "communities of practice." These collaborations connect technical engineering and science efforts (on the left-hand-side of **Figure 1**) with on-the-ground actions and interventions on the right-hand-side. Going data to information to knowledge to wisdom, we also tend to transition from the general to the specific. On the left-hand-side, we might find an atmospheric model based on universal physical laws or "rocket scientists" who use highly generalized algorithms to translate satellite imagery into precipitation estimates (Kummerow et al., 2015; Skofronick-Jackson et al., 2017; Huffman, 2020). But, as one moves to the right-hand-side in **Figure 1**, we find tailored effective interventions guided by local expertise.

Connecting data providers and responders, we find the sequential contributions of "climate intermediaries." To be actionable, information typically needs to be transformed into impact assessments, answering questions like: "*how might the expected or observed weather or climate conditions affect our crops, water supply, or fire fuels.*" This translation can add great value. For example, a recent study of drought warning activities in Malawi, found that what farmers really wanted and needed was agricultural advice, not weather data (Calvel et al., 2020), i.e., knowledgeable actionable guidance, not just data or information.

Shared conceptual frameworks can facilitate effective collaboration and communication across these communities of practice, guiding the translation of data and information into knowledge and appropriate action. For example, the Famine Early Warning Systems Network (http://www.

[1]https://www.wired.com/story/a-unique-alliance-could-help-warn-us-of-toxic-algae/

[2]https://gca.org/reports/adapt-now-a-global-call-for-leadership-on-climate-resilience/

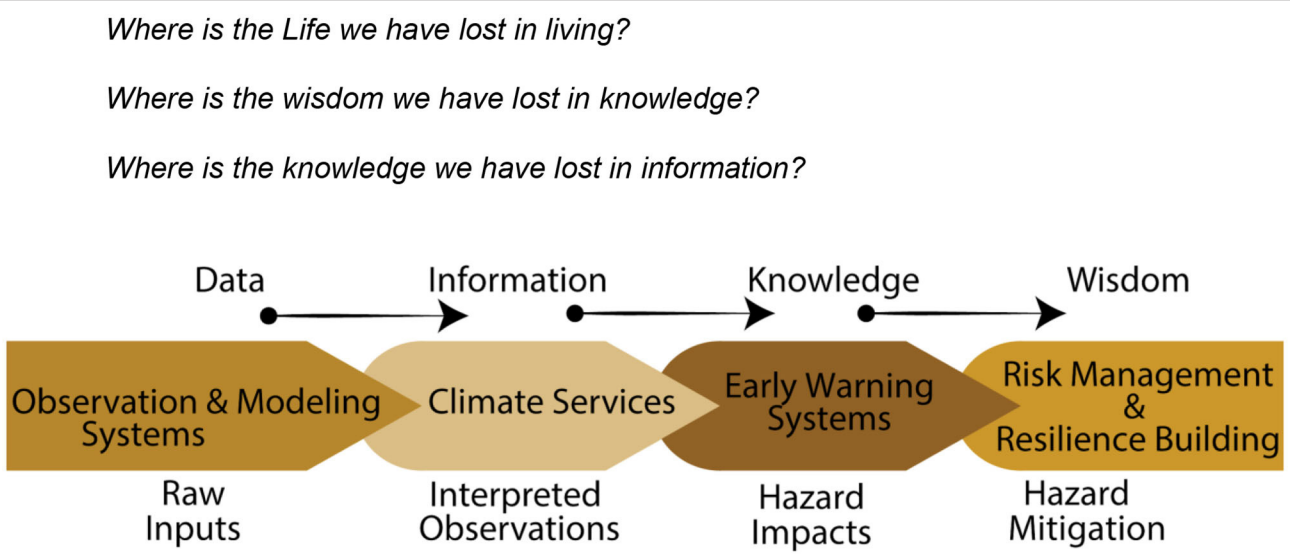

FIGURE 1 | A schematic diagram showing how multiple communities of practice can all contribute to effective hazard mitigation, risk management, and capacity-building.

fews.net/) identifies severely food insecure populations by developing scenarios[3] that analyze household level food economies, but these scenarios use a rigorous multi-agency "food security outlook[4]" process to translate climate information into likely impacts on incomes, food access and food availability.

Yes—we need to translate climate data into information that drives impact models that provide accessible outputs that can support effective actions, and each of those verbs typically manifests as thousands of lines of code and extensive computations, but no, computation alone does not suffice.

The transitions described in **Figure 1** describe a series of coherent social interactions, emergent collaborative complex behavior, and when thinking about such structures the climate services community can learn from experts who study how cultures evolve. Seen from this perspective, successful early warning communities are subcultures that evolve to address specific threats, such as drought or food insecurity, and their success depends on translating data into wise action (**Figure 1**) using shared models "for" reality supported by accurate models "of" reality. Hence, such systems spend considerable effort on describing how hazards are detected and defined (Pulwarty and Sivakumar, 2014; Wilhite and Pulwarty, 2017; Funk and Shukla, 2020). Crisp definitions of drought (Wilhite and Glantz, 1985; Svoboda and Fuchs, 2016), and food insecurity (FEWS NET, 2021), can form a shared basis for collaboration and coherent climate services development. But these definitions, and the associated impact assessments and risk management responses, will be highly location specific—thereby requiring local knowledge.

But climate change is accelerating the need for climate services, and demanding that we have the best possible models "for" early warning. Surveys of extreme events, such as the book "Drought Fire Flood" (Funk, 2021)[5] can help guide climate service development. Analyses focusing on the new science of climate change attribution evaluate how climate change may or may not contribute to extreme events. Such studies can also provide search patterns, or models "for" hazards that can guide prediction and monitoring (i.e., a, b, c, d, e). For example, many studies have suggested that climate change will produce more frequent extreme El Niño and La Niña events. For La Niñas, it turns out that numerical models "of" the climate can predict these conditions very early, in June[6], providing a very valuable opportunity for early warning, predicated on a conceptual model "for" climate change impacts built around the assumption that extreme sea surface temperatures will provide a solid foundation for forecasting. Given that ENSO is the leading component of seasonal forecasting skill, linking our successful model "of" the climate to models "for" early action can help us move effectively from data to information to wise interventions (**Figure 1**). But there are as many opportunities for effective climate services as there are categories of climate impacts. Our age offers us many exciting opportunities to contribute to the production of data, information, knowledge, and wise action.

[3]https://fews.net/our-work/our-work/scenario-development
[4]https://public.wmo.int/en/resources/bulletin/how-climate-forecasts-strengthen-food-security
[5]https://www.cambridge.org/core/books/drought-flood-fire/96E0EB1519F5175B68079D294D0B0E93
[6]https://blog.chc.ucsb.edu/?p=757

These contributions are helping us cope with an increasing hazardous world.

AUTHOR CONTRIBUTIONS

All authors listed have made a substantial, direct and intellectual contribution to the work, and approved it for publication.

FUNDING

Primary support for this work came from the National Aeronautics and Space Administration (NASA) GPM mission grant #80NSSC19K0686 and the United States Agency for International Development (USAID) cooperative agreement #72DFFP19CA00001 and the Famine Early Warning Systems Network.

REFERENCES

Calvel, A., Werner, M., Van den Homberg, M., Cabrera Flamini, A., Streefkerk, I., Mittal, N., et al. (2020). Communication structures and decision making cues and criteria to support effective drought warning in Central Malawi. *Front. Clim.* 2:16. doi: 10.3389/fclim.2020.578327

Eliot, T. S. (1934). *Choruses From the Rock*. The complete poems and plays of TS Eliot. New York, NY: Harcourt, Brace & World, Inc.

FEWS NET (2021). *Integrated Phase Classification*. Available online at: https://fews.net/sectors-topics/approach/integrated-phase-classification

Funk, C. (2021). *Drought, Flood, Fire: How Climate Change Contributes to Catastrophes*. Cambridge: Cambridge Press. Available online at: https://www.cambridge.org/core/books/drought-flood-fire/96E0EB1519F5175B68079D294D0B0E93

Funk, C., and Shukla, S. (2020). *Drought Early Warning and Forecasting: Theory and Practice*. Oxford: Elsevier Press.

Geertz, C. (1973). *The Interpretation of Cultures*, Vol. 5019. New York, NY: Basic Books.

Huffman, G. J., Bolvin, D. T., Braithwaite, D., Hsu, K. L., Joyce, R. J., Kidd, C. (2020). "Integrated multi-satellite retrievals for the global precipitation measurement (GPM) mission (IMERG)," in *Satellite Precipitation Measurement*, eds K. C. V. Levizzani, D. Kirschbaum, C. Kummerow, K. Nakamura, and F. Turk (Cham: Springer), 343–354. doi: 10.1007/978-3-030-24568-9_19

Kummerow, C. D., Randel, D. L., Kulie, M., Wang, N. Y., Ferraro, R., Joseph Munchak, S., et al. (2015). The evolution of the Goddard profiling algorithm to a fully parametric scheme. *J. Atmos. Ocean. Technol.* 32, 2265–2280. doi: 10.1175/JTECH-D-15-0039.1

Pulwarty, R. S., and Sivakumar, M. V. (2014). Information systems in a changing climate: early warnings and drought risk management. *Weather Clim. Extremes* 3, 14–21. doi: 10.1016/j.wace.2014.03.005

Skofronick-Jackson, G., Petersen, W. A., Berg, W., Kidd, C., Stocker, E. F., Kirschbaum, D. B., et al. (2017). The global precipitation measurement (GPM) mission for science and society. *Bull. Am. Meteorol. Soc.* 98, 1679–1695. doi: 10.1175/BAMS-D-15-00306.1

Svoboda, M., and Fuchs, B. (2016). *Handbook of Drought Indicators and Indices. Integrated Drought Management Tools and Guidelines Series 2. I. D. M. P. (IDMP)*. Geneva: World Meteorological Organization (WMO) and Global Water Partnership (GWP). doi: 10.1201/b22009-11

Wallace, D. P. (2007). *Knowledge Management: Historical and Cross-Disciplinary Themes*. Exeter: Libraries Unlimited.

Wilhite, D., and Glantz, M. (1985). Understanding: the drought phenomenon: the role of definitions. *Water Int.* 10, 111–120. doi: 10.1080/02508068508686328

Wilhite, D., and Pulwarty, R. S. (2017). *Drought and Water Crises: Integrating Science, Management, and Policy*. Boca Raton, FL: CRC Press. doi: 10.1201/b22009

Conflict of Interest: The authors declare that the research was conducted in the absence of any commercial or financial relationships that could be construed as a potential conflict of interest.

frontiers in Climate

ORIGINAL RESEARCH
published: 30 October 2020
doi: 10.3389/fclim.2020.578785

On the Robustness of Annual Daily Precipitation Maxima Estimates Over Monsoon Asia

Phuong-Loan Nguyen[1]*, *Margot Bador*[1], *Lisa V. Alexander*[1], *Todd P. Lane*[2] and *Chris C. Funk*[3,4]

[1] Climate Change Research Centre and Australian Research Council Centre of Excellence for Climate Extremes, UNSW Sydney, Sydney, NSW, Australia, [2] Australian Research Council Centre of Excellence for Climate Extremes, School of Earth Science, The University of Melbourne, Melbourne, VIC, Australia, [3] US Geological Survey, Centre for Earth Resources Observation and Science, Sioux Falls, SD, United States, [4] Santa Barbara Climate Hazard Centre, University of California, Santa Barbara, Santa Barbara, CA, United States

Understanding precipitation extremes over Monsoon Asia is vital for water resource management and hazard mitigation, but there are many gaps and uncertainties in observations in this region. To better understand observational uncertainties, this study uses a high-resolution validation dataset to assess the consistency of the representation of annual daily precipitation maxima (Rx1day) over land in 13 observational datasets from the Frequent Rainfall Observations on Grids (FROGS) database. The FROGS datasets are grouped into three categories: *in situ*-based and satellite-based with and without corrections to rain gauges. We also look at three sub-regions: Japan, India, and the Maritime Continent based on their different station density, orography, and coastal complexity. We find broad similarities in spatial and temporal distributions among *in situ*-based products over Monsoon Asia. Satellite products with correction to rain gauges show better general agreement and less inter-product spread than their uncorrected counterparts. However, this comparison also reveals strong sub-regional differences that can be explained by the quantity and quality of rain gauges. High consistency in spatial and temporal patterns are observed over Japan, which has a dense station network, while large inter-product spread is found over the Maritime Continent and India, which have sparser station density. We also highlight that while corrected satellite products show improvement compared to uncorrected products in regions of high station density (e.g., Japan) they have mixed success over other regions (e.g., India and the Maritime Continent). In addition, the length of record available at each station can also affect the satellite correction over these poorly sampled regions. Results of the additional comparison between all considered datasets and the sub-regional high resolution dataset remain the same, indicating that the overall quality of the station network has implications for the reliability of the *in situ*-based products derived and also the satellite products that use a correction to *in situ* data. Given these uncertainties in observations, there is no single best dataset for assessment of Rx1day in Monsoon Asia. In all cases we recommend users understand how each dataset is produced in order to select the most appropriate product to estimate precipitation extremes to fit their purpose.

Keywords: precipitation extremes, observational uncertainties, *in situ*, satellite observation, satellite correction

OPEN ACCESS

Edited by:
Dann Mitchell,
University of Bristol, United Kingdom

Reviewed by:
Milind Mujumdar,
Indian Institute of Tropical Meteorology (IITM), India
Jun Matsumoto,
Tokyo Metropolitan University, Japan

***Correspondence:**
Phuong-Loan Nguyen
phuongloan.nguyen@student.unsw.edu.au

Specialty section:
This article was submitted to Climate Services, a section of the journal Frontiers in Climate

Received: *01 July 2020*
Accepted: *30 September 2020*
Published: *30 October 2020*

Citation:
Nguyen P-L, Bador M, Alexander LV, Lane TP and Funk CC (2020) On the Robustness of Annual Daily Precipitation Maxima Estimates Over Monsoon Asia. Front. Clim. 2:578785. doi: 10.3389/fclim.2020.578785

INTRODUCTION

Asia is home to about 60% of the world's population and is the largest and most populous continent in the world (Hijioka et al., 2014). The extensive Asian monsoon system which spans South Asia, Southeast Asia, and East Asia plays an important role in large scale climate variability over much of the globe. This region is vulnerable to extreme weather, notably extreme precipitation (Fujibe et al., 2006; Jung et al., 2011; Zhao et al., 2014; Ren et al., 2015; Roxy et al., 2017). To monitor and understand the change and risk from precipitation extremes in Asian countries, accurate and reliable precipitation observations are required.

Numerous observational products are now available in a consistent format from the Frequent Rainfall Observations on GridS (FROGS) database (Roca et al., 2019), enabling easier intercomparisons. The FROGS database contains a variety of observational daily gridded precipitation datasets that have all been interpolated onto a common 1°x1° grid. These products differ in their data sources (e.g., *in situ*, satellite and blended sources) and the methods by which they are produced, and they have different spatial coverage (regional to global). *In situ* precipitation products have been developed solely from station (gauge) observations, which are typically used to measure precipitation at a point. Many stations have very long records, and this is an advantage for detecting climate trends. However, *in situ* data have disadvantages, including incomplete spatial coverage, deficiencies over most oceanic regions and sparsely populated areas (Kidd et al., 2017) and they are not normally representative of rainfall (especially convective rainfall) over a broader area. As discussed in the data section, there are also complexities associated with gauge undercatch correction (Legates and Willmott, 1990). Satellite observations, on the other hand, offer advances in terms of spatial coverage and temporal completeness for vast areas of the globe, but have records that are much shorter and inhomogeneous due to different instruments used through time and potential algorithm changes in how estimates are calculated. In addition, precipitation from satellite-based products are instantaneous and indirect measures inferred from infrared (IR) or passive microwave (PMW). IR observations can see clouds but not precipitation, and IR estimates must link cloud-top temperature or reflectivity to rain rates through empirical relationships. PMW observations, on the other hand, can detect the radiation from hydrometeors, but PMW observations are sparse and intermittent. Both IR and PMW data streams rely on changing constellations of satellites that require additional data processing and calibration. These factors are major sources of uncertainty and error (Iguchi et al., 2009; Tapiador et al., 2012). Many attempts have been made to merge different sources of information to utilize the advantages of individual types of products. For example, multiple satellite fields are merged and/or scaled with rain gauge analyses over land, which helps improve the accuracy of precipitation measurements (Sun et al., 2018). Popular products used in climate studies, such as the Global Precipitation Climatology Project (GPCP) precipitation analysis, merge gauge observations with satellite microwave data and infrared radar (IR). The launch of precipitation radars in some satellite measurements, for example over the Tropical Rainfall Measuring Mission (TRMM) (Huffman et al., 2007) helps capture the three-dimensional structure of rain. In particular, the long-term TRMM on-board radar had obvious advantages for detecting the heavy precipitation that is associated with distinct orographic features and coastal effects (Shige et al., 2013, 2015, 2017). Other products such as CMORPH (Xie et al., 2017) and version 6 of the Global Precipitation Mission (GPM) Integrated Multi-Satellite Retrievals for GPM (IMERG) (Huffman et al., 2019, 2020) use a "morphing" based approach to estimate precipitation. Sparse and intermittent PMW observations are used to derive instantaneous rain rates, which are then combined with motion vectors to derive a detailed two-dimensional rain rate structure that covers every location.

Precipitation extremes estimated from these numerous datasets present a heterogeneous picture at both regional [e.g., Australia (Contractor et al., 2015), Europe (Prein and Gobiet, 2017), the United States (Beck et al., 2019), South-East Asia (Kim et al., 2018), and global (Herold et al., 2016a,b; Alexander et al., 2020; Bador et al., 2020)] scales owing to their different data sources, quality control schemes, and procedures in how precipitation estimates are calculated. At the global scale, *in situ* products are most similar to each other in their representation of extreme precipitation compared to other product types (Herold et al., 2016b; Sun et al., 2018). In addition, and as expected, satellite products that use rain gauge corrections show a better agreement with *in situ*-based observations than uncorrected satellite products (Alexander et al., 2020; Bador et al., 2020). The specific details of the gauge-satellite blending process, however, can have important ramifications for product performance. Satellite estimates having relatively low mean bias are less likely to experience non-stationary systematic errors and spurious trends associated with shifts in gauge network (Maidment et al., 2015).

Very few studies, however, have examined the consistency in how different observational products represent precipitation extremes over the Asian domain. One exception is Kim et al. (2018) who conducted an intercomparison of precipitation across different observational products (and in an ensemble of models) with only a minor focus on extremes. They examined the spatial-temporal characteristics of rainfall exceeding the 95th percentile threshold across 7 gridded *in situ*, satellite and reanalysis daily precipitation products. Their results revealed small differences among the datasets over India, Korea and Japan but large differences over Southeast Asian countries and the Maritime Continent. In addition, they found that decadal trends in extreme precipitation are consistent over some parts of South Asia (e.g., India) and East Asia (e.g., South Korea, Japan) while no trend in precipitation extremes was found over Southeast Asia (e.g., the Maritime Continent). However, the study focused on only a small subset of available products and on a limited aspect of "moderate extremes" of precipitation. Therefore, there are still many gaps in our understanding of the representation and analysis of observed precipitation extremes over Monsoon Asia. These better understanding will help to better inform data development and others

research activities like model evaluation, monitoring, and projections etc.

For this study, we conduct an intercomparison of various existing observational products to evaluate their consistency in terms of representing the annual maxima of daily precipitation (Rx1day) over Monsoon Asia, in terms of their climatology and trends. We chose to focus on Rx1day because this metric represents an annual extreme value that is often used to infer potential flooding events (Lestari et al., 2019). Supplemental results examine the annual wettest 5-days period (Rx5day), the annual sum of precipitation on wet days (PRCPTOT), the simple daily intensity index (SDII) and the annual total count of days when daily precipitation exceeds 10 mm (R10mm). Our objective is to better understand observational uncertainties from different data sources and over different sub-regions of Monsoon Asia. We do this by investigating the influence of the underlying station density and correction methods that satellites use to estimate precipitation on the consistency of annual maxima of daily precipitation. Finally, we make recommendations for the regional assessment of precipitation extremes over Monsoon Asia and its sub-regions.

The remainder of the paper is organized as follows. Section data and methods describes the observational datasets used in this study along with the definition of precipitation extremes and the description of the methods used. Results on the comparison of precipitation extremes from different datasets is presented in section results, followed by our discussion of results in section discussion and our conclusions in section 5.

DATA AND METHODS

Observational Datasets and Domain

At present, there are many precipitation datasets available, including those from the FROGS database (Roca et al., 2019). This database has been developed recently to provide a variety of gridded observational precipitation datasets from *in situ*, satellite, blended and reanalyses sources on a common daily 1°x1° latitude/longitude grid format mostly covering global land and/or ocean. Here we utilize 13 products from FROGS (**Table 1**) which have sufficient coverage over our chosen Asian domain (60^0E-150^0E; 15^0S-50^0N) and a suitable length of record for this analysis (see below). We do not include reanalyses, which generally have uncertainties that are too large to support the analysis of precipitation extremes (Alexander et al., 2020; Bador et al., 2020). Besides, they are not purely observations, but observation data assimilated into numerical models. Therefore, precipitation information in reanalysis is of questionable quality since it relies, almost entirely, on the parameterization of

TABLE 1 | List of observational datasets of daily precipitation used in this study.

Cluster	No	Product name	Short name	Input data	Temporal coverage	Original resolution	References
Reference	1	APHRODITE	APHRODITE	GTS, local organization and own APHRODITE	1951–2015	$0.5° \times 0.5^0$	Yatagai et al. (2012)
In situ (3)	2	REGEN_ALL_v2019	REGEN_ALL	GPCC, GHCN	1950–2016	1°× 1°	Contractor et al. (2020)
	3	GPCC_FDD_v1.0	GPCC_FDD	GPCC	1988–2013	1°× 1°	Schamm et al. (2014)
	4	CPC_v1.0	CPC	CPC	1979–2017	$0.5° \times 0.5^0$	Xie (2008)
Satellite with correction to rain gauge (6)	5	GSMAP-gauge-RNLv60	GSMAP-RNL	IR, PMW, sate_radar, CPC gauges	2001–2013	1° × 1°	Okamoto et al. (2005)
	6	GPCP_CDR_v1.3*	GPCP_CDR	IR, PMW GPCC gauges	1997–2017	0.25°/8 km	Huffman et al. (2001)
	7	CMORPH_v1.0_CRT	CMORPH_CRT	IR, PMW CPC gauges	1998–2017	0.25° × 0.25°	Xie et al. (2017)
	8	IMERG_V6_FC*	IMERG_FC	IR, PMW GPCC gauges, sate_radar	2001–2018	0.25° × 0.25°	Huffman et al. (2019)
	9	3B42_v7.0	3B42	IR, PMW sat_radar, GPCC gauges	2001–2013	$0.1° \times 0.1^0$	Huffman et al. (2007)
	10	CHIRPS_v2.0	CHIRPS2	IR, TMPA 3B42, gauges (GHCN and other sources), CFS2, CHPclim	1981–2016	0.1° × 0.1°	Funk et al. (2015)
Satellite without correction to rain gauge (4)	11	CMORPH_v1.0_RAW	CMORPH_RAW	IR, PMW	1998–2017	0.25°/8 km	Xie et al. (2017)
	12	IMERG_v6_FU	IMERG_FC	IR, PMW, sate_radar	2001–2018	0.25° × 0.25°	Huffman et al. (2019)
	13	3B42_IR_V7.0	3B42_IR	IR	1998–2016	0.25° × 0.25°	Huffman et al. (2007)
	14	CHIRP_V2	CHIRP	IR	1981–2016	$0.1° \times 0.1^0$	Funk et al. (2015)

**Gauge under-catch correction; IR, thermal infrared; PMW, passive microwave; sate_radar: satellite radar; CSF2, Coupled Forecast System (CFS) version 2; CHPclim, Climate Hazards group Precipitation climatology; GHCN, the Global Historical Climate Network; TMPA 3B42, Tropical Rainfall Measuring Mission Multi-satellite Precipitation Analysis version 7.*

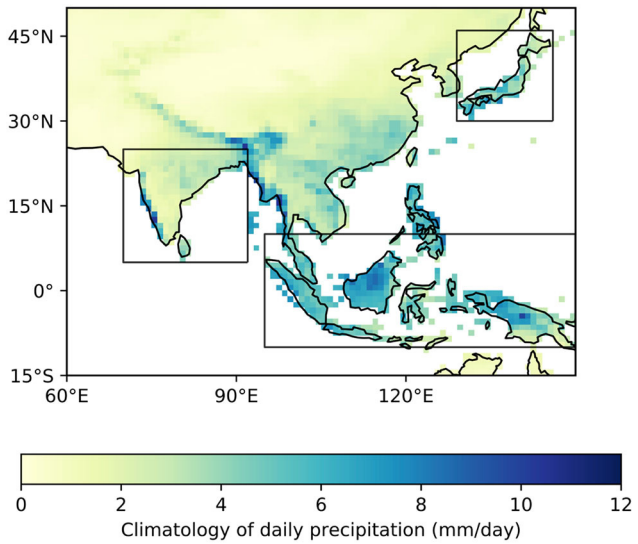

FIGURE 1 | Climatology of the annual daily precipitation (mm/day) extracted from APHRODITE. Black boxes show the regions used in this document: Japan (129°E-146°E, 30°N-46°N), India (70°E-92°E, 5°N-25°N), and the Maritime Continent (95°E-150°E, 10°S-10°N).

convection and simulation of rainfall in numerical models and is not constrained by precipitation observations (Bosilovich et al., 2011; Dee et al., 2011). In addition, some product "families" include more than one dataset, but we select only one dataset from each product family where we believe that either the best quality control has been applied or where one dataset is deemed preferable for the purposes of this study.

To intercompare datasets with respect to product types, we cluster the 13 products into three groups organized by data type: *in situ*-based (three datasets); satellite with (six datasets) and without (four datasets) a correction to rain gauges. The products range in the time period covered, from 13 years (GSMAP-RNL) to 67 years (REGEN_ALL). All products share the common overlapping period of 2001–2013, which is therefore used to intercompare climatologies between the different datasets.

Additionally, we include the $0.5^0 \times 0.5^0$ gridded precipitation dataset: Asian Precipitation—Highly Resolved Observational Data Integration Towards Evaluation of Water Resources (APHRODITE) (Yatagai et al., 2012). This continental-scale daily product contains a dense network of daily rain gauge data for Asia obtained from different sources: Global Telecommunication System (GTS) based data, data precompiled by other projects or regional organizations and APHRODITE's own collection. Various versions of the product have been developed including: V1101, V1101_EXR1, V1801, and V1901. Note that the newest version of APHRODITE, V1901, that applies updated algorithms has been released, but it only covers the period 1998–2017. Therefore, for this study we merged version V1101 (covering 1950-2007) and V1101_EXR1 (covering 2008–2015) to get as long a record as possible. Two versions of this dataset were merged to get the longest covered period (1950–2005). We acknowledge that this regional dataset is not necessarily "the truth," but with the extensive exchange of real time data from these national hydrological and meteorological services, APHRODITE has a substantially improved station precipitation network in many parts of Asia, notably around the Himalayas, Southeast Asia, and mountainous regions compared to other available global precipitation datasets (see **Figure 2** and further discussion on this in section climatology of the mean daily precipitation). Therefore, in this study we use APHRODITE as a reference dataset with which to compare the 13 precipitation products we have accessed from FROGS. In order to enable a fair comparison, the daily precipitation data from APHRODITE were interpolated using a first-order area-conservative remapping method (Jones, 1999) to the same 1°x1° resolution as the other datasets. This interpolation method conserves the integral of precipitation that does not necessarily hold for other remapping methods. Then extreme precipitation indices outlined in the next section were then calculated.

Wind and evaporation effects on gauge measurements, typically resulting in gauge undercatch is one of the dominant errors in precipitation estimates over high-latitude and mountainous areas (Prein and Gobiet, 2017). Several observational datasets are corrected for gauge-precipitation undercatch (see **Table 1**). The applied correction method, however, varies from one product to another. For example, a bulk correction factor (Legates and Willmott, 1990) usually was applied to monthly climatological means in GPCP_CDR (Huffman et al., 2001) and IMERG_FC (Huffman et al., 2019). Note that APHRODITE does not apply a gauge-undercatch correction, but rather uses an improved quality-control method and orographic correction of precipitation.

Our domain covers a large area with a heterogeneous distribution in the number of gauges per 1°x1° grid, as extracted from APHRODITE (**Figure 2e** and also **Supplementary Figure 1** for a zoom in). We also defined different station density (s) following categories: rare ($0 < s < 1$); low ($1 \leq s < 5$), medium ($5 \leq s < 10$), and high ($s \geq 10$) to try to better quantify this heterogeneity. To account for spatial-temporal variations in the characteristics of precipitation extremes, we investigate several sub-regions in more detail, namely: Japan (129^0E-146^0E; 30^0N-46^0N); the Maritime Continent (95^0E-150^0E;10^0S-10^0N); and India (70^0E-90^0E; 5^0N-25^0N) (**Supplementary Figure 1**) for further analyses. These three sub-regions cover a large area of land with very different station density and spatial characteristics such as orography and coastal complexity. We chose these regions because they provide a good representation of different extreme rainfall estimation challenges. Japan has a very dense *in situ* gauge network. Indian and the Maritime Continent are poorly instrumented.

APHRODITE lacks good station coverage over India and the Maritime Continent (**Supplementary Figure 1**). At more local scales, the Southeast Asian Climate Assessment and Dataset (SACA&D) (Van Den Besselaar et al., 2017) and the high resolution long-term India Meteorological Department (IMD) (Pai et al., 2014) dataset might provide better precipitation estimates in these regions since they have much more station information than the products we have assessed over the wider region. Therefore, we conduct additional comparison

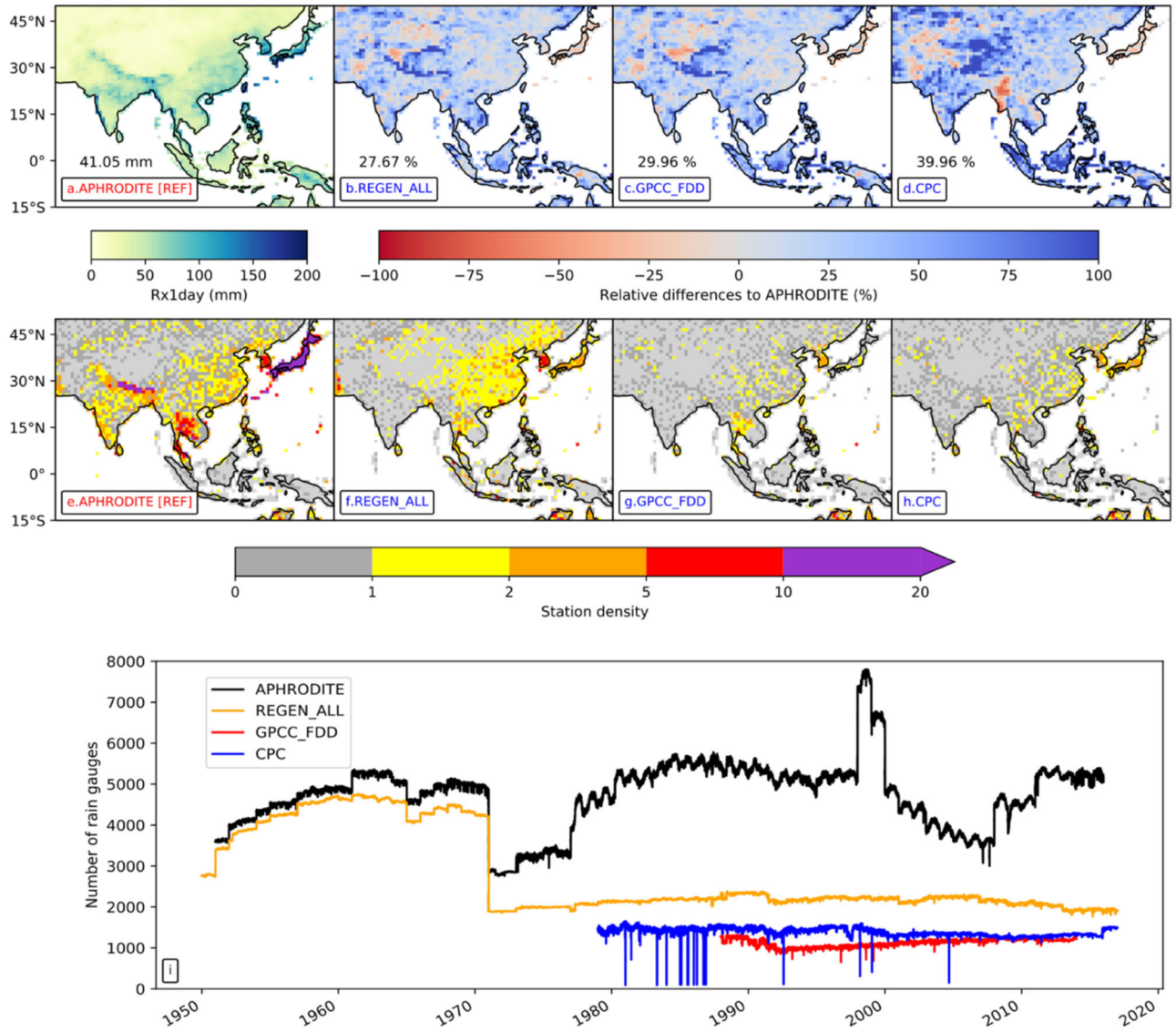

FIGURE 2 | Upper panel: Climatological values (over the period of 2001–2013) of the annual wettest-day (Rx1day; in mm) for **(a)** APHRODITE and the relative difference to APHRODITE (in %) of climatological Rx1day for the *in situ*-based products (blue labels): **(b)** REGEN_ALL **(c)** GPCC_FDD, **(d)** CPC. The number inserted on each panel indicates the regional average of these relative differences. Middle panel: Climatological station density in each *in situ*-based dataset: averaged number of rain gauges per 1°x1° grid cell over the 2001–2013 period in **(e)** APHRODITE, **(f)** REGEN_ALL, **(g)** GPCC_FDD, **(h)** CPC. Note that the light gray color indicates no station and the dark color indicates very sparse-station regions (i.e., have station density <1 station per grid cell). Bottom panel: **(i)** Time evolution of station density: daily total number of rain gauges over the Asian Monsoon area in (black) APHRODITE, (orange) REGEN_ALL, (red) GPCC_FDD, and (blue) CPC.

between all the products from **Table 1** and these local datasets (**Supplementary Part**). Note that the local datasets are at 0.25° × 0.25° resolution and contain only precipitation information for Indonesia and India. To enable a fair comparison with the other products analyzed here, SACA&D and IMD were interpolated into a common 1° × 1° grid using a conservative remapping method.

Precipitation Extremes

Note that most regional precipitation extremes of monsoon Asia are associated with Asian summer monsoon circulation features. However, to characterize extreme precipitation, we select the annual maximum 1-day precipitation (Rx1day) as recommended by the Expert Team on Climate Change and Detection Indices (ETCCDI) (Zhang et al., 2011) from each 1^0x1^0 grid box. This index represents the type of extreme event that might lead to flooding for example (You et al., 2011; Liu et al., 2014). In addition, most the annual daily precipitation maxima do actually mostly reflect the summer precipitation maxima [whether that is Northern Hemisphere summer (June, July, August, and September for the "mainland" of monsoon Asia) or Southern Hemisphere summer (December, January,

and February for Southeast Asia)] (Figure not shown). We also extract other precipitation indices [i.e., the maximum 5-days precipitation (Rx5day), the simple daily intensity (SDII), the total annual wet-day precipitation (PRCPTOT) and the annual counts of day when precipitation exceeds 10 mm (R10mm)]. Analysis of these are found in the **Supplementary Material**.

We use some basic statistics including an assessment of the climatology over the longest overlapping period of data (i.e., 2001–2013); and time series of regional averages for the whole period of available data (which varies by observational product—see **Table 1**). Note that time series of regional averages are calculated relative to the Rx1day annual average over the 1961–1990 baseline period in APHRODITE. Only areas that have common data between all datasets are used to calculate area-averaged time series. In order to draw conclusions about inter-product spread, the coefficient of variation (cov) (i.e., standard deviation normalized by the multiproduct mean of climatology for each cluster is calculated over the common period of 2001–2013).

Finally, we compare trends and temporal correlations over 1988–2013 for each product that covers this (longer) period and has a sufficient amount of non-missing data (i.e., 70% of data has to be present for an annual value to be calculated). Therefore, all satellite products are excluded except the CHIRP2 family, which have temporal coverage from 1981 to 2016 (see **Table 1**). Since some annual extremes do not follow a Gaussian distribution, we use a non-parametric linear trend estimator, Sen's slope (Sen, 1968). Trend significance is estimated using a Mann-Kendall test at the 5% level of significance (Kendall, 1975).

RESULTS

Climatology of the Mean Daily Precipitation

Figure 1 illustrates the spatial distribution of the 13-years mean (2001–2013) of daily precipitation in the APHRODITE dataset over different regions of monsoon Asia. Clearly, the precipitation pattern is strongly dependent on orography. In particular, large amounts of precipitation are located in the western Ghats of India, central and northeast of India (South Asia), the coastline of Myanmar (Southeast Asia), and parts of Japan. This heavy orographic rainfall is on the windward side of high-elevation regions and the rapid decrease of rainfall is observed on the leeward side of these regions. This feature has been mentioned in previous literature (Krishnan et al., 2012; Pai et al., 2014; Priya et al., 2016; Kim et al., 2018). In addition, there is heavy rainfall over Eastern China, Korea while lower intensities of daily precipitation are observed over the Tibetan Plateau and higher latitudes of Asia.

Climatology, Inter-Product Spread, and Trends in Rx1day

Precipitation in *in situ*-based products are directly estimated from surface stations and therefore different datasets often share similar underlying data (Sun et al., 2018). For this reason, we start with a comparison among *in situ*-based products to see whether there is consistency in their representation of precipitation extremes. **Figure 2a** shows a 13-years climatology (2001–2013) for Rx1day (mm) in the APHRODITE dataset (taken as reference; see section observational datasets and domain) and the relative difference (%) for three of the available *in situ*-based products from the FROGS database compared with APHRODITE (**Figures 2b–d**). Intense extreme rainfall (i.e., Rx1day $>$ 150 mm) is found in Japan, South Korea, and the western coastal part of India while lower intensities of extreme precipitation are observed over the Tibetan Plateau and higher latitudes of Asia (**Figure 2a**). Overall, *in situ*-based products tend to show spatially coherent patterns of extreme precipitation difference compared to APHRODITE, that is, they are consistently wetter almost everywhere. This feature can not only be seen in other intensity-based indices such as Rx5day, PRCPTOT, and SDII but also in frequency-based indices like R10mm (**Supplementary Figures 3–6**).

Some exceptions are found over Japan, Korea and Pakistan where all global *in situ* datasets are drier than APHRODITE in their extremes (see **Supplementary Figures 2A–D** for a zoom in over Japan). It is worth noting that over Japan, APHRODITE has at least an order of magnitude more stations than any of the other *in situ*-based datasets so it could be picking up more severe local storms contributing to the wetter Rx1day. This extremely dense gauge network may also be capturing events in remote mountainous regions with orographic enhancement. Precipitation gauges tend to be preferentially located in valleys and low-lying areas. REGEN_ALL and GPCC_FDD have very similar spatial patterns with regional means wetter than APHRODITE (27.67 and 29.96%, respectively). This is expected as these two products utilize the rain gauges from GPCC_FDD (Schamm et al., 2014; Contractor et al., 2020) although REGEN_ALL also includes other sources. Meanwhile, CPC has higher estimates of Rx1day on the whole than APHRODITE (39.96%) (and the other two products) but regions clearly stand out as having drier extremes. It is easy for example to see the borders of Myanmar, Pakistan, and Laos highlighting that there are data availability issues over these particular countries in CPC. The considered period of 2001–2013 exhibits a strong decrease in the number of total ground-based measurements globally due to migration and abandonment of sites and operational costs, particularly for CPC and GPCC_FDD as mentioned in Sun et al. (2018). A common feature among the three *in situ*-based datasets is that the Himalayas stand out as having consistently wetter Rx1day than APHRODITE.

The newest version of APHRODITE, V1901, applied some improvements to quality control and used an updated interpolation algorithm to represent "extreme" values. To test the sensitivity of the above results to the choice of version of APHRODITE, we conduct the same analyses with APHRODITE_MA version V1901 (**Supplementary Figure 7**). Our main conclusions remain the same whatever version of APHRODITE is used.

The differences among gauge-based products may come largely from the different gauge networks used to derive each dataset, as well as differences in the background climatologies used to interpolate these gauge observations. **Figures 2e–h** also highlight the heterogeneous distribution of rain gauges in the overlapping period of 2001–2013. Note that the light

gray color indicates no stations present in a grid box while the gray color indicates a very sparse station network (i.e., with averaged station density less than one station per grid cell). APHRODITE has the highest number of stations overall (**Figure 2e**) although this might not always hold regionally [e.g., REGEN_ALL has more stations over China (**Figure 2f**)]. GPCC_FDD and CPC have fewer stations than REGEN_ALL and APHRODITE (**Figures 2g–h**). Some regions are well-covered by stations in all the *in situ* products such as Japan, South Korea and Thailand while Myanmar is a data-sparse region for all products. As a result, estimates of precipitation extremes over the dense-station regions usually show a consistent spatial pattern e.g., over Japan with slightly drier extremes compared to APHRODITE (see also– **Supplementary Figure 2**). On the contrary, the representation of the annual maxima precipitation over the data-sparse regions (i.e., station density <1) e.g., Myanmar is largely different among *in situ* products. Interestingly, the Himalayas has lots of stations (station density is >5, some locations are >10) in APHRODITE (**Figure 2e**) but no stations in the other *in situ*-based products (**Figures 2f–h**). In addition, APHRODITE applied the orographic precipitation correction over high-elevation regions like the Himalayas which other *in situ*-based products do not apply. These features might help to explain the consistently wetter pattern compared with APHRODITE in all *in situ*-based products over the Himalayas.

Focusing on the time evolution of station density across the *in situ*-based products (**Figure 2i**), it is interesting to note that there is a large decrease in the total number of stations used in APHRODITE and REGEN_ALL around 1970, which relates to a substantial reduction of rain gauges over India in each product (**Supplementary Figure 7**). APHRODITE station numbers recover over subsequent decades, which is explained by the significant increase in gauges over Japan (**Supplementary Figure 9**), though this increase does not occur for REGEN_ALL (**Supplementary Figure 9**). These changes in the total number of available rain gauges are expected to impact inter-product differences, which is further investigated hereafter.

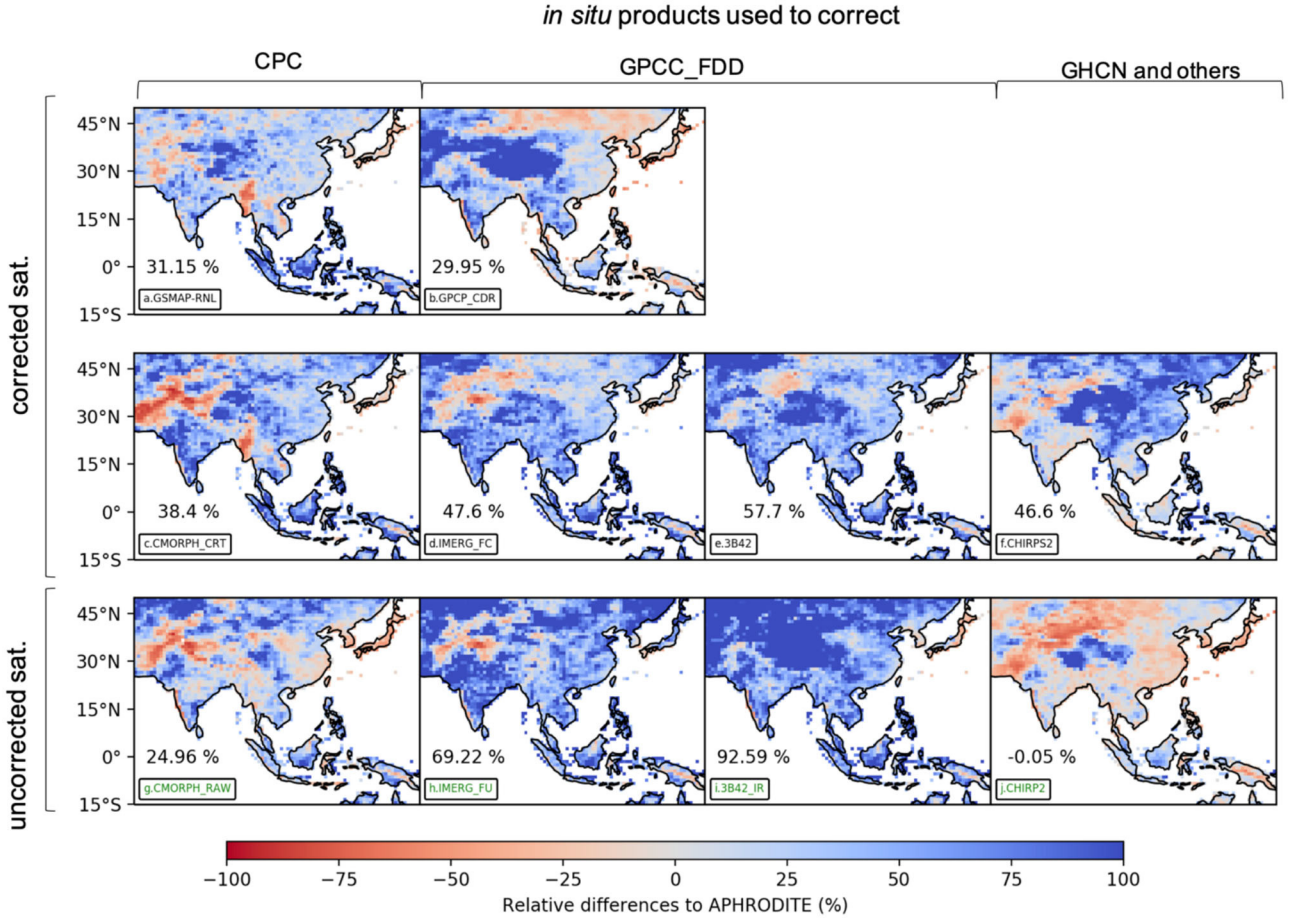

FIGURE 3 | The relative difference to APHRODITE (in %) of the climatological (over the period of 2001–2013) annual wettest day (Rx1day) for corrected satellite products (black labels, two upper panels) **(a)** GSMAP_RNL, **(b)** GPCP_CDR, **(c)** CMORPH_CRT, **(d)** IMERG_FC, **(e)** 3B42, **(f)** CHIRPS2, and uncorrected satellite products (green label, lower panel) **(g)** CMORPH_RAW, **(h)** IMERG_FU, **(i)** 3B42_IR, **(j)** CHIRP2. The number inserted on each panel indicates the regional average of these relative differences. The *in situ* products that satellite products used for their correction to rain gauges are also mentioned at the top of the figure.

Satellite products could potentially reduce issues associated with the lack of *in situ* precipitation observations. For this reason, we next evaluate the consistency of extreme precipitation among satellite products. **Figure 3** compares the representation of Rx1day among all of the satellite products as the relative difference to APHRODITE over the common 2001–2013 period. Interestingly, the annual wettest day estimated from satellites tends to be more spatially inhomogeneous, with regions of underestimation and overestimation compared to APHRODITE for each dataset. This is different to the *in situ* datasets that mostly show wetter estimates of climatological Rx1day (**Figures 2b–d**). We find different estimates across satellite products both with and without correction to rain gauges over Pakistan, the Tibetan Plateau, and Western China. Meanwhile, satellite products with corrections are more consistent with *in situ*-based products over regions that have a higher number of stations (e.g., Eastern China).

We now focus on the overall differences between the corrected and uncorrected satellite products. Generally, the differences from APHRODITE are amplified among the uncorrected satellite products (**Figures 3g–j**) in comparison to the corrected products (**Figures 3a–f**). The diversity of Rx1day estimates among the uncorrected satellite products is clear with relative differences in regional means ranging from 92.59% in 3B42_IR (**Figure 2i**) to −0.05% in CHIRP2 (**Figure 3f**). CHIRP2 is the closest to APHRODITE (**Figure 3f**) in terms of regional average but this hides some regional contrasts (e.g., the Tibetan Plateau and parts of the Maritime Continent are wetter while Pakistan and eastern China are drier than APHRODITE). In a global study of extreme precipitation, Alexander et al. (2020) also showed CHIRP2 to be the driest dataset in terms of extremes over global land areas while 3B42_IR belongs to a group of products with wetter estimates. Ongoing analysis by the Climate Hazards Center suggests that the systematic dry bias of CHIRP2 is related to the fixed intercept terms used to translate thermal infrared satellite observations into estimates of rainfall rates. While CHIRP2 consistently tends to capture well mean precipitation rates, the fixed intercepts used to translate IR data into rainfall rates suppresses the variance of the CHIRP2 product. On the other hand, corrected satellite estimates tend to be consistently wetter than APHRODITE, ranging from the lowest relative difference of 29.95% in GPCP_CDR (**Figure 3b**) to the highest of 57.7% in 3B42 (**Figure 3e**). In addition, by comparing pairs of corrected and uncorrected products for each satellite dataset (which is further explored in section climatology, inter-product spread and trends in Rx1day), we cannot be confident whether the corrections using *in situ* data makes the corrected product overall better over Monsoon Asia (i.e., closer to APHRODITE). For example, both the CMORPH and CHIRP2 family of products are drier (and closer to) APHRODITE in their uncorrected versions compared with their corrected versions, while the opposite is true for products from the 3B42 and IMERG families.

The difference among satellite products can probably partly be explained by the differences in how algorithms are used to estimate precipitation and the techniques used to apply rain gauge corrections, and we now explore this. In particular, among uncorrected satellite products, 3B42_IR and CHIRP2 utilize information from infrared radar (IR) measurements while others integrate information from passive microwave (PMW) measurements (e.g., CMORPH_RAW, IMERG_FU; see **Table 1** for details). These uncorrected satellite products are blended with information derived from rain gauges, forming the rain gauge-enhanced satellite products. It is interesting to note that the choice of the underlying stations used for the rain gauge-enhanced satellite estimates impacts the final product. For instance, the imprint of the underlying CPC *in situ* data that is used to correct them can be clearly seen in some of the spatial patterns of the GSMAP-RNL and CMORPH family of products (e.g., dry bias over Myanmar, Pakistan and Laos; see panels in the left column of **Figure 3**). This is not systematic and indeed other products sharing the same underlying stations (e.g., GPCP_CDR, 3B42, and IMERG product families) show limited similarity in their spatial distribution of differences to APHRODITE although they all utilize GPCC_FDD (**Figure 3**; middle panels).

Monsoon Asia is a vast area and we highlight above that although we can extract some conclusions (e.g., *in situ* and satellite products are generally wetter than APHRODITE), important differences remain at the regional scale. Therefore, we also consider three sub-regions that have been selected because they are characterized by different station density, orography and coastal complexity (see section observational datasets and domain). The consistency among precipitation products over Monsoon Asia and the three sub-regions (namely Japan, India, and the Maritime Continent) are examined through time series of regionally averaged relative differences in Rx1day (**Figure 3**), the coefficient of variation (cov; i.e., Rx1day standard deviation

TABLE 2 | Coefficient of variation (cov) (in percentage (%); see section precipitation extremes) calculated over the 2001–2013 period for each product cluster: *in situ*, corrected satellite, and uncorrected satellite.

Cluster	Monsoon Asia	Japan	India	Maritime Continent
In situ	2.87	3.76	6.65	9.56
Corrected satellite	9.25	16.32	14.07	16.66
Uncorrected satellite	19.35	21.18	19.12	16.35

The cov is calculated for Monsoon Asia and its sub regions: Japan, India, and Maritime Continent based on extracted time series of regional averages in ***Figure 4****.*

TABLE 3 | Temporal correlation of regionally averaged relative differences (in %) for the annual wettest day (Rx1day) for each considered products with APHRODITE, calculated for each product covering the period of 1988–2013.

Dataset name	Monsoon Asia	Japan	India	Maritime Continent
REGEN_ALL	0.57	0.51	−0.03	0.30
GPCC_FDD	0.54	0.71	−0.17	0.33
CPC	0.67	0.64	−0.26	0.42
CHIRPS2	0.21	0.65	0.23	0.49
CHIRP2	0.17	0.52	0.07	0.12

The temporal correlation is calculated from extracted time series of regional averages in ***Figure 4****. Products are selected if they have <2 years of missing values during this period. See also* ***Supplementary Figure 6*** *for additional information.*

divided by mean) taken as a measure of the inter-product spread within each cluster (**Table 2**) and the temporal correlation with APHRODITE taken as a measure of inter-annual variability (**Table 3**).

We first focus on the Monsoon Asia region as a whole. *In situ*-based products (**Figure 4A**) show some robustness with less inter-product spread compared to the other two classes of product (**Figures 4B,C**), as further shown by smaller cov values for the *in situ*-based products compared to the corrected and uncorrected satellite products (2.87% compared to 9.25 and 19.35%, respectively; **Table 2**). Note that three particular years of CPC (i.e., 1983–1985) contain a lot of missing grid cells over whole Monsoon Asia and its sub-regions, therefore these three years were excluded in the calculation of Rx1day. Corrected satellite products are more closely aligned with *in situ*-based products (**Figure 4B**) compared with uncorrected versions. Focusing on inter-annual variability, we find relatively high temporal correlations with APHRODITE for *in situ*-based products (from 0.54 to 0.67; **Table 3**) compared to CHIRPS2 (0.21; **Table 3**) and its uncorrected counterpart CHIRP2 (0.17; **Table 3**). While we cannot extract general conclusions based on these temporal correlations for the corrected and uncorrected satellite clusters due to their limited time coverage, this further tends to show that *in situ*-based products are generally more reliable than satellite data over the whole region studied.

We then further investigate the consistency in the representation of Rx1day over the three sub-regions (Japan, India, and the Maritime Continent; second, third and last rows of **Figure 4** respectively). First, we focus on the *in situ* cluster. As over Monsoon Asia, we find relatively strong consistency among *in situ*-based datasets over the high-station density region of Japan (cov value of 3.76 %, **Table 2**). We also find high

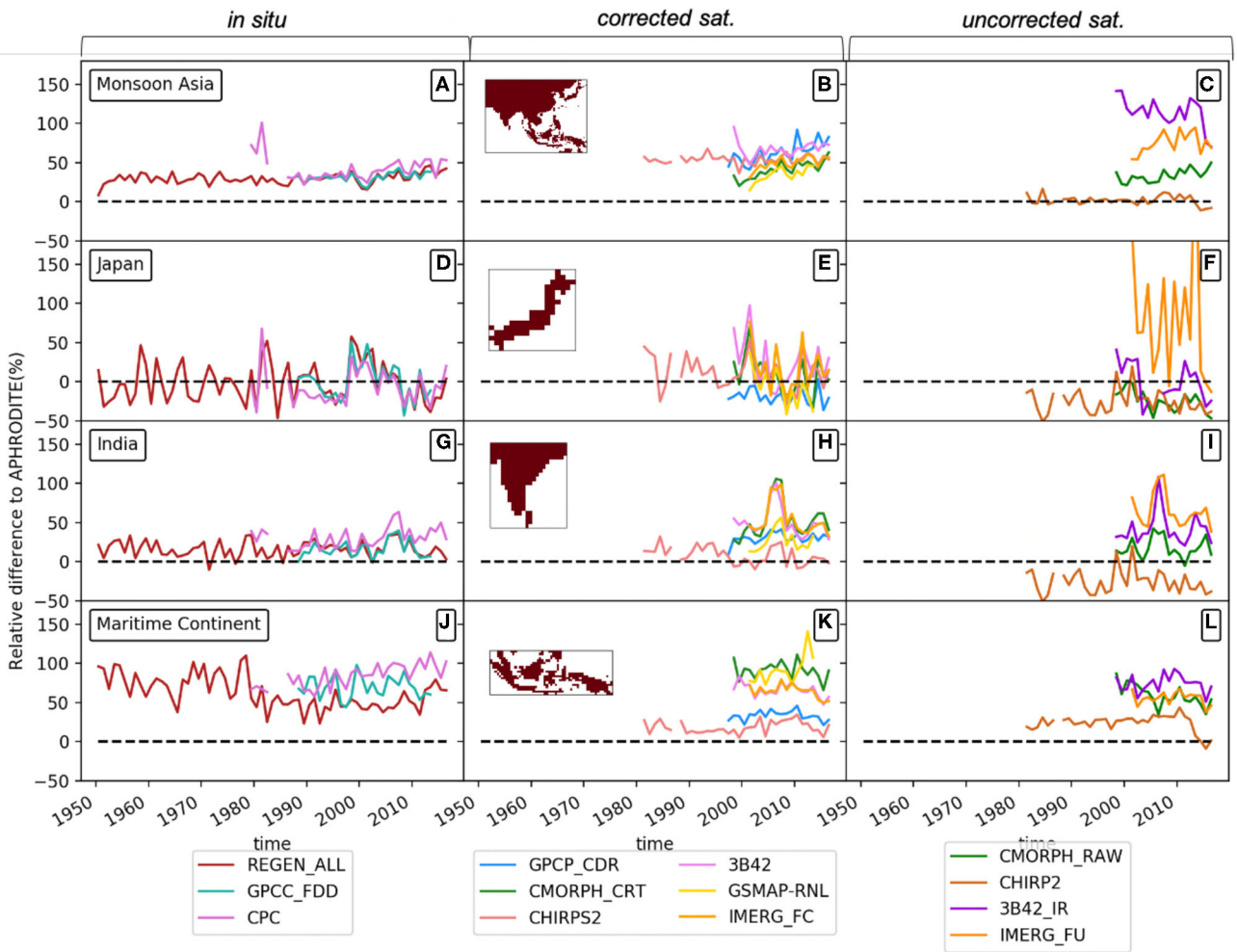

FIGURE 4 | Time series of regionally averaged relative differences (in %) for the annual wettest day (Rx1day) for each considered product compared to the baseline period (1961–1990) of APHRODITE. Products are clustered into three groups: *in situ* (the left column), corrected satellite (the middle column), and uncorrected satellite (the right column). Four regions are considered: **(A–C)** Monsoon Asia (60°E-150°E, 15°S-50°N), **(D–F)** Japan (129°E-146°E, 30°N-46°N), **(G–I)** India (70°E-92°E, 5°N-25°N), and **(J–L)** the Maritime Continent (95°E-150°E, 10°S-10°N). Regionally averaged Rx1day is calculated over the common area across all datasets (as shown by the inserted maps in the middle panel of each row).

consistency in terms of inter-annual variability for *in situ*-based products in estimating Rx1day over Japan (ranging from 0.51 to 0.71; **Table 3**). It is also worth noting that *in situ* data are generally closer to each other and temporally more consistent to APHRODITE over Japan compared to the whole Monsoon Asia region (**Figures 4A,D**). On the other hand, we find reduced consistency over the Maritime Continent where only a few gauges are available (temporal correlations among *in situ* products vary from 0.30 to 0.42), as well as larger differences to APHRODITE compared to that in other regions (**Figure 4J**). Interestingly, India, which is also a region of poor station density like the Maritime Continent, shows better agreement among *in situ* products with smaller inter-product spread (0.14 %, **Table 2**) compared with the Maritime Continent (0.25%, **Table 2**). Therefore, the station network alone does not account for all uncertainties in each dataset. Other factors like geography and climate can lead to these observational uncertainties. Surprisingly, all considered *in situ*-products show negative temporal correlations with APHRODITE over India (ranging from −0.26 to −0.03), revealing some important issues in the data that will be further discussed later.

Next, we focus on the representation of Rx1day among the satellite products, with and without a correction to rain gauges (middle and right columns of **Figure 4**). Compared to the *in situ* inter-product spread described above, the inter-product spread for satellite data is generally higher. This is particularly true for uncorrected products and applies to all four regions investigated here. In addition, we generally find a similar bias to APHRODITE for satellite data compared to *in situ* data, with an overestimation of Rx1day over Monsoon Asia, the Maritime Continent and India (to a lesser extent) and estimates closer to APHRODITE over Japan. The inter-product spread in the uncorrected satellite cluster is the largest and relatively similar across all four regions (last column of **Figure 3**), with cov values between 16.35 and 21.18% (**Table 2**). The inter-product spread is reduced in the corrected satellite cluster compared to uncorrected products cluster and in particular over Monsoon Asia and Japan, with a reduction in cov values from 19.35 to 9.25% and from 21.18 to 16.32%, respectively (**Table 2**), whereas little difference is seen over the Maritime Continent. Interestingly, higher temporal correlation is found for the regional average of Rx1day between APHRODITE and CHIRPS2 compared to its uncorrected counterpart CHIRP2 for all four regions and in particular for the Maritime Continent and India (**Table 3**). However, we find low temporal correlations (ranging from 0.12 to 0.49, **Table 3**) over the Maritime Continent, which highlights inconsistencies in inter-annual variability across different precipitation products and strongly limits the confidence that can be associated with these observational datasets over this region when assessing the annual daily precipitation maxima. It is also striking to see that temporal correlations over India are not only very low but also negative for satellite products. This is a major problem and again demonstrates that observations over India should be considered with care, in particular for studies focusing on inter-annual variations. This can partly be explained by the instability of the total number of observational stations in all considered *in situ*-based products (APHRODITE, REGEN_ALL, GPCC_FDD, and CPC) over India (**Supplementary Figure 10B**). For example, India experienced a major variation in available station coverage using in APHRODITE with a sudden increase during 1998–1999 and decrease during 2004–2006 (**Supplementary Figures 11B–D**).

TABLE 4 | Trends per decade in the annual Rx1day (mm/decades and %/decade) for each product that has data covering the period of 1988–2013.

Dataset name	Monsoon Asia	Japan	India Continent	Maritime
APHRODITE	1.12 (2.8%)	3.06 (3%)	−3.1 (−5.0%)	6.01 (12%)
REGEN_ALL	0.71 (1.8%)	−6.03 (−6%)	−1.67 (−2.7%)	1.30 (2.6%)
GPCC_FDD	0.71 (1.8%)	−2.35 (−2.2%)	0.82 (1.3%)	−1.23 (−2.7%)
CPC	2.93 (7.3%)	3.1 (3.1%)	6.07 (9.6%)	6.20 (12.4%)
CHIRPS2	0.61 (1.5%)	0.61 (0.6%)	−2.40 (−3.8%)	3.15 (6.3%)
CHIRP	0.08 (0.2%)	0.08 (0.08%)	−0.67 (−0.5%)	1.31 (2.6%)

Products are selected if they have <2 years of missing values during this period. Trends are calculated using Sen slope estimation and significant test at the 5% level using Mann-Kendall test (see section precipitation extremes). Dark (light) background colors indicate significant (non-significant) trends, with blue referring to an increase and orange to a decrease in Rx1day. Note that trends are calculated over the common area across all considered datasets for each sub-region (see inserted maps in ***Figure 3****).*

The time series (**Figure 4**) also indicate there might be trends over the observational record in some products. We further quantify whether temporal trends are present in the regionally averaged Rx1day values and how robust these trends are across the different observational products for Monsoon Asia and its sub-regions. We consider here only products having at least 25 years of data available between 1988 and 2013 (**Table 4**), which covers the same time period as for the temporal correlations in **Table 3** and gives us a sufficient record length for analysis. We find coherent (positive) trends across all products over the entire Monsoon Asia although only GPCC_FDD and CPC show a significant intensification, but with quite different magnitudes (0.71 mm/decade and 2.93 mm/decade, i.e., 1.8%/decade and 7.3%/decade, respectively). Focusing on the three selected sub-regions of Monsoon Asia, we find that four products out of six agree on a significant increase in the annual wettest day over the Maritime Continent, but the magnitude of their trend varies quite substantially (from 1.31 to 6.20 mm/decade, i.e., 2.6%/decade to 12.4%/decade). There is no consensus between observational products over India, with only APHRODITE and CPC showing significant trends yet of opposite signs (−3.10 and 6.07 mm/decade, i.e., −5.0%/decade and 9.6%/decade, respectively). Japan has non-significant trends in all products.

Corrected Satellite and Uncorrected Satellite Comparison

Our results show substantial differences in how observational datasets represent Rx1day. It is clear that how well products agree depends on the region of interest, and in particular the agreement between the corrected and uncorrected satellite product estimates. Therefore, we further focus on how the satellite data with and without correction to rain gauges compare to each other for the representation of climatological Rx1day

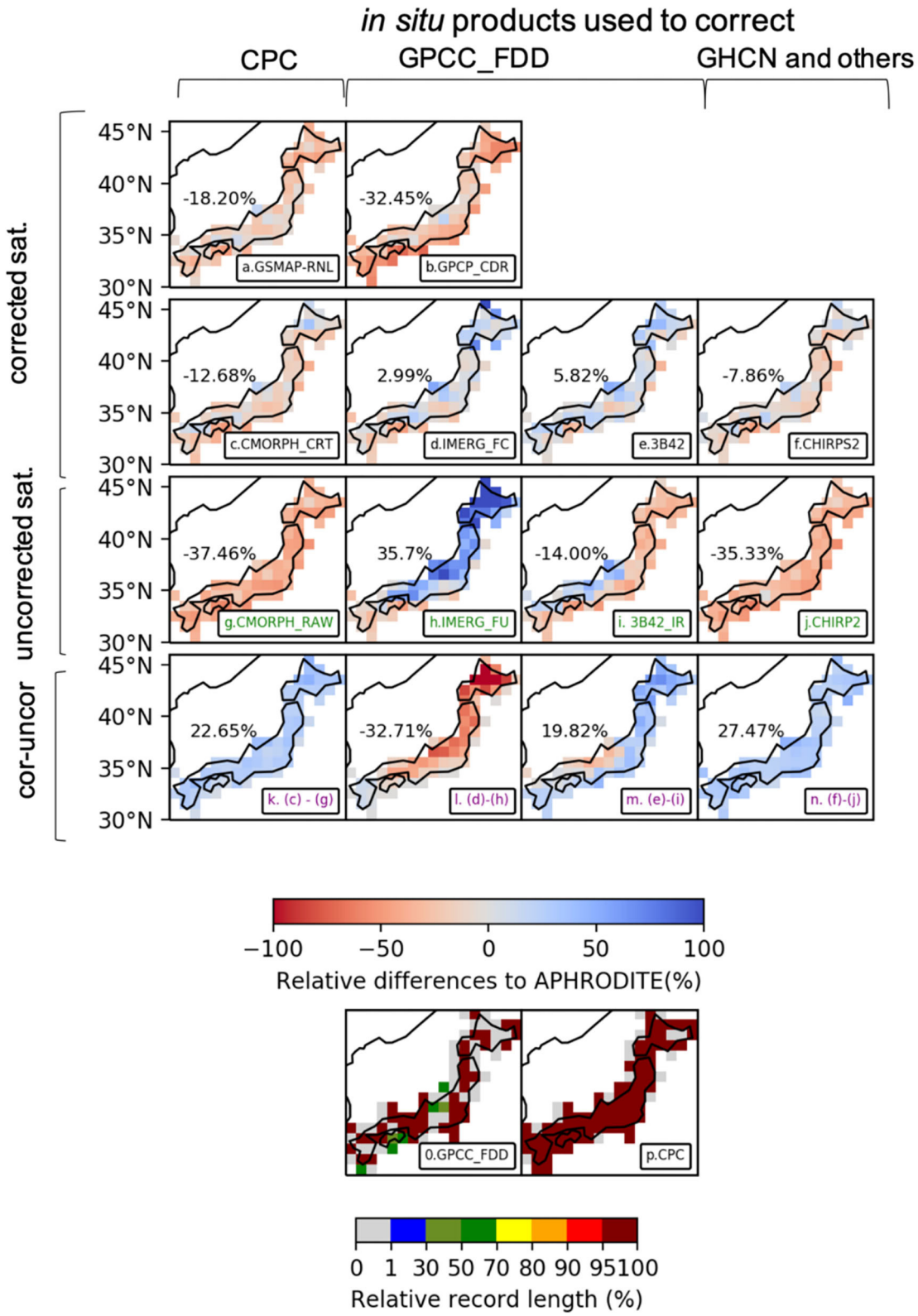

FIGURE 5 | Upper panel: relative difference to APHRODITE (in %) of the climatological (over the period of 2001–2013) annual wettest day (Rx1day) for corrected satellite products (black labels, two upper rows): **(a)** GSMAP_RNL, **(b)** GPCP_CDR, **(c)** CMORPH_CRT, **(d)** IMERG_FC, **(e)** 3B42, **(f)** CHIRPS2; uncorrected satellite

(Continued)

FIGURE 5 | products (green label, the third row): **(g)** CMORPH_RAW, **(h)** IMERG_FU, **(i)** 3B42_IR, **(j)** CHIRP2; and the differences between the corrected and uncorrected products **(k–n)**. The number inserted on each panel indicates the regional average of these relative differences. The *in situ* products that satellite products used to correct are also mentioned at the top of the figure. The last two panels also show the percentage of data available for each grid cell during the 2001–2013 period in these *in situ*-based datasets [**(o)** GPCC_FDD, **(p)** CPC] used for correction of satellite products.

(over the 2001–2013 period) over the three sub-regions of Monsoon Asia (**Figures 5**–**7**).

Figures 5a–j show the spatial map of relative differences (to APHRODITE) in the climatology of Rx1day for corrected satellite products (**Figures 5a–f**) and uncorrected versions (**Figures 5g–j**) over Japan. The difference between pairs of datasets from the same family are also presented (**Figures 5k–n**). Three uncorrected satellite products (CMORPH_RAW, 3B42_IR, and CHIRP2; **Figures 5g,i,j**) tend to be drier than APHRODITE whereas IMERG_FU is generally wetter (**Figure 5h**). The corrected satellite versions of these four family products usually show reduced bias spatially (**Figures 5c–f**), in particular for IMERG products (as seen in **Figures 5e,f**). Note that the direction of correction among product families is different (**Figures 5k–n**). Hence, a strong correction is applied over Japan that shifts the satellite products closer to APHRODITE (and therefore to each other). This highlights that the dense rain gauge network presents other benefits than simply a better estimation of precipitation extremes in *in situ*-based datasets as it also leads to improvement (i.e., closer to APHRODITE) in Rx1day estimates in satellite products when a correction to *in situ* data is applied. **Figures 5o,p** indicates the percentage of station data available during the 2001–2013 period for each grid box in the *in situ* datasets used to correct these satellite products. Stations from CPC cover the whole of Japan with almost all station information being fully available (nearly 100%) during the considered period. On the other hand, station networks from GPCC_FDD only partly cover Japan and in which the length of available data for some grid boxes is <50%, However, it is interesting that the imprint of underlying station networks among corrected satellite-products (as mentioned in section climatology of the mean daily precipitation) does not appear to have a strong impact over Japan. This is likely because there are enough stations in the underlying rain gauge networks over Japan to produce corrections that shift the satellite products closer to APHRODITE.

Figure 6 focuses on India which covers a large area of land only partially covered by *in situ* stations. Overall, both satellite products with and without rain gauge correction tend to overestimate climatological Rx1day compared to APHRODITE, over most areas of India except a thin band on the west coast. This excludes CHIRPS2 and CHIRP2 that are closer to APHRODITE (**Figures 6f,j**). Contrary to the results for Japan, the correction to rain gauges has smaller impacts (**Figures 6k–n**) and each pair of corrected and uncorrected products presents a relatively similar distribution of climatological Rx1day, except over the western coast of India where the correction to *in situ* data makes precipitation extremes slightly closer to APHRODITE. This interesting feature can be probably explained by the fact that over the west coast of India *in situ* stations used for the correction generally have a nearly complete temporal coverage (i.e., greater than 95%) during 2001–2013 period (**Figures 6o–p**). Meanwhile, in other parts of India, the percentage of data available through time in each grid box varies (from 1 to 70%). Another possible explanation might be related to lower station density over India compared with that over Japan. This seems to limit the improvement in the representation of Rx1day from the correction of satellite products to *in situ* data.

Finally, we focus on the Maritime Continent in **Figure 7**. Conclusions similar to those drawn for India can be made for the Maritime Continent. Generally, both satellite products with and without correction to rain gauges are much wetter compared with APHRODITE. In addition, almost all products are fairly similar to each other (both spatially and in their regional averages; **Figures 7a–j**) in terms of representing Rx1day. Some notable exceptions include the highest elevation regions of New Guinea and the island of Sulawesi, which both have positive differences in some datasets (GSMAP-RNL and CMORPH_CRT; **Figures 7a,c**) and negative in others. Comparing both corrected and uncorrected satellite clusters reveals some potential issues related to the rain gauge networks that satellite products use to correct their precipitation estimation. The issues might be related to the lack of stations across different rain gauge networks and also emphasize the dubious quality of available stations over the Maritime Continent.

Generally, the gauge-based correction applied to satellite estimates acts differently from region to region and product to product, and we show here that this also depends on the station network utilized in addition to the method itself (for instance some products have stronger corrections than others even when using the same underlying network). We find a clear distinction in the impact of the correction between regions of high and sparse station density, for instance over Japan where there are a lot of stations with good temporal coverage, it brings satellite estimates closer to APHRODITE and reduces inter-product spread. Over regions poorly sampled by stations, how well the correction to *in situ* acts depends on the length of record available and this can lead to regional contrasts but generally we find minor improvements in the representation of climatological Rx1day between the corrected and uncorrected version of the satellite products over such regions, which implies that not only does poor station coverage affect the representation of precipitation extremes in *in situ*-based datasets but it also has clear impact in most satellite products that rely on ground networks.

DISCUSSION

We find that the estimation of Rx1day is generally wetter in *in situ*-based products compared to APHRODITE. This wet

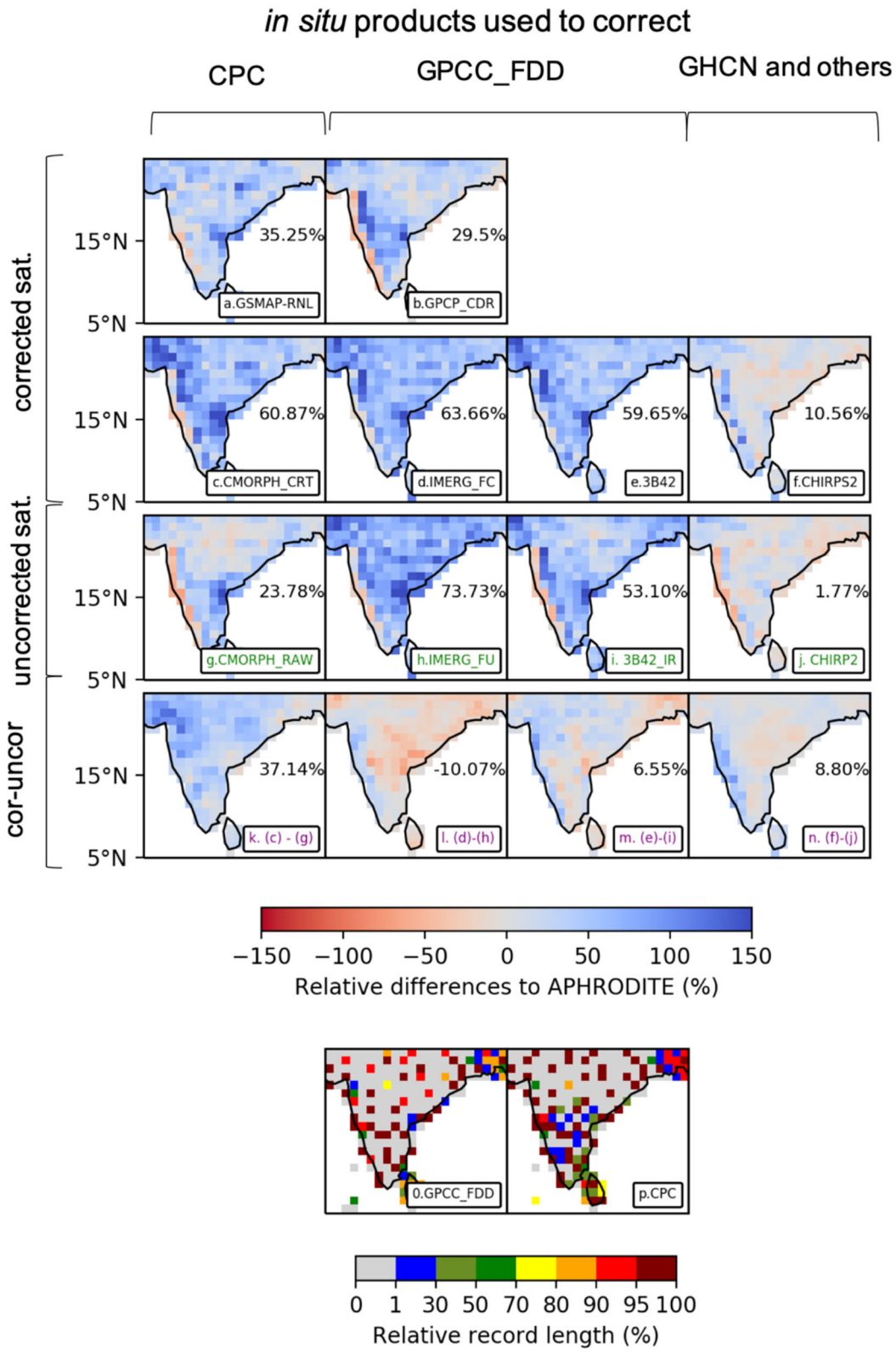

FIGURE 6 | Same as **Figure 5** for India. Upper panel: relative difference to APHRODITE (in %) of the climatological (over the period of 2001–2013) annual wettest day (Rx1day) for corrected satellite products (black labels, two upper rows): **(a)** GSMAP_RNL, **(b)** GPCP_CDR, **(c)** CMORPH_CRT, **(d)** IMERG_FC, **(e)** 3B42, **(f)**

(Continued)

FIGURE 6 | CHIRPS2; uncorrected satellite products (green label, the third row): **(g)** CMORPH_RAW, **(h)** IMERG_FU, **(i)** 3B42_IR, **(j)** CHIRP2; and the differences between the corrected and uncorrected products **(k–n)**. The number inserted on each panel indicates the regional average of these relative differences. The *in situ* products that satellite products used to correct are also mentioned at the top of the figure. The last two panels also show the percentage of data available for each grid cell during the 2001–2013 period in these *in situ*-based datasets [**(o)** GPCC_FDD, **(p)** CPC] used for correction of satellite products.

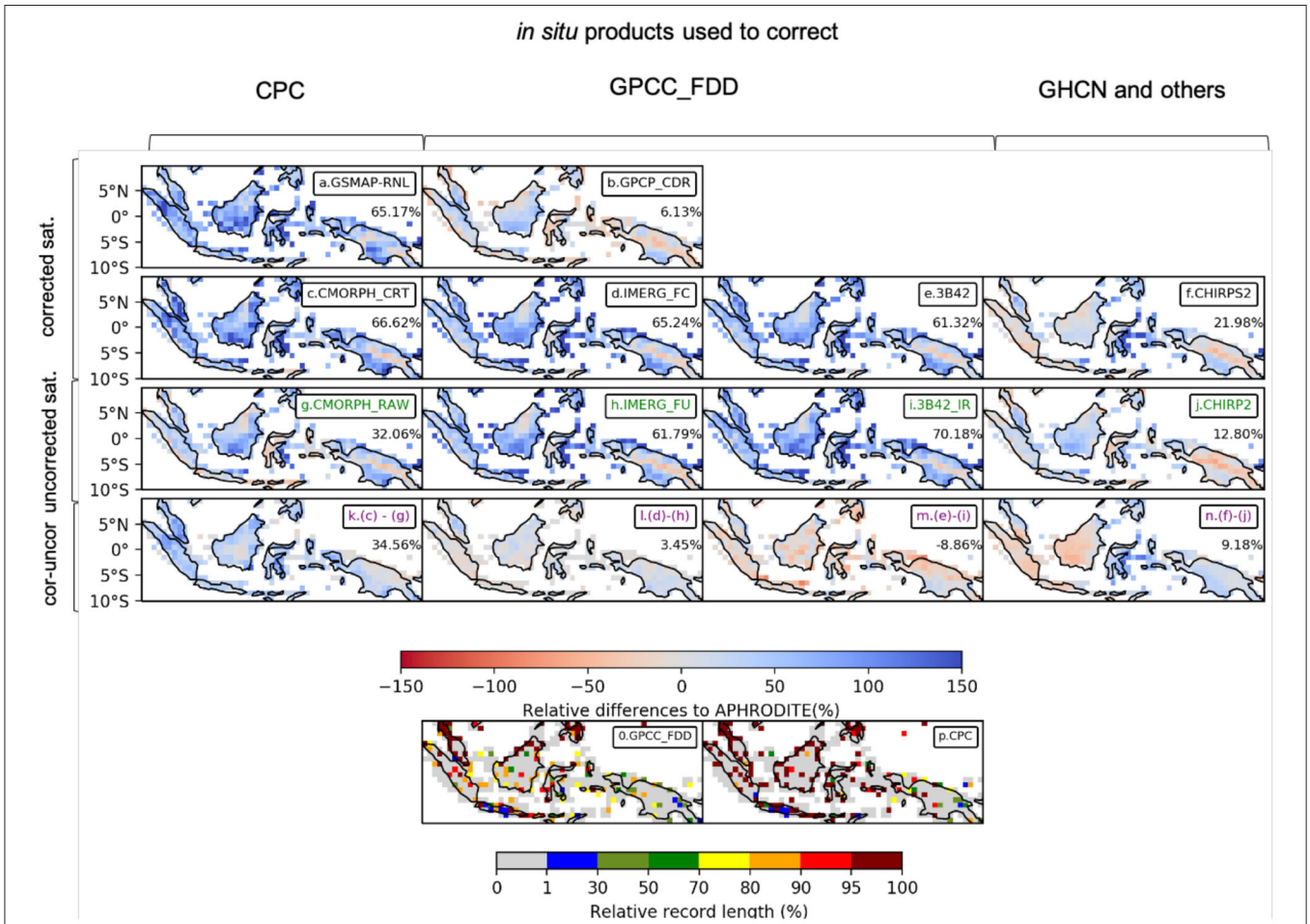

FIGURE 7 | Same as **Figure 5** for the Maritime Continent. Upper panel: relative difference to APHRODITE (in %) of the climatological (over the period of 2001–2013) annual wettest day (Rx1day) for corrected satellite products (black labels, two upper rows): **(a)** GSMAP_RNL, **(b)** GPCP_CDR, **(c)** CMORPH_CRT, **(d)** IMERG_FC, **(e)** 3B42, **(f)** CHIRPS2; uncorrected satellite products (green label, the third row): **(g)** CMORPH_RAW, **(h)** IMERG_FU, **(i)** 3B42_IR, **(j)** CHIRP2; and the differences between the corrected and uncorrected products **(k–n)**. The number inserted on each panel indicates the regional average of these relative differences. The *in situ* products that satellite products used to correct are also mentioned at the top of the figure. The last two panels also show the percentage of data available for each grid cell during the 2001–2013 period in these *in situ*-based datasets [**(o)** GPCC_FDD, **(p)** CPC] used for correction of satellite products.

"bias" is also apparent in other precipitation indices [e.g., Rx5day (**Supplementary Figure 3**), SDII (**Supplementary Figure 4**), PRCPTOT (**Supplementary Figure 5**), and R10mm (**Supplementary Figure 6**)]. One source of these differences is that APHRODITE contains substantially more rain gauges than any other *in situ*-based product (**Figure 2i**). This could be related to the "central limit theorem," which explains that averaging more observations in each grid cell can lead to lower variance weighted averages of original station values. For instance, three considered *in situ*-based products have a wetter bias compared with APHRODITE over Thailand which (**Figure 2a** compared with **Figures 2b–d**). However, this "central limit theorem" cannot be applied over Japan, Korea, and Pakistan with being slightly drier in other products compared to APHRODITE (**Supplementary Figure 2**). The potential reason might be related to a very high-density station network over Japan and Korea in all *in situ* dataset. Other possible sources of difference could be related to the quality control procedures and interpolation method applied in APHRODITE [see Yatagai et al. (2012) for details]. Particularly, Yatagai et al. (2012) recognized that there are some features in APHRODITE that don't exist in other products such as narrower rainbands. The authors

show that this is a result of the Mountain Mapping technique [see Schaake et al. (2004) for more details] they employed and which allows better estimates of precipitation averages in the merging algorithm over data-sparse areas. This technique avoids the false penetration of precipitation from wet areas into adjacent and relatively drier areas, which can hence induce narrower rainbands in APHRODITE than in other datasets. The Maritime continent combining both dry and wet regions illustrates this nicely with generally much wetter estimates in all other datasets compared to APHRODITE, and in particular over the mountainous regions of Indonesia and Malaysia (**Supplementary Figures 2F–H**).

We note that CPC has a drier bias compared with APHRODITE in regions with little or no stations and that such regions coincide well with country borders (e.g., Myanmar, Pakistan) (**Figure 2d**). According to Xie (2008) and Chen et al. (2008) the dry bias can also potentially be explained by the fact that GTS values are used everywhere outside of China and missing values can sometimes be reported incorrectly as zero precipitation.

Our results indicate the limitations in estimating precipitation extremes in gridded precipitation products, especially in *in situ-based* products over poorly sampled regions with few (e.g., the Maritime Continent, Myanmar) or no stations (e.g., the Tibetan Plateau). These *in situ* products have been used in many model evaluations studies as the observational reference ("ground truth"). Therefore, our recommendation is to carefully apply these datasets, notably over data-sparse regions like the Maritime Continent. We find better agreement among sole gauge-based products over high station density (i.e., >10 station per grid) regions like Japan. These results are perhaps not surprising and are consistent with the findings of Kim et al. (2018), although we observe large differences in the quantity of observational stations over Japan (**Supplementary Figure 8A**) in APHRODITE compared to other considered *in situ*-based products. That makes us question whether there is a minimum number of stations required to obtain good agreement in the representation of rainfall extremes.

The regional high-resolution datasets (e.g., IMD for India and SACA&D for the Maritime Continent) might provide a better precipitation information than APHRODITTE as they have higher resolution and include many more stations compared to APHRODITE. Therefore, additional comparison between all the products from **Table 1** and local datasets are conducted to get better views in terms of the uncertainties among different observational products regrading to various references datasets. **Supplementary Figures 12, 13** show the differences between IMD and SACA&D and other observation products respectively. All products are drier than IMD in their estimates of Rx1day. This "drier bias" is consistent with the spatial pattern found over Japan and Korea, which can be explained by a very dense station density in IMD compared with other products. The pattern over the Maritime Continent for SACA&D is similar to APHRODITE, with all products generally wetter than SACA&D. Although different bias patterns are observed when adding these two local high-resolution datasets, our main conclusions remain the same in that there is high consistency among *in situ*-based products irrespective of the station density. Satellite products with gauge-corrections show better agreement with each other in estimating Rx1day than those that are uncorrected.

Due to insufficient observational evidence and/or spatially varying trends, the Fifth Assessment Report (AR5) of IPCC (2013) stated only *low to medium confidence* in the trends in extreme precipitation over various regions of Asia (see IPCC AR5 Table 2.13). Since AR5, more attempts have been made to examine changes in different aspects of precipitation extremes over Asian countries. To date, significant decadal trends in precipitation extremes have been identified over India (Prakash et al., 2015; Rana et al., 2015), Japan (Fujibe et al., 2006; Duan et al., 2015), but not over Southeast Asia [including the Maritime Continent e.g., Kim et al. (2018)]. However, all these studies have been limited either in the number of observational products they used and/or the time period they covered [e.g., seven datasets used and 10 years considered in Kim et al. (2018)], or the different definitions of extreme precipitation used. Here, we have considered 13 observational datasets that cover 25 years (1988–2013) for the estimation of observed trends in the annual 1-day precipitation maxima across the different considered sub-regions. There is low confidence in the presence of a trend in Rx1day over India during 1988–2013 because of a lack of agreement between products, which is likely linked to a lack of *in situ* data. This inconsistency still exists when considering the IMD dataset (**Supplementary Table 5**). Note that there have been significant increasing trends in frequency and intensity of extreme heavy rainfall over central and southern India since 1950 where regional climates are controlled by the Asian monsoon system (Krishnan et al., 2015; Roxy et al., 2017; Venkata Rao et al., 2020) (i.e., the core monsoon zones). Interestingly, despite a poor station coverage over the Maritime Continent, we find significant positive trends in four out of six datasets. On the other hand, Japan is a region of very high station density and yet we do not find significant trends in any of the considered datasets. Other studies found a significant increasing trend in Rx1day over Japan (Fujibe et al., 2006; Duan et al., 2015) but in these cases a much longer period was studied (1901–2004 and 1901–2012, respectively) which might explain these differences. Further results based on different extreme indices [e.g., Rx5day (**Supplementary Table 1**), SDII (**Supplementary Table 2**), PRCPTOT (**Supplementary Table 3**), and R10mm (**Supplementary Table 4**)] show little differences in terms of trends depending on regions and indices over 1988–2013. In particular, we find significant trends in SDII over Japan with three datasets including: REGEN_ALL, GPCC_FDD and CHIRPS but opposite signs (−0.82 mm/decade, 0.67 mm/decade, and −0.57 mm/decade respectively; **Supplementary Table 2**). On the other hand, coherent positive significant trends in Rx5day, SDII, PRCPTOT, and R10mm are found over India in at least two out of five considered products (the third column; **Supplementary Tables 1–4**). Similar results on decadal trends are obtained for different extreme indices over the Maritime Continent.

Comparing inter-annual variability in different products, we highlighted the reliability of *in situ* products over Monsoon Asia. In addition, we also found high consistency over

dense-station areas like Japan, whereas very low temporal correlation was found over India in all considered products. This is likely due to the instabilities in time-varying station networks in APHRODITE, for example over India during 1988–2013 (**Supplementary Figures 8B, 9**). Note that a substantial international "reporting crisis" has been recorded in many regions of the world, referring to either a substantial decrease in observations or major variations in station networks over time (Funk et al., 2015; Alexander et al., 2019). These temporal changes in network distribution can lead to very different climatologies from year to year and hence inconsistencies in inter-annual variability, simply because of differences in spatial coverage from year to year.

Further issues in how satellite products ingest data, use algorithms to bias adjust or merge input data together to produce final products (see **Table 1**) also add to the uncertainties in our results. This could lead to the uncertainties we see in the representation of extremes, especially among the corrected and uncorrected satellite datasets over sub regions, where we found the performance of satellite correction is different between data-sparse (e.g., Indonesia and India) and high station density regions (e.g., Japan). Understanding the method behind the creation of a rainfall product is the best way to know how robust it is and to which extent one can trust it. Some diagrams from Le Coz and Van De Giesen (2020)-the review on how products are developed can facilitate such understanding. It also acknowledged that the "reporting crisis" mentioned above might also affect products differently. For example, satellite estimates that start with lower bias are more resilient to changes in the gauge networks.

We do not have all of the required information to be able to better quantify the reasons behind the uncertainties among precipitation products and to reduce these uncertainties because of the inhomogeneities in precipitation records and the lack of station information from regional products like IMD and SACA&D. Efforts still need to be pursued on how to reduce the uncertainties in observed precipitation extremes. However, this study does indicate some inherent types of uncertainties in datasets through the employed station network and applied satellite correction over Monsoon Asia. The idea of this research is not to recommend any single observational dataset but rather to highlight the commonalities and differences among different products and product clusters when they are compared within a common framework. This can be used to better inform research activities like model evaluation, monitoring, and projections etc. Previous studies suggested that there is no single best observational dataset for global assessment of annual wettest day precipitation (Alexander et al., 2020; Bador et al., 2020). However, as we focus on a whole of Monsoon Asia regional scale study, APHRODITE could be considered as being better than any other existing global datasets because this regional data product often has access to much more data than any of its global dataset counterparts. However, if we consider smaller sub-regions, most develop their own high-resolution datasets which should generally be considered as the first choice for evaluation purposes since they employ the most rain gauges and the most effort has gone into their development for applications in the specific region.

CONCLUSIONS

This study focused on the robustness of 1-day precipitation annual maxima (Rx1day) over Monsoon Asia by comparing the climatological value of Rx1day across multiple observational precipitation products and exploring the influence of the underlying station density and the correction methods that satellites use to estimate precipitation. To explore how different data sources represented observed precipitation extremes, all considered products were clustered into three groups based on their data sources: *in situ*, corrected satellite and uncorrected satellite. We investigated their consistency in the representation of precipitation extremes across the multiple products principally through their spatial and temporal distribution of Rx1day, the inter-product spread, temporal correlation and trends over the 1988–2013 period. We further investigated three sub-regions of particular interest: Japan (a region of high station density and strong spatial contrast), India (a large region covered by a sparse station network with orographic contrasts), and the Maritime Continent (a poorly sampled region with strong coastal complexity).

We find that there are broad similarities in the spatial and temporal distributions among *in situ*-based products compared to satellite products (with or without a correction to *in situ*). Better general agreement in climatology and less inter-product spread and higher temporal correlation is found for satellite estimates with correction to rain gauges than for the uncorrected versions of the satellite products. These findings are generally true over Monsoon Asia and are consistent with results from quasi-global studies [e.g., Bador et al. (2020)].

These general results also contain strong sub-regional differences, and we show in this study that these differences can partly be explained by the quantity and quality of the rain gauges over the considered region. First, focusing on *in situ* datasets only, we find a better agreement among *in situ*-based products over dense data regions like Japan. Conversely, regions with no stations (e.g., Myanmar, Tibetan Plateau) or sparse station networks (e.g., the Maritime Continent) stood out over other regions as having the largest differences in precipitation extreme estimates. Secondly, over the data dense region of Japan, corrected satellite products show similar spatial and temporal patterns between themselves and compared to the *in situ*-based products that are used to correct them. In addition, the inter-product spread among corrected satellite estimates is closer to the spread for *in situ*-based products than for their uncorrected counterparts despite the larger number of satellite products. On the contrary, over poorly sampled regions (e.g., India and the Maritime Continent), both uncorrected and corrected satellite clusters are similar to each other and have much larger spread compared with *in situ*-based products. In addition, we also showed that the length of record available at each station can also affect the satellite correction over these poorly sampled regions.

Clearly, the quantity and quality of the station network have implications for the reliability of the *in situ*-based products derived and also the satellite products that use a correction to *in situ* data over Monsoon Asia. We showed that satellite products can have the spatial imprints of the underlying *in situ* data.

Therefore, they cannot be considered as the "perfect solution" to replace the lack of *in situ* data over data-sparse regions.

Finally, and based on our results, we would like to make some recommendations for data selection for the study of the annual wettest day over the three sub-regions studied here. First, we found large observational uncertainties among uncorrected satellite products over all considered regions, so preference should be given to the corrected version over the uncorrected version of each product family. There might potentially be areas where the uncorrected products could be better than their corrected counterparts e.g., where stations are not representative of the region and therefore the correction to *in situ* does not lead to an improvement for precipitation extreme estimates. However, such conclusions did not arise from our analyses and therefore we only consider the satellite products from the corrected cluster in addition to *in situ*-based products for some recommendations that we detail for each region individually:

Japan has a dense network of stations with good completeness in terms of length of record in APHRODITE. We recommend the selection of *in situ*-based observations as they tend to have very similar spatial and temporal patterns. Furthermore, satellite products can also be recommended as they show good agreement with *in situ*-based products and slightly larger inter-product spread than *in situ*-based products. However, it should be noted that there is some inconsistency in long-term extreme precipitation trends among *in situ*-based products.

Over India, we recommend using *in situ*-based datasets with great care. Indeed, this large region suffers from a substantial reduction in the station density and some inconsistencies in its station network over the last few decades. This leads to differences among *in situ* products for both spatial and temporal patterns of precipitation extremes, and also affects trend estimates that cannot be extracted with confidence. This might also have a negative impact on satellite datasets that also show large inter-product spread over India. Therefore, we suggest a careful selection of both *in situ* and satellite products over this region. Note that India does have its own high-resolution gridded datasets which might provide better local precipitation extremes estimates.

The Maritime Continent, which features highly complex terrain, is sampled by only a few rain gauges for which data quality is also questionable. This causes substantial differences in climatology and inconsistency in inter-annual variability among *in situ* products. There is also a little satellite correction applied over the Maritime Continent due to data spare networks. We recommend users are knowledgeable of data issues when choosing *in situ* products.

Our research focuses on uncertainties among different observational products in estimating precipitation extremes by understanding the impact of the underlying station networks and satellite corrections. It is important to acknowledge that these factors do not account for the full range of uncertainties in each dataset. Other factors like geography and climate might also contribute. Therefore, we recommend understanding how each dataset is produced in order to make the best decision about what products are fit for purpose in estimating precipitation extremes for individual regions.

DATA AVAILABILITY STATEMENT

All datasets generated for this study are included in the article/**Supplementary Material**.

AUTHOR CONTRIBUTIONS

All authors listed have made a substantial, direct and intellectual contribution to the work, and approved it for publication.

FUNDING

P-LN, LA, and MB are supported by the Australian Research Council (ARC) grant DP160103439. P-LN and TL are supported by the ARC grant CE170100023. CF has been supported by the US Geological Survey Drivers of Drought project and NASA GPM grant 80NSSC19K0686. Information about the datasets provided by FROGS are given here https://data.ipsl.fr/ and the data are freely available from ftp://ftp.climserv.ipsl.polytechnique.fr/FROGs/. Indices were calculated using ClimPACTv2 software (https://climpact-sci.org/get-started/). All analyses and graphics have been performed using Climate Data Operator (CDO) and Python.

SUPPLEMENTARY MATERIAL

The Supplementary Material for this article can be found online at: https://www.frontiersin.org/articles/10.3389/fclim.2020.578785/full#supplementary-material

REFERENCES

Alexander, L. V., Bador, M., Roca, R., Contractor, S., Donat, M., and Nguyen, P. L. (2020). Intercomparison of annual precipitation indices and extremes over global land areas from *in situ*, space-based and reanalysis products. *Environ. Res. Lett.* 15:055002. doi: 10.1088/1748-9326/ab79e2

Alexander, L. V., Fowler, H. J., Bador, M., Behrangi, A., Donat, M. G., Dunn, R., et al. (2019). On the use of indices to study extreme precipitation on sub-daily and daily timescales. *Environ. Res. Lett.* 14:125008. doi: 10.1088/1748-9326/ab51b6

Bador, M., Alexander, L. V., Contractor, S., and Roca, R. (2020). Diverse estimates of annual maxima daily precipitation in 22 state-of-the-art quasi-global land observation datasets. *Environ. Res. Lett.* 15, 1–10. doi: 10.1088/1748-9326/ab6a22

Beck, H. E., Pan, M., Roy, T., Weedon, G. P., Pappenberger, F., Van Dijk, A. I. J. M., et al. (2019). Daily evaluation of 26 precipitation datasets using Stage-IV gauge-radar data for the CONUS. *Hydrol. Earth Syst. Sci.* 23, 207–224. doi: 10.5194/hess-23-207-2019

Bosilovich, M., Robertson, F., and Chen, J. (2011). Global energy and water budgets in MERRA. *J. Clim.* 24, 5721–5739. doi: 10.1175/2011JCLI4175.1

Chen, M., Shi, W., Xie, P., Silva, V. B. S., Kousky, V. E., Wayne Higgins, R., et al. (2008). Assessing objective techniques for gauge-based analyses of global daily precipitation. *J. Geophys. Res. Atmospheres* 113:9132. doi: 10.1029/2007JD009132

Contractor, S., Alexander, L. V., Donat, M. G., and Herold, N. (2015). How well do gridded datasets of observed daily precipitation compare over Australia? *Adv. Meteorol.* 2015, 1–15. doi: 10.1155/2015/325718

Contractor, S., Donat, M. G., Alexander, L. V., Ziese, M., Meyer-Christoffer, A., Schneider, U., et al. (2020). Rainfall Estimates on a Gridded Network (REGEN)—a global land-based gridded dataset of daily precipitation from 1950 to 2016. *Hydrol. Earth Syst. Sci.* 24, 919–943. doi: 10.5194/hess-24-919-2020

Dee, D. P., Uppala, S. M., Simmons, A. J., Berrisford, P., Poli, P., Kobayashi, S., et al. (2011). The ERA-Interim reanalysis: configuration and performance of the data assimilation system. *Quart. J. Roy. Meteorol. Soc.* 137, 553–597. doi: 10.1002/qj.828

Duan, W., He, B., Takara, K., Luo, P., Hu, M., Alias, N. E., et al. (2015). Changes of precipitation amounts and extremes over Japan between 1901 and 2012 and their connection to climate indices. *Clim. Dyn.* 45, 2273–2292. doi: 10.1007/s00382-015-2778-8

Fujibe, F., Yamazaki, N., and Kobayashi, K. (2006). Long-term changes of heavy precipitation and dry weather in Japan (1901–2004). *J. Meteorol. Soc. Japan* 84, 1033–1046. doi: 10.2151/jmsj.84.1033

Funk, C., Peterson, P., Landsfeld, M., Pedreros, D., Verdin, J., Shukla, S., et al. (2015). The climate hazards infrared precipitation with stations—a new environmental record for monitoring extremes. *Sci. Data* 2:150066. doi: 10.1038/sdata.2015.66

Herold, N., Alexander, L. V., Donat, M. G., Contractor, S., and Becker, A. (2016a). How much does it rain over land? *Geophys. Res. Lett.* 43, 341–348. doi: 10.1002/2015GL066615

Herold, N., Behrangi, A., and Alexander, L. (2016b). Large uncertainties in observed daily precipitation extremes over land: uncertainties in precipitation extremes. *J. Geophys. Res. Atmospheres* 122, 668–681. doi: 10.1002/2016JD025842

Hijioka, Y., Lin, E., Pereira, J. J., Corlett, R. T., Cui, X., Insarov, G. E., et al. (2014). "Asia," in *Climate Change 2014: Impacts, Adaptation, and Vulnerability. Part B: Regional Aspects. Contribution of Working Group II to the Fifth Assessment Report of the Intergovernmental Panel on Climate Change,* eds *V.R. Barros, C.B. Field, D.J. Dokken, M.D. Mastrandrea, K.J. Mach, T.E. Bilir,* et al. *(United Kingdom and New York, NY: Cambridge University Press, Cambridge),* 1327–1370.

Huffman, G., Bolvin, D., Braithwaite, D., Hsu, K.-L., Joyce, R., Kidd, C., et al. (2020). "Integrated multi-satellite retrievals for the global precipitation measurement (gpm) mission (IMERG)". in *Satellite Precipitation Measurement. Advances in Global Change Research, Vol 67*. eds V. Levizzani, C. Kidd, D. Kirschbaum, C. Kummerow, K. Nakamura, F. Turk (Cham: Springer) 343–353. doi: 10.1007/978-3-030-24568-9_19

Huffman, G. J., Adler, R. F., Morrissey, M. M., Bolvin, D. T., Curtis, S., Joyce, R., et al. (2001). Global precipitation at one-degree daily resolution from multisatellite observations. *J. Hydrometeorol.* 2, 36–50. doi: 10.1175/1525-7541(2001)002<0036:GPAODD>2.0.CO;2

Huffman, G. J., Bolvin, D. T., Braithwaite, D., Hsu, K., Joyce, R., Kidd, C., et al. (2019). *NASA Global Precipitation Measurement (GPM) Integrated Multi-Satellite Retrievals for GPM (IMERG).* (Greenbelt, MD: NASA Algorithm Theoretical Basis Doc), 1–34.

Huffman, G. J., Bolvin, D. T., Nelkin, E. J., Wolff, D. B., Adler, R. F., Gu, G., et al. (2007). The TRMM multisatellite precipitation analysis (TMPA): quasi-global, multiyear, combined-sensor precipitation estimates at fine scales. *J. Hydrometeorol.* 8, 38–55. doi: 10.1175/JHM560.1

Iguchi, T., Kozu, T., Kwiatkowski, J., Meneghini, R., Awaka, J., and Okamoto, K. I. (2009). Uncertainties in the rain profiling algorithm for the TRMM precipitation radar. *J. Meteorol. Soc. Japan* 87A, 1–30. doi: 10.2151/jmsj.87A.1

Jones, P. W. (1999). First- and second-order conservative remapping schemes for grids in spherical coordinates. *Mon. Wea. Rev.* 127, 2204–2210. doi: 10.1175/1520-0493(1999)127<2204:FASOCR>2.0.CO;2

Jung, I. W., Bae, D.-H., and Kim, G. (2011). Recent trends of mean and extreme precipitation in Korea. *Int. J. Clim.* 31, 359–370. doi: 10.1002/joc.2068

Kendall (1975). *Rank Correlation Coefficient. (New York, NY: Springer New York)*, 278–281.

Kidd, C., Becker, A., Huffman, G. J., Muller, C. L., Joe, P., Skofronick-Jackson, G., et al. (2017). So, how much of the Earth's surface is covered by rain gauges? *Bull. Am. Meteorol. Soc.* 98, 69–78. doi: 10.1175/BAMS-D-14-00283.1

Kim, I.-W., Oh, J., Woo, S., and Kripalani, R. (2018). Evaluation of precipitation extremes over the Asian domain: observation and modelling studies. *Clim. Dyn.* 52, 1–26. doi: 10.1007/s00382-018-4193-4

Krishnan, R., Sabin, T. P., Vellore, R., Mujumdar, M., Sanjay, J., Goswami, B. N., et al. (2015). Deciphering the desiccation trend of the South Asian monsoon hydroclimate in a warming world. *Clim. Dyn.* 47, 1007–1027. doi: 10.1007/s00382-015-2886-5

Krishnan, R., T P, S., D. C, A., A, K., Sugi, M., Murakami, H., et al. (2012). Will the South Asian monsoon overturning circulation stabilize any further? *Clim. Dyn.* 40, 187–211. doi: 10.1007/s00382-012-1317-0

Le Coz, C., and Van De Giesen, N. (2020). Comparison of rainfall products over sub-Saharan Africa. *J. Hydrometeorol.* 21, 553–596. doi: 10.1175/JHM-D-18-0256.1

Legates, D. R., and Willmott, C. J. (1990). Mean seasonal and spatial variability in global surface air temperature. *Theor. Appl. Climatol.* 41, 11–21. doi: 10.1007/BF00866198

Lestari, S., King, A., Vincent, C., Karoly, D., and Protat, A. (2019). Seasonal dependence of rainfall extremes in and around Jakarta, Indonesia. *Weather Clim. Extremes* 24:100202. doi: 10.1016/j.wace.2019.100202

Liu, M., Xu, X., Sun, A., Wang, K.-L., Liu, W., and Zhang, X. (2014). Is southwestern China experiencing more frequent precipitation extremes? *Environ. Res. Lett.* 9:064002. doi: 10.1088/1748-9326/9/6/064002

Maidment, R. I., Allan, R. P., and Black, E. (2015). Recent observed and simulated changes in precipitation over Africa. *Geophys. Res. Lett.* 42, 8155–8164. doi: 10.1002/2015GL065765

Okamoto, K. I., Ushio, T., Iguchi, T., Takahashi, N., and Iwanami K. (2005). "The global satellite mapping of precipitation (GSMaP) project," in *Proceedings. 2005 IEEE International Geoscience and Remote Sensing Symposium, IGARSS '05* (Seoul: IEEE), 3414–3416. doi: 10.1109/IGARSS.2005.1526575

Pai, D., Sridhar, L., Rajeevan, M., Sreejith, O.P., Satbhai, N.S., and Mukhopadhyay, B. (2014). Development of a new high spatial resolution ($0.25^\circ \times 0.25^\circ$) long period (1901-2010) daily gridded rainfall data set over India and its comparison with existing data sets over the region. *Mausam* 65, 1–18.

Prakash, S., Mitra, A. K., Momin, I. M., Rajagopal, E. N., Basu, S., Collins, M., et al. (2015). Seasonal intercomparison of observational rainfall datasets over India during the southwest monsoon season. *Int. J. Climatol.* 35, 2326–2338. doi: 10.1002/joc.4129

Prein, A. F., and Gobiet, A. (2017). Impacts of uncertainties in European gridded precipitation observations on regional climate analysis. *Int. J. Climatol.* 37, 305–327. doi: 10.1002/joc.4706

Priya, P., Krishnan, R., Mujumdar, M., and Houze, R. A. (2016). Changing monsoon and midlatitude circulation interactions over the Western Himalayas and possible links to occurrences of extreme precipitation. *Clim. Dyn.* 49, 2351–2364. doi: 10.1007/s00382-016-3458-z

Rana, S., Mcgregor, J., and Renwick, J. (2015). Precipitation seasonality over the Indian subcontinent: an evaluation of gauge, reanalyses, and satellite retrievals. *J. Hydrometeorol.* 16, 631–651. doi: 10.1175/JHM-D-14-0106.1

Ren, Z., Zhang, M., Wang, S., Qiang, F., Zhu, X., and Dong, L. (2015). Changes in daily extreme precipitation events in South China from 1961 to 2011. *J. Geogr. Sci.* 25, 58–68. doi: 10.1007/s11442-015-1153-3

Roca, R., Alexander, L. V., Potter, G., Bador, M., Jucá, R., Contractor, S., et al. (2019). FROGs: a daily 1°x1° gridded precipitation database of rain gauge, satellite and reanalysis products. *Earth Syst. Sci. Data*. 11, 1017–1035. doi: 10.5194/essd-11-1017-2019

Roxy, M. K., Ghosh, S., Pathak, A., Athulya, R., Mujumdar, M., Murtugudde, R., et al. (2017). A threefold rise in widespread extreme rain events over central India. *Nat. Commun.* 8:708. doi: 10.1038/s41467-017-00744-9

Schaake, J., Spring, S., Henkel, A., and Cong, S. (2004). *"Application of PRISM climatologies for hydrologic modeling and forecasting in the western U.S," in 18th conference on hydrology*. (Seattle, WA: American Meteorology Society).

Schamm, K., Ziese, M., Becker, A., Finger, P., Meyer-Christoffer, A., Schneider, U., et al. (2014). Global gridded precipitation over land: a description of the new GPCC First Guess Daily product. *Earth Syst. Sci. Data* 6, 49–60. doi: 10.5194/essd-6-49-2014

Sen, P. K. (1968). Estimates of the regression coefficient based on kendall's Tau. *J. Am. Stat. Assoc.* 63, 1379–1389. doi: 10.1080/01621459.1968.10480934

Shige, S., Kida, S., Ashiwake, H., Kubota, T., and Aonashi, K. (2013). Improvement of TMI rain retrievals in mountainous areas. *J. Appl. Meteorol. Climatol.* 52, 242–254. doi: 10.1175/JAMC-D-12-074.1

Shige, S., M. K., Yamamoto, and Taniguchi, A. (2015). Improvement of TMI rain retrieval over the Indian subcontinent. *Remote Sensing Terrestrial Water Cycle, Geophys. Monogr.* 206, 27–42. doi: 10.1002/9781118872086.ch2

Shige, S., Nakano, Y., and Yamamoto, M. K. (2017). Role of orography, diurnal cycle, and intraseasonal oscillation in summer monsoon rainfall over the western ghats and Myanmar coast. *J. Clim.* 30, 9365–9381. doi: 10.1175/JCLI-D-16-0858.1

Sun, Q., Miao, C., Duan, Q., Ashouri, H., Sorooshian, S., and Hsu, K.-L. (2018). A review of global precipitation data sets: data sources, estimation, and intercomparisons. *Rev. Geophys.* 56, 79–107. doi: 10.1002/2017RG000574

Tapiador, F., Turk, J., Petersen, W., Hou, A., García-Ortega, E., Machado, L., et al. (2012). Global precipitation measurement: methods, datasets and applications. *Atmos. Res.* 104–105, 70–97. doi: 10.1016/j.atmosres.2011.10.021

Van Den Besselaar, E. J. M., Van Der Schrier, G., Cornes, R. C., Iqbal, A. S., and Klein Tank, A. M. G. (2017). SA-OBS: a daily gridded surface temperature and precipitation dataset for Southeast Asia. *J. Clim.* 30, 5151–5165. doi: 10.1175/JCLI-D-16-0575.1

Venkata Rao, G., Venkata Reddy, K., Srinivasan, R., Sridhar, V., Umamahesh, N. V., and Pratap, D. (2020). Spatio-temporal analysis of rainfall extremes in the flood-prone Nagavali and Vamsadhara Basins in eastern India. *Weather Clim. Extremes* 29:100265. doi: 10.1016/j.wace.2020.100265

Xie, P. (2008). "CPC unified gauge-based analysis of global daily precipitation," in: *Western Pacific Geophysics Meeting*. (Cairns, Australia).

Xie, P., Joyce, R., Wu, S., Yoo, S.-H., Yarosh, Y., Sun, F., et al. (2017). Reprocessed, bias-corrected CMORPH global high-resolution precipitation estimates from 1998. *J. Hydrometeorol.* 18, 1617–1641. doi: 10.1175/JHM-D-16-0168.1

Yatagai, A., Kamiguchi, K., Arakawa, O., Hamada, A., Yasutomi, N., and Kitoh, A. (2012). APHRODITE: constructing a long-term daily gridded precipitation dataset for asia based on a dense network of rain gauges. *Bull. Am. Meteorol. Soc.* 93, 1401–1415. doi: 10.1175/BAMS-D-11-00122.1

You, Q., Kang, S., Aguilar, E., Pepin, N., Flügel, W.-A., Yan, Y., et al. (2011). Changes in daily climate extremes in China and their connection to the large scale atmospheric circulation during 1961–2003. *Clim. Dyn.* 36, 2399–2417. doi: 10.1007/s00382-009-0735-0

Zhang, X., Alexander, L., Hegerl, G., Jones, P., Tank, A., Peterson, T., et al. (2011). Indices for monitoring changes in extremes based on daily temperature and precipitation data. *Wiley interdisciplinary reviews. Clim. Change* 2, 851–870. doi: 10.1002/wcc.147

Zhao, Y., Zhang, Q., Du, Y., Jiang, M., and Zhang, J. (2014). Objective analysis of circulation extremes during the 21 july 2012 torrential rain in Beijing. *Acta Meteorol. Sinica* 27, 626–635. doi: 10.1007/s13351-013-0507-y

Conflict of Interest: The authors declare that the research was conducted in the absence of any commercial or financial relationships that could be construed as a potential conflict of interest.

The handling editor is currently organizing a Research Topic with one of the authors, CF, and confirms the absence of any other collaboration.

frontiers in Climate

ORIGINAL RESEARCH
published: 04 December 2020
doi: 10.3389/fclim.2020.576653

Building an Improved Drought Climatology Using Updated Drought Tools: A New Mexico Food-Energy-Water (FEW) Systems Focus

Lindsay E. Johnson[1]*, *Hatim M. E. Geli*[2,3], *Michael J. Hayes*[1] and *Kelly Helm Smith*[4]

[1] School of Natural Resources, University of Nebraska, Lincoln, NE, United States, [2] Animal and Range Science Department, New Mexico State University, Las Cruces, NM, United States, [3] New Mexico Water Resources Institute, New Mexico State University, Las Cruces, NM, United States, [4] National Drought Mitigation Center, University of Nebraska, Lincoln, NE, United States

Drought is a familiar climatic phenomenon in the United States Southwest, with complex human-environment interactions that extend beyond just the physical drought events. Due to continued climate variability and change, droughts are expected to become more frequent and/or severe in the future. Decision-makers are charged with mitigating and adapting to these more extreme conditions and to do that they need to understand the specific impacts drought has on regional and local scales, and how these impacts compare to historical conditions. Tremendous progress in drought monitoring strategies has occurred over the past several decades, with more tools providing greater spatial and temporal resolutions for a variety of variables, including drought impacts. Many of these updated tools can be used to develop improved drought climatologies for decision-makers to use in their drought risk management actions. In support of a Food-Energy-Water (FEW) systems study for New Mexico, this article explores the use of updated drought monitoring tools to analyze data and develop a more holistic drought climatology applicable for New Mexico. Based upon the drought climatology, droughts appear to be occurring with greater frequency and magnitude over the last two decades. This improved drought climatology information, using New Mexico as the example, increases the understanding of the effects of drought on the FEW systems, allowing for better management of current and future drought events and associated impacts.

Keywords: drought, drought monitoring, food-energy-water systems, drought impacts, triggers

OPEN ACCESS

Edited by:
Chris C. Funk, United States Geological Survey (USGS), United States

Reviewed by:
Jian Peng, University of Oxford, United Kingdom
Ladislaus Benedict Chang'A, Tanzania Meteorological Agency, Tanzania

***Correspondence:**
Lindsay E. Johnson
lindsay.johnson@huskers.unl.edu

Specialty section:
This article was submitted to Climate Services, a section of the journal Frontiers in Climate

Received: *26 June 2020*
Accepted: *09 October 2020*
Published: *04 December 2020*

Citation:
Johnson LE, Geli HME, Hayes MJ and Smith KH (2020) Building an Improved Drought Climatology Using Updated Drought Tools: A New Mexico Food-Energy-Water (FEW) Systems Focus. Front. Clim. 2:576653. doi: 10.3389/fclim.2020.576653

INTRODUCTION

Since 2000, 16 drought events classified as "Billion Dollar Disasters" have occurred across the United States (U.S.) according to a national web-based archive of these types of disasters for a variety of natural hazards (NOAA NCEI, 2020). The estimated economic losses from the 16 drought-specific events total $133.2 billion. These losses illustrate that drought is a key disaster that can have dramatic local and regional impacts across the U.S. Droughts are different from other hazards in that they can develop slowly, extend over large regions, and have a long duration, making

it very difficult for officials to tally both the direct and indirect impacts that result (Ding et al., 2011). Because of their widespread and long-lasting nature, droughts also affect multiple sectors of a region's economy. Therefore, it is important to consider drought impacts when analyzing the dynamics of Food-Energy-Water (FEW) systems in a location.

The complex and costly impacts of the recent drought events across the U.S. highlight the need for a proactive drought risk management approach to help officials be better prepared for future drought events (Wilhite, 2018). Historically, most efforts of drought management have focused on responding to drought impacts after an event, which has often meant that these responses have been uncoordinated and untimely, and little is done to reduce potential impacts in the next events (Wilhite and Pulwarty, 2005; Wilhite et al., 2007). Drought risk management, however, places the attention on improving drought early warning, drought planning, and drought mitigation strategies that will hopefully reduce future drought impacts (Wilhite et al., 2014).

Drought early warning is often considered the foundation of successful drought risk management (Hayes et al., 2018). It consists of both the assessment of current conditions (or drought monitoring) as well as an outlook for future conditions. In the past several decades, there have been remarkable advancements in the capacity of early warning, particularly with new drought monitoring tools, remote sensing technologies, and improved understanding of oceanic-atmospheric interactions to assist with drought outlooks. The advancements have particularly highlighted the improved spatial and temporal resolutions that are now available with many of these tools (Hayes et al., 2012).

An important aspect of drought early warning is having a solid understanding of a location's drought climatology (i.e., historical drought events' frequency, magnitude, duration, and impacts), so that current and future drought conditions are placed into a proper historical perspective and impacts can be anticipated or projected based upon drought severity levels (Steinemann et al., 2015; Svoboda et al., 2015; Martin et al., 2020). Decision-makers often ask specific questions during a drought event that link to the climatology such as how the current severity compares with historical records, how often the current severity has occurred in the past, when was the last time the drought event was this severe, what impacts have occurred, and what does the past record indicate as to what can be expected ahead (Svoboda et al., 2002). These questions relate directly to the decision-makers' understanding drought and having access to drought climatologies. Timely answers with key information derived from an accurate drought climatology, especially when combined with real-time drought early warning information, provide powerful resources for decision-makers to use for improving drought response and drought risk management strategies.

Drought and Food-Energy-Water Systems of New Mexico, U.S.A

This analysis was conducted within the context of providing an improved understanding of how natural hazard events such as drought can affect the sustainability and resilience of New Mexico's FEW systems (Geli et al., 2017). This article thus highlights the value of an updated drought climatology for the state while also investigating the role drought (among other factors) has had, and will have, on the FEW systems across the state. New Mexico is specifically included in 11 of the Billion Dollar drought designations since 2000, and the three-year 2011–13 period that severely affected New Mexico had an estimated $59.6 billion of losses nationally from the direct and indirect impacts that occurred (NOAA NCEI, 2020). For New Mexico, drought impacts affect crop and livestock productivity (Sawalhah et al., 2019; Zaied et al., 2019, 2020; Gedefaw et al., 2020); water supplies for public and ecosystem consumption; human, animal, and wildlife health; forests and wildfires; and recreation and tourism. These sectors have also become more vulnerable to natural hazards (i.e., droughts and wildfires) given changes occurring in the climate (NMOSE and NMWRRI, 2018). **Figure 1** is a time series that highlights drought has been a regular feature in New Mexico since the beginning of the U.S. Drought Monitor (USDM) record in 2000 (USDM, 2019), and the recent 2018–2019 drought reached the "extreme" (D3) and "exceptional" (D4) categories for parts of the state. In addition to this recent drought, parts of New Mexico were in the exceptional category during 2002, 2003–2004, 2006, 2011–2012, and 2013.

These recent droughts in New Mexico, and the availability of new drought early warning tools and information for use by decision-makers, emphasize the importance of building a strong drought climatology. This article provides a historical drought perspective for New Mexico within the context of providing an improved understanding of FEW systems response during drought, and how a drought climatology can potentially improve drought risk management. Updating the state's drought history is also important for using drought early warning information to establish a baseline that can also be helpful for multiple other applications, such as developing indicators and thresholds of resiliency for FEW systems monitoring shifts in the dynamic equilibrium of these systems, and can serve as a model (and provide guidelines) for other states and regions on how to update the drought climatology in their locations (Svoboda et al., 2015). The New Mexico case study will also support ongoing efforts in the state to evaluate the response of state's FEW systems under drought. FEW systems are extremely important for New Mexico because they are highly interconnected and they collectively support the well-being and livelihood of New Mexicans (Geli et al., 2017).

New Mexico is diverse in its topography, climate, and economic sectors. Its economy is driven by a number of principal sectors that include energy, agriculture, mining, and recreation (USDA NASS, 2018, 2019; NMDA, 2019; NMSU, 2019; USDA – FSA, 2020). The state has abundant land resources suitable for grazing of livestock and to some extent for crop production as well as large reserves of crude oil and natural gas.

However, the state is challenged by limited and variable water supplies that affect the sustainability of its interconnected FEW systems. The World Resources Institute (WRI, 2020), for example, identifies much of New Mexico in the "extremely high" category for current water quantity risks. This challenge is

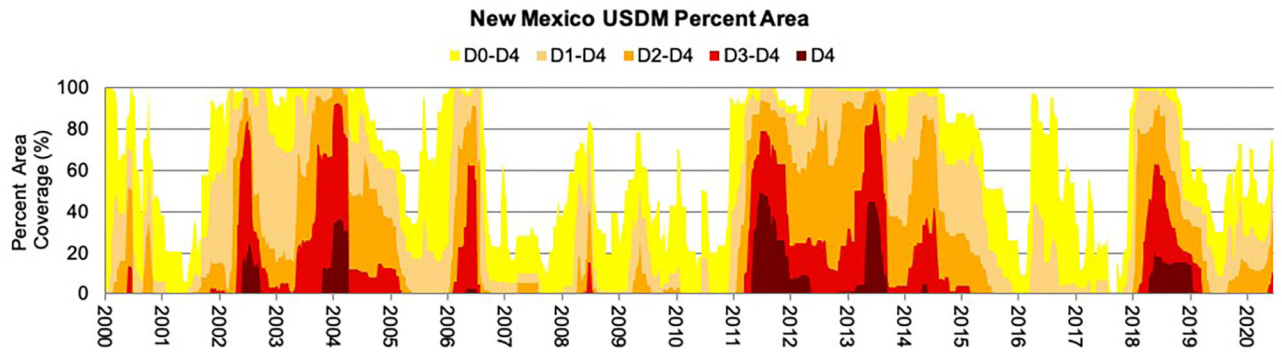

FIGURE 1 | A time series of the weekly percent area of the USDM spatial coverage by severity category across New Mexico for the 2000–2020 period (NDMC, 2020). The colors represent the five USDM drought categories.

highlighted by the fact that the state of New Mexico has been in at least "Moderate Drought" (D1) for 999 weeks since January 2000 (93%), as designated by the USDM, more than any other state in the U.S. (USDM, 2020a).

Therefore, the goals of this article are to: (1) highlight how the availability of data and tools have rapidly advanced over the past two decades; (2) demonstrate how these data and tools can now be leveraged to build improved drought climatologies using a New Mexico example; and (3) illustrate how these drought climatologies can support drought risk management.

DATA

Tremendous progress in drought early warning strategies has occurred over the past two decades, with more tools providing greater spatial and temporal resolution for a variety of variables, including drought impacts. For a considerable amount of time, the Palmer Drought Severity Index (PDSI) (Palmer, 1965) was nearly the only drought monitoring indicator available for decision-makers to use. The Standardized Precipitation Index (SPI) (McKee et al., 1993) was introduced as an indicator in the mid-1990s, and the USDM product was first available in 1999. These developments, and the increased availability of remote sensing data, were catalysts spurring the rapid growth of products that had both improving spatial and temporal resolutions. That growth continues today with the added capacity of mapping and spatial analysis through Geographic Information Systems (GIS), computing power, and online tools.

This influx of available drought early warning information and data, while advantageous, does come with a suite of corresponding limitations as well (Finnessey et al., 2016). For example, there can actually be so much climate and drought data, tools, and information available for decision-makers that it can be challenging to find the appropriate valid and reliable data to address the particular issue. This can lead to frustration when trying to understand drought information for either building a drought climatology or making current assessments of an evolving event. Because of the importance that decision-makers understand the available resources, **Table 1** was developed to provide a comprehensive overview of key sources for climate and drought data that are now available to be used to build a drought climatology. As far as the authors are aware, no similar table exists in the literature and this table can serve as a valuable resource for decision makers.

Enhancement of Existing Drought Monitoring Tools

There are a large number of drought and climate resources that are beneficial in drought monitoring and risk management. Many of the historically popular drought indices and indicators have been improved to incorporate new available data, temporal and spatial scales, and enhanced computing power. The U.S. Drought Monitor (USDM), Drought Risk Atlas (DRA), and Drought Impact Reporter (DIR) are three tools that are continually evolving in order to provide useful and robust data for scientists and decision-makers.

The U.S. Drought Monitor

In the U.S., one of the most widely-used drought monitoring tools is the U. S. Drought Monitor (NDMC, 2020). The USDM is a map-based assessment of drought intensity produced weekly since 1999. The assessment is made using a wide range of inputs representing the entire spectrum of the hydrological cycle, including real-time climate, water, and remotely-sensed data. The responsibility for the operational weekly updates of the product is a partnership between the National Drought Mitigation Center (NDMC), the U.S. Department of Agriculture (USDA), and the National Oceanic and Atmospheric Administration (NOAA) (NDMC, 2020). The product is also unique because it relies heavily on a continuous feedback process based on the interactions from a large number of climate and water experts from around the country (Svoboda et al., 2002). **Figure 2** shows a USDM map for 2 October 2018 for New Mexico, which was a time when dryness or drought covered almost the entire state. Exceptional (D4) and extreme (D3) conditions covered northwest New Mexico. There was also extreme (D3) drought in the central Pecos River Basin. **Figure 2** also provides a table with statistics related to the percent area of the state in each category of drought, as well as comparisons to what was being experienced in the state the previous week, 3 months ago, the

TABLE 1 | Climate and drought data sources.

	WestWide drought tracker	U.S. drought monitor	Climate at a glance	Drought risk atlas	NCEI	Centers for disease control
	1895 - present Gridded data, 4 km (PRISM) File Format: NetCDF	2000 – present Data: shapefile	Period of record dependent upon individual station Station based data	Period of record dependent upon individual station Station based data	Period of record dependent upon variable File format: HTML, XML, JSON	1989–2016 File format: CSV, RDF, RSS, TSV (for excel), EM
Temporal scale	- Annual - Monthly	- Weekly	- Annual - Monthly	- Annual - Monthly - Weekly	- Annual - Weekly - YTD - Aggregate by number of months	- Monthly - Weekly - Quarter (seasonal)
Spatial coverage	- CONUS - State - County - Climate division - HUC	- National - State - Climate region and division - County - FEMA region - HUC (2, 4, 6, and 8 digits) - NWS region - River forecast center - Urban areas - USACE district and division - USDA climate hubs - Other regions	- Climate region and division - State - County - FEMA region - HUC (2, 4, 6, and 8 digits) - NWS region - River forecast center - Urban areas	- Individual stations	- FEMA region - HUC (2, 4, 6, and 8 digits)	- FEMA region - HUC (2, 4, 6, and 8 digits)
Climate data	- Temperature (anomaly, avg., max., and min.) - Precipitation (total and anomaly) - Heating degree days - Colling degree days - Growing degree days	- PDSI, SPI, and other climatological inputs; the Keech-Byram Drought Index for fire, satellite-based assessments of vegetation health, and various indicators of soil moisture; and hydrologic data, SWSI & Snowpack	- Temperature (avg., max., and min.) - Precipitation - Cooling degree days - Heating degree days	- Temperature (anomaly, avg., max. and min) - Precipitation (total and anomaly) - Decilies (1–96 months) - Standardized Streamflow Index	- Daily summaries - Global summaries (month & year) - Normals (hourly, daily, monthly, seasonally, annually) - Precipitation (15-minute intervals, hourly) - Weather Radar	- Population-weighted global horizontal irradiance - Population-weighted UV irradiance - Flood vulnerability - Future projections of extreme heat & precipitation - Heat stress, heat vulnerability, and heat-related mortality - Historical extreme heat days, events, precipitation - Temperature distribution
Drought indices	- PDSI - sc-PDSI - Palmer-Z - SPI (1–72 months) - SPEI (1–72 months)	- USDM (Drought categories D0–D4) - DSCI	- PDSI - PHDI - PMDI - Palmer-Z	- PDSI - sc-PDSI - PHDI - PMDI - SPI (1–96 months) - SPEI (1–96 months)	- PDSI - sc-PDSI - SPI (1–96 months) - SPEI (1–96 months) - Drought monitor	- PDSI - SPEI - SPI - USDM - Max. number of consecutive months of mild drought or worse - Number of months of mild drought or worse

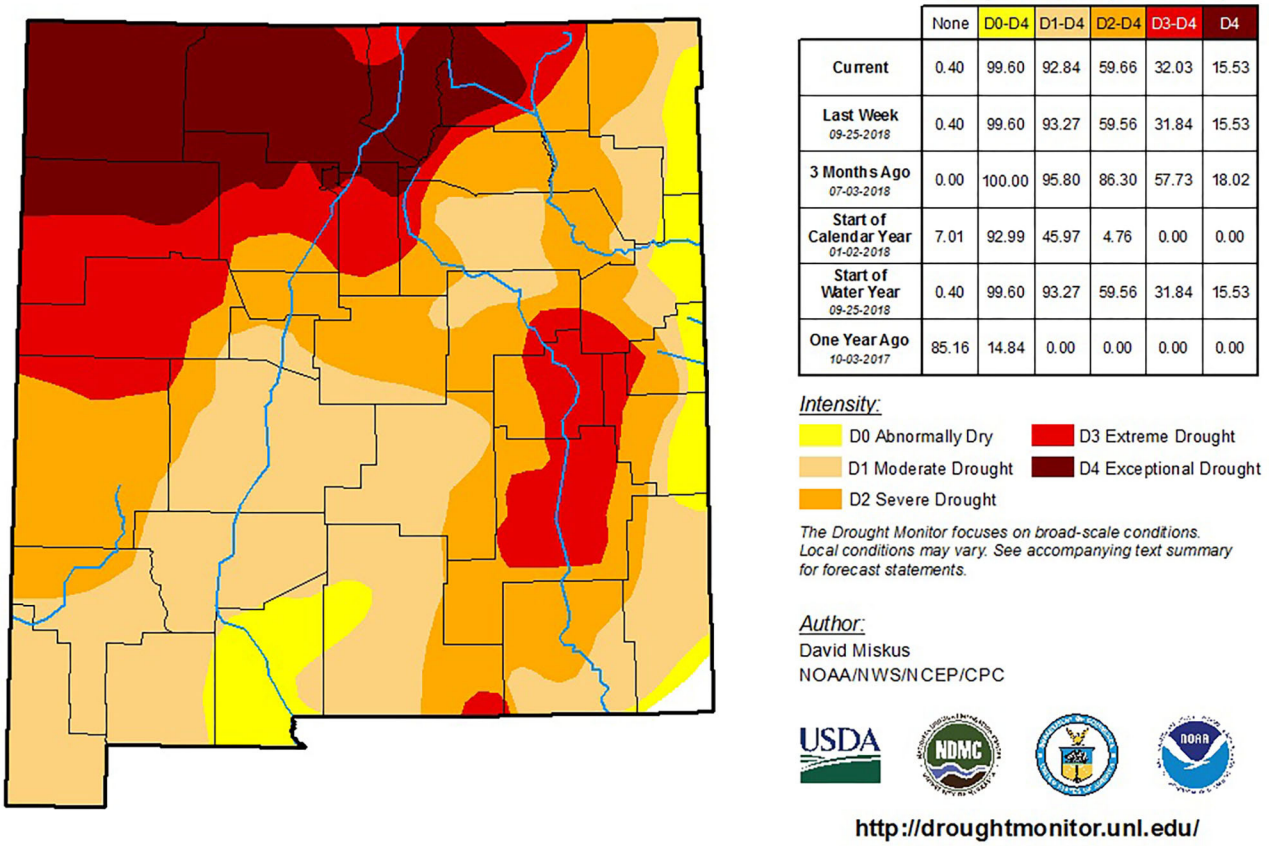

FIGURE 2 | A USDM map of New Mexico for 2 October 2018 and an associated table with relevant statistics comparing the drought coverage with other past time periods (NDMC, 2020).

beginning of the calendar year, the beginning of the "Water Year" or October 1, and 1 year ago. These are also the same types of questions that decision-makers might ask that are related to how a current drought compares with previous conditions readily understood by the decision-maker. The map and table in **Figure 2**, combined with the time series in **Figure 1**, can be highly valuable as part of a drought climatology and in helping to make drought-related decisions.

The USDM's website [http://droughtmonitor.unl.edu] and associated web-based tools include an archive of the weekly maps and a timeline product of the drought intensities for a variety of scales. The maps, data tables, and time series can also be produced at national, county, river basin, and several different climate-related scales. The USDM is used by several government agencies to trigger a variety of drought responses (NDMC, 2020). For example, the Farm Service Agency (FSA) of the USDA uses the USDM to determine its livestock disaster payment program (LFP). The FSA has a tool designed to help livestock producers know if their county is eligible for this drought relief that is also featured on the USDM's website.

The Drought Risk Atlas (DRA)

The Drought Risk Atlas (DRA) tool was developed by the NDMC to provide decision-makers with more details about historical drought events (Svoboda et al., 2015). As with the development of other drought tools, the DRA was inspired by decision-makers' needs to assess their risks related to climate variability and extremes. The current DRA is an evolution from the National Drought Atlas (NDA) developed in 1996 and primarily focused on hydrology and the PDSI data for stations around the country. The updated DRA not only increased the number of observation stations to 4,183 as of 2016, but also the number of calculated indices and indicators available; including the PDSI, SPI and many more. The DRA's goal was to provide usable information and to increase the ability of users and decision-makers to analyze their potential risk to drought at a specific location and time (Svoboda et al., 2015). The DRA has aided in improving the

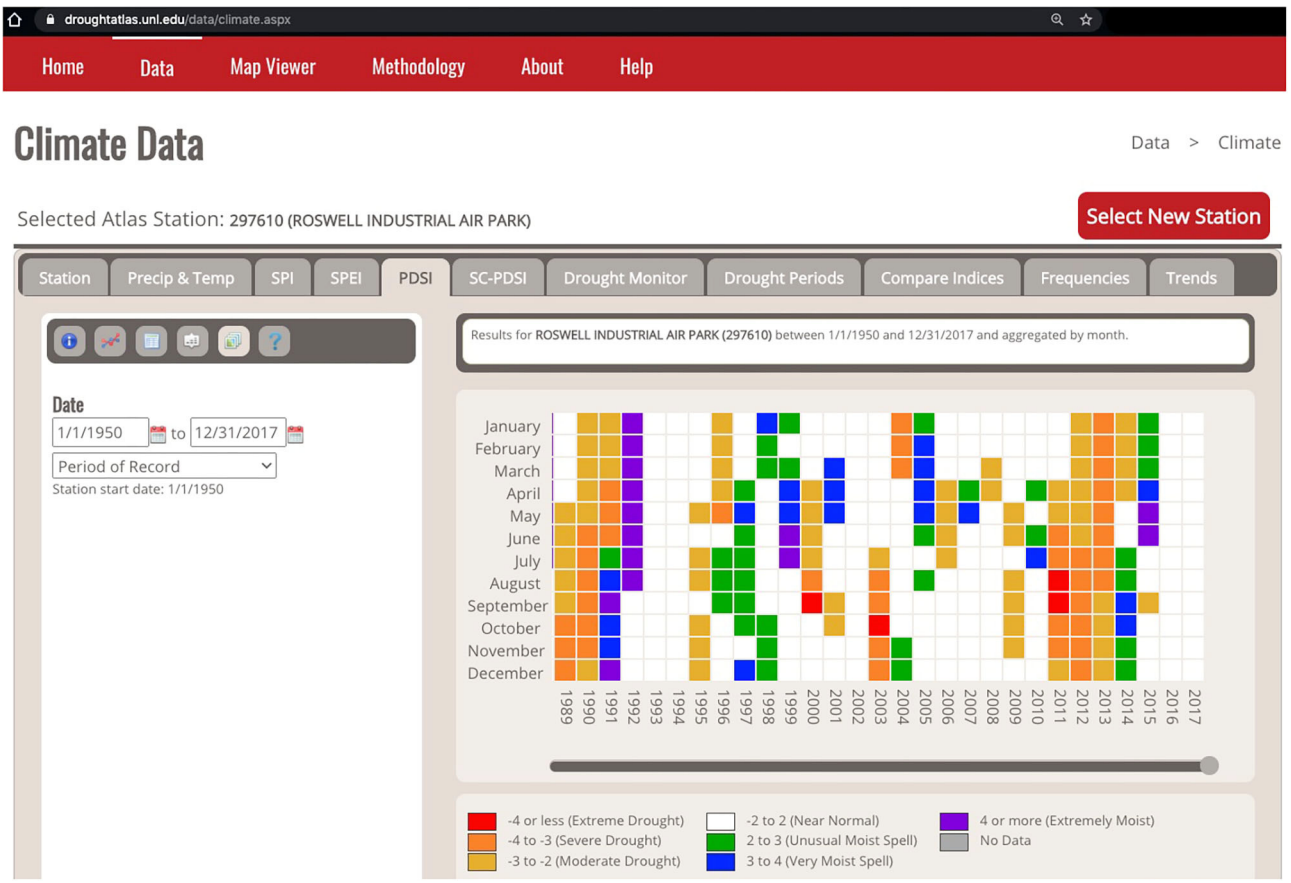

FIGURE 3 | An example of the Drought Risk Atlas [http://droughtatlas.unl.edu/data/climate.aspx] that highlights the monthly PDSI heat map of PDSI values for Roswell, NM, from 1988 to 2017.

analysis of drought as an extreme event by providing data and visualization tools to help them better understand the drought climatology for different spatial extents (Svoboda et al., 2015). **Figure 3** is a screen capture of the Drought Risk Atlas tool showing the recent PDSI record (1988–2017) for Roswell, NM. The heat map display is one feature of the tool that, in this case, provides a visual representation of the PDSI values by month and year in a slightly different format than a more traditional time series, which is also available. The DRA is a continuously evolving tool, with an option to investigate dryness "trends" added in 2020 to the already numerous options for the station data in the tool. Because the DRA focuses on station-based data, its information was not used for this statewide analysis for New Mexico.

Drought Impacts and the Integration of Monitoring Tools

The USDM and DRA are powerful drought monitoring tools that can help in developing drought climatologies, but they lack one key element that is beneficial for improving decision making: drought impacts. Redmond (2002) advocated the importance of defining drought by considering impacts, and because of their unique local nature, monitoring these impacts along with other drought monitoring indicators is critical. Unlike other natural hazards, droughts are often difficult to detect until after impacts have already begun to appear. Drought impacts can also extend past the end point given by many drought indicators. Because of the complexity of possible impacts, drought impact collection and monitoring has always been difficult and usually lacking for use in decision making (Redmond, 2002). This has made the incorporation of impacts difficult in the development of drought climatologies as well.

Given this challenge, the NDMC launched the Drought Impact Reporter (DIR) in 2005 as the nation's first comprehensive, web-based archive of drought impacts. The DIR is a moderated database of events drawn from a variety of sources, documenting the occurrence of drought impacts. Moderators scan daily results of automated news searches for evidence of a quantifiable or observable change at a specific place and time that can be attributed to drought. When they find a report that meets these criteria, they add it to the DIR as an impact (Smith et al., 2015). Impacts are categorized by sectors and can be displayed on a map. Other sources of information on drought impacts are reports from agencies or organizations, and on observations submitted by individuals

across the country. These types of sources are now represented in one location at the NDMC [droughtimpacts.unl.edu]. Understanding drought impacts helps decision-makers at all levels identify vulnerabilities so that actions can be taken to address and reduce those vulnerabilities. Impacts can also assist in the early warning system by helping connect drought indicator levels with impact occurrences. As the archive of impacts has grown, the DIR has been used in planning as a historic record highlighting vulnerability to drought [https://drought.unl.edu/archive/plans/Drought/state/SD_2015.pdf]. It provides context and interpretation of U.S. Drought Monitor depictions (Noel et al., 2020). Reports from observers in the national Community Collaborative Rain, Hail, and Snow (CoCoRaHS) network and from other contributors provide near real-time perspectives on what individual producers are experiencing (Smith et al., 2015). Researchers have also experimented with comparing impacts from a European database of drought impact events with physical indicators of drought (Bachmair et al., 2017).

Recent Drought Monitoring Tools for Drought Climatologies

This section features two of the more recently developed tools that can assist decision-makers with building drought climatologies.

The Drought Severity and Coverage Index (DSCI)

The USDM as it is represented in **Figures 1**, **2** is very helpful illustrating how information on drought severity can be provided at different spatial scales, but the information remains primarily a qualitative comparison of historical drought conditions. It is difficult to compare conditions between two or more separate drought events, either in one location or in multiple locations, and then make a determination regarding which events were more severe (Martin et al., 2020). For example, using **Figure 1**, it is difficult to quantify how the droughts of 2002, 2003–2004, 2006, 2011–2012, 2013, and 2018–2019 in New Mexico compare with each other. Therefore, to enhance the quantitative capabilities of the USDM to better determine spatial coverage and intensity together, and allow for better comparisons between drought events for locations or between locations, an index called the Drought Severity and Coverage Index (DSCI) was developed as a method for converting categorical USDM drought levels to a single continuous aggregated value for a specified area [https://droughtmonitor.unl.edu/About/AbouttheData/DSCI.aspx] (Akyuz, 2017; Smith et al., 2020). To compute the DSCI using a weighted average, a weight of 1 through 5 is given to each USDM category (D0–D4), and this weight is then multiplied by the categorical percent area for the drought category, and these totals are summed together (Equation 1). This results in a DSCI value that has a continuous scale of 0–500 (**Figure 4**).

$$DSCI = 1\,(D0) + 2\,(D1) + 3\,(D2) + 4\,(D3) + 5(D4) \qquad (1)$$

Figure 4 demonstrates the transformation process for New Mexico of the categorical USDM time series (**Figure 1**) to the continuous DSCI time series using Equation 1. Two advantages can result from converting the percent of an area in each USDM drought category into the DSCI: (1) it provides a single numerical value describing current drought extent and intensity and (2) it allows for drought to be quantified over time. While the USDM provides real-time maps of the spatial extent of drought, it does not provide a simple way to analyze drought over time as do some of the other drought indices. With that in mind, the DSCI is a new tool that increases the capacity of the USDM for further drought monitoring and analysis. The usefulness of the USDM is limited when a long-term historical context is needed since it has only been operational since 2000.

The West Wide Drought Tracker (WWDT)

Another tool that can be very useful for a decision-makers is the WestWide Drought Tracker [WWDT, https://wrcc.dri.edu/wwdt/] (Abatzoglou et al., 2017). One of the features of the WWDT that is attractive for decision making is that it provides a variety of data options available back to 1895. The tool was designed to provide fine-scale drought and climate data for the states covered by the Western Regional Climate Center (WRCC), including New Mexico. These western states all consist of vast areas of complex terrain where local precipitation and temperature can vary dramatically, affecting local drought conditions (Abatzoglou et al., 2017). The western U.S. is unique in that the geopolitical boundaries are large and consist of diverse land surfaces and topographies, adding to the complexity of an already intricate topic of drought monitoring in these regions. To rectify these drought monitoring challenges, the WWDT is using the PRISM Climate Mapping Program that provides climate and drought data at a 4-km resolution (**Table 1**) (Abatzoglou et al., 2017). All the data focused on New Mexico applied in this paper, aside from the DSCI, were acquired from the Time Series Tool of the WWDT. These data, and the long historical record, provide an excellent opportunity to build drought climatologies for locations with improved spatial and temporal resolutions that were not available before.

While there are a number of other climate and drought tools that can be used by decision-makers, the tools described here were selected because of the types of available data, the spatial and temporal scales available, and the robustness of the available data. The data and tools discussed happen to be focused on the United States, but significant progress in drought monitoring is also being made around the world, and several examples of these are highlighted in **Table 2**. The processes described in this article can be applied to any location having historical data available with the appropriate spatial and temporal resolutions.

METHODS

The process of building a drought climatology is unique for every location. Ensuring that there are available historical data to provide the appropriate context is a key consideration for highlighting the frequency, magnitude, duration, and impacts of previous drought events. Additional factors to consider in this process include understanding how the drought climatology addresses the drought perspectives and management activities of the decision-makers. It is also important to understand

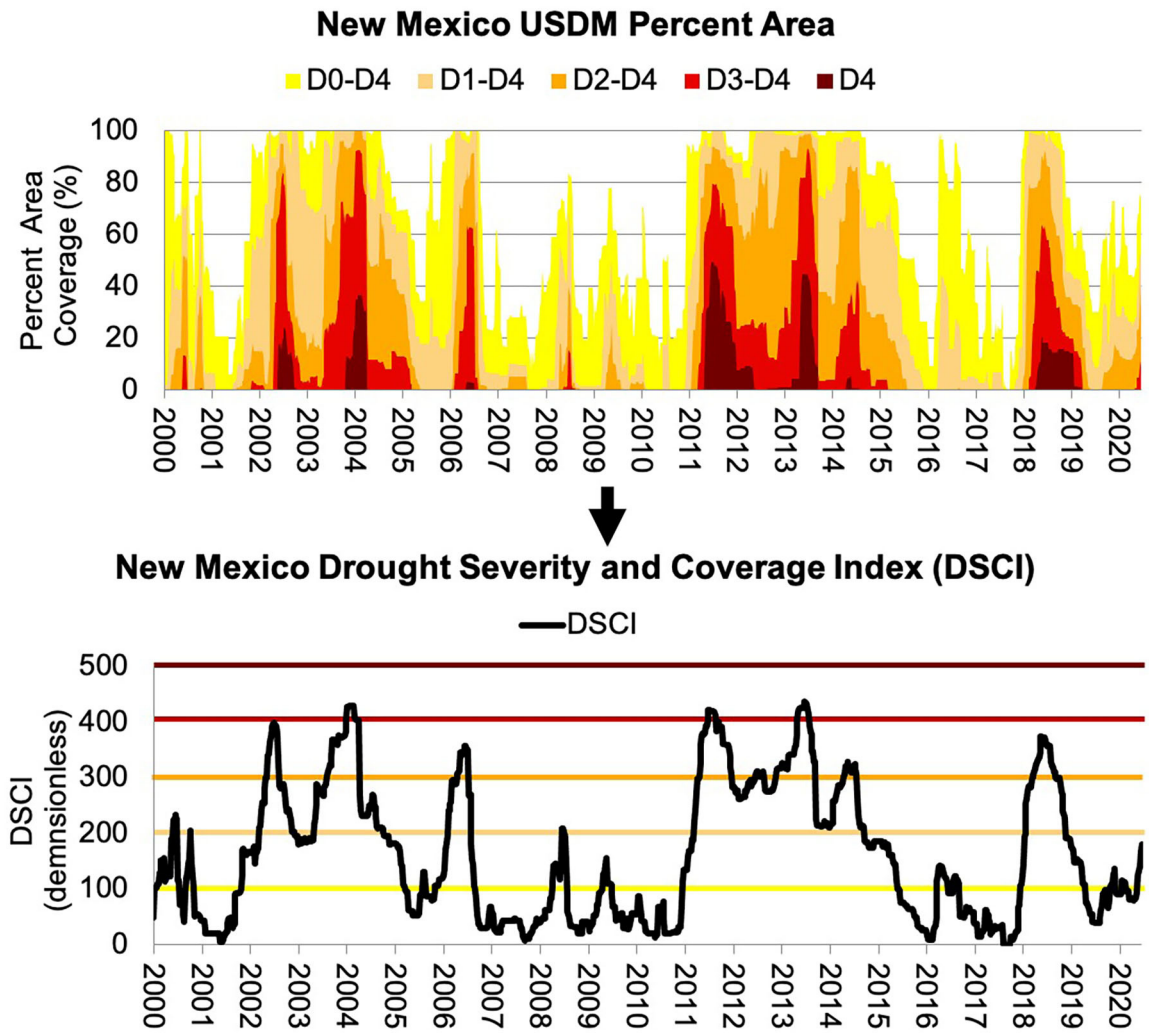

FIGURE 4 | Weekly time series that show how the USDM categorical plot is transformed into the continuous DSCI. The continuous DSCI (*USDM*) values are 0–99 (*None*), 100–199 (*D0*), 200–299 (*D1*), 300–399 (*D2*), 400–499 (*D3*), and 500 (*D4*).

the spatial scale most relevant for the decision-makers. As with a more traditional climatology where both temperature and precipitation are the main components, temperature- and precipitation-related indicators are very important for a drought climatology as they both represent important components of the hydrological cycle and are a good starting point.

For this analysis of New Mexico's drought, all temperature, precipitation, and drought indices data used were taken from the WWDT tool. Although provided for New Mexico on a statewide scale in this case, similar analyses can be conducted for a variety of spatial scales including individual stations, counties, river basins, and climate divisions where historical data are available for more than 30 years. The WWDT data are available for the 1895 through 2019 period, which allows anomalies to be compared to longer averages from 1900 to 1999.

Drought Events Using the Self-Calibrated Palmer Drought Severity Index

One indicator that has been used regularly for assessing drought and building drought climatologies is the PDSI (Palmer, 1965). The PDSI uses both precipitation and temperature data to estimate drought and wetness conditions. Wells et al. (2004) updated the PDSI, called the Self-Calibrated PDSI (sc-PDSI), using a methodology that better incorporates characteristics present at each individual station. This is an important distinction because it accounts for local variability and allows for better comparisons between locations (Wells et al., 2004). Both the PDSI and the sc-PDSI can be calculated back to the beginning of the instrumental record in 1895. **Figure 5** illustrates a sc-PDSI time series for New Mexico and provides a general qualitative snapshot of how drought has been a fairly persistent feature in New Mexico.

TABLE 2 | International drought monitoring activities.

Tool/Dataset	References/Links	Description
North American Drought Monitor (NADM)	Lawrimore et al. (2002)	Users have access to a monthly drought monitoring composite maps and data for Canada, the United States, and Mexico, with an archive of the NADM dating back to 2002
Monitor de Secas do Nordeste (the Northeast Drought Monitor, or MSNE)	Hayes et al. (2018)	A tool adapted directly from the USDM process for 13 states in northeastern Brazil and operational since July 2014
Global Drought and Flood Catalog (GDFC)	He et al. (2020)	Users can access *in situ* and remote sensing datasets and products of droughts and floods, 1950–2016, to provide an estimate of extremes in regions of the world
Anywhere DEWS (AD-EWS)	Sutanto et al. (2020)	In addition to real-time drought information for multiple aspects of the water cycle, users can get high resolution seasonal drought predictions for Europe
European Drought Observatory (EDO)/Global Drought Observatory	EDO GDO	Users have access to current drought information and a database of drought events back to 1950 for Europe and around the world. The GDO is mainly for emergency response information
European Drought Report Impact Inventory (EDII)/European Drought Reference Database (EDR)	Stahl et al. (2015)	The European Drought Center (EDC) provides an archive of drought impacts (EDII) or summaries of historical European droughts and an SPI visualization tool (1958–2009). Users can also submit drought impacts as well
African Flood and Drought Monitor (AFDM), Princeton University	Sheffield et al. (2014)	The AFDM provides drought assessments and forecasts for the African continent at various temporal and spatial scales. Current conditions are compared with historical reconstructions of the water cycle

While the sc-PDSI time series itself is valuable, additional analyses can be made on the time series to provide quantitative comparisons of drought events based on their duration, magnitude, and severity. In this study for New Mexico, the method adapted by Nam et al. (2015) is used to calculate the drought severity for the drought events that have occurred during the state's climate history based on the sc-PDSI. The first step is to define a Drought Event (DE_P). The subscript "P" represents Drought Events specifically identified by the sc-PDSI. The common threshold of PDSI or sc-PDSI values ≤-2.0 (classified as "Moderate Drought") was used to define the initiation of a DE_P (Palmer, 1965; World Meteorological Organization (WMO) and Global Water Partnership (GWP), 2016). In addition, to provide some consistency and prevent individual 1-month DE_Ps, a baseline criterion was established that a DE_P must have at least two consecutive months of sc-PDSI values ≤-2.0 to be counted.

Using the long-term sc-PDSI time series for New Mexico, the duration of a DE_P is the number of consecutive months (two or more) where the sc-PDSI threshold of −2.0 or less was met. The magnitude of a DE_P is the absolute value of the sum of the sc-PDSI values for all months within a designated DE_P (Equation 2).

$$DE\ Magnitude = \left| \sum scPDSI \leq -2.0 \right| \tag{2}$$

Using the duration and magnitude, the severity can be calculated for each DE_P using Equation 3. This method is simple and provides a quick and easy way to analyze how droughts compare through history.

$$Severity = \frac{Magnitude}{Duration} \tag{3}$$

Table 3 shows all 31 DE_Ps as defined by the process described above for New Mexico since 1895. The DE_Ps in red are designated as the Top 10 events in New Mexico's history. The DE_Ps for 1895–2019 period were ranked on the calculated drought severity (Equation 3). It is important to note that the 1950s drought, which is often considered New Mexico's worst drought since the beginning of the instrumental record, is broken into two separate drought events using this method. This is because there were 4 months during 1952 when the magnitude threshold was not met. Otherwise, if this gap was not present, the cumulative 1950s drought would rank as the most severe drought event for the state.

However, the method does have one limitation in that duration and magnitude are given the same weight. This means that a drought with a very large magnitude, but short duration can be calculated to have the same severity as a longer drought with moderate magnitude. This is observed comparing DE_P02 and DE_P12 in **Table 3**, where DE_P02, which only lasted for 10 months, is ranked as more severe than DE_P12, which lasted for 61 months.

Drought Events Using the DSCI

As with the sc-PDSI, end-users (i.e., stakeholders, decision-makers, and researchers) can get a time series of the U.S. Drought Monitor for their state or more localized region (**Figure 1**). This time series record only goes back to 2000, however. To provide a more quantitative perspective of the drought severity categories and the spatial coverage, the Drought Severity and Coverage Index (DSCI) was created and can be used for that current 20-year record. Although the DSCI is available weekly, for this study of New Mexico, monthly averages of the DSCI were used to provide consistency with the sc-PDSI analysis.

Similar to the sc-PDSI analysis, a baseline of two consecutive months reaching the threshold magnitude was established. A DSCI of 200 is equivalent to 100% of an area being in D1 (or Moderate Drought) and a DSCI of 300 is equivalent to 100% of an area being in D2 ("Severe Drought"). Because this study was looking at a statewide DSCI value, and the goal was to set

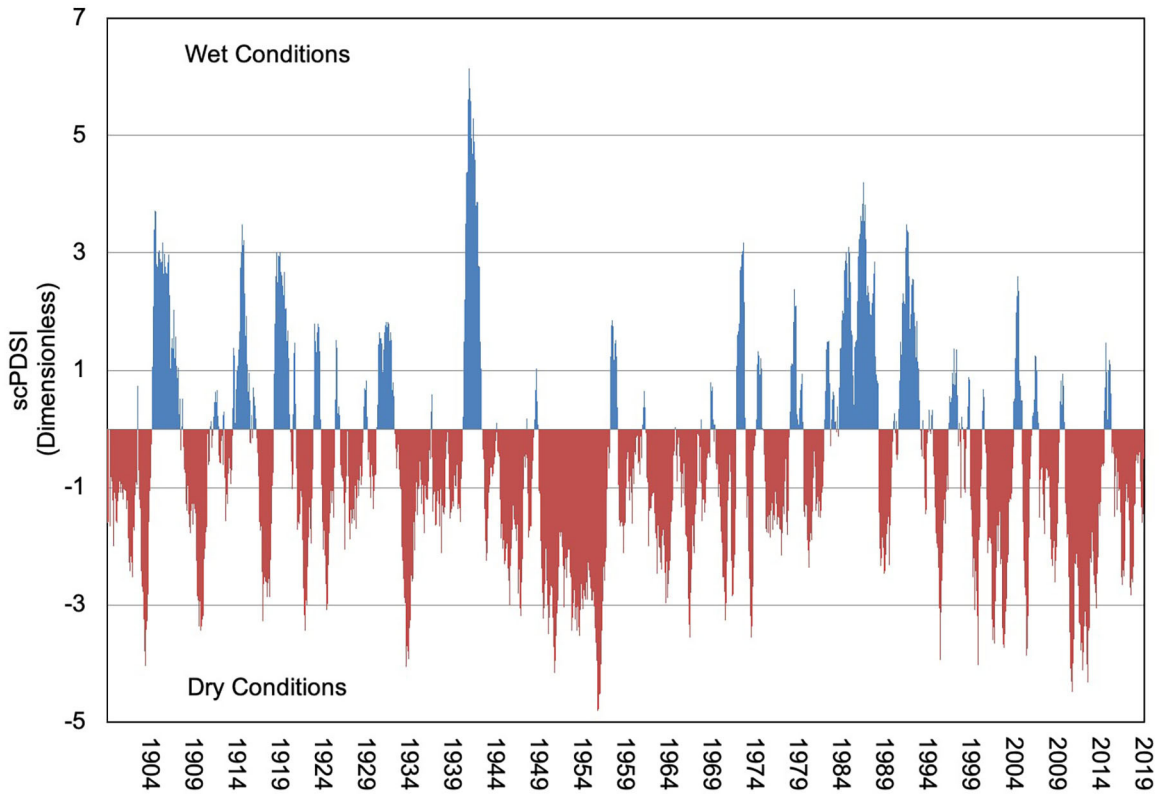

FIGURE 5 | The Self-Calibrating PDSI (sc-PDSC) for the 1900–2019 period. Positive sc-PDSI values (blue) representing wet conditions and negative sc-PDSI values (red) representing dry conditions.

a threshold for drought, the DSCI magnitude threshold was set at 250 to ensure that at least "Moderate Drought" exists for a majority of the state. **Table 4** shows 8 DE_Ds for New Mexico as defined by the temporal step and magnitude threshold described above using Equations 2 and 3. The subscript "D" represents Drought Events specifically identified by the DSCI. The results or the DE_Ds shown on **Table 4** were based on using DSCI instead of sc-PDSI in Equation 2.

RESULTS: BUILDING A NEW MEXICO DROUGHT CLIMATOLOGY

As a good place to begin, the temperature and precipitation records are critical for a New Mexico drought climatology because both represent important components of the hydrological cycle and reveal extremes and trends that provide insights to decision-makers regarding past, present, and potentially future drought events. For New Mexico, **Figure 6** shows annual temperature and precipitation anomalies on a statewide scale compared to the 1900–1999 average. **Figures 6A,B** organizes the historical data into two time series that illustrate distinct warmer/cooler or drier/wetter departures over the period of record from 1895 to 2019. The precipitation record oscillates above and below the long-term average, with the most recent years being generally drier than the 1900–1999 average. The temperature record, however, clearly indicates that there is a warming trend occurring. The annual temperature every year since 2000 in New Mexico has been above the 1900–1999 average according to **Figure 6**.

Figure 6C provides a different perspective that visually combines the temperature and precipitation record. Providing alternative perspectives with the data is another important method in a drought climatology to enhance the understanding of the historical context. In this case, **Figure 6C** uses the historical Water Year, which is an annual representation from October through September of the following year to better represent the water availability in regions like the western U.S., including New Mexico. Many decision-makers manage their activities on a Water Year schedule, so this type of representation would make sense for them. The temperature and precipitation averages for each Water Year are displayed for the 1895–2019 period, with the years since 2000 highlighted in red. In this case, all Water Years in the twenty-first century are warmer than the long-term average, except for 2010, with 10 years being above the long-term average in precipitation (and in the "Wet and Warm" quadrant) and 10

TABLE 3 | New Mexico sc-PDSI identified Drought Events and drought severity since 1895.

Drought event	Drought rank	Start	End	Magnitude	Duration (months)	Severity
DE_P01	25	06/1902	11/1902	13.74	6	2.29
DE_P02	2	11/1903	08/1904	32.37	10	3.24
DE_P03	11	03/1910	03/1911	37.34	13	2.87
DE_P04	16	10/1917	10/1918	34.79	13	2.68
DE_P05	9	08/1922	02/1923	20.28	7	2.90
DE_P06	15	02/1925	07/1925	16.17	6	2.70
DE_P07	4	01/1934	04/1935	48.75	16	3.05
DE_P08	30	10/1943	11/1943	4.37	2	2.19
DE_P09	23	09/1945	09/1946	23.95	10	2.40
DE_P10	17	06/1947	12/1947	18.37	7	2.62
DE_P11	5	03/1950	03/1952	74.91	25	3.00
DE_P12	6	08/1952	09/1957	179.64	61	2.94
DE_P13	31	10/1963	02/1964	10.75	5	2.15
DE_P14	19	06/1964	01/1965	20.65	8	2.58
DE_P15	13	01/1967	07/1967	19.32	7	2.76
DE_P16	18	02/1971	08/1971	18.37	7	2.62
DE_P17	22	03/1972	07/1972	12.44	5	2.49
DE_P18	8	03/1974	08/1974	17.44	6	2.91
DE_P19	28	01/1981	02/1981	4.43	2	2.22
DE_P20	29	05/1989	07/1989	6.57	3	2.19
DE_P21	26	10/1989	01/1990	9.05	4	2.26
DE_P22	14	01/1996	08/1996	21.9	8	2.74
DE_P23	12	02/2000	10/2000	24.94	9	2.77
DE_P24	10	04/2002	01/2003	25.9	9	2.88
DE_P25	7	05/2003	03/2004	32.25	11	2.93
DE_P26	3	01/2006	07/2006	21.85	7	3.12
DE_P27	27	03/2009	11/2009	15.78	7	2.25
DE_P28	1	03/2011	10/2013	106.17	32	3.32
DE_P29	20	01/2014	08/2014	20.43	8	2.55
DE_P30	24	04/2017	09/2017	14.37	6	2.40
DE_P31	21	04/2018	09/2018	15.21	6	2.54

The DE_Ps highlighted in red represent the Top 10 DE_Ps based on the calculated Severity (Equation 3).

TABLE 4 | New Mexico DSCI identified Drought Events (DE_Ds) and drought severity since 2000.

Drought event	Drought rank	Start	End	Magnitude	Duration (months)	Severity
DE_D01	4	05/2002	07/2002	1,099	3	3.66
DE_D02	1	08/2003	03/2004	3,047	8	3.81
DE_D03	6	04/2006	06/2006	991	3	3.30
DE_D04	2	04/2011	12/2011	3,346	9	3.72
DE_D05	8	06/2012	07/2012	607	2	3.04
DE_D06	3	12/2012	08/2013	3,312	9	3.68
DE_D07	7	04/2014	07/2014	1,242	4	3.11
DE_D08	5	03/2018	08/2018	2,019	6	3.37

years below the long-term precipitation average (the "Dry and Warm" quadrant).

Figure 6 shows the co-occurrence of hotter and drier conditions, and highlights the importance of considering their interaction. Increasing temperatures, for example, increase evapotranspiration, which decreases the moisture available for humans, animals, plants, and within the soil.

By evaluating all the above-mentioned drought tools, it can be seen that over the last two decades New Mexico is experiencing more extreme dry periods than wet periods (**Figures 5**, **6**, **Tables 3**, **4**). In **Figure 5**, the sc-PDSI averaged for New Mexico exceeds +2 just one time after 2000, yet regularly falls below −2.0 for the same time period. Based on the data in **Table 3**, each decade during the 1900–1999 period averaged 2.2 DE_Ps, and each DE_P averaging 23.1 months with an average severity value of 2.68. Meanwhile, the two decades since 2000 are averaging 4.5 DE_Ps per decade, each DE_P averaging 47.5 months with an average calculated severity of 2.75. It is also notable, that based of the sc-PDSI, four of the Top 10 DE_Ps occurred since 2000 (**Table 3**).

There have been significant drought events in New Mexico's history, notably DE_P07, DE_P11, and DE_P12 (**Table 3**). But based upon the sc-PDSI it appears that droughts are becoming more frequent and severe in magnitude. This is also supported by the calculated drought severity in **Table 4**. This is in part due to the warming trend New Mexico has been experiencing, especially in the last 20 years. The average temperature from 1900 to 1999 was 11.81°C and the average precipitation was 31.23 mm, where the average temperature from 2000 to 2019 was 12.57°C and average precipitation was 29.79 mm. This combination of an increase in temperature and decrease in precipitation may not seem significant, but for a semi-arid and arid climate that New Mexico's FEW system is built upon, it highly sensitive to these changes in temperature and precipitation.

To further highlight the behavior of the two indices (tools) in representing drought events, **Figure 7** shows a comparison between the sc-PDSI and the DSCI timeseries for New Mexico for the 2000–2019 period. Although the sc-PDSI and DSCI values are opposite in magnitude due to their different scales (**B**), they were consistent in tracking each other for the past 20 years of the USDM data ($r = -0.76$). This demonstrates that both of these tools are detecting similar drought events with slightly different durations and magnitudes, and illustrates the value of looking at more than one drought index to evaluate drought events. Both sources of data confirm key messages and increase the credibility and confidence in the information for the decision-makers. Generally, this also suggest that the use of convergence of evidence approach in drought monitoring is important.

While it is critical to understand historical drought events and how temperature and precipitation have changed over time, a key component for a robust drought climatology is being able to link these drought events with the corresponding drought impacts. The DIR, while a fairly new tool, provides a database that helps to link impacts to different stages of drought events and their magnitude. Understanding this link can help decision-makers understand a drought's progression and anticipate likely future impacts. **Figure 8** depicts all impacts recorded for New

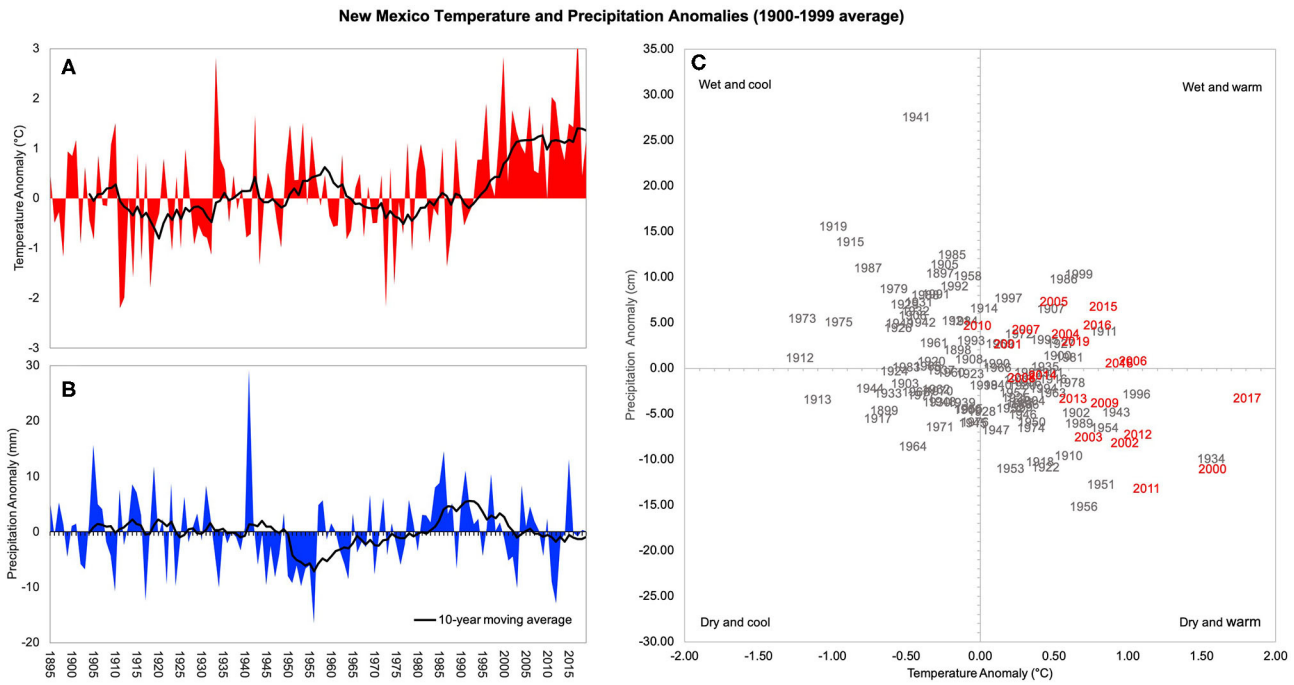

FIGURE 6 | Annual precipitation and temperature anomalies (1900–1999 average) for New Mexico from 1900 to 2019. **(A)** shows a timeseries of New Mexico's annual temperature anomalies and **(B)** precipitation anomalies. **(C)** Compares annual anomalies based on the Water Year (October-September). All 20th century years are gray and 21st century years are red.

Mexico by the DIR since 2005 with an overlay of the DSCI for the same time period. The number of impacts follows the same general trend of the DSCI, and tend to be recorded on the leading edge of a prolonged drought. This makes sense in that impacts in the DIR are recorded as one-off events and plotted here by start date, as end dates are generally unknown. This is an indication that monitoring the conditions leading up to impacts may help provide timely early warning of drought itself, and may actually precede other drought monitoring indicators. It may also relate to different time scales of fast-emerging drought or longer-term drought. Additional analysis is needed to investigate if and when impacts manifest and how this information could be used by decision-makers in drought early warning and drought risk management.

DISCUSSION

New Mexico's economy is highly reliant upon its natural resources. Because of the diverse landscape and arid climate, it is critical for decision-makers to understand the history of previous drought events for effective drought risk management (Finnessey et al., 2016). New Mexico's land cover and land use are characterized by the Chihuahuan Desert in the south and mixed terrains in the west. One of New Mexico's major water resources is the Rio Grande River that runs north-to-south through the center of the state and it supports most of the state's crop production activities through the Elephant Butte Reservoir. A second major river, the Pecos River, originates in the mountains in northern New Mexico and run south, with its basin covering a large part of eastern New Mexico before heading into Texas to eventually join the Rio Grande River.

The agricultural sector brings in ∼$2.5 billion per year into the state's economy and the top two commodities are dairy products and cattle and calves (USDA NASS, 2019). Livestock contributes 81% of the agricultural production value for the state, while crops are the remaining 19% (USDA NASS, 2019). New Mexico's mild climate and its vast land resources (∼92% can be considered as rangelands) provide suitable conditions for grazing for livestock throughout the year (Allison and Ashcroft, 2011; Sawalhah et al., 2019; WRCC, 2019; USDA-NRCS, 2020). However, during winter, summer, drought, and periods with extreme heat events, rangelands productivity decreases leading to increased demand for forage supplements to limit nutritional deficiency of grazing animals (Holechek et al., 2010; Samuelson et al., 2016). A recent study suggested that there have also been some land use land cover changes over some regions in New Mexico that can negatively affected the availability of suitable grazing rangelands that have been attributed mostly to woody plant encroachment (Gedefaw et al., 2020). These feed supplements are mostly based on irrigated and dryland production consisting mainly of combination of hay, grain sorghum, and corn (Schake et al., 1976; Davis et al., 1977; Holechek et al., 1989; Zaied et al., 2020). Agriculture across New Mexico has adapted to its climate, but it also illustrates how important water is for the state, and how droughts and other climate change-related extreme events (Holechek et al., 2020) can have such a significant impact on its economy and the livelihoods of its people.

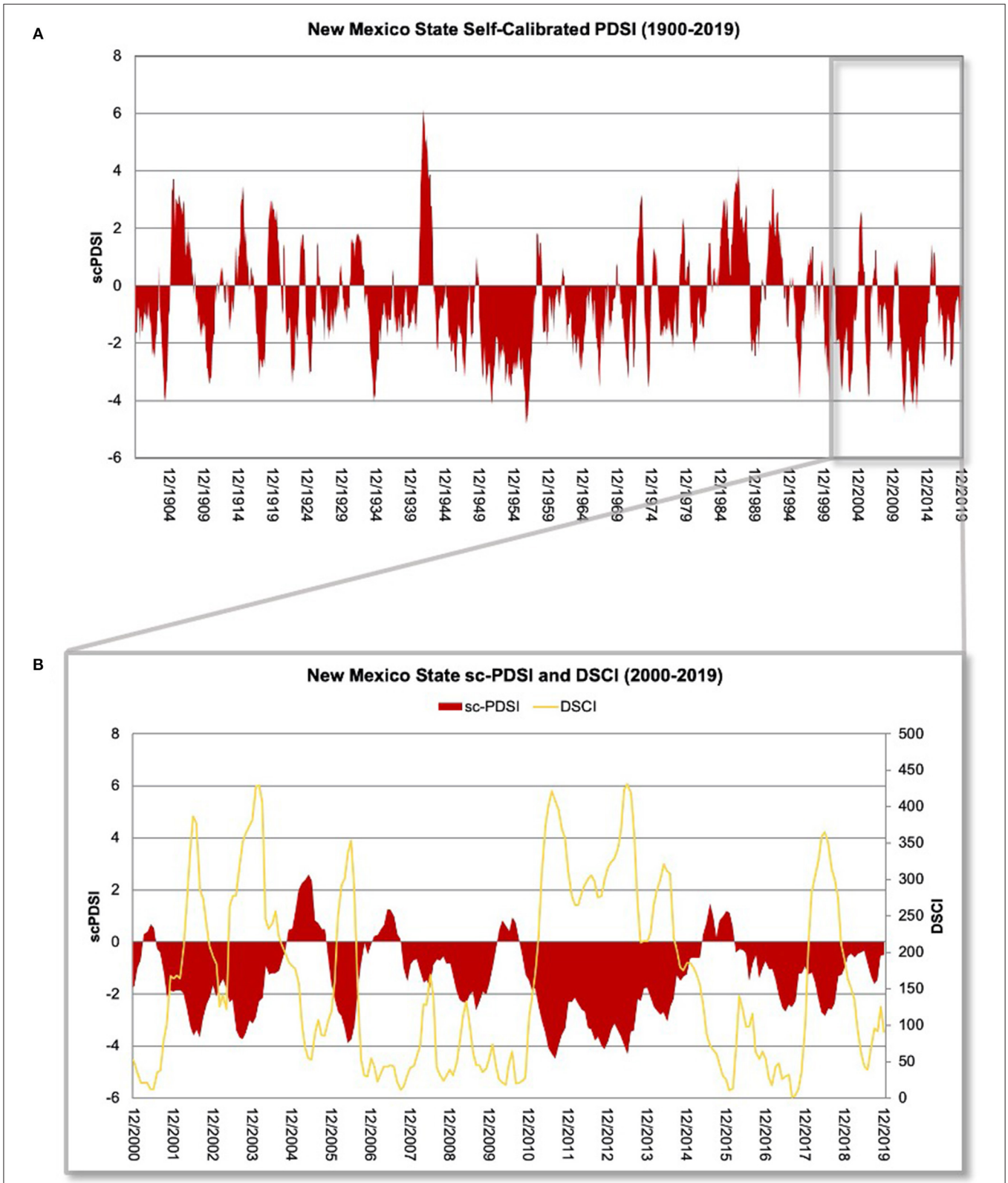

FIGURE 7 | (A) The Self-Calibrating PDSI (sc-PDSC) for the 1900–2019 period and **(B)** a comparison between the sc-PDSI and the DSCI ($r = 0.76$) for the 2000–2019 period over New Mexico.

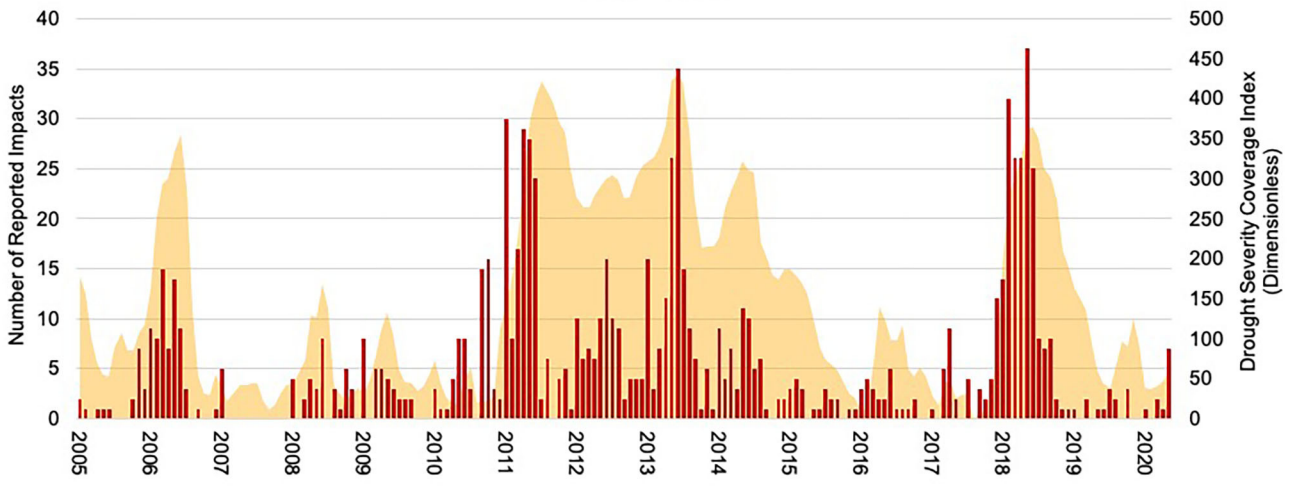

FIGURE 8 | New Mexico monthly drought impacts reported to the DIR and DSCI (2005–2020).

In 2018, New Mexico finished updating the seventh iteration of the New Mexico Drought Plan (NMDP) that was first developed in 1998 (NMOSE and NMWRRI, 2018). The current NMDP has developed a drought response system that is adaptive to changing needs and conditions by incorporating updated and new information. The NMDP has noted the value of triggers to define the timing and selection of drought response actions (NMOSE and NMWRRI, 2018). Previous drought plans had identified seven drought stages used to trigger actions by various entities and the working groups associated with the Drought Task Force (DTF). The 2018 NMDP simplifies and streamlines the previous process by having only three stages, with two triggers responsible for determining the Emergency Drought Stage and the Exception Drought Stage. Drought management actions are outlined for these two stages once the triggers are reached.

The NMDP uses the USDM for its two triggers to initiate the management, adaptation, and mitigation procedures described within the NMDP. These responses are based on the spatial extent of the drought severity categories defined by the USDM. One can use the USDM Tabular Data Archive Tool provided on the USDM (USDM, 2020a) to determine how often the two thresholds have been met in New Mexico. The Emergency Drought Stage has a trigger that is reached when 50% of the state reaches the D2 level on the USDM. The Exceptional Drought Stage reaches its trigger when 20% of the state reaches the D4 level on the USDM (NMOSE and NMWRRI, 2018). Since 2000, the trigger for the Emergency Drought Stage has been exceeded 297 weeks (∼28% of the time). The longest continuous stretch was for 129 weeks between March 2011 and September 2013. The trigger for Exceptional Drought DE_US has been exceeded 64 weeks since 2000, which is ∼6% of the time (**Table 5**). The subscript "U" represents Drought Events specifically identified by the USDM categories. **Figure 9** is a visual representation that highlights when drought conditions met these equivalent triggers. This provides context for how often drought-related management actions take place. It can also provide confidence in the triggers that have been established. The USDM tool allows decision-makers to incorporate similar analyses at a variety of spatial scales for establishing triggers into their decision-making.

TABLE 5 | Drought Events (DE_US) as designated by the USDM thresholds defined in the 2018 New Mexico Drought Plan.

Drought event	Beginning week	Ending week	Duration (Weeks)	Drought stage
DE_U01	May 30, 2000	June 27, 2000	5	Emergency
DE_U02	April 2, 2002	July 2, 2002	14	Emergency
	July 9, 2002	July 23, 2002	3	Exceptional
	July 30, 2002	July 30, 2002	1	Emergency
DE_U03	May 20, 2003	December 16, 2003	31	Emergency
	December 23, 2003	March 30, 2004	15	Exceptional
	April 6, 2004	April 6, 2004	1	Emergency
DE_U04	July 13, 2004	October 5, 2004	13	Emergency
DE_U05	March 7, 2006	July 25, 2006	21	Emergency
DE_U06	March 29, 2011	May 3, 2011	6	Emergency
	May 10, 2011	November 22, 2011	29	Exceptional
	November 29, 2011	April 23, 2013	74	Emergency
	April 30, 2013	August 6, 2013	15	Exceptional
	August 13, 2013	September 3, 2013	5	Emergency
DE_U07	February 18, 2014	July 29, 2014	24	Emergency
DE_U08	January 23, 2018	May 8, 2018	16	Emergency
	May 15, 2018	May 22, 2018	2	Exceptional
	May 29, 2018	October 23, 2018	22	Emergency

The Drought Events (DE_US) identified in the NMDP by the USDM triggers in **Table 5** are very similar to the Drought Events

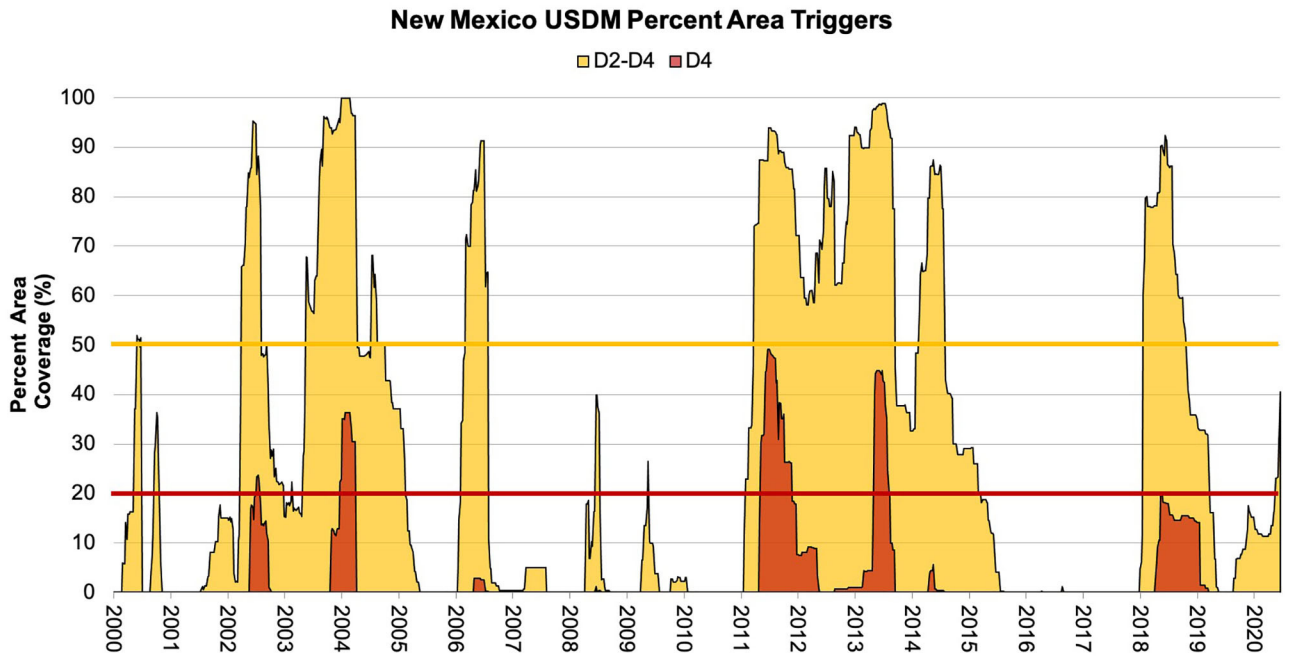

FIGURE 9 | State of New Mexico USDM D2-D4 and D4 categories with the 2018 NMDP equivalent triggers. The yellow line represents the Emergency trigger of 50% area of D2 conditions. The orange line represents the Exceptional trigger of 20% area of D4 conditions.

(DE_{PS}) as depicted by the sc-PDSI in **Table 3** and the DSCI (DE_{DS}) in **Table 4**. The events shown in **Table 5** were defined by weekly conditions, while **Tables 3**, **4** were monthly values. For **Tables 5** and **3**, the 2011–2013 drought stands out as the most severe drought in New Mexico since 2000 with durations of ∼31 and 32 months, respectively. The DSCI threshold for **Table 4** was slightly more restrictive so that the 2011–2013 drought was split into three separate Drought Events during the period for a total of 20 months. No other drought since 2000 in **Table 4** had a duration close to that length.

Understanding how and when drought impacts evolve can help decision-makers make better drought management decisions. Early in the USDM's evolution, a table was developed that provided an overview of how drought impacts might link to the various USDM severity levels (Svoboda et al., 2002). From the outset, this table was meant to provide some guidance on the possible drought impacts and how they relate to drought severity. The table in Svoboda et al. (2002) became a staple item on the USDM website in spite of the recognition that these linkages would be different for different locations around the country (NDMC, 2020). These are broad impacts that do not take into account the location, climatology, or drought history. More recently, Noel et al. (2020) used the DIR to compile the most common impacts for each drought category. **Table 6** displays the most common impacts for each USDM category for the state of New Mexico (USDM, 2020b). The availability of a more tailored table focused on the state or sub-state level will help decision-makers better anticipate impacts associated with emerging drought, and can help inform understanding of historic drought conditions. The combination of **Figure 9** with **Table 6** accomplishes an important aspect of a drought climatology by providing decision-makers with a general idea of what kind of drought impacts might occur with the different drought severity levels on the USDM as a drought event unfolds.

CONCLUSION

New Mexico is highly sensitive to drought conditions due to its variable and limited water supply as well as its normally dry conditions. Climate variability and change increasingly pose significant challenges to the sustainability and resiliency of New Mexico's FEW systems now and into the future, particularly as water resources are further stressed. Drought events and their unique complex human-environment interactions, beyond just the physical drought phenomenon, make them an important climate hazard to focus attention on within the nexus of FEW systems.

Drought early warning and management has advanced significantly over the last 20 years, in large part to the advancement of drought tools. The USDM now has a 20-year history and can be displayed for multiple scales, such as at the state and county levels, and in several different formats. The DSCI is a tool that presents critical information provided by the USDM into a single value for quicker and easier interpretation and response. The simplicity of the DSCI allows decision-makers to use the DSCI as a trigger to initiate drought responses (i.e., NMDP). These advancements in tools lend to more comprehensive drought climatologies to be developed, allowing better understanding how drought has impacted the

TABLE 6 | SDM categories and associated drought impacts for New Mexico (USDM, 2020b).

Category	Description	Reported drought IMPACTS in New Mexico
D0	Abnormally Dry	○ Low soil moisture ○ Increase fire danger
D1	Moderate Drought	○ Supplemental feed and water for Livestock ○ Wildfires abundant
D2	Severe Drought	○ Pasture yield limited; selling livestock ○ Irrigated crops stunted; dry land crops brown? ○ Dust storms ○ Abundance and magnitude of wildfires increase; fuel mitigation practices in effect ○ Wildlife changing feeding patterns ○ Well water decreases
D3	Extreme Drought	○ Livestock suffering; selling herds; high feed costs; emergency CRP grazing ○ Low crop yields ○ Burn bans and firework restrictions could begin; extreme fire ○ Irrigation allotments decrease ○ Vegetation and native trees drying
D4	Exceptional Drought	○ Federal lands begin to close for fire precautions; burn bans increase ○ Bear encroachment; migratory birds changing patterns ○ No surface water left for agriculture; farmers use private wells ○ Rio Grande and other large rivers dry

state of New Mexico in the past and what can be learned from that history. Drought climatologies can be built for any location that has the historical data available, with qualitative (i.e., impacts) and quantitative data providing a more intricate climatology for which more information can be derived by decision-makers.

Until the past few decades, there was not a capability to store and share up-to-date drought impact data. This impact information can elevate already robust drought data, including linking drought indicators with impacts. Our research suggests that monitoring impacts can provide early warning of drought, particularly in conjunction with other drought indicators. Recognizing impacts early can reduce the response time to drought conditions, meaning that decision-makers can take steps to lessen current and future drought impacts.

Drought does not occur in isolation and a state like New Mexico that has an economy heavily dependent upon the land will benefit greatly from having a better understanding of drought and drought impacts throughout the FEW system. Drought climatologies provide valuable information for decision-makers, but there is one limitation that must be considered when building and using historically-derived information, and that is understanding that these climatologies are based upon the assumption of stationarity. Due to climate change, a non-stationarity environment should be taken into consideration when using climatologies to predict future droughts and drought impacts. Regardless, there is still a strong case to understanding how drought has occurred in the past to help with understanding how climate change could influence multiple dimensions of drought.

Another point that was beyond the scope of this study is the discussion about how much the duration of a drought influences the severity, and ultimately the impacts of the drought. A next step is to use the findings from this research and the FEW systems Well-Being Index proposed by Geli et al. (2017) to understand how drought impacts the FEW systems and the well-being of people in New Mexico.

Future research is needed to establish a more detailed link between drought impact information and drought climatologies in New Mexico. Understanding how and when various drought impacts evolve can help prepare decision-makers and stakeholders alike for possible drought impacts in future drought events. Linking drought impacts with drought climatologies will increase the understanding of the effects of drought on FEW systems, allowing for better management of future drought events and the associated impacts.

DATA AVAILABILITY STATEMENT

Publicly available datasets were analyzed in this study. This data can be found at: http://droughtmonitor.unl.edu/; https://wrcc.dri.edu/wwdt/; https://www.fsa.usda.gov/programs-and-services/disaster-assistance-program/index.

AUTHOR CONTRIBUTIONS

LJ conducted the data analysis, in charge of writing the manuscript, and making most of the figures. MH helped to guide the research and manuscript, and provided ideas and edits. HG helped to provide information about New Mexico and how our research applies to New Mexico and the research he is working on. KS provided information on new drought monitoring tools and provided useful data, including advice on the use of the DSCI, to enhance this project. All authors contributed to the article and approved the submitted version.

FUNDING

This research was partially funded by the National Science Foundation (NSF), awards #173935 and #IIA-1301346.

REFERENCES

Abatzoglou, J. T., McEvoy, D. J., and Redmond, K. T. (2017). The west wide drought tracker: drought monitoring at fine spatial scales. *Bull. Am. Meteorol. Soc.* 98, 1815–1820. doi: 10.1175/BAMS-D-16-0193.1

Akyuz, F. A. (2017). *Drought Severity and Coverage Index. United States Drought Monitor.* (Lincoln, NE: The University of Nebraska-Lincoln). Available online

at: https://droughtmonitor.unl.edu/About/AbouttheData/DSCI.aspx (accessed June 24, 2020).

Allison, C. D., and Ashcroft, N. (2011). *New Mexico Range Plants Circular 374 Revised by*. Available online at: https://aces.nmsu.edu/pubs/_circulars/CR374_SM.pdf (accessed September 16, 2020).

Bachmair, S., Svensson, C., Prosdocimi, I., Hannaford, J., and Stahl, K. (2017). Developing drought impact functions for drought risk management. *Nat. Hazards Earth Syst. Sci.* 17, 1947–1960. doi: 10.5194/nhess-17-1947-2017

Davis, D., Schalles, R. R., Kiracofe, G. H., and Good, D. L. (1977). Influence of winter nutrition on beef cow reproduction. *J. Anim. Sci.* 45, 430–437. doi: 10.2527/jas1977.453430x

Ding, Y., Hayes, M. J., and Widhalm, M. (2011). Measuring economic impacts of drought: a review and discussion. *Disaster Prev. Manag.* 20, 434–446. doi: 10.1108/09653561111161752

Finnessey, T., Hayes, M., Lukas, J., and Svoboda, M. (2016). Using climate information for drought planning. *Clim. Res.* 70, 251–263. doi: 10.3354/cr01406

Gedefaw, M. G., Geli, H. M. E., Yadav, K., Zaied, A. J., Finegold, Y., and Boykin, K. G. (2020). A cloud-based evaluation of the National land cover database to support New Mexico's food–energy–water systems. *Remote Sens.* 12:1830. doi: 10.3390/rs12111830

Geli, H. M. E., Hayes, M., Fernald, A., Cibils, A. F., Erickson, C., and Peach, J. (2017). *NSF Award#1739835 - INFEWS/T1 Towards Resilient Food-Energy-Water Systems in Response to Drought Impacts and Socioeconomic Shocks. National Science Foundation*. Available online at: https://www.nsf.gov/awardsearch/showAward?AWD_ID=1739835&HistoricalAwards=false (accessed September 16, 2020).

Hayes, M. J., Svoboda, M., and Redmond, K. T. (2018). "Drought monitoring and early warning: twenty-first century advancements and challenges," in *Drought and Water Crises: Integrating Science, Management, and Policy*, eds D. A. Wilhite and R. S. Pulwarty (Boca Raton, FL: CRC Press), 55–94.

Hayes, M. J., Svoboda, M. D., Wardlow, B. D., Anderson, M. C., and Kogan, F. (2012). "Drought monitoring," in *Remote Sensing of Drought: Innovative Monitoring Approaches*, *eds* B. D. Wardlow, M. C. Anderson, and J. P. Verdin (Back Raton, FL: CRC Press), 1–22.

He, X., Pan, M., Wei, Z., Wood, E. F., and Sheffield, J. (2020). A global drought and flood catalogue from 1950 to 2016. *Bull. Am. Meteorol. Soc.* 101, E508–E535. doi: 10.1175/BAMS-D-18-0269.1

Holechek, J. L., Geli, H. M. E., Cibils, A. F., and Sawalhah, M. N. (2020). Climate change, rangelands, and sustainability of ranching in the Western United States. *Sustainability* 12:4942. doi: 10.3390/su12124942

Holechek, J. L., Pieper, R. D., and Herbel, C. H. (1989). *Range Management. Principles and Practices, 6th Edn*. Englewood Cliffs, NJ: Prentice-Hall.

Holechek, J. L., Pieper, R. D., and Herbel, C. H. (2010). *Range Management: Principles and Practices*, *6th Edn*. London: Pearson. Available online at: https://www.pearson.com/store/p/range-management-principles-and-practices/P100000333785/9780135014165 (accessed February 10, 2020).

Lawrimore, J., Heim, R. R., Svoboda, M., Swail, V., and Englehart, P. J. (2002). Beginning a new era of drought monitoring across North America. *Bull. Amer. Meteor. Soc.* 83, 1191–1192. doi: 10.1175/1520-0477-83.8.1191

Martin, J. T., Pederson, G. T., Woodhouse, C. A., Cook, E. R., McCabe, G. J., Anchukaitis, K. J., et al. (2020). Increased drought severity tracks warming in the United States' largest river basin. *Proc. Natl. Acad. Sci. U.S.A.* 117, 11328–11336. doi: 10.1073/pnas.1916208117

McKee, T. B., Doesken, N. J., and Kleist, J. (1993). "The relationship of drought frequency and duration to time scales," in *8th Conference on Applied Climatology* (Boston), 179–183.

Nam, W.-H., Hayes, M. J., Svoboda, M. D., Tadesse, T., and Wilhite, D. A. (2015). Drought hazard assessment in the context of climate change for South Korea. *Agric. Water Manag.* 160, 106–117. doi: 10.1016/j.agwat.2015.06.029

NDMC (2020). *The National Drought Mitigation Center - United States Drought Monitor*. The National Drought Mitigation Center. Available online at: https://droughtmonitor.unl.edu/ (accessed June 24, 2020).

NMDA (2019). "Rangeland and grazing issues," *in New Mexico Department of Agriculture*. Available online at: https://www.nmda.nmsu.edu/nmda-homepage/divisions/apr/rangeland-and-grazing-issues/ (accessed September 16, 2020).

NMOSE and NMWRRI (2018). *New Mexico Drought Plan: 2018. New Mexico Office of State Engineer & New Mexico Water Resources Research Institute*. Available online at: https://entranosawater.com/documents/711/2018_Drought_Management_Plan__NMDP_Final.pdf (accessed June 6, 2020).

NMSU (2019). *Chaves County Agriculture*. New Mexico State University. Available online at: https://chavesextension.nmsu.edu/adgandhort.html (accessed June 6, 2020).

NOAA NCEI (2020). *U.S. Billion-Dollar Weather and Climate Disasters*. National Centers for Environmental Information NCEI. Available online at: https://www.ncdc.noaa.gov/billions/ (accessed June 6, 2020).

Noel, M., Bathke, D., Fuchs, B., Gutzmer, D., Haigh, T., Hayes, M., et al. (2020). Linking drought impacts to drought severity at the state level. *Bull. Am. Meteorol. Soc.* 101, E1312–E1321. doi: 10.1175/BAMS-D-19-0067.1

Palmer, W. C. (1965). *Meteorological Drought*. Weather Bureau: US Department of Commerce.

Redmond, K. T. (2002). The depiction of drought: a commentary. *Bull. Am. Meteorol. Soc.* 83, 1143–1148. doi: 10.1175/1520-0477-83.8.1143

Samuelson, K. L., Hubbert, M. E., Galyean, M. L., and Löest, C. A. (2016). Nutritional recommendations of feedlot consulting nutritionists: the 2015 New Mexico State and Texas Tech University survey. *J. Anim. Sci.* 94, 2648–2663. doi: 10.2527/jas.2016-0282

Sawalhah, M. N., Holechek, J. L., Cibils, A. F., Geli, H. M. E., and Zaied, A. (2019). Rangeland livestock production in relation to climate and vegetation trends in New Mexico. *Rangel. Ecol. Manag.* 72, 832–845. doi: 10.1016/j.rama.2019.03.001

Schake, L. M., Driedger, A., Riggs, J. K., and Clamme, D. N. (1976). Corn and grain sorghum evaluations for beef cattle. *J. Anim. Sci.* 43, 959–965. doi: 10.2527/jas1976.435959x

Sheffield, J., Wood, E. F., Chaney, N., Guan, K., Sadri, S., Yuan, X., et al. (2014). A drought monitoring and forecasting system for Sub-Sahara African water resources and food security. *Bull. Am. Meteorol. Soc.* 95, 861–882. doi: 10.1175/BAMS-D-12-00124.1

Smith, K. H., Svoboda, M., Hayes, M., Reges, H., Doesken, N., Lackstrom, K., et al. (2015). Local observers fill in the details on drought impact reporter maps. *Bull. Am. Meteorol. Soc.* 95, 1659–1662. doi: 10.1175/1520-0477-95.11.1659

Smith, K. H., Tyre, A. J., Tang, Z., Hayes, M. J., and Akyuz, F. A. (2020). Calibrating human attention as indicator: monitoring #drought in the Twittersphere. *Bull. Am. Meteorol. Soc.* doi: 10.1175/BAMS-D-19-0342.1

Stahl, K., Kohn, I., Blauhut, V., Urquijo, J., De Stefano, L., Acacio, V., et al. (2015). Impacts of European drought events: insights from an international database of text-based reports. *Nat. Hazards Earth Syst. Sci. Discuss.* 3, 5453–5492. doi: 10.5194/nhessd-3-5453-2015

Steinemann, A., Iacobellis, S. F., and Cayan, D. R. (2015). Developing and evaluating drought indicators for decision-making. *J. Hydrometeorol.* 16, 1793–1803. doi: 10.1175/JHM-D-14-0234.1

Sutanto, S. J., Van Lanen, H. A. J., Wetterhall, F., and Llort, X. (2020). Potential of pan-european seasonal hydrometeorological drought forecasts obtained from a multihazard early warning system. *Bull. Am. Meteorol. Soc.* 101, E368–E393. doi: 10.1175/BAMS-D-18-0196.1

Svoboda, M., LeComte, D., Hayes, M., Heim, R., Gleason, K., Angel, J., et al. (2002). The drought monitor. *Bull. Am. Meteorol. Soc.* 83, 1181–1190. doi: 10.1175/1520-0477-83.8.1181

Svoboda, M. D., Fuchs, B. A., Poulsen, C. C., and Nothwehr, J. R. (2015). The drought risk atlas: enhancing decision support for drought risk management in the United States. *J. Hydrol.* 526, 274–286. doi: 10.1016/j.jhydrol.2015.01.006

USDA – FSA (2020). *Disaster Assistance - Livestock Forage Disaster Program LFP. LFP - LivestockForage Disaster Program*. Available online at: https://www.fsa.usda.gov/Assets/USDA-FSA-Public/usdafiles/FactSheets/livestock_forage_program_lfp-fact_sheet.pdf (accessed September 16, 2020).

USDA NASS (2018). "New Mexico agricultural statistics," in *2017 Annual Bulletin*. (Las Cruces, NM). Available online at: https://www.nass.usda.gov/Statistics_by_State/New_Mexico/Publications/Annual_Statistical_Bulletin/2017/2017-NM-AG-Statistics.pdf (accessed September 16, 2020).

USDA NASS (2019). "New Mexico state and county data," in *2017 Census of Agriculture*. Available online at: https://www.nass.usda.gov/Publications/AgCensus/2017/Full_Report/Volume_1,_Chapter_1_State_Level/New_Mexico/nmv1.pdf

USDA-NRCS (2020). *NRI Land Cover Use | NRCS New Mexico.* Available online at: https://www.nrcs.usda.gov/wps/portal/nrcs/detail/nm/technical/dma/nri/?cid=nrcs144p2_068841 (accessed January 20, 2020).

USDM (2019). *What is the U.S. Drought Monitor? United States Drought Monitor.* The United States Drought Monitor. Available online at: https://droughtmonitor.unl.edu/AboutUSDM/WhatIsTheUSDM.aspx (accessed June 6, 2020).

USDM (2020a). *United States Drought Monitor - Tabular Data Archive.* The United States Drought Monitor. Available online at: https://droughtmonitor.unl.edu/Data/DataTables.aspx (accessed June 24, 2020).

USDM (2020b). *United States Drought Monitor - Drought Impacts by State.* The United States Drought Monitor. Available online at https://droughtmonitor.unl.edu/Data/StateImpacts.aspx. (accessed September 15, 2020).

Wells, N., Goddard, S., and Hayes, M. J. (2004). A self-calibrating Palmer drought severity index. *J. Clim.* 17, 2335–2351. doi: 10.1175/1520-0442(2004)017<2335:ASPDSI>2.0.CO;2

Wilhite, D., and Pulwarty, R. S. (2005). "Drought and water crises: lessons learned and the road ahead," in *Drought and Water Crises: Science, Technology, and Management Issues.* 389–398. doi: 10.1201/9781420028386.pt4

Wilhite, D. A. (2018). "National drought management policy guidelines: a template for action," in *Drought and Water Crises: Integrating Science, Management, and Policy*, eds D. A. Wilhite and R. S. Pulwarty (Boca Raton, FL: CRC Press), 55–94.

Wilhite, D. A., Sivakumar, M. V. K., and Pulwarty, R. (2014). Managing drought risk in a changing climate: the role of national drought policy. *Weather Clim. Extremes* 3, 4–13. doi: 10.1016/j.wace.2014.01.002

Wilhite, D. A., Svoboda, M. D., and Hayes, M. J. (2007). Understanding the complex impacts of drought: a key to enhancing drought mitigation and preparedness. *J Water Resour. Manag.* 21, 763–774. doi: 10.1007/s11269-006-9076-5

World Meteorological Organization (WMO) and Global Water Partnership (GWP) (2016). *Handbook of Drought Indicators and Indices (M. Svoboda and B.A. Fuchs). Integrated Drought Management Programme (IDMP), Integrated Drought Management Tools and Guidelines Series 2.* Geneva: World Meteorological Organization (WMO) and Global Water Partnership (GWP).

WRCC (2019). *Climate of New Mexico*. Available online at: https://wrcc.dri.edu/Climate/narrative_nm.php (accessed October 22, 2020).

WRI (2020). *Aqueduct Water Risk Atlas - World Resources Institute. Aqueduct Water Risk Atlas.* Available online at: https://www.wri.org/resources/maps/aqueduct-water-risk-atlas (accessed January 4, 2020).

Zaied, A. J., Geli, H. M. E., Holechek, J. L., Cibils, A. F., Sawalhah, M. N., and Gard, C. C. (2019). An evaluation of historical trends in new mexico beef cattle production in relation to climate and energy. *Sustainability* 11:6840. doi: 10.3390/su11236840

Zaied, A. J., Geli, H. M. E., Sawalhah, M. N., Holechek, J. L., Cibils, A. F., and Gard, C. C. (2020). Historical trends in new mexico forage crop production in relation to climate, energy, and rangelands. *Sustainability* 12:2051. doi: 10.3390/su12052051

Conflict of Interest: The authors declare that the research was conducted in the absence of any commercial or financial relationships that could be construed as a potential conflict of interest.

frontiers in Climate

ORIGINAL RESEARCH
published: 14 December 2020
doi: 10.3389/fclim.2020.571836

Climate Extreme Seeds a New Domoic Acid Hotspot on the US West Coast

Vera L. Trainer[1]*, *Raphael M. Kudela*[2], *Matthew V. Hunter*[3], *Nicolaus G. Adams*[1] and *Ryan M. McCabe*[4,5]

[1] Environmental and Fisheries Science Division, Northwest Fisheries Science Center, National Marine Fisheries Service, National Oceanic and Atmospheric Administration, Seattle, WA, United States, [2] Ocean Sciences Department, University of California Santa Cruz, Santa Cruz, CA, United States, [3] Oregon Department of Fish and Wildlife, Astoria, OR, United States, [4] Joint Institute for the Study of the Atmosphere and Ocean, University of Washington, Seattle, WA, United States, [5] Cooperative Institute for Climate, Ocean, and Ecosystem Studies, University of Washington, Seattle, WA, United States

A heatwave that blanketed the northeast Pacific Ocean in 2013–2015 had severe impacts on the marine ecosystem through altered species composition and survival. A direct result of this marine heatwave was a sustained, record-setting harmful algal bloom (HAB), caused by the toxigenic diatom, *Pseudo-nitzschia*, that led to an unprecedented delay in harvest opportunity for commercial Dungeness crab (*Metacarcinus magister*) and closure of other recreational, commercial and tribal shellfish harvest, including razor clams. Samples collected during a cruise in summer 2015, showed the appearance of a highly toxic "hotspot" between Cape Mendocino, CA and Cape Blanco, OR that was observed again during cruises in the summers of 2016–2018. The transport of toxic cells from this retentive site northward during wind relaxations or reversals associated with storms resulted in economically debilitating delay or closure of Dungeness crab harvest in both northern California and Oregon in 2015–2019. Analyses of historic large-scale *Pseudo-nitzschia* HABs have shown that these events occur during warm periods such as El Niño, positive phases of the Pacific Decadal Oscillation, or the record-setting marine heatwave. In order to reduce the impacts of large-scale HABs along the west coast of North America, early warning systems have been developed to forewarn coastal managers. These early warning systems include the Pacific Northwest and California HAB Bulletins, both of which have documented elevated domoic acid and increased risk associated with the northern California hotspot. These early warnings enable mitigative actions such as selective opening of safe harvest zones, increased harvest limits during low risk periods, and early harvest in anticipation of impending HAB events. The aims of this study are to show trends in nearshore domoic acid along the US west coast in recent years, including the recent establishment of a new seed bed of highly-toxic *Pseudo-nitzschia*, and to explore how early warning systems are a useful tool to mitigate the human and environmental health and economic impacts associated with harmful algal blooms.

Keywords: climate extremes, weather extremes, climate change, climate services, early warning, harmful algal blooms, domoic acid

OPEN ACCESS

Edited by:
Chris C. Funk, United States Geological Survey (USGS), United States

Reviewed by:
Ladislaus Benedict Chang'A, Tanzania Meteorological Agency, Tanzania
Elisa Berdalet, Consejo Superior de Investigaciones Científicas (CSIC), Spain
Dann Mitchell, University of Bristol, United Kingdom

***Correspondence:**
Vera L. Trainer
vera.l.trainer@noaa.gov

Specialty section:
This article was submitted to Climate Services, a section of the journal Frontiers in Climate

Received: *12 June 2020*
Accepted: *13 November 2020*
Published: *14 December 2020*

Citation:
Trainer VL, Kudela RM, Hunter MV, Adams NG and McCabe RM (2020) Climate Extreme Seeds a New Domoic Acid Hotspot on the US West Coast. Front. Clim. 2:571836. doi: 10.3389/fclim.2020.571836

INTRODUCTION

The effects of climate change on marine ecosystems will be long lasting. The impacts of climate change on marine biota, including the shifting range of marine species to higher latitudes, have decreased food security, and enhanced the decline of coral reefs by 70–90% at 1.5°C warming (IPCC, 2018). The International Panel on Climate Change report documented a high confidence of increased frequency and range of harmful algal blooms (HAB) in coastal areas since the 1980s, attributed partly to the effects of ocean warming and marine heatwaves (Collins et al., 2019). The probability of recent high-impact marine heatwaves has increased by more than 20-fold as a result of climate change (Laufkötter et al., 2020). The 2013–2015 marine heatwave that caused large-scale marine ecosystem impacts in the northeast Pacific was five times more likely to occur due to anthropogenic forcing over natural variability alone. This was determined through fraction of attributable risk analysis which compared observed trends and anomalies with model predictions (Weller et al., 2015; Di Lorenzo and Mantua, 2016) to assess the probability of extreme events occurring with and without anthropogenic influences (Stott et al., 2004). A direct result of this marine heatwave was a sustained, record-setting HAB, caused by the toxigenic diatom, *Pseudo-nitzschia*. The toxin, domoic acid (DA), produced by this diatom, accumulated in shellfish, resulting in an unprecedented delay in harvest opportunity for the commercial Dungeness crab (*Metacarcinus magister*) and closure of other recreational, commercial and tribal shellfish harvest (McCabe et al., 2016; McKibben et al., 2017).

Entanglements of mostly humpback whales (*Megaptera novaeangliae*), were an indirect result of the 2015 HAB event because the delay of the crab season opener resulted in higher numbers of crab pot lines than usual along the whale migration routes (NOAA Fisheries, 2018; Saez et al., 2020; Santora et al., 2020). A record number of illnesses and deaths of marine mammals (McCabe et al., 2016) and seabirds (Piatt et al., 2020) were caused both by food web transfer of HAB toxins (McCabe et al., 2016) and habitat compression into a geographically reduced coastal zone of food availability (Santora et al., 2020). An analysis of the historical record of large-scale *Pseudo-nitzschia* HABs has demonstrated that these events tend to occur during periods of anomalously warm ocean conditions such as El Niño, positive phases of the Pacific Decadal Oscillation (PDO), or the record-setting marine heatwave (McCabe et al., 2016; McKibben et al., 2017). Anomalous poleward currents together with fewer reversals (Sanford et al., 2019), facilitated the northward advection of a species of *Pseudo-nitzschia australis*, not usually found northward of California in the springtime (McCabe et al., 2016). Low nutrients were associated with the warm water mass that hosted the *Pseudo-nitzschia* population that subsequently bloomed when advected toward the coast into the nutrient-rich upwelled water (Trainer et al., 2020).

This observation of *P. australis* (McCabe et al., 2016) further north than usual in 2015, exemplified a range extension that included marine fish, mollusks, tunicates, bryozoans, cnidarians, crustaceans, and echinoderms (Sanford et al., 2019). In particular, northern California is a key transition zone between the milder temperate taxa found within the southern California Current and the cooler temperate species found further north, making this region an "ideal barometer" for observing such geographical range expansion in response to warming events (Sanford et al., 2019). Here we analyze annual trends in nearshore DA that were altered by the 2013–2015 marine heatwave by establishing a new seed bed of highly-toxic *Pseudo-nitzschia*, and explore how early warning systems are a useful tool to mitigate the human and environmental health and economic impacts associated with harmful algal blooms.

MATERIALS AND METHODS

Research Cruise Samples

Whole seawater was collected from 3 to 5 m depth on research cruises by Niskin bottle or scientific seawater supply in 1998 (described in Trainer et al., 2000); Niskin bottle (NOAA Ship Bell M. Shimada, 2012; 2016; 2018) and via the scientific seawater system aboard the NOAA Ship Miller Freeman (2009) and NOAA Ship Bell M. Shimada (2015, described in McCabe et al. (2016); also 2017; 2019).

Sea Surface Temperature

Analysis of satellite-derived sea surface temperature for the region of interest utilized the Multi-Scale Ultra-high Resolution Sea Surface Temperature (MURSST) product MUR-JPL-L4-GLOB-v4.1 (JPL MUR MEaSUREs Project, 2015). This is a global, gap-free, gridded, daily 1 km Sea Surface Temperature (SST) dataset created by merging multiple Level-2 satellite SST datasets. For this analysis monthly averages were created by averaging the months September-November 2002–2013 and 2014–2019, and the difference was calculated by subtracting the 2014–2019 average from the 2002–2013 average.

Seawater Domoic Acid

Particulate (cellular) DA was analyzed by filtering 1L seawater collected from surface waters onboard cruises using a bucket or Niskin bottle and analyzed using the [^{3}H]kainic acid-based receptor binding assay for the 1998 cruise (Trainer et al., 2000), or the Biosense or PNW enzyme-linked immunosorbent assay for all other cruises (Eberhart et al., 2012).

Dungeness Crab Domoic Acid

DA in Dungeness crab (*Metacarcinus magister*) was measured using standard high-performance liquid chromatography (Wekell et al., 1994). These data were kindly provided by the OR Department of Agriculture and the California Department of Public Health.

Early Warning System Implementation

Transition plans for the conversion of HAB Bulletins from research to operations have been developed for many regions of the US (https://coastalscience.noaa.gov/research/stressor-impacts-mitigation/hab-monitoring-system/). Some forecasts are fully operational (e.g., Lake Erie); others are in the process of transition. Successful transition will depend on collaborative approaches to ensure full operational support,

including partnerships with the Integrated Ocean Observing System (Anderson et al., 2019), state monitoring organizations such as the Olympic Region Harmful Algal Bloom partnership and health departments (Trainer and Suddleson, 2005) as well as private companies (e.g., https://www.oceanaero.com/) to ensure the availability of advanced technologies to improve forecasts.

RESULTS

A Retentive Feature Is A New Initiation Site for Toxigenic *Pseudo-nitzschia*

Toxigenic *Pseudo-nitzschia* blooms are known to initiate in highly retentive regions, designated as HAB "hotspots" along the west coast, including the Juan de Fuca eddy, Heceta Bank, Monterey Bay, and Point Conception (Trainer et al., 2001, 2012). However, the 2015 bloom was different. The warm water anomaly was found to be a source of *Pseudo-nitzschia* that were delivered to the coast after a series of spring storms, where these cells grew rapidly to bloom proportions when fueled by nutrients from upwelled waters close to shore (McCabe et al., 2016; Trainer et al., 2020). Among the locations that showed record levels of cellular (particulate) DA was a site near the California and Oregon border (McCabe et al., 2016). The emergence of this new toxin source region is also evident from both a compilation of historical observations collected from ships of opportunity and shore stations (**Figure 1**), as well as from the California Harmful Algae Risk Mapping (C-HARM) predictive statistical model (Anderson et al., 2016). Both the observations and the model identified the Humboldt (Trinidad Head) region as particularly toxic during 2015, with maximum total DA (particulate plus dissolved) exceeding 15,000 ng/L and DA in razor clams at a record level of 340 ppm (McClatchie et al., 2016). The C-HARM model continued to predict elevated probabilities of HABs in the region through 2018 (Wells et al., 2017; Thompson et al., 2018).

The coastwide 2015 bloom appears to have "seeded" *Pseudo-nitzschia* cells to a site near Trinidad, California where high concentrations of DA were measured (**Figure 2**, red circled area). Cruises of opportunity prior to 2015, including summer cruises in 1998, 2009, and 2012, showed low concentrations of particulate DA near the California/Oregon border (**Figure 2**), suggesting that either lower abundances or less toxic species of *Pseudo-nitzschia* were found at this site prior to 2015. During a cruise from 7 to 10 August 1997 (data not shown), low concentrations of particulate DA, ranging from 200 to 500 ng/L, were measured at several stations between the Cape Mendocino and the CA/OR border. However, during the cruise in summer 2015 (McCabe et al., 2016), a more toxic DA "hotspot" was observed between Cape Mendocino, CA and Cape Blanco, OR that remained evident over 3–4 subsequent summers (**Figures 2**, **3**). These data suggest that this site was freshly seeded with the more toxigenic species, *P. australis*, promoting higher DA toxicity in filter-feeding organisms in the region. In fact, *Pseudo-nitzschia* measured at this physically-retentive site have impacted Dungeness crab harvest in both CA and OR where frequent DA closures or harvest delays were first observed in 2015 and continued through early 2019 (**Table 1**), with Humboldt County (**Figure 4**) the last county in California to open for harvesting in 2015.

Time series data from 2015, 2017, 2018 demonstrate that northern CA crab were first reported to be toxic (above the regulatory limit of 30 ppm DA), with southern and central

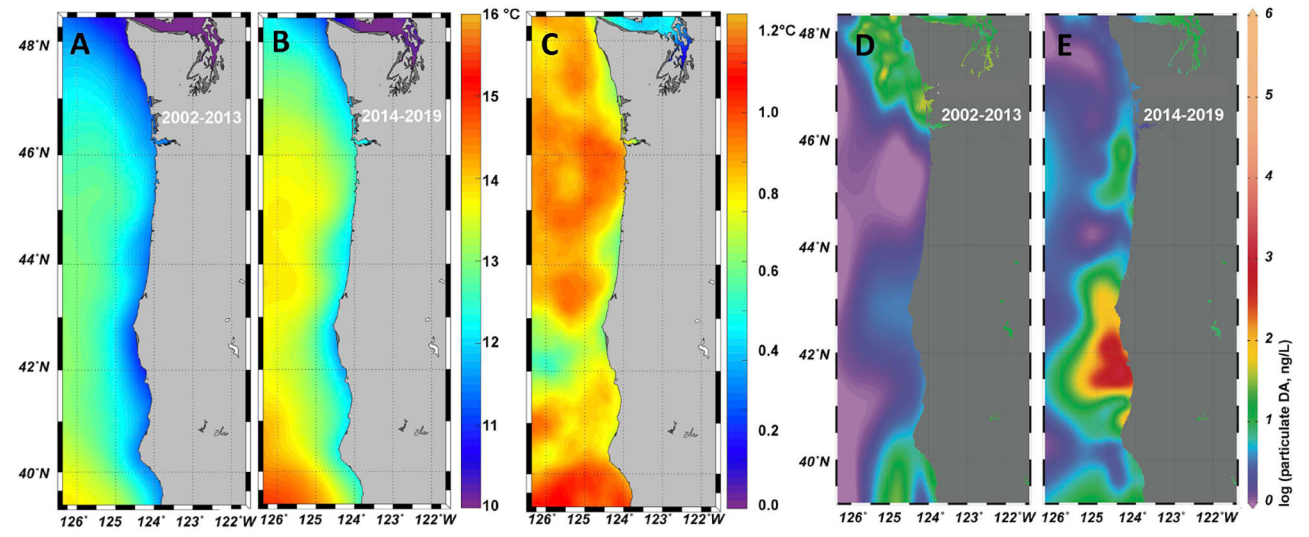

FIGURE 1 | Sea surface temperature from the Multi-scale Ultra-High Resolution Sea Surface Temperature (MURSST) monthly product for September–November is shown for 2002–2013 **(A)** and 2014–2019 **(B)**. The difference **(B–A)** is shown in panel **(C)**. A large dataset of particulate domoic acid (pDA), collated from multiple programs along the US west coast, includes shore-based observations. Data from 2002–2013 **(D)** and 2014–2019 **(E)** were spatially interpolated using DIVA in OceanDataView. The northern California region of enhanced toxicity is prominent in the 2014–2019 dataset, and consistent with the expected optimal temperature for DA production (Ryan et al., 2017; Kudela et al., 2020).

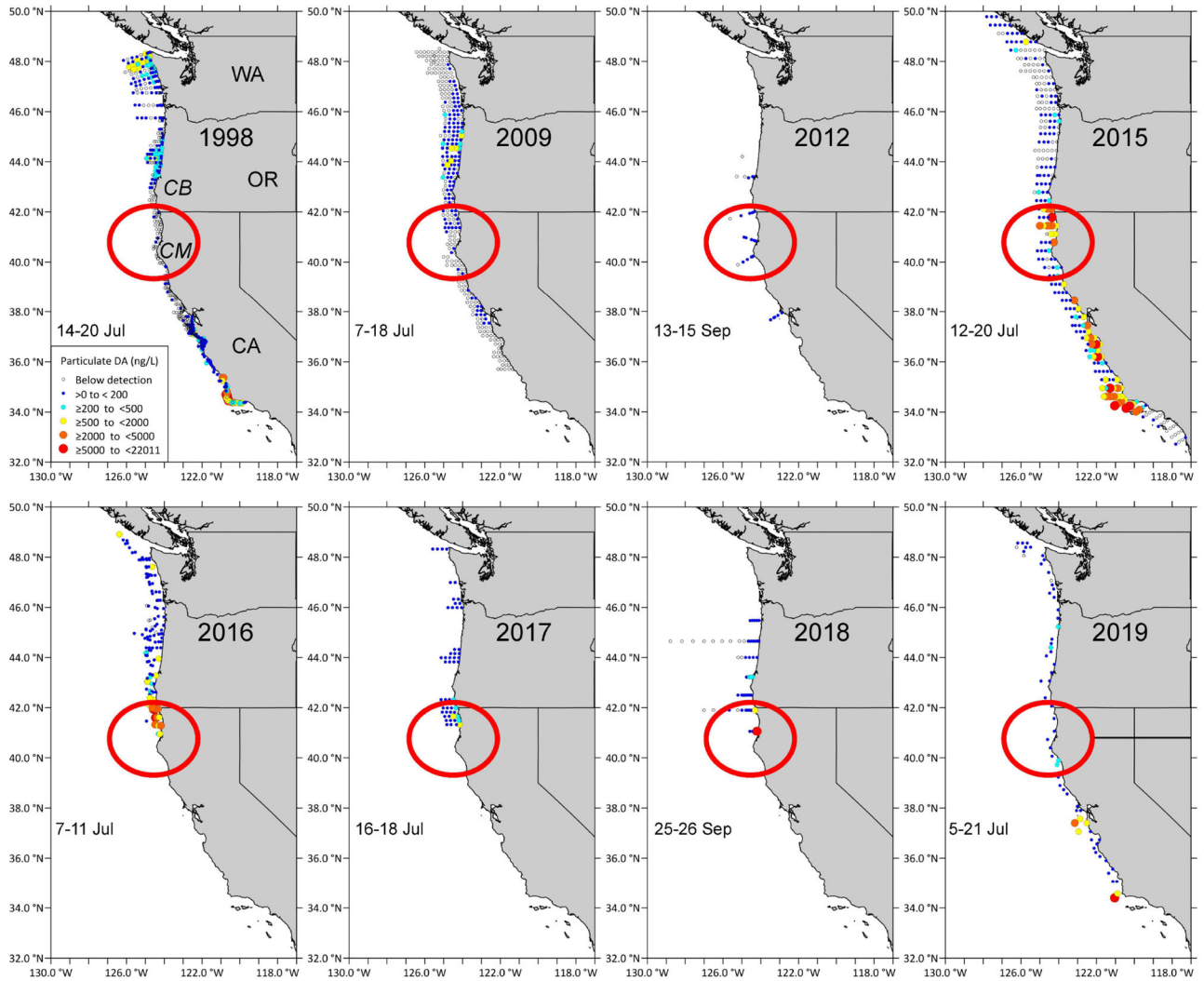

FIGURE 2 | Domoic acid first appeared at the "hotspot" site between Cape Blanco (CB) in OR and Cape Mendocino (CM) in 2015 (red circle). Particulate domoic acid concentrations (ng/L; see legend inside the 1998 map) at stations sampled during summer cruises in 1998, 2008, 2012, 2015, 2016, 2017, 2018, 2019. The dates when stations in the red circled area that is centered around Trinidad, California, were sampled are shown on each panel.

OR crab becoming toxic about 1 week later (**Figure 3**). This is consistent with northward transport of toxigenic cells from the CA hotspot site during periods of relaxations or northward wind reversals associated with storm events near the time of the fall transition (Kosro, 1987; Send et al., 1987). A site of high DA between Cape Blanco and Cape Mendocino was not observed in summer 2019 (**Figure 3**). However, a single station with elevated particulate DA was noted just south of Cape Mendocino.

DISCUSSION

Northern California Transition Zone

The northern CA region has been called an "ideal barometer" (Sanford et al., 2019) for documenting geographic range expansion and shifts in nearshore community composition. This region is an important transition zone where the poleward migration of marine species in response to warming events has been documented (Sagarin et al., 1999; Sanford et al., 2019). During 2014–2016, alongshore currents exhibited anomalously higher poleward flows which were estimated to have transported plankton over maximum distances of ∼500 km in a month (Sanford et al., 2019). Plankton and marine larvae were transported northward over such large distances, with fewer reversals to facilitate their return southward (Sanford et al., 2019), allowing them to be established as new populations in more northern ecosystems. This diffusive transport was enhanced by retentive features or offshore mesoscale eddies especially after the spring transition when mean flow in the California Current System typically is equatorward. The intensified upwelling at coastal headlands (Davis, 1985; Kelly, 1985), including Cape Blanco (Barth et al., 2000) and Cape Mendocino (Largier et al., 1993) provides nutrients to fuel phytoplankton blooms,

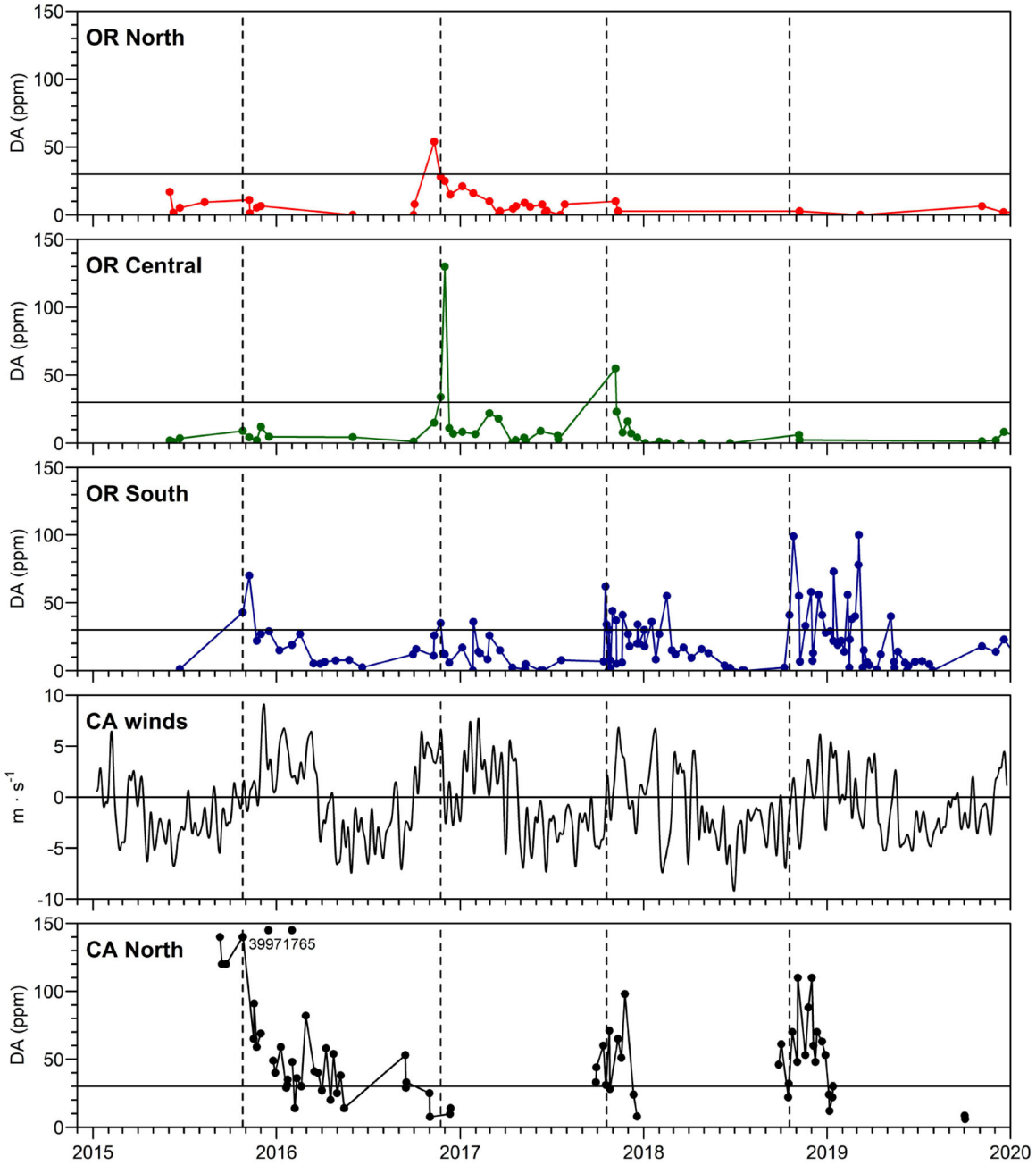

FIGURE 3 | Maximum DA concentrations in Dungeness crab viscera in northern California and southern, central and northern Oregon. The regulatory closure level of 30 ppm DA is shown as a horizontal line on each crab panel. Dotted vertical lines show first appearance of DA above 30 ppm in southern OR crab (which follows DA above 30 ppm in northern CA in all years except 2017). Numbers on the northern CA panel show values of crab DA exceeding the y-axis scale. The north-south component of low pass filtered winds (m s^{-1}), filtered with a 15-day Hanning window, is shown from buoy 46027-6 (location shown in **Figure 4**). Linear regressions with other nearby wind sources were used to fill gaps in the wind time series. Map of regions used for calculation of maximum DA in Dungeness crab, also showing locations of Cape Mendocino (CM) and Cape Blanco (CB). Humboldt County, CA, is found in **Figure 4**.

including HABs (Kudela et al., 2005). Areas on the lee side of coastal headlands are often associated with retentive eddies (Largier et al., 1993; Barth et al., 2000). To summarize, the anomalous poleward flows, such as those observed during 2014–2016, resulted in a higher probability of northward transport of particles (Sanford et al., 2019) such as phytoplankton, and their increased retention near coastal headlands. Indeed, *P. australis*, a highly toxic species typically observed only as far north in the springtime as central California, was detected in northern CA, OR and WA in the spring 2015 (McCabe et al., 2016). This

TABLE 1 | Oregon State harvest actions due to elevated domoic acid in Dungeness crab viscera (2015–2019).

	Ocean commercial crab fishery			Recreational crab fishery		
Year	**Time frame**	**Area**	**Regulatory action**	**Time frame**	**Area**	**Regulatory action**
2015	12/1/15–1/4/16	Coastwide	2015–16 opening delay	11/3/15–11/12/15	Cape Arago to OR/CA border	Evisceration advisory
				11/13/15–12/21/15	Heceta Head to OR/CA border	Closure
2016	12/1/16–12/17/16	Cape Blanco to OR/CA border	2016-17 crab season opening delay	11/18/16–12/20/16	Tillamook Head to OR/CA border	Closure
	12/1/16–12/31/16	OR/WA border to Cape Blanco	2016-17 crab season opening delay			
2017	1/25/17–2/09/17	Heceta Head to Cape Arago	2016–17 in-season evisceration	2/1/17–2/9/17	Heceta Head to Cape Arago	Closure
	12/1/17–1/15/18	Bandon to Cape Blanco	2017–18 crab season opening delay	10/21/17–12/31/17	Bandon to OR/CA border	Closure
	12/1/17–2/6/18	Cape Blanco to OR/CA border	2017–18 crab season opening delay			
2018	2/13/18–2/27/18	Cape Blanco to OR/CA border	2017–18 in-season evisceration	1/1/18–1/31/18	Cape Blanco to OR/CA border	Closure
	12/1/18–1/31/19	Cape Arago to OR/CA border	2018–19 season opening delay	2/16/18–3/4/18	Cape Blanco to OR/CA border	Closure
				10/19/18–12/31/18	Cape Blanco to OR/CA border	Closure
2019	2/11/19–3/27/19	Bandon to OR/CA border	2018–19 in-season evisceration	1/1/19–1/30/19	Cape Blanco to OR/CA border	Closure
	5/8/19–5/22/19	Cape Blanco to OR/CA border	2018–19 in-season evisceration	2/14/19–3/28/19	Bandon to OR/CA border	Closure
				5/10/19–5/24/19	Cape Blanco to OR/CA border	Closure

Time frame indicates periods of regulatory action. If outside that timeframe, harvest was open unless closed by permanent regulations. The commercial ocean crab season spans 2 calendar years with a targeted opening date of 12/1 in calendar year 1 and closing on 8/14 in calendar year 2. The season can be delayed due to low meat yield, elevated DA levels in crab viscera or a combination of both. In mid-2017, the commercial Dungeness crab management authorities created 12 distinct areas along the coast for biotoxin and meat quality determination to avoid confusion over the delineation of a closed/open areas. Recreational Dungeness crab does not use these areas, which explains the different areas for commercial vs. recreational closures. For geographical areas of regulatory actions, see ***Figure 4****. Opening and closings of the crab fishery multiple times in a season caused confusion. The differences in commercial and recreational harvest closures and evisceration regulations in OR but not CA or WA has caused instability to this fishery. The recreational crab harvest in the ocean by boat is closed from 16 October thru 30 November. The recreational season is open in the bays and estuaries and from shore all year. The commercial season is closed 15 August thru 30 November in the ocean but open in the bays and estuaries (except Columbia River) from Labor Day until 30 November.*

provided an opportunity for this high DA-producing species to be "seeded" to the retentive site near the CA/OR border for future initiation of *Pseudo-nitzschia* blooms. During the 2015 event, *P. australis* emerged from a background of multiple *Pseudo-nitzschia* species, and dominated along almost the entire U.S. west coast, whereas during other years, less toxic species such as *P. delicatissima* have dominated, resulting in large blooms but with lower toxicity (Bowers et al., 2018; Smith et al., 2018).

Seeding Techniques

Pseudo-nitzschia species are a major component of marine snow due to their ability to form long chains that can become intertwined while they sink to depths. This shower of organic material that cascades from surface waters to depth can transport DA to the benthos where it has been measured in benthic organisms, including bottom dwelling fish, worms, crustaceans (Vigilant and Silver, 2005, 2007; Kvitek et al., 2008) and Dungeness crab (Taylor, 1993). Toxigenic *Pseudo-nitzschia* and their inherent DA can sink to as deep as 800 m, providing a source of toxin to benthic filter feeders (Schnetzer et al., 2007; Sekula-Wood et al., 2009, 2011). In the Gulf of Mexico, ∼50% of *Pseudo-nitzschia* cells present in the water column sank into sediment traps with ∼10% as live cells (Dortch et al., 1997). *Pseudo-nitzschia* found in sediments were intact, contained pigment and maintained their chain formation (Sekula-Wood et al., 2009). The flux of *Pseudo-nitzschia* to sediments can be as high as 3.2×10^8 cells/m^{-2}/day (Sekula-Wood et al., 2011). More than 80% of DA contained in a surface bloom is estimated to reach sediments >500 m deep (Schnetzer et al., 2017) and previous studies off OR have demonstrated that floc collected from the bottom boundary layer can seed a surface bloom of diatoms, including *Pseudo-nitzschia*, under simulated upwelling conditions (Wetz et al., 2004). Furthermore, sediment trap data suggests that once *Pseudo-nitzschia* are seeded into a retentive region, blooms will be frequent and increasing in intensity. A 15-year time series of sediment from the Santa Barbara Channel indicates that this region was seeded with *Pseudo-nitzschia* in the mid-1990s with increasingly toxic blooms occurring annually (Sekula-Wood

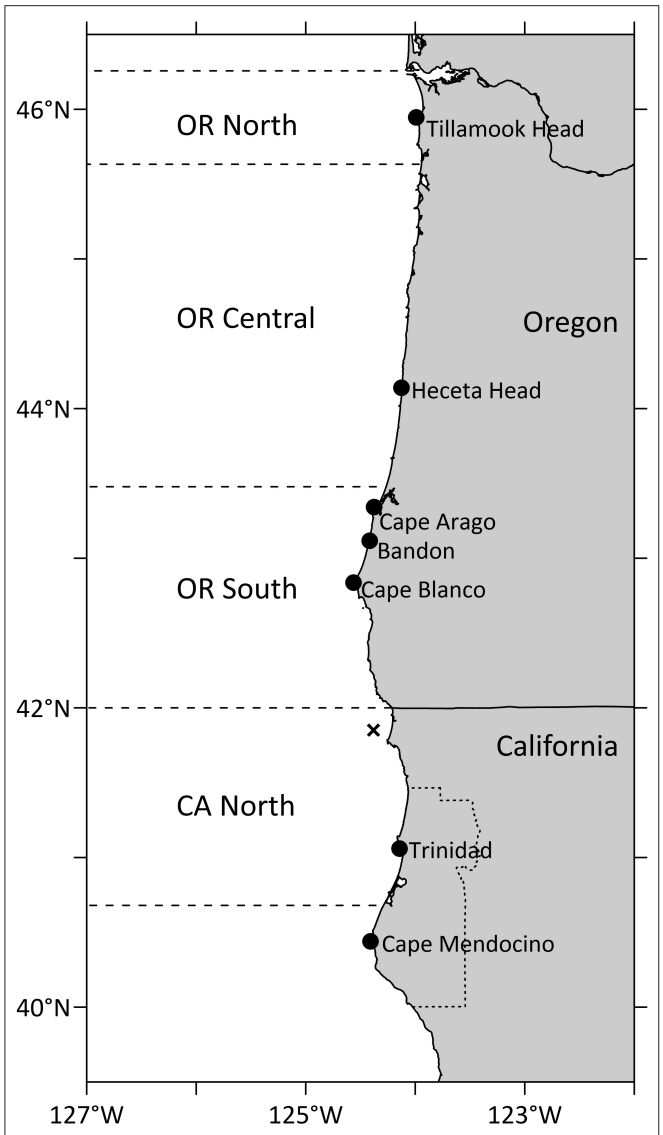

FIGURE 4 | Geographical regions of average domoic acid in Dungeness crab shown in **Figure 3** and reference locations on land for crab closures shown in **Table 1**. Humboldt County, CA, is shown as a dotted line on land. The location of buoy 46027-6, from which wind data in **Figure 3** were retrieved, is shown with an X.

et al., 2011). Therefore, the surficial sediment is a source of *Pseudo-nitzschia* and DA available to initiate the next bloom during upwelling conditions (Seegers et al., 2015).

Dungeness Crab Harvest and HABs

Dungeness crab fishing generates the most income and has the highest vessel participation of all fisheries on the U.S. west coast (Fuller et al., 2017). The harvest yield of the Dungeness crab fishery and the reliability of the timely opening of crab season determines the livelihood of many fishers in rural communities (Ritzman et al., 2018). The Daily Astorian newspaper stated on 23 April 2018, that "HABs have complicated commercial Dungeness crab harvest on the OR coast for the past 3 seasons, threatening the viability of the state's most valuable fishery." The commercial season in northern CA, OR, and WA typically opens December 1 and ends July 15. Unfortunately, after the delay of the crab opener until 15 January 2019 due to high levels of DA, the opportunity for CA crabbers was further limited by statewide fishery closure on April 15, almost 3 months earlier than normal, as stipulated under the terms of a settlement agreement reached between the California Department of Fish and Wildlife (CDFW) and the Centers for Biological Diversity (CBD) to limit whale entanglements in crab nets. The agreement requires CDFW to monitor areas off the central and northern CA coasts where whales feed along their spring migration route (Dillman, 2019). If more than 20 whales are observed in an area, fishery managers must order an immediate closure. Thus, the compression of the crab season by DA events, exacerbated by anomalous ocean warming, will have long-lasting impacts on the accessibility to this fishery and the resulting economic benefits to many rural communities. Small vessel fishers may trade their fishing effort disproportionately to access other fisheries when the crab season is canceled, causing concern for resource managers (Saez et al., 2020). Climate change and related warming have compressed habitats for many organisms (Santora et al., 2020). Both habitat compression and intensified *Pseudo-nitzschia* HABs with range expansion are a result of anomalously warm temperatures in the coastal ocean. In the future, the predicted increased intensity of these HABs (McCabe et al., 2016; McKibben et al., 2017) will reduce fishing opportunity directly due to the presence of toxins in seafood or indirectly through ecosystem impacts such as whale entanglement which may shorten the crab harvest season. Newly seeded HAB retentive sites, resulting from anthropogenic climate change, will challenge managers to ensure the safety of our seafood while having cascading impacts on the health of marine animals and economic welfare of coastal communities.

Forewarning and Mitigation

Early warning systems that anticipate HAB risk at the new hotspot site in northern CA as well as the other known hotspot sites on the US west coast include the Pacific Northwest (PNW) HAB Bulletin (**Figure 5**; http://depts.washington.edu/orhab/pnw-hab-bulletin/) and the California HAB Bulletin (https://sccoos.org/california-hab-bulletin/). Both Bulletins synthesize biological data from coastal and offshore monitoring of HABs and their toxins, a suite of physical environmental data, and output from realistic numerical models, including the LiveOcean model (https://faculty.washington.edu/pmacc/LO/LiveOcean.html) and the California Regional Ocean Modeling System (Anderson et al., 2019), to forecast potential HAB events for coastal managers. The PNW HAB Bulletin is provided to managers prior to razor clam and Dungeness crab openers and can be helpful in pinpointing areas of the coast that are high risk for HABs. When available, data collected from advanced technologies, such as the Environmental Sample Processor (ESP, Doucette et al., 2009; Scholin et al., 2009; Anderson et al., 2019) and autonomous ocean-going vessels (e.g., http://www.nanoos.org/news/index.php?item=Submaran180924) are also implemented

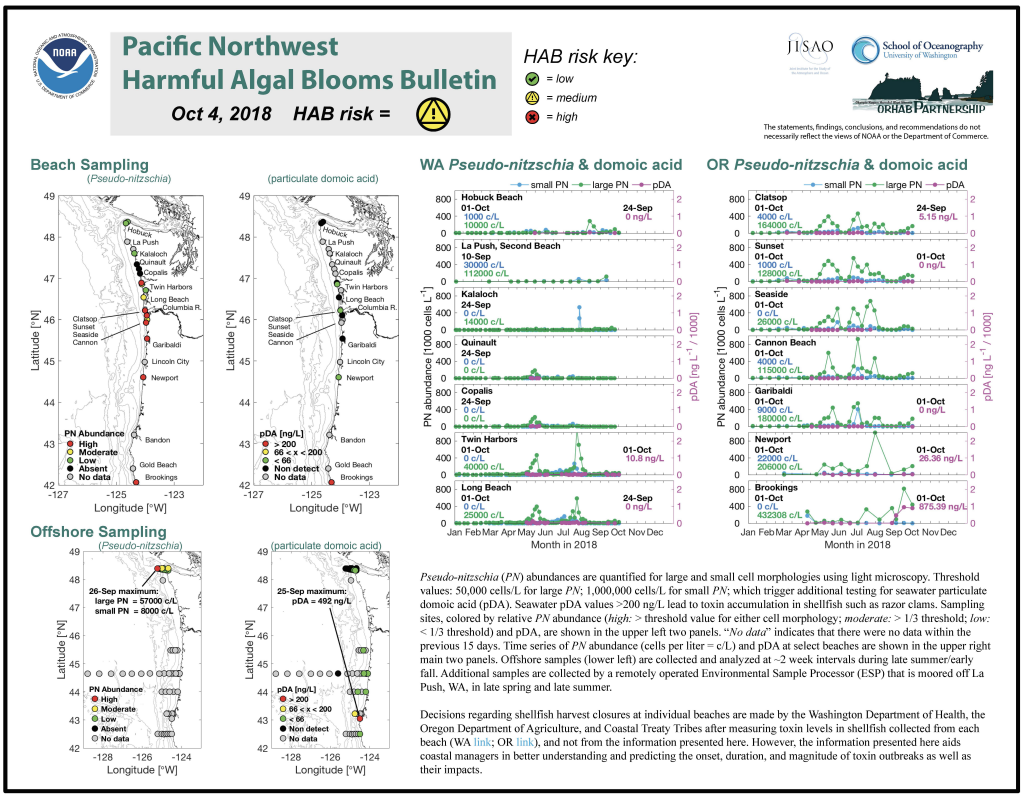

FIGURE 5 | The PNW HAB Bulletin from 4 October 2018 (http://www.nanoos.org/products/habs/forecasts/bulletins/pnw_hab_bulletin-20181004.pdf (accessed 22 Nov 2020)) communicating elevated seawater particulate domoic acid off of Bandon, OR (492 ng/L), Brookings, OR (875 ng/L), and Humboldt, CA (>800 ng/L) in late September 2018. *Pseudo-nitzschia australis* was dominant across those sites at that time.

in the forecasting Bulletins. While regionally specific information is utilized in each Bulletin, the PNW HAB Bulletin also tracks larger scale indices such as the Pacific Decadal Oscillation and El Niño, which have been shown to correlate with DA events throughout the PNW (McCabe et al., 2016; McKibben et al., 2017). In the case of the PNW HAB Bulletin, a summary narrative and a HAB risk assessment (low, medium, high; shown as "traffic light" symbols) are provided as a synthesis of results. The early warnings provided by the Bulletins enable mitigative actions such as selective opening of safe shellfish harvest zones, increased harvest limits during low risk periods, and early harvest in anticipation of upcoming toxin outbreaks. The timely and spatially-refined identification of toxin risk will allow managers to define areas of targeted closure, making these early warning Bulletins potentially more cost-effective than other mitigation methods (Holland and Leonard, 2020). In cases when predictions indicate an increasing risk for toxins, managers often modify workflows in order to collect additional shellfish samples (Dungeness crab, clams, and mussels) to ensure human and marine animal safety.

The new northern CA hotspot has been a repeated feature since the west coast wide 2015 DA event (McCabe et al., 2016), often leading to shellfish harvest closures in southern OR. The higher concentrations of DA in crab in southern OR compared to northern OR in late 2015, 2017, and 2018 (**Figure 3**), suggest that DA originated from northern CA (**Figure 3**, compare crab DA in CA North to OR South and OR North). By contrast, in late 2016, lower concentrations of DA in northern CA crab compared to OR crab suggest that toxigenic *Pseudo-nitzschia* originated from a northern source. Measurement of DA in razor clams provided additional insights regarding the geographical source of toxin. In fact, this northern source of DA in 2016 is supported by the cancellation of razor clam digs in southern WA (https://www.dailyastorian.com/news/local/washington-approves-razor-clam-digs-at-two-beaches-long-beach-still-closed/article_ad972fac-0cd4-5059-a845-fb2b25bb5818.html) and all of OR (DA in razor clams was above the regulatory level of 20 ppm in September and continued to increase, reaching a maximum of 360 ppm on the central OR coast in Dec 2016 [OR Department of Agriculture Food Safety data]; https://www.seattletimes.com/sports/entire-oregon-coast-closed-for-razor-clam-digging-after-marine-toxin-levels-skyrocket/ in the fall due to high DA.

The strong influence of the northern CA hotspot site on OR shellfish safety was documented in several PNW HAB Bulletins that prominently featured the fact that southern OR razor clams, mussels, and crabs all contained elevated DA during fall 2018 (e.g., **Figure 3**). In September 2018, razor clam DA concentrations as high as 180 ppm were measured at Gold Beach, OR, well above the 20 ppm regulatory limit for that species (in contrast to Dungeness crab which have a 30 ppm regulatory limit). Mussels collected off Humboldt, CA, were similarly over the regulatory limit at that same time, suggesting an ongoing toxin event spanning the northern CA/southern OR hotspot. As discussed in the 04-Oct-2018 PNW HAB Bulletin (**Figure 5**; http://www.nanoos.org/products/habs/forecasts/bulletins.php), scanning electron microscopy of *Pseudo-nitzschia* samples collected in late September, confirmed the presence of *P. australis* off both Bandon, OR, and Humboldt, CA. A resurgence of razor clam DA concentrations (from 39 to 140 ppm) at Gold Beach, OR, as well as elevated DA in crab viscera (40 ppm) in early May 2019 indicated the continued risk posed by this new hotspot, even though high particulate DA was not measured in this region in the few samples collected onboard the July 2019 cruise. However, DA poisoning was again a potential risk in October 2019 as seawater particulate DA was documented at an extremely high 5,005 ng/L at Brookings, OR (19-Oct-2019 PNW HAB Bulletin). Crab closures in CA were reported again in 2020 (CDPH report, 2020) demonstrating the persistence of this toxic feature.

PNW HAB Bulletins are emailed to fisheries managers and posted on the ORHAB and NANOOS websites (http://depts.washington.edu/orhab/pnw-hab-bulletin/ and http://www.nanoos.org/products/habs/forecasts/bulletins.php).

There are plans for HAB forecasts across the entire US west coast region to be coordinated through integration with regional Ocean Observing Systems (Anderson et al., 2019) and through the NOAA West Coast Operational Forecast System (WCOFS) effort, currently in development, which eventually will provide consistent ocean modeling across the entire west coast (https://tidesandcurrents.noaa.gov/ofs/dev/wcofs/wcofs_info.html). This dedicated, persistent, and comprehensive monitoring at key transition sites to quantify ocean changes will provide early warning of HABs, allowing management of important resources to promote the health of ocean ecosystems while assisting with safe harvest of seafood.

DATA AVAILABILITY STATEMENT

The raw data supporting the conclusions of this article will be made available by the authors, without undue reservation.

AUTHOR CONTRIBUTIONS

VT conceived of this article and wrote the draft based on input from all authors. RK created **Figure 1**. NA created **Figures 2**, **4**. NA and RM created **Figure 3**. MH and NA created **Table 1**. All authors contributed to editing and improving the final manuscript.

FUNDING

This study was supported by a grant from the NOAA National Centers for Coastal Ocean Science's Monitoring and Event Response to Harmful Algal Blooms (MERHAB) program (NA16NOS4780189), Northwest Fisheries Science Center base funding, funding from the Central and Northern California Ocean Observing System (CeNCOOS; NA16NOS0120021) for toxin analysis from the Trinidad Head region, and by the Joint Institute for the Study of the Atmosphere and Ocean (JISAO) under NOAA

Cooperative Agreement NA15OAR4320063. This is MERHAB contribution number 227, and JISAO contribution number 2020-1109.

ACKNOWLEDGMENTS

We thanked the captains and crews of the R/V New Horizon, NOAA Ship Miller Freeman, R/V Shana Rae, CA Fish and Wildlife Patrol Boat Bluefin, NOAA Ship Bell M. Shimada, and the following volunteers who have been invaluable in helping us over the years with HAB sampling: Tracie Barry, Monica Baze, Brian Bill, Julia Clemons, Madison Drescher, Naomi Estrada, Jennifer Hagen, Alexander Islas, Jessica Knoth, John Kim, Dan Lomax, Anthony Odell, O. Paul Olson, Aaron Parker, Lynne Scamman, Kathleen Schacht, Carla Stehr, Tom Werth. This project contributes to the implementation of the GlobalHAB Programme areas focusing on climate change, human health, and fisheries.

REFERENCES

Anderson, C. R., Berdalet, E., Kudela, R. M., Cusack, C. K., Silke, J., O'Rourke, E., et al. (2019). Scaling up from regional case studies to a global harmful algal bloom observing system. *Front. Marine Sci.* 6:250. doi: 10.3389/fmars.2019.00250

Anderson, C. R., Kudela, R. M., Kahru, M., Chao, Y., Rosenfeld, L. K., Bahr, F. L., et al. (2016). Initial skill assessment of the California Harmful Algae Risk Mapping (C-HARM) system. *Harmful Algae* 59, 1–18. doi: 10.1016/j.hal.2016.08.006

Barth, J. A., Pierce, S. D., and Smith, R. L. (2000). A separating coastal upwelling jet at Cape Blanco, Oregon and its connection to the California Current System. *Deep Sea Res. Pt. II* 47, 783–810. doi: 10.1016/S0967-0645(99)00127-7

Bowers, H. A., Ryan, J. P., Hayashi, K., Woods, A. L., Marin, R., Smith, G. J., et al. (2018). Diversity and toxicity of *Pseudo-nitzschia* species in Monterey Bay: perspectives from targeted and adaptive sampling. *Harmful Algae* 78, 129–141. doi: 10.1016/j.hal.2018.08.006

Collins, M., Sutherland, M., Bouwer, L., Cheong, S.-M., Frölicher, T., Combes, H., et al. (2019). "Extremes, abrupt changes and managing risk," in IPCC Special Report on the Ocean and Cryosphere in a Changing Climate, eds H.-O. Pörtner, D.C. Roberts, V. Masson-Delmotte, P. Zhai, M. Tignor, E. Poloczanska, et al. (in press). Available online at: https://www.ipcc.ch/srocc/chapter/chapter-6/ (accessed November 29, 2019).

Davis, R. E. (1985). Drifter observations of coastal surface currents during CODE-The statistical and dynamical views. *J. Geophys. Res. Oceans* 90, 4756–4772. doi: 10.1029/JC090iC03p04756

Di Lorenzo, E., and Mantua, N. (2016). Multi-year persistence of the 2014/15 North Pacific marine heatwave. *Nat. Climate Change* 6, 1042–1047. doi: 10.1038/nclimate3082

Dillman, T. (2019, December 1). Oregon crab fishery faces regulatory changes. *Fisherman's News*.

Dortch, Q., Robichaux, R., Pool, S., Milsted, D., Mire, G., Rabalais, N. N., et al. (1997). Abundance and vertical flux of *Pseudo-nitzschia* in the northern Gulf of Mexico. *Mar. Ecol. Prog. Ser.* 146, 249–264. doi: 10.3354/meps146249

Doucette, G. J., Mikulski, C. M., Jones, K. L., King, K. L., Greenfield, D. I., Marin, R., et al. (2009). Remote, subsurface detection of the algal toxin domoic acid onboard the Environmental Sample Processor: assay development and field trials. *Harmful Algae* 8, 880–888. doi: 10.1016/j.hal.2009.04.006

Eberhart, B. T. L., Bill, B. D., and Trainer, V. L. (2012). Remote sampling of harmful algal blooms: a case study on the Washington State coast. *Harmful Algae* 19, 39–45. doi: 10.1016/j.hal.2012.05.005

Fuller, E. C., Samhouri, J. F., Stoll, J. S., Levin, S. A., and Watson, J. R. (2017). Characterizing fisheries connectivity in marine social-ecological systems. *ICES J. Mar. Sci.* 74, 2087–2096. doi: 10.1093/icesjms/fsx128

Holland, D. S., and Leonard, J. (2020). Is a delay a disaster? Evaluation of the economic impacts of the delay of the California Dungeness crab fishery due to a harmful algal bloom. *Harmful Algae* 98:101904. doi: 10.1016/j.hal.2020.101904

IPCC (2018). *Global Warming of 1.5°C. An IPCC Special Report on the impacts of global warming of 1.5°C above pre-industrial levels and related global greenhouse gas emission pathways, in the context of strengthening the global response to the threat of climate change, sustainable development, and efforts to eradicate poverty*, eds. V. Masson-Delmotte, P. Zhai, H.-O. Pörtner, D. Roberts, J. Skea, P.R. Shukla, et al. (in press). Available online at: https://www.ipcc.ch/sr15/ (accessed November 22, 2020).

JPL MUR MEaSUREs Project (2015). *GHRSST Level 4 MUR Global Foundation Sea Surface Temperature Analysis (v4.1)*. NASA PO.DAAC. Available online at: http://podaac.jpl.nasa.gov/dataset/MUR-JPL-L4-GLOB-v4.1 (accessed October 29, 2019).

Kelly, K. A. (1985). The influence of winds and topography on the sea-surface temperature patterns over the northern California slope. *J. Geophys. Res. Oceans* 90, 11783–11798. doi: 10.1029/JC090iC06p11783

Kosro, P. M. (1987). Structure of the coastal current field off northern California during the Coastal Ocean Dynamics Experiment. *J. Geophys. Res. Oceans* 92, 1637–1654. doi: 10.1029/JC092iC02p01637

Kudela, R., Pitcher, G., Probyn, T., Figueiras, F., Moita, T., and Trainer, V. L. (2005). Harmful algal blooms in coastal upwelling systems. *Oceanography* 18, 184–197. doi: 10.5670/oceanog.2005.53

Kudela, R. M., Hayashi, K., and Caceres, C. G. (2020). Is San Francisco Bay resistant to *Pseudo-nitzschia* and domoic acid? *Harmful Algae* 92:101617. doi: 10.1016/j.hal.2019.05.010

Kvitek, R. G., Goldberg, J. D., Smith, G. J., Doucette, G. J., and Silver, M. W. (2008). Domoic acid contamination within eight representative species from the benthic food web of Monterey Bay, California, USA. *Mar. Ecol. Prog. Ser.* 367, 35–47. doi: 10.3354/meps07569

Largier, J. L., Magnell, B. A., and Winant, C. D. (1993). Subtidal circulation over the northern California shelf. *J. Geophys. Res. Oceans* 98, 18147–18179. doi: 10.1029/93JC01074

Laufkötter, C., Zscheischler, J., and Frolicher, T. L. (2020). High-impact marine heatwaves attributable to human-induced global warming. *Science* 369, 1621–1625. doi: 10.1126/science.aba0690

McCabe, R. M., Hickey, B. M., Kudela, R. M., Lefebvre, K. A., Adams, N. G., Bill, B. D., et al. (2016). An unprecedented coastwide toxic algal bloom linked to anomalous ocean conditions. *Geophys. Res. Lett.* 43, 10366–10376. doi: 10.1002/2016GL070023

McClatchie, S., Goericke, R., Leising, A., Auth, T. D., Bjorkstedt, E., Robertson, R. R., et al. (2016). State of the California current 2015-16: comparisons with the 1997-98 El Niño. *CalCOFI Reports* 57, 1–61. Available online at: http://calcofi.org/publications/calcofireports/v57/Vol57-SOTCC_pages.5-61.pdf (accessed November 22, 2020).

McKibben, S. M., Peterson, W., Wood, A. M., Trainer, V. L., Hunter, M., and White, A. E. (2017). Climatic regulation of the neurotoxin domoic acid. *Proc. Natl. Acad. Sci. U.S.A.* 114, 239–244. doi: 10.1073/pnas,.1606798114

NOAA Fisheries (2018). *2017 National Report on Large Whale Entanglements*. Available online at: https://www.fisheries.noaa.gov/resource/document/national-report-large-whale-entanglements-2017 (accessed November 22, 2020).

Piatt, J. F., Parrish, J. K., Renner, H. M., Schoen, S. K., Jones, T. T., Arimitsu, M. L., et al. (2020). Extreme mortality and reproductive failure of common murres resulting from the northeast Pacific marine heatwave of 2014-2016. *PLoS ONE* 15:e0226087. doi: 10.1371/journal.pone.0226087

Ritzman, J., Brodbeck, A., Brostrom, S., McGrew, S., Dreyer, S., Klinger, T., et al. (2018). Economic and sociocultural impacts of fisheries closures in two fishing-dependent communities following the massive 2015 US West Coast harmful algal bloom. *Harmful Algae* 80, 35–45. doi: 10.1016/j.hal.2018.09.002

Ryan, J. P., Kudela, R. M., Birch, J. M., Blum, M., Bowers, H. A., Chavez, F. P., et al. (2017). Causality of an extreme harmful algal bloom in Monterey Bay,

California, during the 2014–2016 northeast Pacific warm anomaly. *Geophys. Res. Lett.* 44, 5571–5579. doi: 10.1002/2017GL072637

Saez, L., Lawson, D., and DeAngelis, M. (2020). *Large Whale Entanglements off the U.S. West Coast, from 1982-2017*. NOAA Tech. Memo. NMFS-OPR-63, 48. Available online at: https://www.fisheries.noaa.gov/resource/document/large-whale-entanglements-us-west-coast-1982-2017 (accessed November 22, 2020).

Sagarin, R. D., Barry, J. P., Gilman, S. E., and Baxter, C. H. (1999). Climate-related change in an intertidal community over short and long time scales. *Ecol. Monogr.* 69, 465–490. doi: 10.1890/0012-9615(1999)069[0465:CRCIAI]2.0.CO;2

Sanford, E., Sones, J. L., García-Reyes, M., Goddard, J. H. R., and Largier, J. L. (2019). Widespread shifts in the coastal biota of northern California during the 2014–2016 marine heatwaves. *Sci. Rep.* 9:4216. doi: 10.1038/s41598-019-40784-3

Santora, J. A., Mantua, N. J., Schroeder, I. D., Field, J. C., Hazen, E. L., Bograd, S. J., et al. (2020). Habitat compression and ecosystem shifts as potential links between marine heatwave and record whale entanglements. *Nat. Commun.* 11:536. doi: 10.1038/s41467-019-14215-w

Schnetzer, A., Lampe, R. H., Benitez-Nelson, C. R., Marchetti, A., Osburn, C. L., and Tatters, A. O. (2017). Marine snow formation by the toxin-producing diatom, *Pseudo-nitzschia australis*. *Harmful Algae* 61, 23–30. doi: 10.1016/j.hal.2016.11.008

Schnetzer, A., Miller, P. E., Schaffner, R. A., Stauffer, B. A., Jones, B. H., Weisberg, S. B., et al. (2007). Blooms of *Pseudo-nitzschia* and domoic acid in the San Pedro Channel and Los Angeles harbor areas of the Southern California Bight, 2003-2004. *Harmful Algae* 6, 372–387. doi: 10.1016/j.hal.2006.11.004

Scholin, C., Doucette, G., Jensen, S., Roman, B., Pargett, D., Marin, R. I., et al. (2009). Remote detection of marine microbes, small invertebrates, harmful algae, and biotoxins using the Environmental Sample Processor (ESP). *Oceanography* 22, 158–167. doi: 10.5670/oceanog.2009.46

Seegers, B. N., Birch, J. M., Marin, R., Scholin, C. A., Caron, D. A., Seubert, E. L., et al. (2015). Subsurface seeding of surface harmful algal blooms observed through the integration of autonomous gliders, moored environmental sample processors, and satellite remote sensing in southern California. *Limnol. Oceanogr.* 60, 754–764. doi: 10.1002/lno.10082

Sekula-Wood, E., Benitez-Nelson, C., Morton, S., Anderson, C., Burrell, C., and Thunell, R. (2011). *Pseudo-nitzschia* and domoic acid fluxes in Santa Barbara Basin (CA) from 1993 to 2008. *Harmful Algae* 10, 567–575. doi: 10.1016/j.hal.2011.04.009

Sekula-Wood, E., Schnetzer, A., Benitez-Nelson, C. R., Anderson, C., Berelson, W. M., Brzezinski, M. A., et al. (2009). Rapid downward transport of the neurotoxin domoic acid in coastal waters. *Nature Geosci.* 2, 272–275. doi: 10.1038/ngeo472

Send, U., Beardsley, R. C., and Winant, C. D. (1987). Relaxation from upwelling in the Coastal Ocean Dynamics experiment. *J. Geophys. Res. Oceans* 92, 1683–1698. doi: 10.1029/JC092iC02p01683

Smith, J., Connell, P., Evans, R. H., Gellene, A. G., Howard, M. D. A., Jones, B. H., et al. (2018). A decade and a half of *Pseudo-nitzschia* spp. and domoic acid along the coast of southern California. *Harmful Algae* 79, 87–104. doi: 10.1016/j.hal.2018.07.007

Stott, P. A., Stone, D. A., and Allen, M. R. (2004). Human contribution to the European heatwave of 2003. *Nature* 432, 610–614. doi: 10.1038/nature03089

Taylor, F. J. R. (1993). British Columbia: implications of the North American west coast experience. *Harmful Algae News* 6, 2–3.

Thompson, A. R., Schroeder, I. D., Bograd, S. J., Hazen, E. L., Jacox, M. G., Leising, A., et al. (2018). State of the California Current 2017-18: still not quite normal in the north and getting interesting in the south. *CalCOFI Reports* 59, 1–66. Available online at: https://calcofi.org/publications/calcofireports/v59/Vol59-SOTC2018_1-66.pdf (accessed November 22, 2020).

Trainer, V. L., Adams, N. G., Bill, B. D., Stehr, C. M., Wekell, J. C., Moeller, P., et al. (2000). Domoic acid production near California coastal upwelling zones, June 1998. *Limnol. Oceanogr.* 45, 1818–1833. doi: 10.4319/lo.2000.45.8.1818

Trainer, V. L., Adams, N. G., and Wekell, J. C. (2001). "Domoic acid-producing *Pseudo-nitzschia* species off the US west coast associated with toxification events." in *Harmful Algal Blooms 2000*, eds G. M. Hallegraeff, S. I. Blackburn, C. J. Bolch and R. J. Lewis (Paris: UNESCO), 46–49.

Trainer, V. L., Bates, S. S., Lundholm, N., Thessen, A. E., Cochlan, W. P., Adams, N. G., et al. (2012). *Pseudo-nitzschia* physiological ecology, phylogeny, toxicity, monitoring and impacts on ecosystem health. *Harmful Algae* 14, 271–300. doi: 10.1016/j.hal.2011.10.025

Trainer, V. L., Moore, S. K., Hallegraeff, G., Kudela, R. M., Clement, A., Mardones, J. I., et al. (2020). Pelagic harmful algal blooms and climate change: lessons from nature's experiments with extremes. *Harmful Algae* 91:101591. doi: 10.1016/j.hal.2019.03.009

Trainer, V. L., and Suddleson, M. (2005). Approaches for early warning of domoic acid events in Washington state. *Oceanography* 18, 228–237. doi: 10.5670/oceanog.2005.56

Vigilant, V., and Silver, M. W. (2005). "Domoic acid in the fat innkeeper worm, *Urechis caupo*, at Elkhorn Slough, CA," in *3rd Symposium for Harmful Algae in the US* (Monterey, CA), 152. Available online at: https://www.whoi.edu/cms/files/Abstracts_-_3rd_Symposium_24225.pdf (accessed November 22, 2019).

Vigilant, V. L., and Silver, M. W. (2007). Domoic acid in benthic flatfish on the continental shelf of Monterey Bay, California, USA. *Mar. Biol.* 151, 2053–2062. doi: 10.1007/s00227-007-0634-z

Wekell, J. C., Gauglitz, E. J., Barnett, H. J., Hatfield, C. L., and Eklund, M. (1994). The occurrence of domoic acid in razor clams (*Siliqua patula*), dungeness crab (*Cancer magister*), and anchovies (*Engraulis mordax*). *J. Shellfish Res.* 13, 587–593.

Weller, E., Min, S. K., Lee, D., Cai, W. J., Yeh, S. W., and Kug, J. S. (2015). Human contribution to the 2014 record high sea surface temperatures over the Western Tropical and Northeast Pacific Ocean. *Bull. Amer. Meteor. Soc.* 96, 100–104. doi: 10.1175/BAMS-D-15-00055.1

Wells, B. K., Schroeder, I. D., Bograd, S. J., Hazen, E. L., Jacox, M. G., Leising, A., et al. (2017). State of the California current 2016-17: still anything but "normal" in the north. *CalCOFI Reports* 58, 1–55. Available online at: http://calcofi.org/publications/calcofireports/v58/Vol58-State_of_the_Current_pages_1-55.pdf (accessed November 22, 2020).

Wetz, M. S., Wheeler, P. A., and Letelier, R. M. (2004). Light-induced growth of phytoplankton collected during the winter from the benthic boundary layer off Oregon, USA. *Mar. Ecol. Prog. Ser.* 280, 95–104. doi: 10.3354/meps280095

Conflict of Interest: The reviewer, EB, declared a past co-authorship with two of the authors, VT and RK, to the handling Editor.

The remaining authors declare that the research was conducted in the absence of any commercial or financial relationships that could be construed as a potential conflict of interest.

frontiers in Climate

ORIGINAL RESEARCH
published: 23 December 2020
doi: 10.3389/fclim.2020.577169

Long-Term Land Use Land Cover Change in Urban Centers of Southwest Ethiopia From a Climate Change Perspective

Tesfaye Dessu[1], *Diriba Korecha*[2*], *Debela Hunde*[1] *and Adefires Worku*[3]

[1] College of Agriculture and Veterinary Medicine, Jimma University, Jimma, Ethiopia, [2] Famine Early Warning Systems Network, Addis Ababa, Ethiopia, [3] Ethiopian Environment and Forest Research Institute (EEFRI), Addis Ababa, Ethiopia

Long-term urban land use land cover change (LULCC) dynamics and climate change trends in Southwest Ethiopia's four urban centers were examined for 60 years. Remote sensing, aerial photos, and Landsat, temperature, and rainfall data were analyzed from a climate change perspective over the Jimma, Bedelle, Bonga, and Sokorru urban centers of southwest Ethiopia from 1953 to 2018. Based on geospatial analysis and maximum likelihood supervised image classification techniques to classify LULCC categories, the Mann-Kendall test was applied to perform trend analyses on temperature and rainfall. The LULCC analysis revealed that built-up areas over the urban centers had shown an increasing trend, with the highest increment by 2,360 hectares over Jimma, while vegetation, wetland, and cropland declined due to conversion of plain lands to built-up areas and other similar zones. The pronounced decline of vegetation coverage was 1,427, 185,116, and 32 hectares in Jimma, Bedelle, Bonga, and Sokorru, respectively. Mann-Kendall test results showed a significant sign of intra-seasonal and inter-annual variability of rainfall while the summer and annual rainfall patterns remained less variable compared to other seasons. This study's findings revealed that when the mean between the two climatic normals of 1953–86 is compared with 1987–2018, the temperature has significantly increased in the latter three decades. The rapid expansion of built-up areas coupled with a sharp decline of green space or vegetation and agricultural/croplands could lead to gradual changes in LULCC classes, which have contributed to the changing of the local climate, especially the surface temperature and rainfall over the urban centers of southwest Ethiopia. Therefore, we recommend that the local urban administrations emphasize sustainable urban development by integrating urban planning policies with land use to protect the environment by adopting local municipal adaptation and national climate change strategies. Restoration of the local environment and creation of climate-smart cities could be critical to the resilience of urban dwellers and ecosystems to the changing climate by enhancing grass-root climate services. To that end, we recommend further advanced research to understand how urban LULC-related changes and other factors contribute to local and regional climates, as urban areas of Southwest Ethiopia are undergoing a rapid transformation of their rural surroundings.

Keywords: image classification, LULCC, climate change, Southwest Ethiopia, trend analysis and projection, urban planning and development

OPEN ACCESS

Edited by:
Dann Mitchell,
University of Bristol, United Kingdom

Reviewed by:
Le Yu,
Tsinghua University, China
Markus Adloff,
University of Bristol, United Kingdom

***Correspondence:**
Diriba Korecha
dkorecha@fews.net

Specialty section:
This article was submitted to Climate Services, a section of the journal Frontiers in Climate

Received: *28 June 2020*
Accepted: *01 December 2020*
Published: *23 December 2020*

Citation:
Dessu T, Korecha D, Hunde D and Worku A (2020) Long-Term Land Use Land Cover Change in Urban Centers of Southwest Ethiopia From a Climate Change Perspective. Front. Clim. 2:577169. doi: 10.3389/fclim.2020.577169

INTRODUCTION

Land use land cover (LULC) changes impact weather and climate, both on a local and global spatial scale, which calls for global consideration and continuous monitoring of the changes and subsequent predictions (Mengistie et al., 2013). Changes in the land surface emerge because of both natural and anthropogenic activities. Urbanization leads to changes in the local climate, typically increasing surface air temperature and changing rain patterns and intensity, the magnitude of which varies with season, geographic location, local circulation, climate, and surrounding land cover (Giannaros et al., 2013; Vargo et al., 2013). Using LULC maps based on supervised classification of remote sensing data and local activities offers new possibilities in analyzing effects of LULC due to human activity within the urban area. Indeed, massive changes in LULC patterns significantly affect urban ecosystems (Herold et al., 2003; Patra et al., 2018).

Currently, climate change is accepted as a present reality, and further change is inevitable. For instance, IPCC (2014) documented that between 1906 and 2005, the global average surface temperature rose by 0.7°C. This change occurred in two phases: from the 1910s to the 1940s, and more strongly from the 1970s to the present. The projected global surface warming lies within the range of 0.6 to 4.0°C, while the projected sea level rises are within the range of 0.18 to 0.59 meters by the end of the twenty first century (IPCC, 2014). Urbanization is widely acknowledged to be an upward trend, with 66% of the global population predicted to be living in cities by 2050 (United Nations, 2014). The global urban area estimates, which vary from less than 1–3% of the world's land surface to, are rapidly expanding in different parts of the world, leading to significant changes in other land use land cover types (Liu et al., 2014). Developing countries have begun settlement in urban areas, but they are rapidly urbanizing with unplanned expansion, notably speeding up more than in developed nations (Grimm et al., 2008; Montgomery, 2008). Global climate change is induced by the LULC change because of the considerable effect urban expansion has on the environment, ecosystem, and society (Grimm et al., 2008; Wilson and Chakraborty, 2013).

Ethiopia, the second most populous country in Africa, with an annual population growth rate of 2.3%, has an urban population growth rate of 4.2%. This population growth rate is higher than the average rate (2.2%) for developing countries (United Nations, 2014). In terms of Ethiopian cities' contribution to climate change, cities represent only 15% of Ethiopia's total emissions, although the emission is expected to rise to 35% by 2030 (Cities Alliance, 2017). It is mainly driven by unplanned urban growth, intensive transportation, and energy needs. The country has experienced a significant temperature rise in recent decades, in contrast to a decline in total annual rainfall amounts and recurrent extreme weather events (Cities Alliance, 2017). Various studies were conducted to estimate LULC change in the Ethiopian highlands. However, these studies have shown the dominance of heterogeneity in direction, pattern, type, and magnitude of LULC change in the country (Mengistie et al., 2013). Feyisa et al. (2016), for instance, have analyzed urbanization-induced LULC and surface thermal intensity and its relationship with the biophysical composition in Addis Ababa City using TM and ETM+. The study revealed that the surface temperature around the outskirts of the city has become cooler than urban centers by 3.7°C between 1985 and 2010.

Recent studies have found that there has been an increase in seasonal mean temperatures in many areas of Ethiopia over the last fifty years (Funk et al., 2008). For instance, over the past four decades, the average annual temperature in Ethiopia has increased by 0.37°C per decade, with maximum warming during the second half of the 1990s (EEA, 2008). Studies made on national climate trends since the 1960s showed that mean annual temperatures in the country have increased between 0.5 and 1.3°C (ACCRA, 2012). In contrast, the frequency of cold nights that measure the extent of frost levels during the dry season has decreased significantly in all seasons (McSweeney et al., 2010). In connection to seasonal rainfall trends, Funk et al. (2012) documented that Belg and Kiremt rainfall totals have decreased by 15–20% between 1975 and 2010 in southern, southwestern, and southeastern parts of Ethiopia.

Advances in remote-sensing data improved spatial accuracy and availability of free to less-expensive satellite images coupled with a geographical information system (GIS) that allow quantitative analyses of the rate and pattern of urban LULC change with reasonable cost and better accuracy (Epstein et al., 2002). Information on urban land-use changes is required to visualize growth patterns and improve land use planning and management (Debolini et al., 2015), and allocate services and infrastructure (Witten et al., 2003). Accurate information on urban dynamics is important for predictive urban modeling (He et al., 2008) and assessing ecological changes and their environmental implications on a local scale (Grimm et al., 2008).

Rainfall amounts and distributions in Ethiopia are affected by El Niño-Southern Oscillations (ENSO) and the Indian Ocean Dipole (IOD) phenomena by displacing and weakening rain-producing systems. For instance, Kiremt rain, which accounts for 50–80% of annual rainfall in Ethiopia, has significant contributions to agricultural production and major water reserves, but has been declining in recent decades because of the warming phase of ENSO, and hence is unable to meet the country's agricultural and water resource demands (Korecha and Barnston, 2007; Kassa, 2015). According to Getinet and Woldeamlak (2009), rainfall over southwest Ethiopia showed both high spatial and temporal variability with area-averaged daily rainfall intensity having significantly decreased by 0.44 mm/day per decade. Historically, the southwestern part of Ethiopia is considered the wettest region and the place where tropical rainforest remains clear, and receives moderate to heavy rainfall amounts throughout the year (Korecha, 2013). However, because of ongoing intensive deforestation and expansion of farmland, annual and Kiremt rainfall totals in this part of Ethiopia have shown significant declining trends (Seleshi and Zanke, 2004).

Jimma City, which is the center of this study, is considered one of the major urban centers in southwestern Ethiopia. It is surrounded by steep and hilly topography and subjected to frequent flooding during the main rainy seasons (Getachew and Tamene, 2015). The rapid urban population growth and

economic development led to unplanned urban expansion both in Jimma and in other parts of the country, including southwest Ethiopia's urban areas. However, the extent and spatial characteristics of Jimma's long-term expansion and that of surrounding towns and their LULC implications have not been well-documented. Therefore, this paper examines long-term spatio-temporal trends of land use land cover change in urban areas of southwest Ethiopia from the climate change perspective based on observed environmental, atmospheric, social, and economic data. The outcome of this research finding is expected to provide additional scientific evidence to help to understand the influence of LULC change on the urban microclimate to implement climate change adaptation and mitigation schemes in an urban area to combat the challenges of inevitable climate change at a local scale.

MATERIALS AND METHODS

Description of the Study Area

This study was conducted in southwest Ethiopia's urban area, within the spatial periphery lying between 7°.22'N to 8°.45'N and 36°.23'E to 37°.40' E, representing a grid box of $1^0 \times 1^0$. This area covers the extensive southwestern sector of the country, as depicted in **Figure 1**. The altitude of southwest Ethiopia ranges from the high plateaus of over 2,000 m to flat and low-lying plains of 600 m. Climatically, this region is classified as a temperate-type climate with a mean annual temperature of 14–20°C and a mean annual rainfall of 1,700–2,000 mm. The study area is characterized by two rainy seasons, with the primary rainy season often extending from May through to the end of October and the short rainy season from late February to the end of April. The study is confined within the southwest of Ethiopia (**Table 1**; **Figure 1**), where one of the country's rainfall maxima is located as documented by Getinet and Woldeamlak (2009).

The local urban-rural exchange in urban centers and their surroundings has contributed to significant business activity. The main economic activity in this study of urban centers is commerce and manufacturing enterprises. Except for the newly established Jimma Industrial Park in 2018, no large-scale industrial activity was found in the cities, but small–scale cottage industries were available in each town. The current Town Administration of the study depicts towns structured from a city level to the lowest administrative level (kebele) with decentralized functions of a municipality at Kebele level. As per the Central Statistical Authority (CSA, 2007), the total population of Jimma City is 120,600, which was projected to be more than 200,000 by 2017, with diverse ethnic compositions in the city. Also, the total population of Bonga is 20,858 in 2007, and is projected to be 44,046 by 2022; the total population of Bedelle was 19,517 in 2007 and was projected to reach 31,500 by the year 2017, whereas, Sokorru's total population was 6,233 in 2007 and was projected to reach 16,617 by 2017 (CSA, 2007, 2017).

Each of the four urban centers included in this study has its own historical establishment, land use types, structural plan, or master plan to guide development, even if none of them were established in a planned way at the beginning. Among these, Jimma is the oldest city, founded in the 1830s, and the municipality was established in 1942 under decree number 1/1942, with its activity mainly focused on levy taxes (Yonas and Zahorik, 2017). According to the 2008 city revised master plan, the total area of Jimma City has reached 100.2 km^2(10,200 hectares), expanding further with the ongoing master plan under revision. In contrast, the current total areas of Bonga, Bedelle, and Sokorru towns are 8,846, 2,878, and 300 hectares, respectively, with the major portions of the land being used for residential, infrastructure, and green areas based on the current master plan under revision. Substantial portions of urban regions are green with trees planted and conserved along the roadside and in the compounds of residences and institutions, such as schools, churches, mosques, health centers, and universities. The altitude of Jimma City ranges from the lowest 1,720 meters above sea level (m.a.s.l) of the airfield (kitto) to the highest 2010 m.a.s.l of Jiren, where Abba Jifar Palace (Masara) is situated. Likewise, Bonga, Bedelle, and Sokorru lie at an elevation of 1,779, 2,011, and 1,928 m.a.s.l, respectively (Jimma City Administration, 2019; NMA, 2019; **Table 1**).

Data Sources

Land Use Land Cover Change

Next, we discuss producing the spatial map and assessing the dynamics of urban area changes due to urbanization and quantifying the magnitude and spatial patterns of Land Use Land Cover Changes (LULCC) that environments in and around the four urban centers have undergone between 1953 and 2018 using remote sensing and GIS techniques. Topographic maps and aerial photographs for each study area were collected from Ethiopia Geospatial Agency (EGA), depending on historically available high-resolution Google Earth Pro images, and field observation using handheld Garmin Global Positioning System (GPS), which were used for supervised image classification of the Landsat images. Aerial photos of 1957 for Jimma and Sokorru, 1958 for Bedelle, and 1967 for Bonga were extracted from Landsat Thematic Mappers (TMs) for 1987, and Landsat 8 Operational Land Imager (OLI) for 2018 were used to produce the tri decadal LULCC maps. Identification of the LULC types from the spectral response, the image acquisition dates selected based on the availability of cloud-free images of each town Landsat image (path 168, row 51), and the dry season were downloaded freely from the United States Geological Survey (USGS) (**Table 2**). All images were processed using the ERDAS image processing software version 2015. A change analysis was undertaken by applying a supervised classification and maximum likelihood classifier algorithms change detection procedures. Accuracy of the image classification was assessed using an error matrix, overall accuracy, and kappa coefficient (**Table 2**).

The overall land use land cover change of classes in terms of built-up, vegetation, agriculture/cropland, and wetlands/open space is because of rapid urban expansion and observed changes presented using each town's images. Rainfall and temperature changes were analyzed in line with urbanization, affecting land use land cover change in urban areas.

TABLE 1 | Selected study town station and their geographical location of the study area.

S/No.	Station Name	Location		Altitude in (meter)	Average annual Rainfall (mm)	Average annual mean temp. in (°C)	Year of observation
		Latitude in (North)	Longitude (East)				
1	Jimma	7.66	36.83	1,725	1,523	20.43	1953–2018
2	Bedelle	8.45	36.33	2,011	2,098	20–25	1971–2018
3	Bonga	7.22	36.23	1,779	1,402	19.5	1954–2018
4	Sokorru	7.92	37.40	1,928	1,359	21.5	1980–2018

Source: National Metrological Agency of Ethiopia (2019).

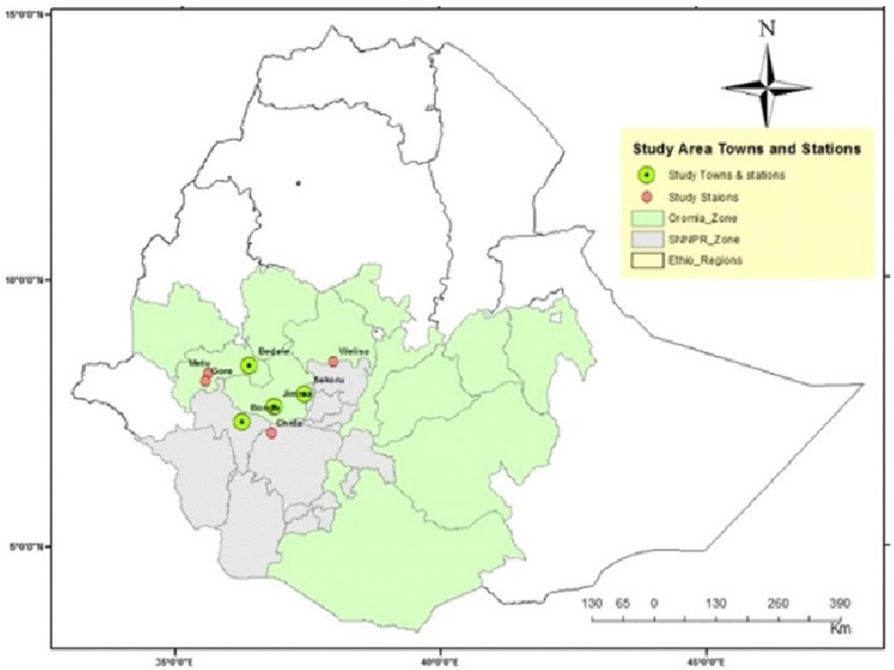

FIGURE 1 | Geographical location of the study area.

Climate Data

Long-term temperature and rainfall data (1953–2018), which were collected from the National Meteorological Agency of Ethiopia (NMA), were aggregated into monthly time series. The study periods were chosen from the period of towns and meteorological station establishments until 2018 in order to increase the quality of data and availability. Quality checks were conducted on available data in order to minimize the errors that could propagate throughout the analysis period and potentially cause bias in the final results. Reliability, accuracy, and homogeneity of these data were checked at 95% significance level using SPSS software. Missing temperature and rainfall data over each meteorological station was filled using the normal ratio method as expressed in Equation (1) below;

$$Px = \frac{Nx}{n}\left(\frac{P1}{N1} + \frac{P2}{N2} + \ldots + \frac{Pn}{Nn}\right) \quad (1)$$

Where Px = Missing value of the climate variable under consideration; Nx = Average value of the climate variable for the station in question for recording period; N1…..Nn = Average value of the climate variable for the neighboring station; P1....Pn = The neighboring station's climate variable during the missing period; and n = number of stations used in the computation. Before conducting this analysis, the consistency of all climate variables, which are rainfall and temperature, in this case, were checked to see if correction was needed.

Methods of Data Analysis and Presentation

Land Use Land Cover Change Classification

Errors are inevitable in any digitally generated land cover maps obtained from remote-sensing imagery. These errors may occur from the source itself, because of errors incurred during data acquisition, or from classification techniques during image processing. As a result, it requires a robust and thorough assessment test on the classification accuracy

TABLE 2 | Land use land cover data based on satellite observation and their sources.

1. Name of Town	Data acquisition year			Path/Raw	Date downloaded or collected	Software used
	1957/58/67 Aerial photograph	1987 Landsat (TM)	2018 Landsat (OLI)			
Jimma	1957	22/11/1987	27/11/2018	169/055	23/10/2019	ERDAS 2015, Arc GIS 10.5 and IDRISI for aerial photo analysis
Bedelle	1958	24/12/1987	24/09/2018	170/054	6/11/2019	
Bonga	1967	15/11/1987	20/11/2018	170/055	1/11/2019	
Sokorru	1957	15/11/1987	20/11/2018	169/055	23/10/2019	Arc GIS 10.5, ERDAS 2015 for Landsat data analysis
2. Source	EGA/ the former EMA/	USGS	USGS	EGA- Ethiopian Geo-Spatial Agency USGS-United States Geological Survey		
3.Resolution(m)	25 m resampled to 30 m	30 m Original	30 m Original			

to guarantee the result's reliability. One very effective and commonly used method of expressing classification accuracy is the preparation of a classification error matrix or a confusion matrix (Congalton, 1991; Lillesand et al., 2004). After preparing land use, land cover data was made and accuracy of the data were further assessed by collecting ground truth points using GPS coordinates and Google Earth.

Image classification is not complete until the accuracy of the land cover classes is assessed using an error matrix. Error matrix or confusion matrix compares the relationship between known reference data or ground truth and the corresponding results generated from the automated classification process (Lillesand et al., 2015). This matrix helps to validate the accuracy of the classified image, which is usually expressed as a percentage and interpreted using overall accuracy, user's accuracy, producer's accuracy, and sometimes as kappa statistics/coefficient. Kappa statistics measure the difference between the actual agreement between reference data and an automated classifier, and the chance of agreement between the reference data and a random classifier (Lillesand et al., 2015).

It is important to note that the producer's accuracy calculated as the total number of accurate pixels in a group category is divided by the total number of pixels of that category as derived from the reference data. This accuracy measure shows the probability of a reference to the pixel being correctly classified. If the total number of correct pixels in a category is divided by the total number of pixels that are classified in that category, it is said that the user's accuracy is reliable. Kappa coefficient measures the agreement between the classifications on the map and the reference data or GCP.

Land Use Land Cover Change Detection

The change in LULC for the periods under consideration was analyzed using the post-classification change detection technique in a GIS environment. Post-classification change detection is selected as it reduces spectral resolution and sensor differences between the multi-temporal images (Lu et al., 2004).

An important feature of change detection is to determine what is changing to what, i.e., which land-use class is changing to the other. This information also assists as a vital tool in management decisions. This process involves a pixel-to-pixel comparison of the study year images through overlay analysis. The land use land cover change matrix depicts the direction of change and the land use type that remains as it is. To calculate the change of LULC in percentage (%), the initial and final LULC area coverage is compared by applying Garai and Narayana (2018) method, as stated in Equation (2).

$$\text{Change percentage} = \left(\frac{\text{final LULC area} - \text{initial LULC area}}{\text{Initial LULC area}}\right) \times 100 \quad (2)$$

The results deduced from this matrix are interpreted as positive and negative percentage values that suggest an increase or decrease in areal coverage.

Climate Data

Quantitative statistical methods were applied to compute the monthly, seasonal, annual, and decadal temperature and rainfall distributions, trends, and variability, taking Jimma as the main hub for urban center, and LULCC and climate change trends for Bedelle, Bonga, and Sokorru towns. Figures, maps, and tables were used to make presentations of the results. It assessed inter-annual and decadal long-term climate variability and changes using Instat, MS Excel, SPSS packages, and other relevant software. GIS software is used for preparing the study area map and analysis.

We computed the mean annual temperature and rainfall based on 30 years+ data record for each station and later aggregated these across the region. In this study, with the rainfall and temperature data, we computed variability using the Standardized Precipitation Anomaly (SPA) and the Coefficient

of Variation (CV). Calculating standardized temperature and rainfall anomalies that enable determining the extent of climate variability and change tested for inter-annual and inter-decadal variability and presented the results graphically (Oliver, 1980; Agnew and Chappel, 1999). CV, which is used to test the variability of rainfall, is computed as expressed in Equation (3).

$$CV = s/\bar{x} * 100\ \% \tag{3}$$

Where CV is the coefficient of variation, s is the standard deviation, and $\bar{x}$ is the mean rainfall. According to Hare (2003), CV is used to classify variability of rainfall events as less (CV < 20), moderate (20 < CV < 30), and high (CV > 30). We calculated a standardized anomaly of rainfall to examine the nature of the trends that enable the effect of determining the dry and wet years in the record and used this to assess the frequency and severity of droughts (Agnew and Chappel, 1999; Conway and Woldeamlak, 2007; Viste et al., 2012; Gebre et al., 2013). We computed standardized Rainfall Anomaly using the Equation (4) below:

$$Z = \frac{(Xi - \bar{X})}{S} \tag{4}$$

Where Z is a standardized Rainfall Anomaly; xi is the annual rainfall total of a particular year; $\bar{x}$ is a long-term mean annual rainfall; and s is the standard deviation of annual rainfall throughout the observation. The inter-annual and decadal temperature patterns, rainfall variability, mean temperature fluctuations, and rainfall are presented graphically for the individual station and for areal averaged value. Linear regression is used to quantify trends, and the non-parametric Kendall-tau test is used to test the statistical significance of trends, which are frequently used to detect trends (Bihrat and Bayazit, 2003).

Since there is potential for outliers to be present in the dataset, the non-parametric Mann-Kendall (MK) test uses a statistic based on the + or – signs, rather than the random variable's values. Thus, the trends determined using MK are less affected by the outliers (Birsan et al., 2005). Trend analysis was carried out on a monthly, seasonal, and annual basis. Each data value was compared with all subsequent data values, using a statistic, S, as expressed using Equation (5). Mann- Kendall (MK) test, a non-parametric, was widely used to detect trends of meteorological variables, as many researchers have well-documented (Seleshi and Zanke, 2004; Mekonnen and Woldeamlak, 2014; Tabari et al., 2015; Gebremedhin et al., 2016). Data analysis was undertaken using the XLSTAT software or excel spreadsheet. The result of the MK test reveals increasing or decreasing trends in the time series data, whereas a value of calculated Z in time series u (t) more than 1.96 shows a positive trend, and a value of u (t) lower than −1.96 reveals a negative trend at the significance level of 95% (Mann, 1945; Kendall, 1975) as expressed in Equation (5).

$$S = \sum_{i=1}^{n-1} \times \sum_{ji+1}^{n} Sgn\,(Xj - Xi) \tag{5}$$

It is documented that when the number of observations is over 10 ($n \geq 10$), the statistic, S, is approximately normally distributed with the mean, and the result value of statistic in the MK test of E(S) becomes 0 (Kendall, 1975). Here, the variance statistic is given as Var (S) and computed using Equation (6).

$$Var(S) = \frac{n(n-1)(2n+5) - \sum_{i=1}^{m} = 1tj\left(tj-1\right)(2tj+5)}{18} \tag{6}$$

Where n is the observations number and tj are the ties of the sample time series. The test statistics Zc is expressed using Equation (6).

$$Zc = \begin{cases} \frac{S-1}{\sigma},\ if\ S > 0 \\ 0,\ if\ S = 0 \\ \frac{S+1}{\sigma},\ if\ S < 0 \end{cases} \tag{7}$$

Theil (1950) and Sen (1968) slope estimator methods predicted the magnitude of the trend. A positive value of β shows an upward trend, which is increasing values with time, while a negative value of β shows a downward trend. Here, the slope (Ti) is of all data pairs computed using the method developed by Sen (1968). It estimated the slope Ti between any two values of a time series x from Equation (8).

$$Ti = \frac{Xj - Xi}{j - i} \tag{8}$$

Where Xj and Xi are considered as data values at time j and i (j>i), correspondingly. The median of these N values of Ti represented as Sen's estimator of the slope, which computed as Qmed=T (N+1) /2 if N appears odd, and it is considered as Qmed = [TN/2+TN+2)/2)/2] if N appears even. A positive value of Qi shows an upward or increasing trend, and a negative value of Qi gives a downward or decreasing trend in the time series.

RESULTS AND DISCUSSIONS

Analysis of Land Use Land Cover Change

Aerial Photo and Satellite Image Analysis

The aerial photos of 1957, 1958, and 1967 for Jimma and Sokorru, Bedelle, and Bonga with a spatial resolution of 25 m × 25 m were used to prepare land use of the land cover of these towns, respectively. The 1987 land-sat TM and 2018 Landsat OLI image of the dry season were used to prepare land use land cover maps of the study area using ERDAS 2015 image processing software (**Table 2**). Pre-processing of the satellite image, band composite, and masking the image for the study area was performed, and then images were visually interpreted, pre-processed, and ready for classification (**Table 2**).

Classification of the satellite images is the process that enables us to classify pixels in the image to the same information, class identification of training points, or signature editor used. Depending on the training point's signature editor value, all the pixel values were classified to the correct class with the parametric rule of a maximum likelihood classification

algorithm. The area was classified into four major categories of land use types practiced based on field survey data, which were collected using GPS as well as structural plan data from the land management office of each town, and was referred and cross-checked using the image from Google Earth. Four thematic LULC classes, built-up, vegetation, agriculture or cropland, and wetlands were generated for the years 1957, 1987, and 2018 using supervised image classification (**Figure 2**). Land uses are classified with a top-level of accuracy. Land use land cover of the study area for Jimma City, Bedelle, Bonga, and Sokorru Towns were mapped through visual interpretation of aerial photographs at a scale of 1:50,000 for 1957, 1958, 1967, and 1957, respectively (**Table 3**; **Figure 2**).

Land Use Land Cover Change in the Urban Areas

The land use land cover change in urban areas of southwest Ethiopia were analyzed by using classification change detection techniques in GIS environment, and then summarized in tables and illustrated in spatial maps. Land use and type change are considered as any change that occurred from the starting year onwards. LULC change detection findings revealed that all urban centers experienced a change in LULC over the past 60 years, even though there seems to be persistence of land cover classes due to their land size throughout the study period, as summarized in **Table 3**.

The analysis of land use land cover change showed, in Jimma City for instance, both cropland and vegetation have a decreasing pattern from 1957 to present by 470 and 1427 hectares, whereas the built-up areas have increased by 2,360 hectares (**Table 4**; **Figure 2**). The results, therefore, revealed that built-up areas increased from the year 1957 (220 ha) to 1987 (372 ha) and 2018 (2,580 ha). Contrary to the highly urbanized trend, vegetation coverage showed a slight increment from 1957 (4,307 ha) to 1987 (4,644 ha) but significantly decreased in 2018 to 2880 ha. Also, the wetland was highly decreased throughout 1957–2018 by 463 ha. Since 1957, vegetation coverage in Jimma City has declined by 1,427 hectares (**Table 2**; **Figure 2**). In contrast, the built-up area of Jimma City has expanded from the central part to eastern and southern directions, with the rate of expansion ranging from 2% in 1957 to 23% in 2018 (**Table 3**; **Figure 2**).

Our findings of a significant increase in built-up areas and a decrease in cropland, wetland, and vegetation in all urban centers under this study are consistent with the previous study as documented by Abebe et al. (2019), which showed that increases in built-up areas resulted because of illegal settlement and transformation of land over the past two decades. The LULC change detection results were also similar to the previous study conducted on green areas of Addis Ababa City by Tesfaye (2017), where vegetation coverage declined, with a significant increase in land surface temperature in the city. The findings we generated for other towns also complied with the results of Herold et al. (2003) and Patra et al. (2018), which identified that the massive changes in LULC patterns had imposed a negative effect on urban environmental conditions.

LULCC Classification Accuracy Assessment and Test

After preparing land use land cover, accuracy assessments were done for LULCC based on ground truth points, which were collected based on GPS coordinates and Google Earth. Error matrix or confusion matrix then were constructed and comparisons were made between known reference data or ground truth and the corresponding results that were generated from the automated classification process as documented by Lillesand et al. (2015). This matrix helps us to validate the classified image's accuracy, which is usually expressed as a percentage and interpreted using Kappa statistics. Based on the Congalton (1991) assessment technique, our findings showed strong agreement between the ground truth and the classified images. The overall accuracy and Kappa statistics (κ) values met the minimum accuracy requirements for LULC change detection studies (Anderson et al., 1976). After applying the above techniques, we summarized the LULC classification accuracy for the Jimma City in the table (**Supplementary Table 1A**).

The overall accuracy of image classification for Jimma City was 88.71%, and its Kappa index agreement was 0.8472. This implies that the LULC classification process avoided 88% of errors that a random classification generates. The accuracy of individual class (Built-up, Vegetation, Cropland, and Wetland) varies from 76.92 to 94.74% for producer's accuracy and from 84.62 to 90.91% for user's accuracy. Thus, all land use land cover classification was found to be accurate with the computed value of over 75%, which elevated to a better standard. Similarly, the overall accuracy and Kappa Statistic for Bedelle, Bonga, and Sokorru towns were found to be 86.67% and 0.8297, 92% and 0.8923, and 88.33% and 0.8422, respectively (**Supplementary Tables 1A–D**). The producer's and user's accuracy range from 81.25 to 90% and 85.71 to 88.89% for Bedelle, 88.89 to 95.24%, and 90.91 to 94.12 for Bonga, and 80 to 93.75% and 81.82 to 88.24% for Sokorru, respectively (**Supplementary Tables 1A–D**).

Land Use Land Cover Change Detection Matrix

This study applied the land change detection assessment technique to individual image classification outputs to identify respective change trajectories of four urban centers under study. The gain, loss, persistence, absolute value of net land change, and total change calculated for all four were classified into image classes (Pontius et al., 2004; Braimoh, 2006). Gain is the amount of land use class i that was added between time t1 and time t2, whereas loss is the amount of land use class j that was lost from time t1 to time t2. Persistence is the land-use class that does not change from time t1 to time t2. Swap is the simultaneous loss and gain of land use class in a landscape, which implied that an area of land use is lost at one location while the same size is gained at a different location. The land use category's total change is the sum of the net change and the swap or the total sum of the gains and losses. Also, the net change is the difference between the gain and losses during the study period.

The major change detection matrix computed between 1957 and 1987 in Jimma City showed that cropland and wetland

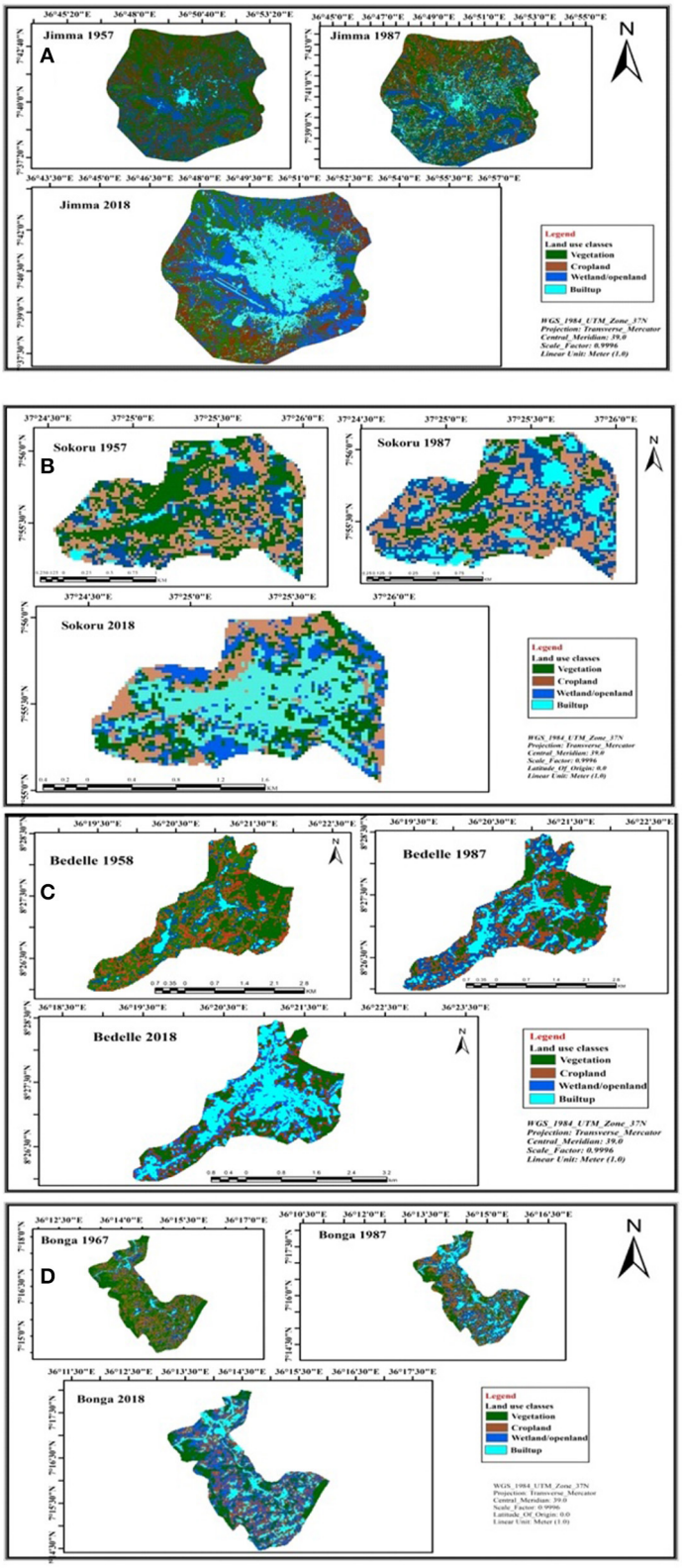

FIGURE 2 | Maps showing land use land cover (LULC) of **(A)** Jimma, **(B)** Sokorru, **(C)** Bedelle, and **(D)** Bonga urban center as observed in1950s.

TABLE 3 | LULC type and change (ha, %) over (A) Jimma, (B) Sokorru, (C) Bedelle, and (D) Bonga urban centers from 1957 to 2018.

(A)	LULC Type	Share of LULC type of total area of the town						LULC type change in hectare (ha)		
Jimma		**1957**		**1987**		**2018**		**1957–1987**	**1987–2018**	**1957–2018**
		ha	**%**	**ha**	**%**	**ha**	**%**			
	Cropland	3,036	29	2,774	27	2,566	24	−262	−208	−470
	Vegetation	4,307	41	4,644	44	2,880	28	337	−1,764	−1,427
	Wetland	2,901	28	2,674	26	2,438	23	−227	−236	−463
	Built-up	220	2	372	3	2,580	25	152	2,208	2,360
(B)	**LULC Type**	**Share of LULC type of total area of the town**						**LULC type change in hectare (ha)**		
Sokorru		**1957**		**1987**		**2018**		**1957–1987**	**1987–2018**	**1957–2018**
		ha	**%**	**ha**	**%**	**ha**	**%**			
	Cropland	129	41	119	37	82	26	−10	−37	−47
	Vegetation	98	31	83	26	66	21	−15	−17	−32
	Wetland	71	22	67	21	54	17	−4	−13	−17
	Built-up	20	6	49	16	116	36	29	67	96
(C)	**LULC Type**	**Share of LULC type of total area of the town**						**LULC type change in hectare (ha)**		
Bedelle		**1958**		**1987**		**2018**		**1958–1987**	**1987–2018**	**1958–2018**
		ha	**%**	**ha**	**%**	**ha**	**%**			
	Cropland	265	31	238	28	189	22	−27	−49	−67
	Vegetation	436	51	352	41	251	30	−84	−101	−185
	Wetland	108	13	106	13	87	10	−2	−19	−21
	Built-up	43	5	156	18	325	38	113	169	282
(D)	**LULC Type**	**Share of LULC type of total area of the town**						**LULC type change in hectare (ha)**		
Bonga		**1967**		**1987**		**2018**		**1967–1987**	**1987–2018**	**1967–2018**
		ha	**%**	**ha**	**%**	**ha**	**%**			
	Cropland	463	34	443	32	395	29	−20	−48	−68
	Vegetation	664	49	589	43	548	40	−75	−41	−116
	Wetland	187	14	145	11	128	9	−42	−17	−59
	Built-up	54	4	191	14	297	22	137	106	243

shrunk from 3,033 ha in 1957 to 2,772 ha in 1987 and from 2,899 ha in 1957 to 2,672 ha in 1987, respectively (**Table 4**). In contrast, the built-up area has expanded from 220 ha in 1957 to 372 ha in 1987 (**Table 4**; **Figure 3**). Parts of the city that were previously covered by vegetation increased from 4,044 ha in 1957 to 4,641 ha in 1987. However, in the following decades, between 1987 and 2018, cropland and vegetation have decreased from 2,754 ha and 4,620 ha in 1987 to 2,249 ha and 2,197 ha in 2018, respectively. Similarly, wetland and built-up land area changed from 2,665 ha and 371 ha in 1987 to 3,129 and 2,835 ha in 2018, respectively, which showed that there is a high transition of land use land cover change in built-up areas because of urbanization and the persistent land use of each class, as shown in bold inside **Table 4**, during the study period.

LULC change detection matrix that was computed between the initial (1957) and final (2018) states was calculated to observe the shifts of land cover classes in Jimma City over the past 60 years (**Table 4**; **Figure 3**). Similarly, of the 2,917 ha of land that was dedicated to crop farming, 566 ha remained as the same class in 2018, with 794, 768, and 21 ha converted to vegetation, wetland, and built-up areas during this period. From vegetation class, 1,140 ha of the area remained as the same class in 2018 with 665, 385, and 6 ha converted to cropland, wetland, and built-up areas, respectively, in 2018. Likewise, from the wetland/open land in Jimma City, 856 ha remained in this class in 2018 while 870, 1,380, and 22 ha converted into cropland, vegetation, and built-up class, respectively, in 2018 (**Table 4**).

The major observed land use and type change during the period between 1957 and 1987 in Sokorru Town increased in cropland, wetland, and built-up areas from 108, 69, 19 ha in 1957 to 118, 107, and 48 ha in 1987, respectively, then later decreased in the areas of vegetation coverage from 120 ha in 1957 to 43 ha in

TABLE 4 | Jimma City LULC change matrix as computed between the 1950s, 1980s, and 2010s.

(A) LULCC in 1987								
From the year 1957	**LULC**	**Cropland**	**Vegetation**	**Wetland/ Open land**	**Built-up**	**Row Total**	**Total change**	**Net change**
	Cropland	**1,857**	933	242	1	3,033	654	1,176
	Vegetation	852	**2,216**	1,192	45	4,305	4,044	3372
	Wetland/ Open land	63	1,491	**1,232**	113	2,899	2,203	2,657
	Built-up	0	1	6	**213**	220	523	1
	Column total	2,772	4,641	2,672	372	**10,457**	4,391	10,457
	Gains	915	3,708	2,430	371	7,424		
	Loss	−261	336	−227	152	−3033		
(B) LULCC in 2018								
From the year 1987	LULC	Cropland	Vegetation	Wetland/ Open land	Built-up	Row Total	Total change	Net change
	Cropland	**557**	629	935	633	2,754	1,187	2,197
	Vegetation	931	**1,251**	1,245	1193	4,620	−855	3,991
	Wetland/ Open land	698	296	**889**	782	2,665	2,658	1,730
	Built-up	63	21	60	**227**	371	4,666	633
	Column total	2,249	2,197	3,129	2,835	**10,410**	4,902	10,410
	Gains	1,692	1,568	2,194	2,202	7,656		
	Loss	−505	−2,423	464	2,464	−2754		
(C) LULCC in 2018								
From the year 1957	LULC	Cropland	Vegetation	Wetland/ Open land	Built-up	Row Total	Total change	Net change
	Cropland	**566**	665	870	816	2,917	815	2,351
	Vegetation	794	**1,140**	1,380	969	4,283	−556	3,618
	Wetland/ Open land	768	385	**856**	879	2,888	2,498	2,018
	Built-up	21	6	22	**171**	220	4,634	816
	Column total	2,149	2,196	3,128	2,835	**10,308**	4,474	10,308
	Gains	1583	1,531	2,258	2,019	7,391		
	Loss	−768	−2,087	240	2,615	−2,917		

The bold values indicate persistence of the same land use land cover during the study period.

1987 (**Figure 4**). Between the year 1987 and 2018, cropland and wetland decreased from 103 to 88 ha in 1987 to 55 and 52 ha in 2018, respectively. In contrast, vegetation and built-up areas have increased from 36 to 43 ha in 1987 to 56 and 107 ha in 2018, respectively. This change happened because of the high transition of land use land cover change to built-up areas because of the fast expansion in urbanization. The change detection matrix, computed as the difference between 1957 and 2018 states, was calculated to detect any shift of land cover classes in Sokorru town over the past 60 years (**Figure 4**).

For instance, from an initial 55 ha of cropland, 15 ha remained as the same class in 2018, while 25, 10, and 5 ha of croplands converted into vegetation, wetland, and built-up areas during this period. The vegetation class change showed that 18 ha of the area persisted, while 23, 13, and 3 ha converted into cropland, wetland, and built-up areas in 2018. For the wetland/open land, 16 ha remained as the same type, whereas 16 ha converted to the cropland class, with the rest converted to vegetation and built-up areas. The cropland, vegetation, and wetland areas have significantly shrunk, but the built-up areas have expanded and override other parts of the town previously dedicated to other land types throughout the study period until 2018 (**Figure 4**).

The major change detection in the period between 1958 and 1987 in Bedelle town displayed an overall area decrease of vegetation from 236 ha in 1958 to 176 ha in 1987 and an increase in cropland, wetland areas, and built-up areas from 213, 107, 42 ha in 1958 to 217, 153, 52 ha in 1987, respectively. Between 1987 and 2018, cropland and vegetation decreased from 211, 430 ha in 1987 to 151, 153 ha in 2018, respectively, whereas wetland and built-up areas increased from 107 to 43 ha in 1987, 163 and 324 ha in 2018, respectively (**Figure 4**). These findings revealed a high transition of plain land cover change into built-up areas due to urbanization.

Change detection matrix computed between the initial (1958) and final (2018) states were calculated to observe the shifts of land cover classes in Bedelle town over 60 years (**Figure 4A**; **Supplementary Table 1B**). Of 152 ha of cropland, 55 ha remained the same class in 2018, 37 ha converted to vegetation, 48 ha to wetland, and 12 ha to built-up areas during this period. The change for vegetation, which was 61 ha of the area, was persistent/remained as the same class in 2018, while 47 ha converted to cropland, 36 ha to wetland, and 36 ha to built-up areas in 2018. For the wetland/open land, 59 ha remained in this class in 2018, 46 ha converted to the cropland class, 32 ha to vegetation class, and 26 ha by the built-up areas. From 324 ha of built-up area, 109 ha remained in this class in 2018, 67 ha converted to the cropland, 44 ha converted to vegetation, and 104 ha converted to wetland/open land through the study period till

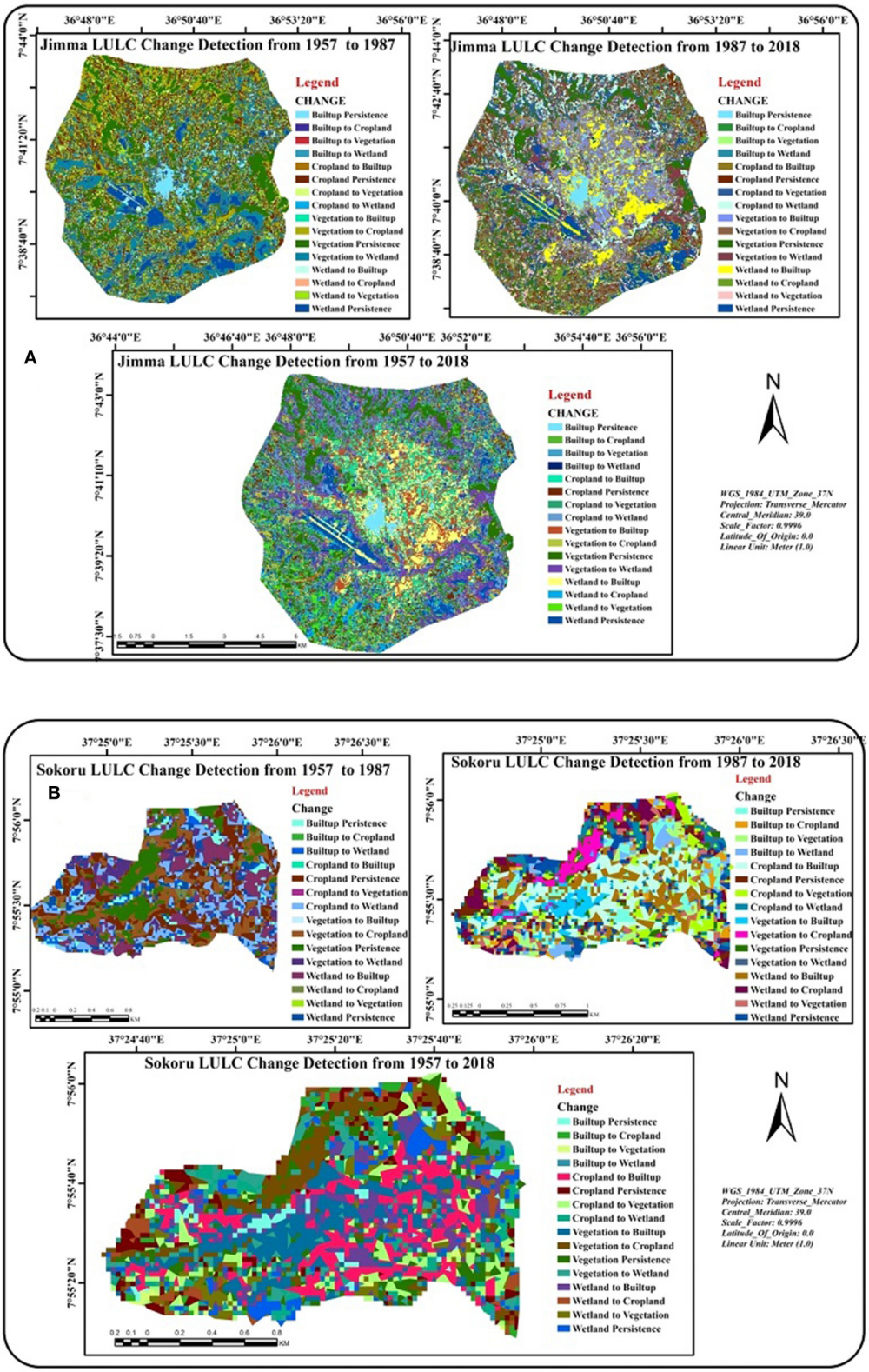

FIGURE 3 | LULC change detection maps of **(A)** Jimma and **(B)** Sokorru from 1957 to 1987, 1987 to 2018, and1957 to 2018.

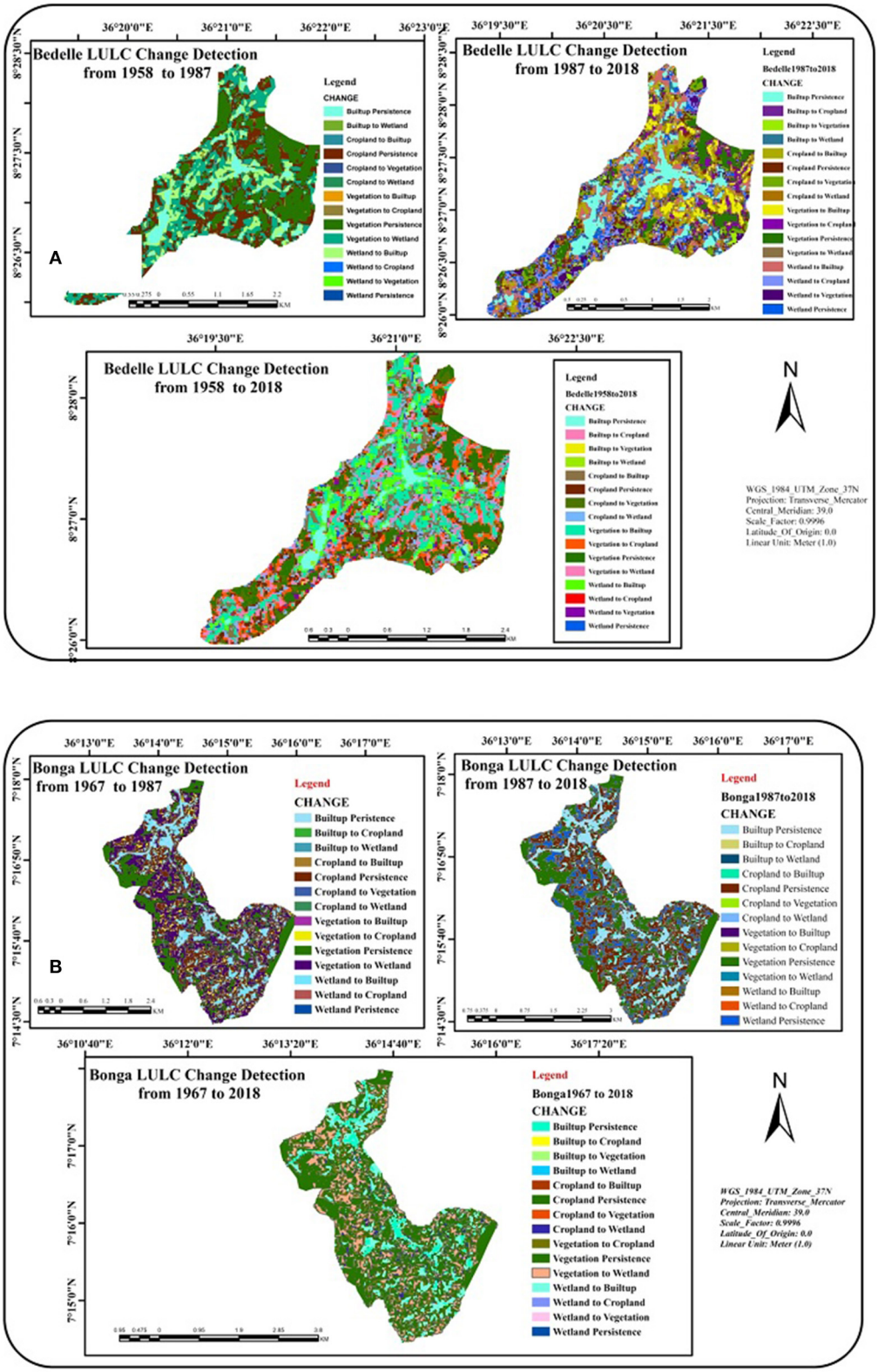

FIGURE 4 | LULC change detection maps of **(A)** Bedelle, and **(B)** Bonga Town from 1958/1967 to 1987, 1987 to 2018, and1958/1967 to 2018.

2018, which showed a high conversion of land use to built-up areas (**Figure 4A**; **Supplementary Table 1B**).

The major change detection matrixes observed in the period between 1967 and 1987 in Bonga town showed an overall area decrease of vegetation from 587 ha in 1967 to 281 ha in 1987 and an increase in the areas of crop land, vegetation, and built-up areas from 363, 33, and 54 ha in 1967 to 413, 413, and 228 ha in 1987, respectively (**Figure 4**). During the period between 1987 and 2018, cropland and wetland/open land decreased from 433, 425 ha in 1987 to 400, 397 ha in 2018, respectively, whereas, vegetation and built-up areas increased from 281 and 228 ha in 1987 and 303 and 267 ha in 2018, respectively, which showed a transition of land use land cover change from one class to another (**Figure 4**).

The change detection matrix computed between the initial (1967) and final (2018) states were calculated to observe the shifts of land cover classes in Bonga town over the period (**Figure 4**). From 380 ha of cropland, 300 ha remained as the same class in 2018, 71 ha converted to vegetation, and the other two to wetland and built-up areas. Vegetation class was the majority with 303 ha of the area remaining as the same class in 2018, with no conversion to other classes observed during the period. For the wetland/open land not in this class in 2018, 29 ha converted to cropland, 68 ha to vegetation, and there was no conversion to built-up areas. From 267 ha of built-up area, 54 ha remained as in this class in 2018, 33 ha was converted to cropland, 2 ha converted to vegetation, and 178 ha converted to wetland/open land through the study period from 1967 to 2018 in Bonga town (**Figure 4**).

Temperature and Rainfall Trends and Variability in Southwest Ethiopia Urban Centers

The computed annual and seasonal mean, CV, Standardized Rainfall Anomaly, and MK test on time series data of climatic parameters, particularly on temperature (maximum and minimum) and rainfall, were analyzed for the urban centers of southwest Ethiopia. The missing data and outlier values were checked for completeness before analysis, and homogeneity was checked using Pitittis curve. Overall, the results have tended toward normally distributed patterns. In the MK test, parameters like Kendall's tau, S-statistic, and the Z-statistic were analyzed to identify the trend in the time series of climatic parameters. The results are discussed separately for each climate parameter in the subsequent subsections.

Seasonal and Annual Rainfall Trends and Variability

The results generated from the annual rainfall analysis showed a positive trend over time during the years of 1953–2018 in Jimma, Bonga, and Bedelle by 10, 3, and 2 mm/year, respectively, with the highest observed rainfall in Jimma (**Table 5**; **Supplementary Figures 1**, **2**). This shows an upward trend in annual rainfall in three urban centers, with a declining trend by −30 mm/decade for Sokorru Town, with Kendall tau-b statistically significant at 95% confidence level (**Table 5**; **Supplementary Figures 1**, **2**). The average areal analysis made over southwestern urban centers revealed that the annual rainfall amount has increased by 25 mm/decade with strong spatiotemporal variations among the urban regions. The average annual rainfall total in the study area was divided into two climatic normals. This enabled us to compare any systematic change in annual rainfall totals between 1953–1986 and 1987–2018 climatic normal periods. We found that southwest urban centers received 1,660 and 1,720 mm of annual rainfall totals during the first and second climatic normals, respectively, with a positive change of rainfall totals by +60 mm. From seasonal time scale analysis, Jimma City, for instance, experienced an increasing rainfall trend during spring, summer, autumn, and winter, with the rate of increment by 40, 34, 29, and 2 mm/decade, respectively (**Table 5**; **Supplementary Figures 1**, **2**).

The study's findings from the Mann-Kendall test revealed that, during the study period of 66 years in all study towns, winter season rainfall signaled a decreasing trend. However, the summer rainfall contribution for annual rainfall totals is 2-fold compared to spring, and an increase/decrease of rainfall totals during one of these seasons significantly impacts southwest Ethiopia urban centers. The results we summarized in **Table 4** are highly comparable with other studies (Korecha and Barnston, 2007; Kassa, 2015), where 50–80% of annual rains fall during Kiremt (summer). Therefore, most severe droughts were related to the failure of Kiremt rain to meet agricultural productivity in Ethiopia. When seasonal rainfall variability was analyzed, the winter, spring, and autumn rainfall were more highly variable than Kiremt rainfall, which implies more inter-seasonal than annual rainfall variability in study towns. Our current results are comparable with the findings of Viste et al. (2013) and Arragaw and Woldeamlak (2017), where more variability in other seasonal rainfall than the Kiremt rainfall in most parts of Ethiopia was disclosed. Philippon et al. (2002) also found a similar finding of a strong interannual variability over the last four decades in equatorial East Africa.

During the study period (1953-2018), the slopes of linear regressions were 10.06, 2.3, and 1.6 mm/year for annual rainfall despite being statistically insignificant over Jimma, Bedelle, and Bonga, respectively (**Table 5**; **Supplementary Figures 1**, **2**).These findings were similar to earlier studies (Getenet and Bewket, 2009; Mohammed, 2018). These scholars argued that the rainfall trend in Jimma and Bedelle was increasing but then substantially declined over Sokorru.

A Standardized Rainfall Anomaly (SRA) method was also applied to assess how inter-annual rainfall fluctuated in the study region. Although the seasons did not exhibit any persistence in the pattern of wet and dry conditions, the dry years and seasons were more frequent than the wet years and seasons during the 66 year study period (**Figure 5**; **Supplementary Figure 2**), with **Figure 6** showing a distinct seasonal rainfall trend in Jimma City. This finding correlated with earlier studies (Getenet and Bewket, 2009; Mohammed, 2018), who argued that since there are no consistent patterns or trends in daily rainfall characteristics or seasonal rainfall, it is difficult to conclude whether the climate of the study area is becoming progressively drier or wetter. However, the observed occurrence of dryness in southwest Ethiopia is becoming apparent, which calls for proactive attention of concerned bodies ahead. Our findings were

TABLE 5 | Mann-Kendall trend test on observed seasonal and annual rainfall time series of the four urban centers from 1953 to 2018 using (two-tailed test at 0.05 significance level) and Sen's Slope Estimator (mm/year).

Study Town/station	Attribute/season	Mean	SD	CV (%)	% Contribution	*P*-value	Sen's slope
Jimma	Winter	115.7	66.8	57.8	7	−0.20	−0.108
	Spring	488.6	179.8	36.8	28	2.43	3.996
	Summer	732.2	171.0	23.4	42	2.11	3.378
	Autumn	398.2	140.6	35.5	23	2.55	3.250
	Annual	1734.7	432.5	24.9		2.09	9.430
Bonga	Winter	167.8	80.0	47.7	9.5	−2.42	−1.265
	Spring	537.3	121.5	22.6	30.4	0.89	1.118
	Summer	628.7	150.8	24	35.6	2.14	1.990
	Autumn	432.3	129.5	30	24.5	0.72	0.614
	Annual	1766.0	284.4	16.1		0.46	1.692
Bedelle	Winter	58.56	37.70	64.4	3	−0.51	−2.41
	Spring	413.00	125.54	30.4	21.4	1.29	1.184
	Summer	932.85	135.21	14.5	48.3	0.00	0.000
	Autumn	527.64	210.03	39.08	27.3	−0.16	−0.567
	Annual	1932.05	373.79	19.3		−0.04	−0.083
Sokorru	Winter	81.8	60.5	74	5.9	−1.87	−1.55
	Spring	345.8	107.4	31.1	25	−0.05	−0.046
	Summer	672.8	108	16	48.7	−1.28	2.76
	Autumn	281.2	97.5	34.7	27.3	1.61	2.617
	Annual	1381.6	176.7	12.8		−1.58	−4.885

also consistent with the Funk et al. (2012), which documented that Belg and Kiremt rainfall have decreased by 15–20% between 1975 and 2010 over southwestern and southeastern parts of Ethiopia.

Monthly, Seasonal, and Annual Temperature Trend Analysis

An increase in temperature is one manifestation of global climate change. To examine the local climate patterns in urban centers of southwest Ethiopia, analysis of monthly, seasonal, and annual temperature was undertaken to detect strong variability and temporal trends in the study area for the periods of 1967–2018. In this study, two climatic normals for maximum, minimum, and mean temperatures from the first period of 1967–1988 were found to be 26. 0, 11.6, and 18.8°C, respectively and for the second period of 1989–2018, 27.0, 12.5, and 19.8°C, respectively. This study further implies that the difference between two consecutive climatic normals resulted in positive changes with the values 1.0, 0.9, and 1.0°C for maximum, minimum, and mean temperatures, respectively. When two climatic normal were compared, the temperature increased in the latter case over the study area, which revealed the global warming footprint in the southwest urban centers of Ethiopia (**Figures 7A–C**, **8A,B**).

Table 5 below summarizes monthly, seasonal, and annual temperature (minimum and maximum) patterns for each urban center and temporal trends during the period under examination, as well as trends for each town depicted in **Supplementary Figures 3**, **4**. The mean minimum and maximum temperature in the study area ranges from 17. 6 to 20.5°C with an annual mean temperature of 19.2°C. Using a linear regression model, the rate of temperature changes over the study region is 0.41, 0.32, and 0.32°C per decade for maximum, minimum, and mean temperature, respectively, between 1967 and 2018 (**Table 6**; **Figures 7A–C**). The long-term anomalies (**Table 7**; **Figures 7**, **8**) of mean annual temperature showed there had been recurrent interannual and seasonal variability (the trend after 1988 has been higher than the long-term average) which is evidence of a warming trend since the last three decades of the twentieth century.

This finding is lower than the global warming rate, which is estimated at 0.6°C, as documented in IPCC (2014) for the past century. Slight differences arose between our findings and a global rate because our study covers only a grid point with only four meteorological observation sites. Besides, we thought that in addition to the presence of vast natural tropical rain forests and 10 months of the rainy period, the region is located far from the country's industrial zones, which might contribute to the low GHGs emissions potential. The results we generated in this study are substantially comparable with previous studies on the average annual temperature of Ethiopia, where the rate of change was documented as +0.37°C per decade (EEA, 2008). Furthermore, as documented by EEA (2008), Ethiopia has been warming for the past four decades, with most warming occurring through the second half of the 1990s. This implies that the warming trend in southwest urban centers of Ethiopia is slower than the rest of the country because of the remnants of natural forests and the presence of better moisture status in the region.

As shown in **Table 7**, MK trend test results revealed that maximum and minimum average temperatures have increased since the 1950s, and the trend is statistically significant at the 95%

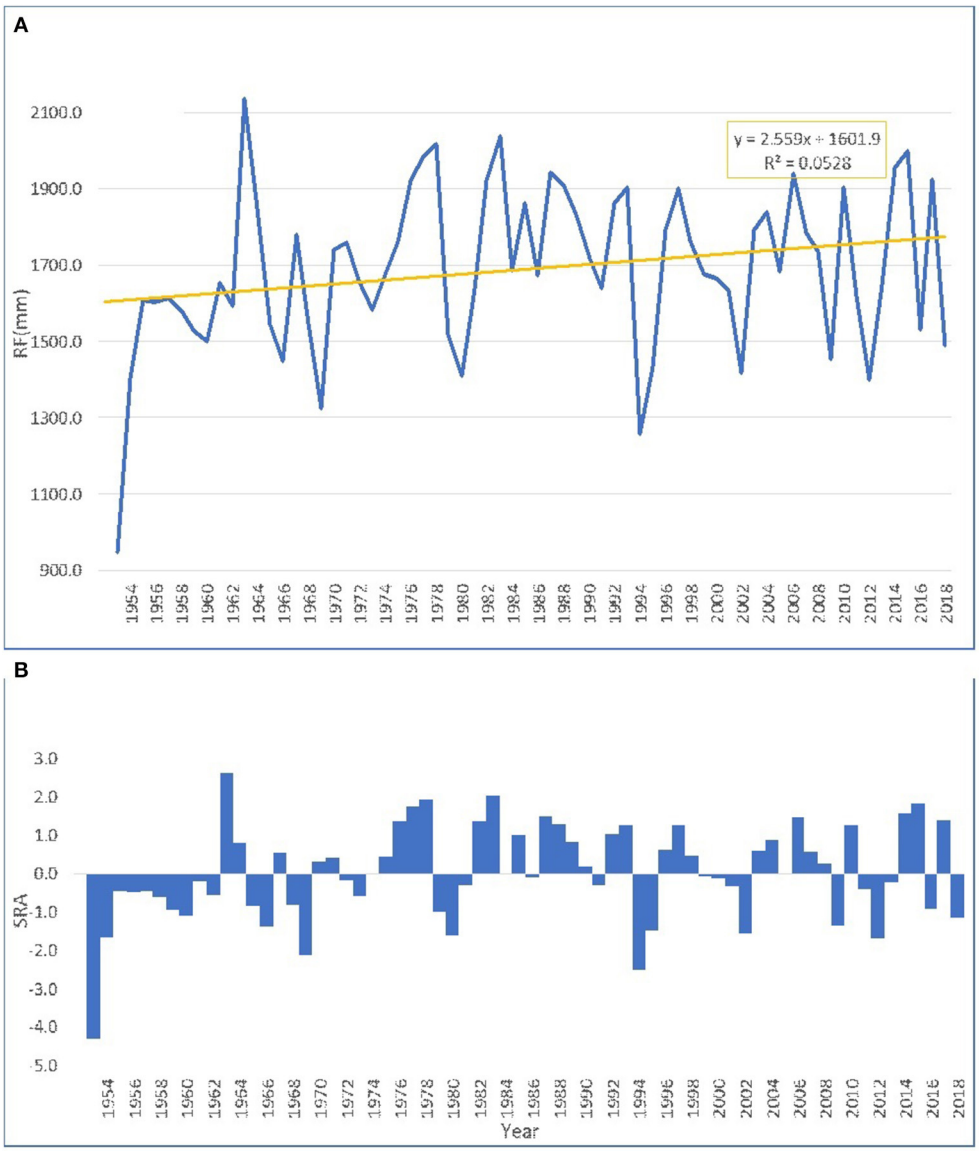

FIGURE 5 | Areal-averaged **(A)** annual rainfall trend, and **(B)** standardized rainfall anomaly computed for Southwest urban centers of Ethiopia dining the period 1953–2018.

level. The monthly maximum temperature has also increased, and for many months the trend is statistically significant at a 95% significance level.

Mann Kendall tests, both seasonal and annual for minimum and maximum temperature, showed to be statistically significant with the increasing trend at $\alpha = 0.05$ level spatial variations over towns (**Table 7**). In Jimma City, the maximum temperature increased in all seasons and annually except during the winter, whereas the minimum temperature had a significant increase during winter and summer seasons. For Bedelle town, both minimum and maximum temperatures have an increasing trend during autumn. In Sokorru town, maximum temperature has an increasing trend, but it is not statistically significant for most seasons or annually except during summer when both minimum and maximum temperatures have significantly increased (**Table 7**; **Supplementary Figure 4**). Regarding inter-seasonal and annual variability of temperature during the study period, the minimum temperature has higher seasonal variability with the lowest Coefficient of variation (4.3%) in summer over Jimma City and the highest CV (19.7%) during autumn over Bonga, while the maximum temperature showed lower variability (**Table 7**).

The overall increase in annual temperature observed in the study area was attributed to an increase in the minimum temperature (the minimum temperature increment is more pronounced than the maximum). The empirical result is in

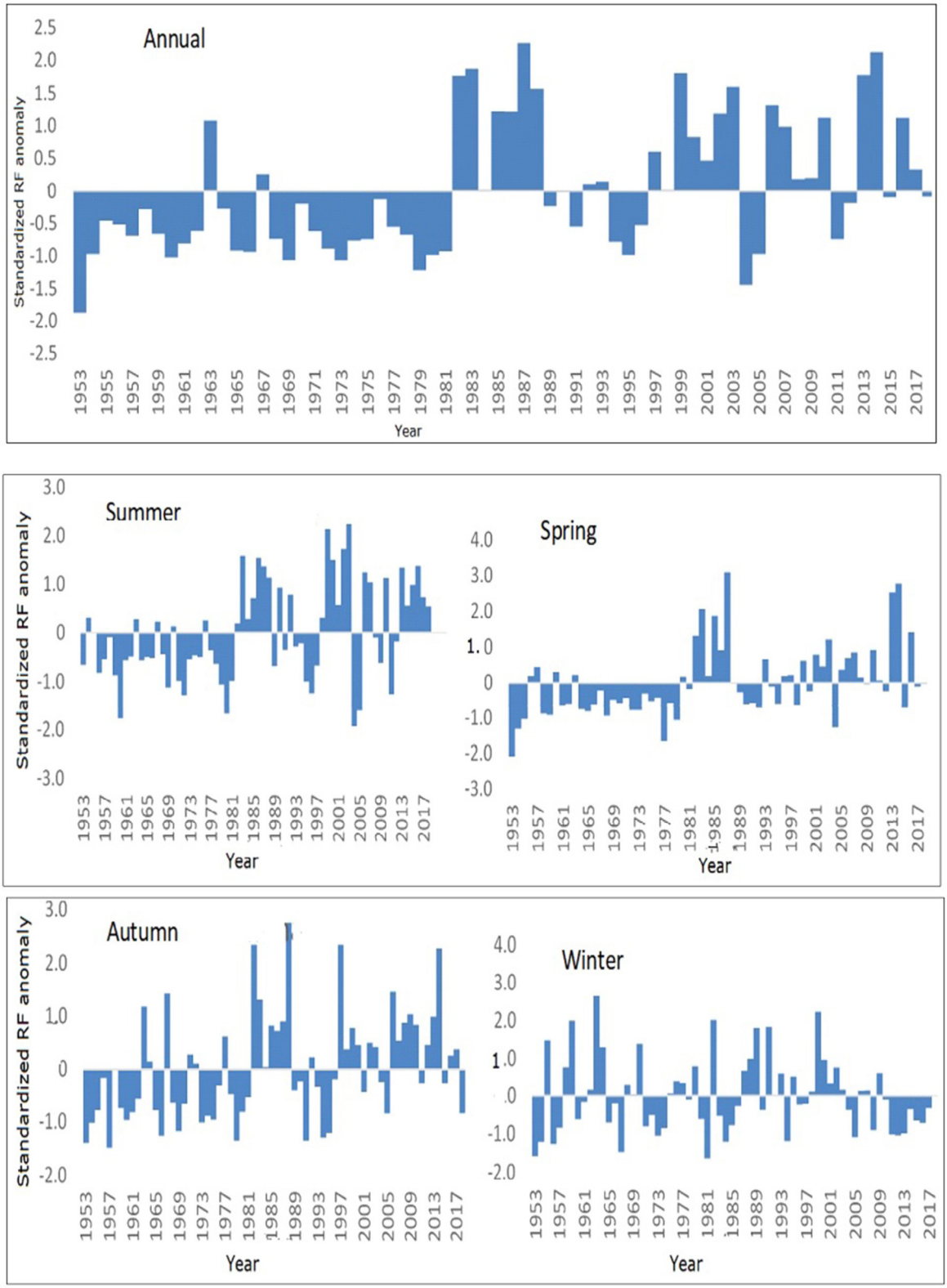

FIGURE 6 | Time series of Standardized annual and seasonal Rainfall Anomaly (SRA) as computed for Jimma urban center during 1953 to 2018.

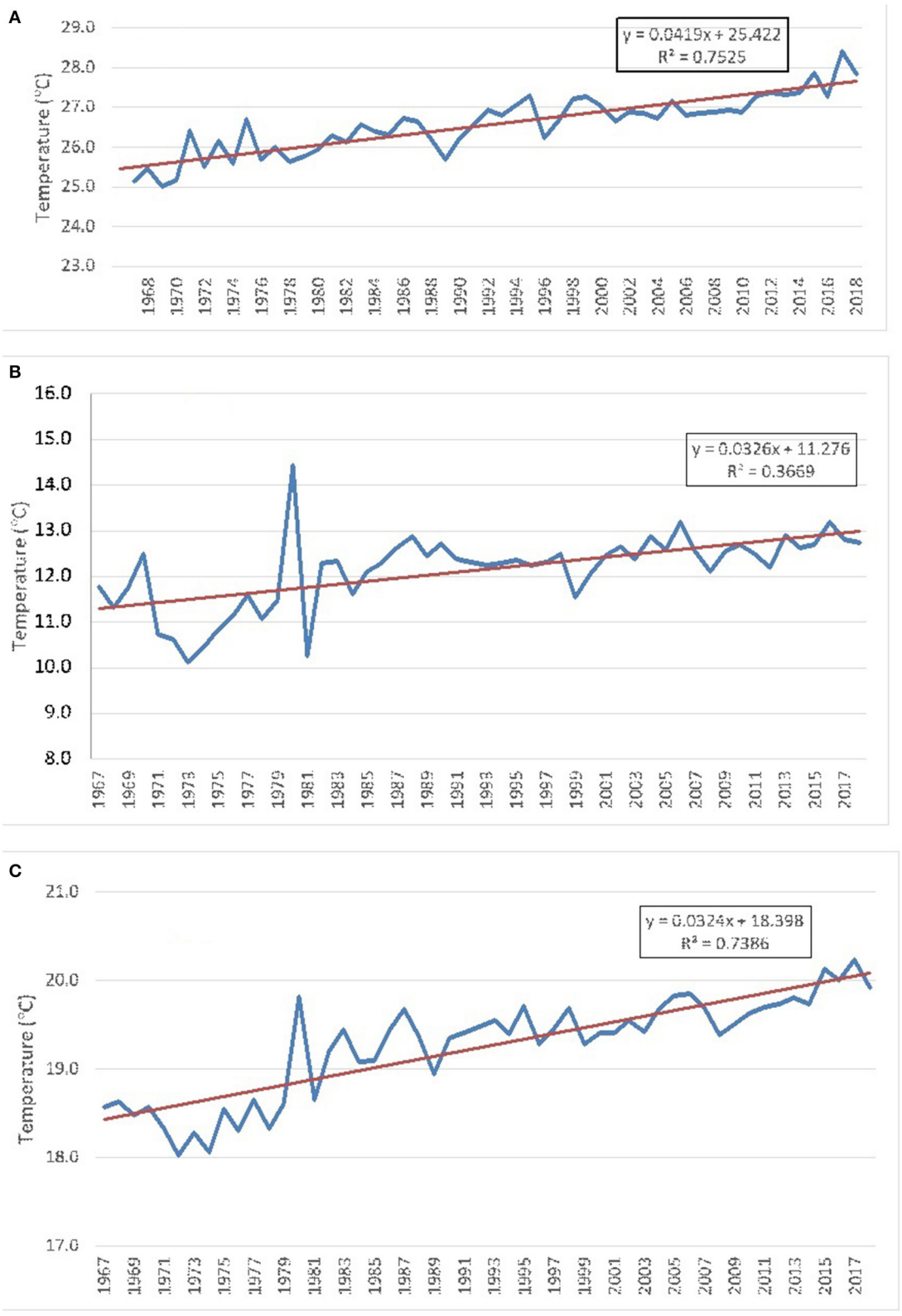

FIGURE 7 | Time series graph showing areal-averaged **(A)** Maximum, **(B)** Minimum, and **(C)** Mean temperature as computed for the southwest urban centers of Ethiopia during the period 1967–2018.

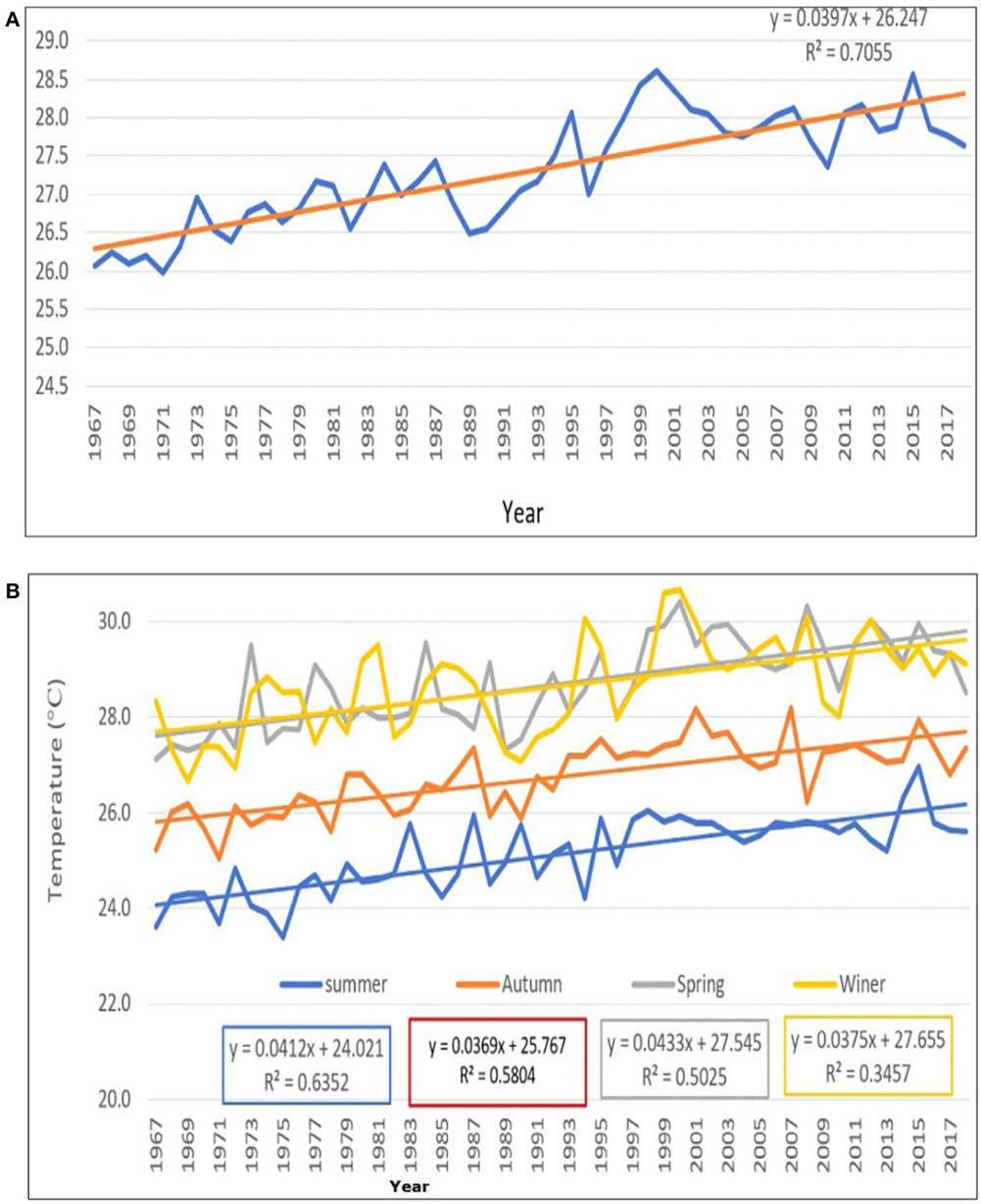

FIGURE 8 | Time series graph showing **(A)** Annual, **(B)** Seasonal maximum temperature trend over Jimma urban center during the period 1967–2018.

agreement with the findings of similar studies conducted in various parts of Ethiopia (Conway et al., 2004; Tabari and Talaee, 2011; Roy and Das, 2013; Daniel et al., 2014; Asfaw et al., 2018), where the increasing trends in the minimum temperature series were higher than those in the maximum temperature. The result generated from our study, which is based in southwest Ethiopia, is consistent with similar research made for Addis Ababa (Feyisa et al., 2016). Therefore, it is apparent that temperatures in urban centers are warmer than the outskirts and its bio-physical conditions are up to 3.7°C, which needs further research in the study area. This study's findings are also complementary to the findings documented in the Cities Alliance (2017). One of the driving forces behind this narrative is that in Ethiopia, cities developed and expanded because of unplanned urban growth, unmanaged old and new vehicles for transportation, and energy needs in cities, which resulted in a temperature rise in recent decades, decline in rainfall totals, and increased incidences of extreme events. It was also found that very low rainfall anomaly values, which correspond to severe drought periods, had links to ENSO events and other global changes. Therefore, it is imperative to adjust the urban development under extreme variation in climate systems because of the changing climate. The data will also help in designing effective urban planning and implementation of climate change adaptation strategies ahead of

TABLE 6 | Results from linear regression analysis of rainfall (1953–2018) and temperature (1967–2018), and their temporal changes in urban centers of Southwest Ethiopia.

S/N	Attribute	Jimma	Bedelle	Bonga	Sokorru	Areal-averaged change
I	**Rainfall**					
1	Change of RF (mm/year)	10.06	1.618	2.342	−2.95	2.559
2	Change of RF (mm/decade)	100.6	16.18	23.42	−29.5	25.59
3	R^2	0.222	0.00	0.024	0.027	0.036
II	**Minimum Temperature**					
	Change of temp (°C/year)	0.028	0.057	−0.002	0.021	0.032
	Change of temp (°C/decade)	0.28	0.57	−0.02	0.21	0.32
	R^2	0. 393*	0. 533*	0.000	0.178	0. 366*
III	**Maximum temperature**					
	Change of temp (°C/year)	0.037	0.013	0.076	0.012	0.041
	Change of temp (°C/decade)	0.37	0.13	0.76	0.12	0.41
	R^2	0. 666*	0.062	0. 656*	0.000	0. 752*
IV	Mean temperature	0. 32°C/decade) R^2 =0. 705*				

**indicates that R^2 is statistically significant at 0.05 significant level.*

TABLE 7 | Mann-Kendall trend test on seasonal and annual temperature in urban centers of Southwest Ethiopia.

Town	Attribute/	Mean (°C)		SD (°C)		CV (%)		*P*-value		Sen's slope	
/station	Season	Tmax	Tmin	Tmax	Tmin	T max	T min	T max	T min	Tmax	Tmin
Jimma	Winter	28.7	8.2	0.94	1.5	3.3	18.7	1.83	2.35	0.017	0.014
	Spring	28.7	12.3	0.9	1.1	3.1	8.6	2.17	2.2	0.023	0.016
	Summer	25.0	13.4	0.82	0.6	3.3	4.3	2.02	2.17	0.290	0.013
	Autumn	26.8	11.2	0.73	1.1	2.7	10.2	2.16	1.83	0.017	0.010
	Annual	27.3	11.3	0.7	0.8	2.6	7.3	2.06	1.9	0.025	0.014
Bonga	Winter	28.6	10.7	2.0	1.7	7.1	15.9	0.73	0.02	0.000	0.000
	Spring	27.8	12.5	1.7	1.7	6.2	12.5	0.97	0.79	0.000	0.006
	Summer	25.7	12.6	1.5	1.8	6.0	14.3	0.95	0.98	0.000	0.007
	Autumn	26.8	11.8	1.7	2.31	6.2	19.7	1.63	1.43	0.000	0.010
	Annual	27.7	11.9	2.84	1.7	16	13.9	0.83	1.17	0.000	0.008
Bedelle	Winter	27.8	13.3	1.4	0.6	5.3	4.8	1.75	0.74	0.018	0.067
	Spring	27.5	14.3	1.2	0.8	4.3	5.7	0.93	1.75	0.003	0.059
	Summer	23.1	12.3	0.9	0.8	3.8	6.5	0.13	0.56	0.000	0.000
	Autumn	24.5	12.6	0.8	0.8	0.9	5	3.28	2.35	0.160	0.027
	Annual	25.6	13.3	0.8	0.6	3.0	4.5	1.60	0.34	0.013	0.040
Sokorru	Winter	27.8	13.3	0.8	0.6	2.8	4.8	0.65	1.98	0.023	0.030
	Spring	27.7	14.3	1.1	0.8	3.8	5.7	1.74	1.42	0.029	0.009
	Summer	23.8	13.2	0.8	0.7	2.9	6.2	2.37	1.99	0.031	0.011
	Autumn	25.6	12.6	0.7	0.8	2.9	6.2	0.48	2.32	0.000	0.035
	Annual	26.2	13.3	0.6	0.6	2.2	4.5	1.09	1.53	0.013	0.025

time and mitigation actions to scale up the adaptive capacity and resilience of southwest Ethiopia's urban centers.

Impacts of Urbanization on LULCC and Local Climate

The rapid increase in built-up areas was the central cause behind various social, economic, and environmental changes throughout the study period. In this study, the results from LULC classification and climate variables, noticeably temperature and rainfall data analyses, showed that urban expansion induced significant impacts on land use land cover changes. Built-up areas expanded at the expense of shrinking of vegetation, cropland, and wetland areas (**Table 3**). This study has indicated the rapid expansion of anthropogenic influence on the LULC, where urban areas increased highly in the last three decades. Minimum temperature has also increased at a rate higher than that of mean and maximum temperature during the entire study period. Thus, this study revealed that during the early 2000s, the

rate of change of areal averaged temperature over entire urban centers was greater than the 1990s, with the mean, minimum, and maximum increased by 0.7, 1.3, and 0.3°C, respectively. In East India, Partha et al. (2019) documented that an increase in areal-averaged temperatures was associated with LULC changes of urbanization, and with spatio-temporal variation, up to half of the warming due to LULC change in urban centers. Similarly, over four urban centers in Southwest Ethiopia, LULCC could possibly be attributed to the areal-averaged observed minimum, maximum, and mean temperature change with the order of 0.32, 0.41, and 0.32°C/decade, respectively (**Tables 3**, **6**; **Figure 7**; **Supplementary Figures 2–4**). LULCC, therefore, induced a significant warming in urban centers as a result of changing in vegetation cover. In contrast, a change in rainfall amounts varied from place to place, where it increased over Jimma, but decreased more over Bedelle, Bonga, and Sokorru in the last 30 years than in the first 30 years of the study period.

In Ethiopia, much research has been done to examine the impact of urban expansion on LULCC. For instance, the study carried out in Addis Ababa (Abebe and Megento, 2016); Adama (Sinha et al., 2016); Mekelle (Tahir et al., 2013); Hawassa (Gashu and Gebre-Egziabher, 2018); and Dire Dawa (Taffa et al., 2017) showed that there was a significant increment in built-up areas, while there was a decline in green areas and open spaces. These findings are similar to the results we deduced in this study. Similar studies made for other major towns in Ethiopia also indicated that the temperature increased in recent decades and was projected to increase in the future, with no clear trend on precipitation change. For instance, the temperature change has shown an increasing trend over Mekelle, Bahirdar, Gondar, Adama, Diredawa, Gode, Jigjiga, Batu, Arbaminch, and others (Beyene, 2016; Mulugeta et al., 2017), as well as fluctuations in annual rainfall trends (Abebe, 2016). Climate-related impacts have also been highly reported for urban centers in part due to urban land use land cover change that directly related to a systematic rise in temperature, as well as intensive urban flooding during rainfall seasons. Results that were generated from similar studies resembled our findings, which revealed that urbanization could trigger substantial LULC changes that in turn resulted in local climate changes in urban centers of Southwest Ethiopia. In fact, as this study focused on four heterogenic urban centers, more research is required to understand comprehensive urban LULC changes and other factors linked to local and regional climate change. Nevertheless, as urban areas are currently undergoing rapid transformation due to intensive developmental activities, this could accelerate the rate of climate change in urban areas.

CONCLUSION

This study adopted a combined method of multi-temporal remote sensing image interpretation and GIS spatial analysis to characterize the dynamics of urban land use land cover change and emerging climatic extremes in the urban area of southwest Ethiopia during the period of 1957 to 2018. The LULCC analysis, which we carried out in four main urban centers, revealed a substantial land use land cover change between 1957 and 2018 due to the use of urban land for different human activities. As a result, the built-up areas showed an increasing trend over the last six decades in all urban centers, in contrast to the decline of vegetation, wetland, and cropland because of the conversion of lands to built-up areas. The rapid increase of built-up areas coupled with the sharp decline of green space because of urban expansion and urbanization led to the fast decline of agricultural and crop lands, which is practiced in many developing countries, leading to the changing of the local microclimate of the urban centers. The urban centers' surface temperature is warmer than the outskirts; the findings coincided with many studies claiming cities are "Heat high lands." Areal-averaged rainfall totals of southwest Ethiopia urban centers have declined since the 1950s, coupled with recurrent extreme rainfall events with a strong spatial and temporal variation.

Since the early 1950s, annual rainfall totals have somewhat increased by <5 mm/year over parts of the urban centers, although the change is not statistically significant. The Mann Kendal test results showed there is intra seasonal and inter-annual rainfall variability while the summer and annual rainfall is less variable than other seasons. In this study we identified that there is a warming trend in the southwest urban centers and hence the latter half of the study period is warmer than the first half of the period. The local warming trend is accounted for because of the expansion of urbanization with buildings, the use of excessive energy sources, and expansion of new factories, business centers, and vehicles that contribute to localized warming in central parts of urban regions. Therefore, the study results revealed that the maximum, minimum, and mean daily temperatures have increased by 0.3, 1.3, and 0.7°C during 1987–2018 and from 1953 to 1986. Whereas, the results generated from a linear regression model showed an increasing trend of daily mean, minimum, and maximum temperatures by 0.21, 0.24, and 0.18°C per decade, respectively, from 1953 to 2018. These values are relatively comparable with the national (NMSA, 2001) and IPCC (2013) values, which is 0.3°C/decade on average.

Over the second study period, the urban centers of southwest Ethiopia experienced abrupt land use land cover change because of the momentum of urbanization and human activities, which also showed a similar temperature trend over recent decades. Thus, the urban centers of southwest Ethiopia are under the threat of climate change. Similar to other developing countries, urban centers that emerge from unplanned urban expansion and development at the expense of the urban environment and local climate, should devise strategies to comply with sustainable urban development so they can become more livable and resilient cities in the dynamic world of challenging climate change.

For many nations, the heart of politics, technological development, and economic growth lie in their urban centers, which also hosting rampant poverty, inequality, environmental hazards, and communicable diseases. Urban

centers in developing countries are hampered by shortages of infrastructure services, and the unplanned development and lack of infrastructural development in urban areas of study towns escalated the effects of climate change.

Climate change is expected to exacerbate several threats to urban dwellers' health and well-being through direct physical injuries from the recurrence of extreme weather events, such as intense heavy rainfall that leads to flooding, often damage trees and infrastructure facilities, and disrupts access to clean water and food. Also, it causes water-borne diseases, food-borne diseases resulting from bacterial growth in foods exposed to higher temperatures, illnesses from a range of vector-borne infectious diseases, respiratory illnesses because of a worsening of poor air quality related to changes in temperature and precipitation resulting in the formation of smog, and vulnerability because of stress from hotter and longer heat waves, which are aggravated by the urban heat island effect. Climate change imposes an additional expense for more energy consumption even for buildings that use air conditioning and other technologies during hot summers. Most of the urban poor live in in environmentally unsuitable neighborhoods of urban regions, for instance along the hillsides, riverbanks, and water basins subject to landslides, flooding, or hazards which favor the spread of communicable and non-communicable diseases, pollution, poor nutrition, and other catastrophes. How much these environmental changes could associate with newly emerging climatic factors, land use land cover change, building, and infectious diseases needs further epidemiological research.

Although extensive urbanization has become an irreversible phenomenon, urban governments have to consider policies that enhance community participation in poverty reduction, addressing proper urban environmental issues, improving rural-urban linkages to improve food security, implementing urban safety net programs for social protection and health services, and increasing the capacity of urban dwellers to adapt to the challenges of climate change while seeking to reduce unplanned urbanization, which reduces the land use land cover change of urban areas.

DATA AVAILABILITY STATEMENT

The raw data supporting the conclusions of this article will be made available by the authors, without undue reservation.

AUTHOR CONTRIBUTIONS

TD and DK devised the project, the main conceptual ideas, and the proof outline. TD worked out almost all of the technical details, performed the numerical calculations for the manuscript, and wrote the manuscript under the close supervision of DK. DK closely worked out the supervision, involved almost in all technical details, and verified the numerical results of all sections with help from TD. DH and AW contributed to framing the manuscript and made valuable inputs. All authors contributed to the article and approved the submitted version.

ACKNOWLEDGMENTS

The authors would like to acknowledge the following institutions in the acquisition of necessary data and technical support for this work: United States Geological Survey (USGS), Jimma, Bedelle, Bonga and Sokorru City Administration Offices, Ethiopia Geo-Spatial Agency, and West Oromia Meteorological Services Center. We are also grateful to Jimma University College of Agriculture and Veterinary Medicine for writing supporting letters to study towns and institutions to undertake ethical procedures of the research and those friends who stand on our side during the research work. Finally, we would like to thank Juliet Way-Henthorne of the University of California Santa Barbara, who reviewed language coherency and consistency of this manuscript to the best standard.

SUPPLEMENTARY MATERIAL

The Supplementary Material for this article can be found online at: https://www.frontiersin.org/articles/10.3389/fclim.2020.577169/full#supplementary-material

REFERENCES

Abebe, M. (2016). *Remote sensing and geographic information system based suitability analysis of urban green space development in Addis Ababa: a case study of bole sub-city* [M.Sc. thesis]. Addis Ababa University, Addis Ababa, Ethiopia.

Abebe, M., and Megento, T. (2016). The city of Addis Ababa from "Forest City" to "Urban Heat Island": assessment of urban green space dynamic. *J. Urban Environ. Eng.* 10, 254–262. doi: 10.4090/juee.2016.v10n2.254262

Abebe, M. S., Derebew, K. T., and Gemeda, D. O. (2019). Exploiting temporal, spatial patterns of informal settlements using GIS and remote sensing technique: a case study of Jimma City, Southwestern Ethiopia. *Environ. Syst. Res.* 8:6. doi: 10.1186/s40068-019-0133-5

ACCRA (2012). *Climate Trends in Ethiopia: Summary of ACCRA Research in Three Sites*. CDKN and DfID.

Agnew, C. T., and Chappel, A. (1999). Drought in the Sahel. *Geojournal* 48, 299–311. doi: 10.1023/A:1007059403077

Anderson, J. R., Hardy, E. E., Roach, J., and Witmer, R. E. (1976). *A Land Use/Cover Classification System for Use With Remote Sensor Data*. Sious Falls, SD: US Geological Survey Professional. Available online at: https://pubs.usgs.gov/pp/0964/report.pdf

Arragaw, A., and Woldeamlak, B. (2017). Local spatio temporal variability and trends in rainfall and temperature in the central highlands of Ethiopia. *Geogr. Ann. Phys. Geogr.* 99, 85–101. doi: 10.1080/04353676.2017.1289460

Asfaw, A., Simane, B., Hussein, A., and Bantider, A. (2018). Variability and time series trend analysis of rainfall and temperature in north central Ethiopia: a case study in Woleka sub-basin. *Weather Clim. Extremes* 19, 29–41. doi: 10.1016/j.wace.2017.12.002

Beyene, A. (2016). Precipitation and temperature trend analysis in Mekelle city, Northern Ethiopia, the case of Illala meteorological station. *J. Earth Sci. Clim. Change*. 7:1. doi: 10.4172/2157-7617.1000324

Bihrat, O., and Bayazit, M. (2003). The power of statistical test for trend detection. *Turkish J. Eng. Env. Sci.* 27, 247–251. Available online at: https://www.semanticscholar.org/paper/The-Power-of-Statistical-Tests-for-Trend-Detection-%C3%96n%C3%B6z-Bayazit/e05ceac33dcaba5ad8e451009ab8188063ccc4ec

Birsan, M., Molnar, P., Burlando, P., and Pfaundler, M. (2005). *Stream Flow Trends in City A. The Climate Change and Energy Debate in Ethiopia*. Brussels: Pegasys Institute and Ethio Resources Group.

Braimoh, A. K. (2006). Random and systematic land-cover transitions in northern Ghana. *Agric. Ecosyst. Environ*. 113, 254–263. doi: 10.1016/j.agee.2005.10.019

Cities Alliance (2017). *About CDS* [Online]. Available online at: http://www.citiesalliance.org/about-cds (accessed February 6, 2020).

Congalton, R. G. (1991). A review of assessing the accuracy of classifications of remotely sensed data. *Remote Sens. Environ.* 37, 35–46. doi: 10.1016/0034-4257(91)90048-B

Conway, D., Mould, C., and Woldeamlak, B. (2004). Over one century of rainfall and temperature observations in Addis Ababa, Ethiopia. *Int. J. Climatol*. 24, 77–91. doi: 10.1002/joc.989

Conway, D., and Woldeamlak, B. (2007). A note on the temporal and spatial variability of rainfall in the drought-prone Amhara region of Ethiopia. *Int. J. Climatol*. 27, 1467–1477. doi: 10.1002/joc.1481

CSA (2007). *Population Statistical Abstract*. Addis Ababa: Federal Democratic Republic of Ethiopia, Population Census Commission. Democratic Republic of Ethiopia, Population Census Commission.

CSA (2017). *Population Projections for Ethiopia 2007-2037*. Addis Ababa.

Daniel, M., Woldeamlak, B., and Lal, R. (2014). Recent spatiotemporal temperature and rainfall variability and trends over the upper Blue Nile river basin, Ethiopia. *Int. J. Climatol*. 34, 2278–2292. doi: 10.1002/joc.3837

Debolini, M., Valette, E., and Chery, J. P. (2015). Mapping land use competition in the rural-urban fringe and future perspectives on land policies: a case study of Meknès (Morocco). *Land Use Policy* 47, 373–381. doi: 10.1016/j.landusepol.2015.01.035

EEA (2008). *Climate Change and Development Adaptation Measures*. Addis Ababa: Ethiopian Economic Association.

Epstein, J., Payne, K., and Kramer E. (2002). Techniques for mapping suburban sprawl. *Photogr. Eng. Remote Sens.* 63, 913–918.

Feyisa, G. L., Meilby, H., Darrel Jenerette, G., and Pauliet, S. (2016). Locally optimized separability enhancement indices for urban land cover mapping: exploring thermal environmental consequences of rapid urbanization in Addis Ababa, Ethiopia. *Remote Sens. Environ*. 175, 14–31. doi: 10.1016/j.rse.2015.12.026

Funk, C., Dettinger, M. D., Michaelsen, J. C., Verdin, J. P., Brown, M. E., Barlow, M., et al. (2008). Warming of the Indian Ocean threatens eastern and southern African food security but could be mitigated by agricultural development. *Proc. Natl. Acad. Sci. U.S.A.* 105, 11081–11086. doi: 10.1073/pnas.0708196105

Funk, C., Rowland, J., Eilerts, G., Kebebe, E., Biru, N., White, L., and Galu, G. (2012). *A Climate Trend Analysis of Ethiopia, Fact Sheet 2012-3053*. U.S. Geological Survey. doi: 10.3133/fs20123053

Garai, D., and Narayana, A. C. (2018). Land use/land cover changes in the mining area of Godavari coal fields of southern India. *Egypt J. Remote Sens. Space Sci.* 21, 375–381. doi: 10.1016/j.ejrs.2018.01.002

Gashu, K., and Gebre-Egziabher, T. (2018). Spatiotemporal trends of urban land use/land cover and green infrastructure change in two Ethiopian cities: Bahir Dar and Hawassa Kassahun. *Environ. Syst. Res.* 7:8. doi: 10.1186/s40068-018-0111-3

Gebre, H., Kindie, T., Girma, M., and Belay, K. (2013). Trend and variability of rainfall in Tigray, Northern Ethiopia: analysis of meteorological data and farmers' perception. *Acad. J. Environ. Sci.* 1, 159–171. doi: 10.15413/ajar.2013.0117

Gebremedhin, K., Shetty, A., and Nandagiri, L. (2016). Analysis of variability and trends in rainfall over northern Ethiopia. *Arab J. Geosci.* 9:451. doi: 10.1007/s12517-016-2471-1

Getachew, K., and Tamene, A. (2015). Assessment of the effect of urban road surface drainage: a case study at Ginjo Guduru Kebele of Jimma town. *Int. J. Sci. Technol. Soc*. 3, 164–173. doi: 10.11648/j.ijsts.20150304.20

Getenet K., and Bewket, W. (2009). Variations in rainfall and extreme event indices in the wettest part of Ethiopia. *SINET* 32, 129-140.

Giannaros, T. M., Melas, D., Daglis, I. A., Keramitsoglou, I., and Kourtidis, K. (2013). Numerical study of the urban heat island over Athens (Greece) with the WRF model. *Atmos. Environ*. 73, 103–111. doi: 10.1016/j.atmosenv.2013.02.055

Grimm, N. B., Faeth, S. H., Golubiewski, N. E., Redman, C. L., Wu, J., Bai, X., et al. (2008). Global change and the ecology of cities. *Science* 319, 756–760. doi: 10.1126/science.1150195

Hare, W. (2003). Assessment of Knowledge on Impacts of Climate Change-Contribution to the Specification of art. *2 of the UNFCCC: Impacts on Ecosystems, Food Production, Water and Socio-Economic Systems*. Available online at: https://www.researchgate.net/publication/ (accessed March 12, 2020).

He, C., Okada, N., Zhang, Q., Shi, P., and Li, J. (2008). Modelling dynamic urban expansion processes incorporating a potential model with cellular automata. *Landsc. Urban* Plann. 86, 79–91. doi: 10.1016/j.landurbplan.2007.12.010

Herold, M., Goldstein, N. C., and Clarke, K. C. (2003). The spatiotemporal form of urban growth. *Remote Sens. Environ*. 86, 286–302. doi: 10.1016/S0034-4257(03)00075-0

IPCC (2013). "Climate change 2013: the physical science basis," in *Contribution of Working Group I to the Fifth Assessment Report of the Intergovernmental Panel on Climate Change*, eds T. F. Stocker, D. Qin, G.-K. Plattner, M. Tignor, S. K. Allen, J. Boschung, A. Nauels, Y. Xia, V. Bex, and P. M. Midgley (Cambridge; New York, NY: Cambridge University Press), 1535.

IPCC (2014). *Climate Change 2014: Impacts, Adaptation, and Vulnerability; Part A: Global and Sectoral Aspects. Contribution of Working Group II to the Fifth Assessment Report of the Intergovernmental Panel on Climate Change*. Cambridge; New York, NY: Cambridge University Press.

Jimma City Administration (2019). *Spatial Planning and Socioeconomic Assessment of the Master Plan Under the Revision Document*.

Kassa, F. (2015). Ethiopian seasonal rainfall variability and prediction using canonical correlation analysis (CCA). *Earth Sci.* 4, 112–119. doi: 10.11648/j.earth.20150403.14

Kendall, M. G. (1975). *Rank Correlation Method*, 4th Edn. London: Charles Griffin.

Korecha, D. (2013). *Characterizing the predictability of seasonal climate in Ethiopia* [Dissertation for the degree philosophiae doctor (PhD) in Meteorology]. University of Bergen, Bergen, Norway.

Korecha, D., and Barnston, A. G. (2007). Predictability of June–September rainfall in Ethiopia. *Mon. Weather Rev*. 135, 628–650. doi: 10.1175/MWR3304.1

Lillesand, T., Kiefer, R. W., and Chipman, J. (2015). *Remote Sensing and Image Interpretation*. Hoboken, NJ: John Wiley and Sons.

Lillesand, T. M., Keifer, R. W., and Chipman, J. W. (2004). Remote sensing and image interpretation. 5th ed. (New York: Wiley). Geogr. J. 146. doi: 10.2307/634969

Liu, Z., He, C., Zhou, Y., and Wu, J. (2014). How much of the world's land has been urbanized, really? A hierarchical framework for avoiding confusion. *Landscape Ecol.* 29, 763-771. doi: 10.1007/s10980-014-0034-y

Lu, D., Mausel, P., Batistella, M., and Moran, E. (2004). Land-cover binary change detection methods for use in the moist tropical region of the Amazon: a comparative study. *Int. J. Remote Sens.* 26, 101–114. doi: 10.1080/0143116041000172074 8

Mann, H. B. (1945). Non-parametric tests against trend. *Econometrica* 13, 245–259. doi: 10.2307/1907187

McSweeney, C., New, M., Lizcano, G., and Lu, X. (2010). Improving the accessibility of observed and projected climate information for studies of climate change in developing countries. *Bull. Am. Meteorol. Soc*. 91, 157–167. doi: 10.1175/2009BAMS2826.1

Mekonnen, A. D., and Woldeamlak, B. (2014). Variability and trends in rainfall amount and extreme event indices in the Omo-Ghibe River Basin, Ethiopia. *Reg. Environ. Change* 14, 799–810. doi: 10.1007/s10113-013-0538-z

Mengistie, K., Thomas, S., Demel, T., and Thomas, K. (2013). Land use/land cover change analysis using an object based classification approach in the Munesa Shashemene Landscape of the Ethiopian highlands. *Remote Sens*. 5, 2411–2435. doi: 10.3390/rs5052411

Mohammed, Y. (2018). Meteorological drought assessment in north east highlands of Ethiopia. *Int. J. Clim. Change Strateg. Manag*. 10, 142–160. doi: 10.1108/IJCCSM-12-2016-0179

Montgomery, M. R. (2008). The urban transformation of the developing world. *Science* 319, 761-764. doi: 10.1126/science.1153012

Mulugeta, M., Tolossa, D., and Abebe, G. (2017). Description of long-term climate data in Eastern and Southeastern Ethiopia. *J. Data Brief* 12, 26–36. doi: 10.1016/j.dib.2017.03.025

NMA (2019). *Observed Monthly Rainfall and Temperature data over Ethiopia*. Available online at: http://www.ethiomet.gov.et (accessed March 16, 2020).

NMSA (2001). *Initial National Communication of Ethiopia to the United Nations Framework Convention on Climate Change (UNFCCC).* National Meteorological Services Agency under the GEF supported Climate Change Enabling Activities Project of Ethiopia.

Oliver, J. E. (1980). Monthly precipitation distribution: a comparative index. *Prof. Geogr*. 32, 300–309. doi: 10.1111/j.0033-0124.1980.00300.x

Partha, P. G., Vinoj, V., Roberts, D. S. G., Dash, J., and Tripathy, S. (2019). Land use and land cover change effect on surface temperature over Eastern India. *Natu. Sci. Rep*. 9:8859. doi: 10.1038/s41598-019-45213-z

Patra, S., Sahoo, S., Mishra, P., and Mahapatra, S. C. (2018). Impacts of urbanization on land use /cover changes and its probable implications on local climate and groundwater level. *J. Urban Manag*. 7, 70–84. doi: 10.1016/j.jum.2018.04.006

Philippon, N., Camberlin, P., and Fauchereau, N. (2002). Empirical predictability study of October–December East African rainfall. *Q. J. R. Meteorol. Soc*. 128, 2239–2256. doi: 10.1256/qj.01.190

Pontius, R. G. Jr., Shusas, E., and McEachern, M. (2004). Detecting important categorical land changes while accounting for persistence. *Agricult. Ecosyst. Environ.* 101, 251–268. doi: 10.1016/j.agee.2003.09.008

Roy, T. D., and Das, K. K. (2013). Temperature trends at four stations of Assam during the period 1981-2010. *Int. J. Sci. Res. Publ*. 3, 1–3.

Seleshi, Y., and Zanke, U. (2004). Recent changes in rainfall and rainy days in Ethiopia. *Int. J. Climatol.* 24, 973–983. doi: 10.1002/joc.1052

Sen, P. K. (1968). Estimates of the regression coefficient based on Kendall's tau. *J. Am. Stat. Switzerland. J. Hydrol*. 314, 312–329. doi: 10.1080/01621459.1968.10480934

Sinha, P., Verma, N., and Ayele, E. (2016). Urban built-up area extraction and change detection of Adama municipal area using time-series landsat images. *Int. J. Adv. Remote Sens. GIS*. 5, 1886–1895. doi: 10.23953/cloud.ijarsg.67

Tabari, H., Meron, T. T., and Willems, P. (2015). Statistical assessment of precipitation trends in the upper Blue Nile River basin. *Stoch. Environ. Res. Risk Assess*. 29, 1751–1761. doi: 10.1007/s00477-015-1046-0

Taffa, C., Mekonen, T., Mulugeta, M., and Tesfaye, B. (2017). Data on spatiotemporal urban sprawl of Dire Dawa City, Eastern Ethiopia. *Data Brief* 12, 341–345. doi: 10.1016/j.dib.2017.04.008

Tahir, M., Imam, E., and Hussain, T. (2013). Evaluation of land use/land cover changes in Mekelle City, Ethiopia using Remote Sensing and GIS. *Comput. Ecol. Softw*. 3, 9–16. Available online at: http://www.iaees.org. (accessed March 12, 2020).

Tesfaye, G. A. (2017). *Monitoring trends of greenness and LULC (land use/land cover) change in Addis Ababa and its surrounding using MODIS time-series and LANDSAT Data*. Lund University GEM thesis series NGEM01 20171, Department of Physical Geography and Ecosystem Science. Available online at: http://lup.lub.lu.se/student-papers/record/8917891

Theil, H. (1950). "A rank invariant method of linear and polynomial regression analysis, i, ii, iii," in *Proceedings of the Koninklijke Nederlandse Akademie Wetenschappen, Series A Mathematical Sciences*, Vol. 53, 386–392, 521–525, 1397–1412.

United Nations (2014). *World Urbanization Prospects, The 2014 Revision*. Available online at: http://esa.un.org/unpd/.

Vargo, J., Habeeb, D., and Stone, B. (2013). The importance of land cover change across urban– rural typologies for climate modeling. *J. Environ. Manag*. 114, 243–252. doi: 10.1016/j.jenvman.2012.10.007

Viste, E., Korecha, D., and Sorteberg, A. (2013). Recent drought and precipitation tendencies in Ethiopia. *Theor. Appl. Climatol.* 112, 535-551. doi: 10.1007/s00704-012-0746-3

Viste, E.,Korecha, D., and Sorteberg, A. (2012). Recent drought and precipitation tendencies in Ethiopia. *Theoret. Appl. Climatol*. 2018, 29–41.

Wilson, B., and Chakraborty, A. (2013). The environmental impacts of sprawl: emergent themes from the past decade of planning research. *Sustainability* 5, 3302–3327. doi: 10.3390/su5083302

Witten, K., Exeter, D. J., and Field, A. (2003). The quality of urban environments: mapping variation in access to community resources. *Urban Stud*. 40:161–177. doi: 10.1080/00420980220080221

Yonas S., and Zahorik, J. (2017). Jimma Town: Foundation and Early Growth from ca. 1830 to 1936. *Ethnol. Actualis* 17. doi: 10.2478/eas-2018-0003

Conflict of Interest: The authors declare that the research was conducted in the absence of any commercial or financial relationships that could be construed as a potential conflict of interest.

frontiers in Climate

ORIGINAL RESEARCH
published: 28 January 2021
doi: 10.3389/fclim.2020.589282

Mobilizing Climate Information for Decision-Making in Africa: Contrasting User-Centered and Knowledge-Centered Approaches

Blane Harvey[1]*, *Ying-Syuan Huang*[1], *Julio Araujo*[2], *Katharine Vincent*[3,4], *Jean-Pierre Roux*[2,5], *Estelle Rouhaud*[6] and *Emma Visman*[7]

[1] Department of Integrated Studies in Education, McGill University, Montréal, QC, Canada, [2] SouthSouthNorth, Cape Town, South Africa, [3] Kulima Integrated Development Solutions (Pty) Ltd., Pietermaritzburg, South Africa, [4] School of Architecture and Planning, University of the Witwatersrand, Johannesburg, South Africa, [5] Department of Geography, University of Exeter, Exeter, United Kingdom, [6] London School of Economics and Political Science, Grantham Research Institute on Climate Change and the Environment, London, United Kingdom, [7] UK Centre for Ecology & Hydrology (UKCEH), Wallingford, United Kingdom

OPEN ACCESS

Edited by:
Andrew Hoell, Physical Sciences Division, United States

Reviewed by:
Scott Ronald Bremer, University of Bergen, Norway
Tufa Dinku, Columbia University, United States

***Correspondence:**
Blane Harvey
blane.harvey@mcgill.ca

Specialty section:
This article was submitted to Climate Services, a section of the journal Frontiers in Climate

Received: *30 July 2020*
Accepted: *31 December 2020*
Published: *28 January 2021*

Citation:
Harvey B, Huang Y-S, Araujo J, Vincent K, Roux J-P, Rouhaud E and Visman E (2021) Mobilizing Climate Information for Decision-Making in Africa: Contrasting User-Centered and Knowledge-Centered Approaches. Front. Clim. 2:589282. doi: 10.3389/fclim.2020.589282

This study examined ways in which climate information was mobilized for use under Future Climate for Africa (FCFA), an applied research program to improve the use of climate information to support medium-term (5–40 years) policies and planning in sub-Saharan Africa. Past research has underscored the interdependent relationship between user engagement and knowledge mobilization in effective climate knowledge uptake. The study used a document analysis of 46 program ou tputs and semi-structured interviews with 13 FCFA researchers to contrast user-centered and knowledge-centered approaches to effectively mobilize climate information uptake for use. A total of 20 knowledge mobilization tools and approaches were identified across the program and analyzed. This analysis reveals a complex interplay between user engagement and knowledge mobilization processes, including the strategic or flexible use and re-use of knowledge products as the user engagement process evolved. These findings have important implications for future programmatic design and planning in promoting engagement and mobilization approaches that can contribute to long-term policy and decision-making.

Keywords: climate information, climate services, knowledge mobilization, knowledge co-production, user engagement, Africa

INTRODUCTION

Despite the widely-documented exposure of lives, livelihoods, and assets in the global South to rising climate risks, the integration of information about those risks into planning and decision remains limited (Webber, 2019). In particular, researchers have highlighted challenges associated with encouraging the use of medium to longer-term climate information in many developing countries (Jones et al., 2017). As a recent review by (Singh et al., 2017: 394) notes, despite the critical need to consider decadal and multi-decadal time scale information in planning,

"there are very few clear examples of long-term climate information linking directly to on-the-ground decision-making." Numerous recent studies have sought to better understand the barriers to this integration, highlighting factors related to the nature of the climate information (its salience, legitimacy, credibility, and accessibility); and the nature of the ties between producers and users of that information (Cash et al., 2003; Jones et al., 2017). They also point to individual, organizational and systemic constraints that affect actors' capacities to act appropriately on information, including technical, financial, social, and psychological barriers to action (Watkiss and Cimato, 2015; Singh et al., 2017; Vincent et al., 2017, 2020b; Carr et al., 2020).

The challenges related to the uptake of this information are particularly salient in the context of the growing number of investments being made through bilateral and multilateral funding initiatives into research and capacity strengthening for National Meteorological and Hydrological Services (NMHSs), particularly in sub-Saharan Africa (see Harvey et al., 2019a; Mahon et al., 2019; Carr et al., 2020). Rising investment into major applied climate research programs aspiring to improve both the quality and use of climate-related information offers an opportunity to advance our understanding of this gap between knowledge production and its integration into use. These programs reflect a growing range of strategies, tools and approaches to knowledge mobilization and, hence, an important opportunity to assess their effectiveness. The programs also stand to contribute to improved outcomes for communities in the sites where they are being implemented.

This study addresses this opportunity space by examining an array of user engagement strategies and knowledge mobilization approaches, which were implemented over a common time period and under a common program, and which sought to improve medium- to long-term (5–40 years) policies, planning and investment by African stakeholders and donors. More specifically, we look at work carried out under the Future Climate for Africa (FCFA) program in 14 African countries between 2015 and 2019. We have focused our analysis on two complementary entry points for promoting the use of climate information: *user-centered* engagement (strategies used to identify and build links to particular communities of potential users of the information), and *knowledge-centered* approaches (knowledge mobilization used to organize, translate, and present this information for users). Through this work we sought to understand:

1. How user engagement strategies and knowledge mobilization approaches were put into practice across particular user groups and decision contexts; and
2. The reported barriers and enablers of their effectiveness.

Analysis for these two questions, however, also revealed important additional insights on the ways that user engagement and knowledge mobilization are being brought together within successful program strategies. We explore these insights in the discussion that ensues.

Limited comparative evidence of this nature has been published to date. In doing so we are able to draw lessons related to particular forms of engagement and mobilization of climate information, as well as broader lessons about how climate research programs can better contribute to positive social and political outcomes.

Evolutions in Climate Information Use in Sub-Saharan Africa

There is no single universal strategy or solution to promoting the use of climate information amongst a range of users, especially considering the wide range of contexts in which it might be used. Initially it was the inherent uncertainty in the climate system itself, as well as limits in forecasting capacity, that significantly impeded the availability of weather and climate information (Hulme et al., 2001). Subsequent critiques highlighted that the scientific presentation of information, for example use of terciles in probabilistic seasonal forecasts, impeded its use (Patt and Gwata, 2002). Case studies in a variety of locations across Africa highlighted that issues of accessibility and comprehension were impeding its use in decision-making (Vogel and O'Brien, 2006; Roncoli et al., 2009; Hansen et al., 2011). In short, the information produced in early iterations of user-oriented climate information did not meet the criteria for "actionable knowledge," namely for it to be legitimate, credible, and salient (Cash et al., 2003).

The recognition that decision-makers often failed to take up climate information prompted the development of the field of climate services. The rise of climate services has placed much more explicit focus on providing timely and tailored information to suit decision contexts (Hewitt et al., 2012; Buontempo et al., 2014; Vaughan and Dessai, 2014). This has led to increased interest in strategies that can most effectively *mobilize*[1] climate information for use in decision contexts—whether by improving availability of information, translating information into more accessible formats, or enlisting "intermediaries" to broker more effective communication between climate information producers and users (McNie, 2012; Jones et al., 2016; Vaughan et al., 2016; Harvey et al., 2019a). Despite these advances, there remain well-recognized challenges with many climate service initiatives, including concerns about institutional capacity to develop and sustain the services (Dinku et al., 2014; Harvey et al., 2019a); availability of and access to the climate information itself (Jones et al., 2017; Vaughan et al., 2019); as well as concerns about the impact of commercializing services as a means of ensuring their availability and sustainability (Webber and Donner, 2017).

The combined challenges of lower-than-expected engagement of users of climate services, weak accuracy and availability of highly localized or contextualized climate information, and broader concerns about the presumed primacy of Western science in some African decision contexts have also prompted an epistemological shift toward co-producing climate services (Lemos et al., 2012; Meadow et al., 2015; Bremer and Meisch, 2017; Vincent et al., 2018). In co-production

[1]Canada's Social Sciences and Humanities Research Council (SSHRC), describes knowledge mobilization as "an umbrella term encompassing a wide range of activities relating to the production and use of research results, including knowledge synthesis, dissemination, transfer, exchange, and co-creation or co-production by researchers and knowledge users" (SSHRC, 2019).

processes, rather than emphasizing the supply and "transfer" of knowledge to specific audiences (also referred to as "push"-style communication), the aim is to transform the process of knowledge construction to one where the ontological pluralism of producers and users is leveraged to generate new, actionable knowledge (Dilling and Lemos, 2011; Mach et al., 2020). As such, knowledge co-production often brings user engagement and knowledge mobilization together into a single process where the distinction between producers and users of knowledge becomes blurred (Pohl et al., 2010). However, empirical evidence on how this process of co-production is undertaken in practice, or agreement on how to best gauge its impacts remains scarce (Jagannathan et al., 2020; Mach et al., 2020; Vincent et al., 2020a). As a consequence of this ambiguity, argue Mach et al. (2020, p. 31), co-production persists as an "idealized, yet also diversely and imprecisely defined concept that inevitably falls short of meeting its own standards," and risks crowding out other forms of interactive science methods and practices.

FRAMEWORK AND METHODS

This study examined the user engagement and knowledge mobilization activities undertaken under the Future Climate for Africa program, a 5-year, £20 million program funded by the UK Department for International Development (DFID) and Natural Environment Research Council (NERC). The program was implemented by five research consortia, each featuring an international set of partner institutions (see **Table 1**). Together these consortia worked toward FCFA's three primary aims:

- Significantly improving scientific understanding of climate variability and change across Africa and the impact of climate change on specific development decisions.
- Demonstrating flexible methods for integrating improved climate information and tools in decision-making.
- Improving medium term (5–40 years) decision-making, policies, planning, and investment by African stakeholders and donors.

FCFA research consortia adopted a range of different strategies for and approaches to promoting the uptake of climate information, thus creating a valuable opportunity to compare and draw lessons from across their practices. Preliminary data collection was undertaken through an analysis of 46 program publications to identify the range of user engagement and knowledge mobilization tools and approaches that were used and the lessons that were documented on their use. A total of 20 different tools and approaches were identified, with some being used by more than one consortium. We then conducted semi-structured interviews with representatives from all five FCFA consortia to better understand how the tools and approaches that were identified were used in practice, and whether that use evolved over time. A total of 13 researchers were identified using purposeful sampling, based on their roles in developing or implementing the tools and approaches identified. This included interviews with two Principal Investigators, 10 Co-Investigators and one Early Career Researcher, of whom four were from partner organizations based in Africa. In terms of disciplinary focus, four respondents were from the physical climate sciences, three were social scientists, and six were from applied sciences.

In line with principles of action learning (Zuber-Skerritt, 2002), our analysis also draws on the extensive experiential knowledge of four members of the author team, who were active participants in many of the consortium meetings and field activities over the life of the program. These insights informed our collective analysis of the data, and were critical in understanding the generalizability of evidence from anonymized interview data. One member of the author team was also an interview participant, though her responses (along with all other interview data) were anonymized prior to collective analysis.

Recent research has increasingly underscored the interdependent relationship between *user engagement* and *knowledge mobilization* in the uptake of climate information into decision-making (Dilling and Lemos, 2011; Lemos et al., 2012; Harvey and Cook, 2018). As noted at the outset of the paper, user-centered and knowledge-centered approaches are different entry points to achieve the same output (knowledge uptake). User engagement strategies often seek to establish connection, contextual awareness, and trust between producers and specific communities or individual users of climate information. Knowledge mobilization, in contrast, tends to start with the information or knowledge that producers aim to see used more frequently or effectively. It involves identifying and implementing approaches that best align with the specific information type, intended use contexts, users, and desired outcomes or impacts (Phipps et al., 2016).

However, the nature of the links between these processes is not consistently set out in the literature, or in practice (Harvey et al., 2019b). The reasons for this inconsistent framing of the relationship are multiple, but often stem from competing ontological and epistemological positions on the nature of knowledge and knowledge production. Differing disciplinary starting points have also shaped orientations to both the potential users of climate information and the processes aimed at promoting the integration of this information into practice. Researchers and practitioners have, for instance, adopted approaches grounded in communications and social marketing theories, knowledge brokering and knowledge management theories, theories from participatory development, from the learning sciences, as well as more recent theories specifically focused on knowledge co-production, not to mention initiatives that have brought two or more of these orientations together (Harvey et al., 2012). While there are clearly intersections between these different disciplinary orientations, each brings its own norms and assumptions regarding the sequencing, prioritization, and assumed relationship between engagement with potential users of information and the development of tools, technologies and other products to synthesize or translate information and facilitate its use. To study these two inter-related dimensions of promoting the uptake of climate information—user

TABLE 1 | FCFA Consortia and their respective focus areas.

Acronym	Full name	Research and geographical focus
AMMA-2050	African Monsoon Multidisciplinary Analysis 2050	Understand how the West African monsoon will change in future decades, and how this information can be used to support climate-compatible development in the region; case studies in Burkina Faso (water resources) and Senegal (agriculture)
FRACTAL	Future Resilience for African Cities and Lands	Increase the climate resilience of nine southern African cities by including climate knowledge in decision-making processes; case studies in Lusaka, Maputo, Windhoek, Cape Town, Johannesburg, Durban, Blantyre, Harare, Gaborone.
HyCRISTAL	Integrating Hydro-Climate Science into Policy Decisions for Climate Resilient Infrastructure and Livelihoods in East Africa	Improve understanding of East African climate variability and change, their impacts, and support effective long-term (5–40 years) decision making; case studies in Uganda and Kenya on climate-resilient livelihoods and water management
IMPALA	Improving Model Processes for African Climate	Develop a very high-resolution pan-African climate model that better captures key processes and local-scale weather phenomena, including extremes.
UMFULA	Uncertainty Reduction in Models for Understanding Development Applications	Improve climate information for decision-making in the water-energy-food sectors in central and southern Africa; case studies in the Rufiji basin in Tanzania and Shire basin in Malawi.
CCKE	Coordination, Capacity Development and Knowledge Exchange Unit	Cross-cutting support to the five research consortia.

engagement and knowledge mobilization—we conducted a thematic analysis of the data drawing on two established frameworks:

Examining User Engagement Through the Lens of Co-production

There is a recognized need to identify and engage potential users of climate information, whether to understand their information needs, build trust, or to prioritize who should be engaged. Knowledge co-production has increasingly been framed as a "gold standard" of sorts for engaged science (Lemos et al., 2018: 722) and climate services (e.g., Vincent et al., 2018; Bremer et al's., 2019; Carter et al., 2019), albeit one that remains idealized, as noted above. Descriptions of co-production processes (e.g. Mauser et al., 2013; Vincent et al., 2018; Carter et al., 2019) often begin with stages of stakeholder identification, trust-building, and joint meaning-making before advancing to the collective development of products or solutions. This offers a useful framing for applying a "user-centric" analysis of how climate information and services have been conceived and developed for use in FCFA. To capture the full extent of this engagement, we coded participant responses by adapting Carter et al. (2019) and Vincent et al.'s (2018) frameworks for knowledge co-production, which set out four stages of climate services co-production: Identifying actors and building partnerships; co-exploring need; co-developing; co-delivering solutions; and evaluating the results of user engagement. Our adoption of this framing does not imply that all user engagement activities in the field of climate services were (or indeed should be) instances of co-production. However, the framework's four stages provide a useful point of reference for understanding the form and extent of user engagement that has shaped the approaches under study.

A Spectrum of Knowledge Mobilization Practices

We use the term "knowledge mobilization" to describe a range of approaches and processes used to organize, translate, and present information for users at the science-to-decision interface. Interpretations of how terms like knowledge brokering, knowledge translation, knowledge transfer, knowledge exchange, and knowledge mobilization differ from one another vary across the literature, leading Shaxson et al. (2012) to coin the term "K*" to highlight the fuzzy boundaries between definitions and functions of these terms. To clarify the distinctions between these different orientations to knowledge mobilization, Shaxson et al. (2012) and other scholars in the field of climate and environment (e.g. Michaels, 2009; Harvey et al., 2012; Hammill et al., 2013; Jones et al., 2016) developed a spectrum of approaches to knowledge mobilization categorizing forms of knowledge mobilization, from relatively linear information provision (information intermediation), which tends to focus on making information available in appropriate formats, to approaches aimed at influencing the decision contexts and the wider climate services system (innovation brokering) (see **Figure 1**). Jones et al.'s (2016) use of this framework for studying the contributions of NGOs in supporting climate service delivery provides a reference point for our own analysis.

There is always an element of subjectivity in situating activities on a spectrum, for instance in deciding whether a particular knowledge mobilization activity is better described as knowledge brokering or innovation brokering. To address areas of uncertainty we reviewed our assessment collectively as an author team and compared written descriptions of particular activities with FCFA members' interpretations of how these unfolded in practice.

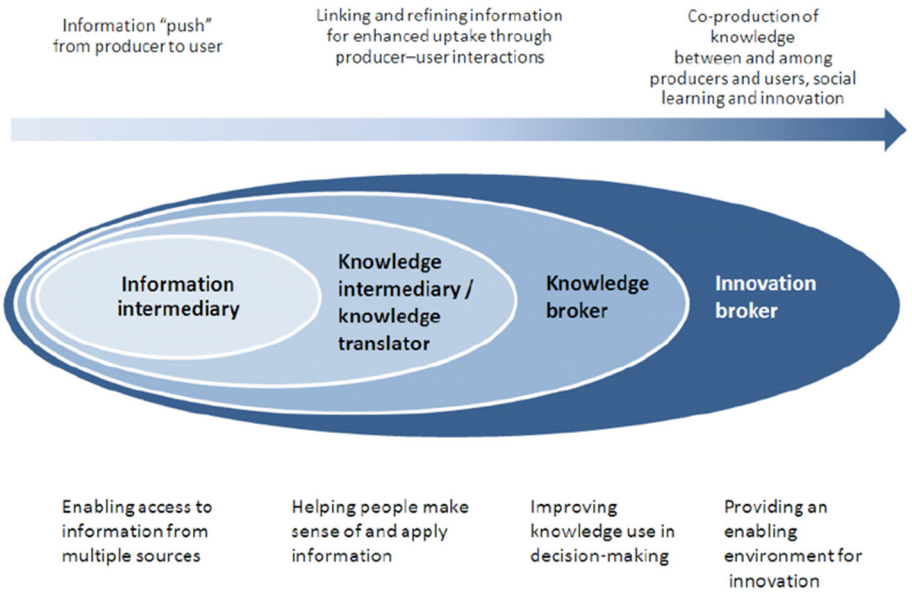

FIGURE 1 | A spectrum of knowledge mobilization approaches (from Hammill et al., 2013).

It is also important to note that, while our analysis considers user engagement processes and knowledge mobilization approaches in turn, in some cases these have been planned together and exist under a common strategy. In other cases, these are attended to sequentially, with user engagement and knowledge mobilization building upon one another. The dynamics between these processes ultimately form an important dimension to how we understand efforts to promote the use of climate information. In doing so we seek to extend Lemos et al.'s (2012) call to "delve deeper into understanding the processes and mechanisms that move information from what producers of climate information hope is useful, to what users of climate information know can be applied in their decision-making" (p. 789).

RESULTS

Strategies for User Engagement

Regardless of the approaches to knowledge mobilization adopted, there is a need to identify and engage with potential users of climate information. Through a series of interviews, we sought to understand which strategies they deemed effective in engaging potential users of climate information and knowledge. We used thematic coding to group responses around the four stages of climate services co-production adapted from Vincent et al. (2018) and Carter et al. (2020) and have noted the frequency with which respondents from one of the five consortia mentioned each strategy listed as being effective (**Table 2**).

We find close alignment between the user engagement strategies highlighted by interview respondents and those set out in the co-production framework. Consortia have used a wide range of strategies to engage current and potential knowledge users, but we see clear trends in using in-person engagement (directly or via trusted intermediaries) for identifying entry points and engaging with potential users, and use of long-term multi-prolonged engagements in building trust with key stakeholders (e.g., Steynor et al., 2020). These are not unusual practices but they underscore the fact that effective engagement strategies start early and remain intensive through the duration of program activities—regardless of the approaches to knowledge mobilization that accompany them. Given FCFA's focus on medium term climate change, the process of co-exploring needs included an emphasis on being open about the inherent limits in data and models.

The third stage of the user-engagement framework sees users and researchers engaging in the co-production of specific knowledge products or processes. In practice, not all tools or processes that emerged from the user engagement were co-produced—as we discuss in the sections that follow. Respondents reported instances where these strategies were not used and the consequences that sometimes resulted. One researcher recounted the challenges of effectively sequencing research plans and developing knowledge mobilization strategies that met the needs of a range of users:

> The first kick-off meeting we talked about what the key metrics of high impact on climate change were in different sectors and that was good to get [...] everybody on the same wavelength, and then the climate scientists went off and produced those [in] a long and technical way, bringing in new bias corrected data sets and training early career scientists. So that process was [...] definitely good in terms of building the skills of early career scientists. But then we, you know, produced big [...] documents that hang off our website, they were [...] even within the consortium, people found some of them a bit tricky. [...] The way that they were presented made sense to a scientist but not necessarily to a policy-maker.

TABLE 2 | User engagement strategies highlighted by FCFA consortia mapped to stages of co-production.

Identify actors and build partnerships	• Stakeholder meetings, early scoping visits, and in-person visits (4/5); • Draw on well-connected personnel and prior contacts (4/5); • Enhance receptivity by using project brochures/presentations to communicate goals and potential outcomes (4/5). • Monitor demands for information and training that are communicated directly or indirectly to the project (1/5). • Prolonged engagement through events and regular communication (3/5); • Joint production of knowledge products (2/5); • Establish a relationship coordinator and personal rapport (2/5); • Draw on credibility of partnering institutions, reputation of the project team (3/5);
Co-explore need	• Demonstrate commitment to partners' needs (3/5). • Transparency about the uncertainties in data, models, research process, and futures (4/5); • Knowledge sharing through workshops or training sessions (2/5); • Communicate through scenarios, instead of uncertainty (3/5); • Use visual aids paired with in-person support for interpreting (3/5).
Co-develop and co-deliver solution	• Ensure that the communication formats of climate information are most accessible to users (4/5); • Encourage participation through co-production (2/5); • Use iterative engagements to inform development (2/5)
Monitor/evaluate the results of engagement	• Monitor changes in policy or user engagement through key informant interviews, surveys, and document analysis (3/5); • Monitor requests from partners coming through ongoing correspondence (2/5); • Look for evidence of use noted in other data collection activities (3/5); • Specific case studies of evidence use (1/5)

The final stage of the co-production process cycle is to evaluate the effectiveness of the process and its results. Here we found limited evidence of results from the evaluation of user engagement activities that aimed to promote use of climate information, though some consortia reported having conducted some preliminary investigations. Respondents for three consortia suggested that it was premature to assess whether there had been uptake of the information or recommendations being shared. A member of the AMMA-2050 consortium, for instance, noted that the results of uptake would take time to unfold, so their current strategy was to look for "evidence of change" through informal discussions and email exchanges with partners. This strategy was part of AMMA-2050's broader evaluation framework for tracking institutional and individual changes against project baselines.

Respondents in other consortia shared some common approaches to monitoring uptake, as set out in **Table 2** above. While these are effective monitoring approaches, we note that only one of the approaches highlighted involves a structured analysis of context-specific progress or outcomes. Claims that it is premature to evaluate impact have merit, particularly in longer-term behavioral change processes. However, past research highlights the risk that evaluation plans left until the closing stages of the program often encounter time, human and financial resources constraints that impinge on their implementation (see Harvey et al., 2019c), as well as lack of reliable data if baselines and monitoring processes have not been set up to gather the data required for effective analysis. This concern was recognized by one consortium co-lead who noted the need for tracking long-term program impacts "after the project ended," but observed that doing so requires the project management team to "maintain a strong network."

Categorization of Knowledge Mobilization Activities in FCFA

Having reviewed the strategies used in FCFA to engage users, we then looked at how knowledge was mobilized to enable access to new climate information for decision-making among the range of potential users. Particular attention was paid to how the function of knowledge varied according to context. **Figure 2** illustrates the distribution of the categories of FCFA's knowledge mobilization activities.

While we see a distribution of tools and approaches across this spectrum, we find a predominance of cases in the intermediary and translation categories, which emphasize ensuring that information and knowledge are available and are in accessible language or formats. This is perhaps unsurprising, given that such tools (such as the production of policy briefs and brochures) have long been used by projects to translate and communicate information for targeted audiences. However, evidence suggests that, used in isolation, such tools tend to be less effective for engaging with non-expert audiences, for building capacity, or for shifting behavior (Bielak et al., 2008; Turnhout et al., 2013). They may nonetheless be helpful for raising the awareness among actors already active in the climate information and services field (such as other researchers). Also worth considering in these intermediary and translation categories is the ways in which these activities are embedded in wider processes or strategies of engagement to enable knowledge uptake. We explore this point in section Interplay Between User Engagement and Knowledge Mobilization Processes below.

We also find examples of more interactive approaches to knowledge mobilization being used by most consortia. These include the co-development of stories and narratives describing climate risk, and forums. These approaches have tended to be used as conversation starters to engage targeted stakeholders in more sustained knowledge mobilization processes. As one FRACTAL researcher noted in speaking about the power of these interactive knowledge production and uptake process,

> Fundamentally it's the process that has produced the uptake of the information, but I just want to emphasize, it's not just information, it's the understanding. It's the relational capacity amongst the participant groups, it's the exchanges across the cities.

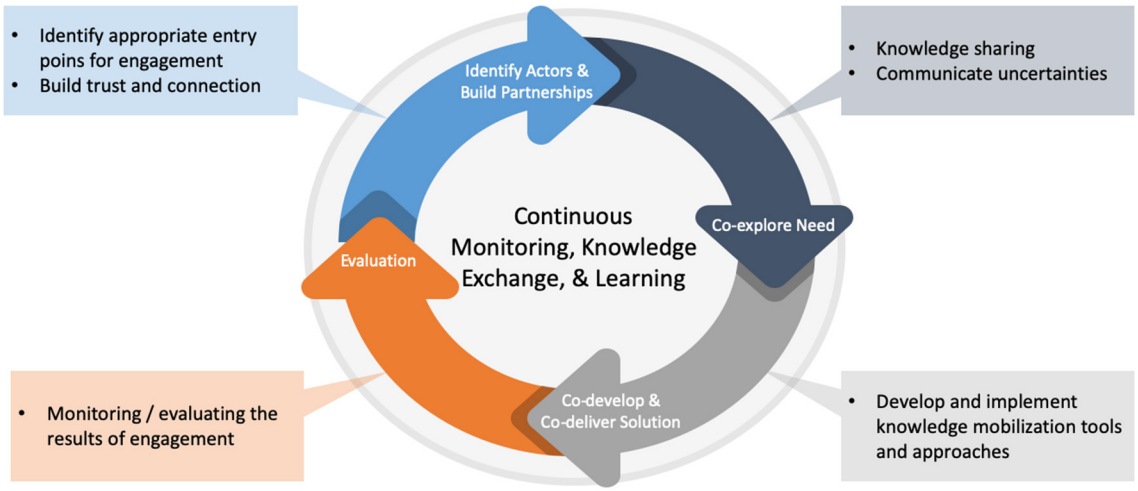

FIGURE 2 | Stages and indicative strategies for user engagement in knowledge co-production.

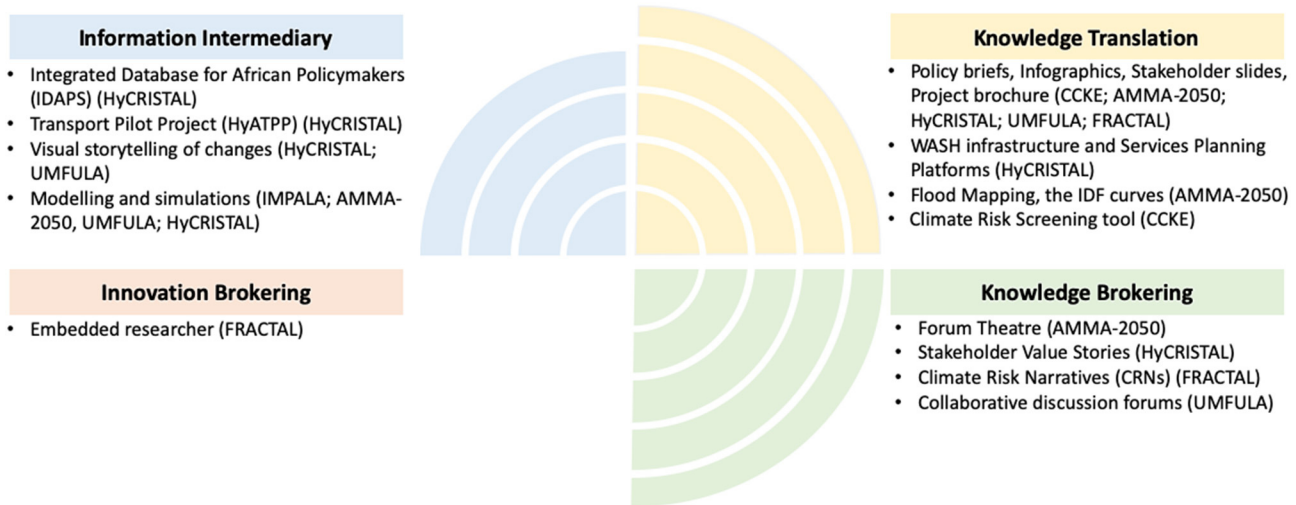

FIGURE 3 | Categorization of knowledge mobilization tools and approaches used in FCFA.

The lack of examples categorized as "innovation brokering" is also noteworthy. These are tools and approaches that operate at the level of climate information systems (the network of actors, institutions, policies, and infrastructure that govern the production and use of climate information) to open up the possibility for innovations in practice. These systems-scale approaches can offer scope for deeper transformations in the technical, social and institutional relationships that shape knowledge production and use, but require time and sustained resourcing required to affect this kind of change (Klerkx, 2012). Recent studies have highlighted the potential mismatch between project-based initiatives and these more systemic efforts at transformation, and may help to explain the relative lack of these systems-level approaches in FCFA (Harvey et al., 2019b).

Distribution of Tools and Approaches by Context and Intended User Groups

Having established the overall distribution of the categories of knowledge mobilization activities, we then looked at the alignment between the tools and approaches used and the contexts and audiences that were targeted. As evidenced in **Table 3**, the tools and approaches used by FCFA consortia spanned a wide range of user types and scales. While some tools and approaches appeared to target a diverse set of users, the majority target a clearly defined audience and/or use context. This is in line with the growing awareness of the importance of context-informed knowledge mobilization, and may also be due to the expectation that all FCFA activities have clearly targeted stakeholder groups at the proposal development stage. However, in looking at categories of mobilization and their

TABLE 3 | Tools and approaches to knowledge mobilization and uptake by targeted users.

Category of mobilization	Name of tool or approach	Tool type	Targeted users	Example of outcomes
Informational functions (Information intermediary)	Integrated Database for African Policymakers (IDAPS) (HyCRISTAL)	Online database of climate modeling, agronomy and hydrology	Policy-makers at national, district, and sub-district levels	The modules of IDAPS have been tested in Uganda to support livelihood and policy decisions
	Transport Pilot Project (HyTPP) (HyCRISTAL)	Reports on current- and future-climate analysis	World Bank and their consultants	The reports were shared by the World Bank at a workshop in October 2018
	Visual storytelling of changes (HyCRISTAL; UMFULA)	Videos	Local communities; Local government; International donors	Too early to assess.
	Modeling and simulations (IMPALA; AMMA-2050, UMFULA; HyCRISTAL)	Large-scaled synthesized data with simulations and modeling	Research institutions	A high resolution meteorological dataset is expected to be published in the UK CEDA and used in collaboration with other universities
Informational-Relational functions (Knowledge translation)	Policy briefs, Infographics, Stakeholder slides, Project brochures (CCKE; AMMA-2050; HyCRISTAL; UMFULA; FRACTAL)	Written briefs; infographics; summary slides; brochures; etc.	A wide range of stakeholders (e.g., farmers, researchers, NGOs, policy-makers)	The briefs are used in various policy documents.
	WASH infrastructure and Services Planning Platforms (HyCRISTAL)	A web-based data sharing platform	Policy-makers and practitioners	
	Flood Mapping, IDF curves (AMMA-2050)	Maps of inundated area with land use scenarios	City planners, infrastructure companies	Decision-makers have requested IDF curves for particular infrastructure project
	Climate Risk Screening tool (CCKE)	Screening tool	Rwanda Green Fund staff, expert reviewers and project developers	Too early to assess
Relational functions (Knowledge brokering)	Theater Forum (AMMA-2050)	Play designed to enable dialogue.	Scientists, government officials, farmers, and more.	Promoted discussion on adaptation options with National and regional decision-makers, and researchers.
	Stakeholder Value Stories (HyCRISTAL)	Stakeholder narratives of information use	Policy-makers	Used to inform the IDAPS database development.
	Climate Risk Narratives (CRNs) (FRACTAL)	Textual descriptions of plausible climate futures	City decision-makers	Contributed to the city-specific strategy and action plan in Windhoek, Namibia
	Collaborative learning fora (UMFULA)	Multi-stakeholder discussion on climate impacts, decision trade-offs and robust options	Policy and decision-makers at the national and river basin levels	Too early to assess (ongoing)
Systems functions (Innovation brokering)	Embedded researcher (FRACTAL)	Researchers embedded in city government	City decision-makers	Developed networks with decision-makers

alignment to user types, no strong trends emerge. We do see a tendency for interactive knowledge brokering approaches to focus on policy makers (at a range of scales), which is in line with past reviews (see Harvey et al., 2012). While this could suggest a lack of clear consensus on which categories of knowledge mobilization are most effective with particular stakeholder groups, it may also highlight that the alignment of knowledge mobilization tools and approaches with specific user groups can depend on additional factors. Indeed, we find that additional variations in the use of similar tools (briefing notes, for instance) such as the intended outcomes and stage of user engagement at which they are used, can greatly shape how they "fit" within the knowledge generation process. We explore this finding below.

Interplay Between User Engagement and Knowledge Mobilization Processes

Our analytical framework examined approaches to user engagement and knowledge mobilization processes in turn, recognizing them to be complementary entry points to achieve common outcome (knowledge uptake). However, interviews with consortium members underscored the significance of the interplay between these two processes and the varied ways that they were brought together in program initiatives. One HyCRISTAL researcher, for example, noted that, although "each pilot [study] has its own specific knowledge product, [...] they were not used independently" as "a source of knowledge" for a specific targeted user group. Instead, a combination of knowledge tools and approaches was used "in conjunction with the [climate] narratives and other tools" to engage stakeholders. This use of combinations of tools and knowledge products within user engagement processes helped the teams achieve smaller, interim steps toward their overall project objectives. One FRACTAL researcher also explained that their policy briefs "were not targeting [city learning lab] participants," but were rather designed to help participants "in their roles [...] to inform their bosses or their stakeholders." In the context of the learning labs, which focused on co-learning and co-production of solutions, knowledge mobilization tools could "only work within a process that allows for engagement and conversation" to build "relationships and trust." As the researcher argued, "were any of those products outside of that process, I don't think we'd really have achieved much."

In other cases the interplay between mobilization and engagement processes revealed a strategic or flexible use and re-use of knowledge mobilization tools as user engagement processes evolved. For example, policy briefs in UMFULA were initially designed to translate project baseline evidence, but ultimately served as "the key" in getting consortium researchers invited to contribute to Tanzania's national climate policies. In FRACTAL's work in Zambia, although the primary objective of developing policy briefs was to increase awareness of climate change in Lusaka, the process of co-producing the briefs guided the rest of "the research activities [and] all the engagement activity for most of the learning lab process." Policy briefs thus acted as a boundary object shared by the researchers and stakeholders in both FRACTAL and UMFULA to initiate more extended engagement processes, some of which included knowledge co-production activities (see **Box 1**).

The dynamic use of knowledge products in concert with extended user engagement processes highlights the importance of being "responsive and flexible" in enhancing the uptake of climate information. FRACTAL members emphasized the learning component of "listening to what participants were requesting" and being willing to change the research team's view about "what was either needed or important or how things [should] be communicated" in their City Learning Labs. As one member described, the Maputo City lab "was an example where the engagement didn't work very well" at the beginning, so the team had to "reframe the information" and "change directions [...] a few times to try and find some traction."

These examples of the successful interplay between user engagement and knowledge mobilization processes reveal a number of important insights. First, in many of these cases the contribution of knowledge products themselves (briefs, guides, etc.) rested less on the credibility, legitimacy and saliency of their content (in terms of knowledge translated or transferred), and more on the spaces they opened up for more extended interactions. Second, the co-productive dimensions of many of these processes were emergent over time, rather than designed. Together, these insights suggest a more complex relationship between production and use of climate knowledge than is reflected in many models of evidence use. We reflect on these insights below.

DISCUSSION

FCFA consortia have used a wide range of tools and approaches to promote greater use of climate information in planning and decision-making, which we have loosely grouped into "*user-centered*" and "*knowledge-centered*" entry points to knowledge uptake. This offers an opportunity to better understand how and why particular tools and approaches have been beneficial, for whom, and in what contexts. Having a better understanding of what has or has not worked, we argue, can help to improve the ways in which researchers engage with "user" communities, and potentially challenge perceptions about those relationships. Looking across the analysis we find some evidence to advance our understanding of how best to mobilize medium-term climate information, but also some important questions that will require further exploration.

Applying Principles of Co-production for Engaging Users of Medium and Longer-Term Climate Information

We find a strong alignment between the principles of effective knowledge co-production set out in the wider literature and practices cited as effective across the 20 FCFA examples we studied. This seems particularly significant given the range of approaches that were inventoried in **Figure 3**. The value of long-term engagement, trust-building, and in-person engagement is emphasized by respondents. This underscores the need to consider both process and product in the development of any resources for knowledge mobilization. Emphasizing the value of these principles of co-production offers a good starting point for future initiatives, particularly at planning and design stages.

Dynamic Interplay Between User Engagement and Knowledge Mobilization

While our analysis examines user engagement processes and knowledge mobilization approaches in turn, in many cases these were planned together and exist under a common strategy or approach to co-production. Though our review of literature on knowledge mobilization strategies confirms the importance of tailoring tools to particular stakeholder groups, our review of the alignment of specific categories and tools/approaches with particular stakeholder types did not reveal clear trends in FCFA.

BOX 1 | Policy briefs as boundary objects in FRACTAL's City Learning Labs in Lusaka.

The city learning processes in Lusaka have led to the "fundamental changes in key decision pathways (around water, flooding, land use and infrastructure development) to increase the [city's] resilience" (Koelle et al., 2019, p. 25). One important factor that contributed to this policy impact was the process of co-developing policy briefs with the decision-makers. In Lusaka, policy briefs acted as boundary objects (Michaels, 2009) that resided between the social worlds of the decision-makers and scientists. Boundary objects are objects or ideas that emerge through collaboration and dialogue which are both adaptable to local needs yet "robust enough to maintain a common identity" (Star and Griesemer, 1989, p. 393).

In fact, the development of policy briefs was not a pre-planned output of Lusaka's City Learning Labs. The idea came from the participants during a media training event where they recognized the need for media statements about the "burning issues" in Lusaka related to climate change. Therefore, co-developing policy briefs became a mutual priority. As boundary objects, the briefs brought city planners and scientists together for more in-depth dialogue and became "the red thread" that guided "research activities [and] all the engagement activity for most of the learning lab process in Lusaka." In the fourth and fifth Learning Labs, the decision-makers and the project teams even sat and wrote the policy briefs together "over a number of days (and evenings)" (Mwalukanga et al., 2018, p. 1). As a result, these policy briefs are now a shared product between all members involved. A shared ownership of such products is essential for medium to long-term knowledge uptake, as it allows all members to use these policy briefs as a new form of boundary objects to initiate diverse dialogues and engage future collaborations with other decision-makers, researchers and practitioners.

Since the Lusaka learning labs concluded, city representatives have expressed a desire to continue an engagement similar to the learning lab. In keeping with the aims of innovation brokering, this outcome suggests a newly established norm of policy learning in the decision-making space. It also indicates a potential benefit of the co-productive practice in establishing long-term engagement and trusting relationships between partners.

What we did find, however, were numerous cases where similar mobilization tools and approaches were being embedded in wider user engagement strategies toward quite different ends—often with those strategies being in a regular state of flux.

To take the case of the "briefing note"—one of the most commonly used knowledge translation tools for policy stakeholders—these performed a range of different functions in FCFA. This included a more traditional "gap filling" function of matching an evidence "supply" with a perceived knowledge "need;" a "priming" function where briefs served to stimulate more in-depth user engagement; a "help desk" function where briefs were generated later in the engagement process in response to stakeholder-identified needs; and a "co-production" function where jointly-produced brief served as the boundary object in a joint meaning-making process. As noted above, some of these functions emerged out of engagement practices rather than being established through a design process. While past research has distinguished between science-driven "push;" user-driven "pull;" and iterative "co-production" models of knowledge production (Dilling and Lemos, 2011), case evidence from FCFA demonstrates how extended knowledge mobilization processes may combine or move between these modes, either strategically or adaptively, as user engagement dynamics evolve.

Not all of the tools and approaches reviewed in the study reflected this form of interplay, of course. There remain knowledge mobilization activities that reflect a push to showcase research evidence with limited awareness of how the evidence might be taken up in use, or by whom. We note that the wider climate research system, including many funders and academic institutions, continues to rely on incentives and performance metrics that prioritize research "outputs" (products) over "outcomes" (societal impacts) (Jones et al., 2018). Further, we cannot conclude that those tools or approaches that did feature the interplay described here were necessarily more impactful over time. Indeed, the lack of evaluative data on these strategies within the program makes it challenging to draw firm conclusions on how to best align mobilization approaches with particular user groups, as we discuss below.

What we do observe from these examples, is the diversity of trajectories toward effectively supporting the use of climate information, even when pursued under a common programmatic framework and in line with a relatively common set of principles of good practice, as found in FCFA. We find that extended engagement processes toward co-production with intended users will not necessarily be the product of careful design as they might be in more controlled environments such as research teams (see Cundill et al., 2019). This makes the task of monitoring progress and tracking the effects of these forms of engagement over time particularly challenging, yet critical.

These insights reflect earlier reviews of knowledge mobilization practice from Ward et al. (2009), who observed that "the boundaries between [approaches] are often blurred" with many projects combining elements of different tools and approaches to meet users' needs. "This is often done" they suggest, "without recourse to any underlying model or framework of knowledge transfer or knowledge brokering and causes difficulties when evaluating individual brokering interventions" (p. 274–275). While Ward et al. appear to raise concerns about a seemingly haphazard approach to combining strategies, our results suggest that this may actually be indicative of a type of strategic agility within teams.

Better Assessing Outcomes and Impacts

Despite being a relatively large, lengthy, and well-resourced initiative, our document analysis yielded limited data reporting on the effectiveness of specific approaches to promoting the use of climate information in FCFA. Where data did exist, it was largely in relation to ongoing expressions of demand, or responses to information that had been shared rather than assessments of the outcomes or impacts of evidence use. Many respondents cited the project timeline as the biggest barrier to gathering this outcome and impact-level information—as they felt it was too early to meaningfully assess. This gap limits our ability to assess whether there are clear "best matches" between tools/approaches and particular audiences, aims, or stages of engagement, or

whether there are tools or approaches that have particularly wide-ranging utility. These are important questions for the future of research-to-action linkages on climate information services in Africa. A more robust testing of tools and approaches could yield important insights. Some preliminary analysis has been undertaken by FCFA consortia to compare the advantages and challenges of some knowledge mobilization tools and approaches (see Harold et al., 2019 for a comparison of tailored slides, policy briefs, infographics and narratives). Future investigation could examine a wider range of approaches and contexts.

A call for more robust evaluation of these approaches should not be perceived as a push for researcher accountability but rather as an opportunity to better understand how particular strategies for knowledge mobilization and user engagement contribute to evidence use and behavior change. Evaluations that focus on outcomes with specific stakeholder groups and decision settings and at different points across the co-production process seem particularly important based on the evidence from these cases. Addressing these needs would demand new emphasis on monitoring during a program lifespan, as well as methods for assessing the longer-term impacts of knowledge mobilization activities, many of which may not emerge until long after the conclusion of program activities. One promising monitoring approach that emerged from the strategies of some FCFA consortia is the use of incremental progress markers that identify and track evidence of interim steps toward longer-term changes in the use of climate information in planning and decision-making. These can include shifts in attitudes, knowledge, and behavior, for example. AMMA-2050 developed a key informant score card, combining qualitative and quantitative questions administered to a panel of researchers and decision-makers at program base-, mid- and end-line. Use of progress indicators is not new to monitoring and evaluation (see Earl et al., 2001) but their use in this context remains limited. Applying such process markers would better enable rigorous analysis of progress toward the intended impacts that are often only seen long after the end of a program. However, where responsibility for this "post-project" impact monitoring should rest remains unclear.

Limited Strategies Aimed at System-Scale Knowledge Mobilization

Finally, we note the relative absence of knowledge mobilization tools and approaches falling in the "innovation brokering" category, where attention is typically placed on enabling systems-scale changes. In an emergent field of practice like climate services, where there is a recognized need to strengthen the overall functioning of the climate information system (Dinku et al., 2014) this form of mobilization would seem to be of critical importance. However, past research has suggested that the time-bound and closely focused nature of most project-based initiatives (such as FCFA) makes efforts to support systems-scale changes (Harvey et al., 2019b). This does not mean, however, that other types of knowledge mobilization activities did not ultimately have systems-level impacts. The case of FRACTAL's City Learning Labs (**Box 1**), for instance, appears to have led to a more fundamental shift in local practices, while AMMA-2050 reports changes in institutional norms in terms of attention to decision-making needs within collaborating research institutions.

Work at this systems level involves engaging with the established norms and institutional cultures that shape work on climate services. This can be a significant challenge for initiatives led by outside organizations, or organizations working to strict timelines and budgeting constraints. Klerkx (2012), for instance, describes the "funding paradox" of innovation brokers in the context of agricultural systems, where efforts to tackle market and system failures are themselves undermined when the initiatives aiming to do so are subject to the same flawed system. Similar challenges can be found in the field of climate services (Daly and Dilling, 2019; Harvey et al., 2019a) highlighting the need to examine approaches beyond specific initiatives or programs.

CONCLUSIONS

This study has sought to better understand the growing range of ways that user engagement and knowledge mobilization are being used to promote the use of medium-term climate information in planning and decision-making in sub-Saharan Africa. To do so, we studied a sample of 20 tools and approaches emerging from a common program (Future Climate for Africa), loosely grouping them into "user-centered" or "knowledge-centered." This framing allowed us to look across a wide range of approaches to evidence uptake and use, from more traditional, linear modes of information intermediation and knowledge translation to forms of knowledge co-production that have increasingly become seen as a model of practice in climate services.

Our findings reveal the central role of co-production principles in engaging potential users of climate information, regardless of the knowledge mobilization approach being used. They also highlight the complex interplay that can unfold between user engagement and knowledge mobilization processes, dynamics that belie the sometimes narrow depictions of the relationship between knowledge production and use in the literature. These insights reflect Bremer, Wardekker, Dessai, Sobolowski, Slaattelid and van der Sluijs (2019) assertion that "recognizing knowledge co-production as a multi-faceted phenomenon, able to be worked on along several different dimensions, could help climate services scholars and practitioners more fully realize the potential of this process" (p. 49).

Recognizing the complex and often-iterative dynamics of these processes, where seemingly linear modes of engagement may actually serve to initiate, or provide boundary objects that support more extended pathways toward knowledge co-production, highlights the need for better approaches to monitoring and assessing their impact. Investment into more nuanced and longer-term assessments of the impacts and outcomes that user engagement and knowledge mobilization efforts yield for particular stakeholders and contexts, remains a significant gap. We hope that these findings serve to highlight this need, as well as opportunities for continued work to ensure climate information supports effective decision making and climate resilience in Africa.

DATA AVAILABILITY STATEMENT

The raw data supporting the conclusions of this article will be made available by the authors, without undue reservation.

ETHICS STATEMENT

The Research Ethics Board 2 reviewed and approved this project by delegated review in accordance with the requirements of the McGill University Policy on the Ethical Conduct of Research Involving Human Participants and the Tri-Council Policy Statement: Ethical Conduct for Research Involving Humans. (File # 50-0619). The patients/participants provided their written informed consent to participate in this study.

AUTHOR CONTRIBUTIONS

Y-SH and JA led data collection. BH and J-PR contributed to data collection. BH and Y-SH led data analysis with contributions from all other authors. BH led drafting of the manuscript with contributions from all other authors. All authors contributed to the study design.

FUNDING

BH and Y-SH's contributions to this study were carried out with financial support from SouthSouthNorth (grant ref. G251310) as part of the Future Climate for Africa Program, as well as Quebec's Fonds de Recherche Société et Culture (FRQSC) (grant ref. FRQ-SC NP-253637). KV, ER, and EV's contributions were carried out with financial support from the UK Natural Environment Research Council (NERC) (grant ref. NE/M020010/1 Kulima, NE/M020398/1 LSE, and NE/M020428/1 CEH), and the UK Government's DFID.

ACKNOWLEDGMENTS

The authors wish to thank members of the FCFA program and the UK Department for International Development for their valuable contributions to this study, and for their feedback on earlier versions of the study.

REFERENCES

Bielak, A. T., Campbell, A., Pope, S., Schaefer, K., and Shaxson, L. (2008). "From science communication to knowledge brokering: the shift from 'science push'to "policy pull," in *Communicating Science in Social Contexts*, eds D. Cheng, M. Claessens, T. Gascoigne, J. Metcalfe, B. Schiele, and S. Shi (Springer), 201-226.

Bremer, S., and Meisch, S. (2017). Co-production in climate change research: reviewing different perspectives. *WIREs Clim. Change* 8:e482. doi: 10.1002/wcc.482

Bremer, S., Wardekker, A., Dessai, S., Sobolowski, S., Slaattelid, R., and van der Sluijs, J. (2019). Toward a multi-faceted conception of co-production of climate services. *Clim. Serv.* 13, 42–50. doi: 10.1016/j.cliser.2019.01.003

Buontempo, C., Hewitt, C. D., Doblas-Reyes, F. J., and Dessai, S. (2014). Climate service development, delivery and use in Europe at monthly to inter-annual timescales. *Clim. Risk Manag.* 6, 1–5. doi: 10.1016/j.crm.2014.10.002

Carr, E. R., Goble, R., Rosko, H. M., Vaughan, C., and Hansen, J. (2020). Identifying climate information services users and their needs in Sub-Saharan Africa: a review and learning agenda. *Clim. Dev.* 12, 23–41. doi: 10.1080/17565529.2019.1596061

Carter, S., Steynor, A., Vincent, K., Visman, E., and Waagsaether, K. L. (2020). *Manual-Co-production in African Weather and Climate Services*, 2nd Edn. WISER and Future Climate for Africa.

Carter, S., Steynor, A., Vincent, K., Visman, E., Waagsaether, K. L., Araujo, J., et al. (2019). *Co-production in Weather and Climate Services.* Cape Town: Future Climate for Africa. Available online at: https://futureclimateafrica.org/coproduction-manual/

Cash, D. W., Clark, W. C., Alcock, F., Dickson, N. M., Eckley, N., Guston, D. H., et al. (2003). Knowledge systems for sustainable development. *Proc. Natl. Acad. Sci. U.S.A.* 100, 8086–8091. doi: 10.1073/pnas.1231332100

Cundill, G., Harvey, B., Tebboth, M., Cochrane, L., Currie-Alder, B., Vincent, K., et al. (2019). Large-scale transdisciplinary collaboration for adaptation research: challenges and insights. *Glob. Challenges* 3:1700132. doi: 10.1002/gch2.201700132

Daly, M., and Dilling, L. (2019). The politics of "usable" knowledge: examining the development of climate services in Tanzania. *Clim. Change* 157, 61–80. doi: 10.1007/s10584-019-02510-w

Dilling, L., and Lemos, M. C. (2011). Creating usable science: opportunities and constraints for climate knowledge use and their implications for science policy. *Global Env. Change* 21, 680–689. doi: 10.1016/j.gloenvcha.2010.11.006

Dinku, T., Block, P., Sharoff, J., Hailemariam, K., Osgood, D., del Corral, J., et al. (2014). Bridging critical gaps in climate services and applications in Africa. *Earth Perspect.* 1:15. doi: 10.1186/2194-6434-1-15

Earl, S., Carden, F., and Smutylo, T. (2001). *Outcome Mapping: Building Learning and Reflection Into Development Programs*. Ottawa, ON: IDRC.

Hammill, A., Harvey, B., and Echeverria, D. (2013). Knowledge for action: an analysis of the use of online climate knowledge brokering platforms. *Knowl. Manag. Dev. J.* 9, 72–92. doi: 10.1093/oso/9780198792154.003.0009

Hansen, J. W., Mason, S. J., Sun, L., and Tall, A. (2011). Review of seasonal climate forecasting for agriculture in Sub-Saharan Africa. *Exp. Agric.* 47, 205–240. doi: 10.1017/S0014479710000876

Harold, J., Coventry, K., Visman, E., Diop, I. S., Kavonic, J., Lorenzoni, I., et al. (2019). *Approaches to Communicating Climatic Uncertainties With Decision-Makers.* Future Climate for Africa. Available online at: https://futureclimateafrica.org/wp-content/uploads/2019/09/approaches-to-communicating-climatic-uncertainties-with-decision-makers_final.pdf

Harvey, B., Cochrane, L., Jones, L., and Vincent, K. (2019c). *Programme design for climate resilient development: A review of key functions*. Ottawa, ON: International Development Research Centre.

Harvey, B., Cochrane, L., and Van Epp, M. (2019b). Charting knowledge co-production pathways in climate and development. *Env. Policy Govern.* 29, 107–117. doi: 10.1002/eet.1834

Harvey, B., and Cook, C (2018). *Knowledge Resources for National Climate Action: An Analysis of Developing Country Needs and Perspectives*. Research Report Commissioned by the NDC Partnership and World Resources Institute, Washington, DC.

Harvey, B., Ensor, J., Carlile, L., Garside, B., Patterson, Z., and Naess, L. O. (2012). "Climate change communication and social learning: review and strategy development for CCAFS," in *CCAFS Working Paper 22* (Copenhagen: CGIAR Research Programme on Climate Change, Agriculture and Food Security (CCAFS)). Available online at: www.ccafs.cgiar.org

Harvey, B., Jones, L., Cochrane, L., and Singh, R. (2019a). The evolving landscape of climate services in sub Saharan Africa: what roles have

NGOs played? *Clim. Change* 157, 81–98. doi: 10.1007/s10584-019-02410-z

Hewitt, C., Mason, S., and Walland, D. (2012). The global framework for climate services. *Nat. Clim. Change* 2, 831–832. doi: 10.1038/nclimate1745

Hulme, M., Doherty, R., Ngara, T., New, M., and Lister, D. (2001). African climate change: 1900-2100. *Clim. Res.* 17, 145–168. doi: 10.3354/cr017145

Jagannathan, K., Arnott, J. C., Wyborn, C., Klenk, N., Mach, K. J., Moss, R. H., et al. (2020). Great expectations? Reconciling the aspiration, outcome, and possibility of co-production. *Curr. Opin. Env. Sus.* 42, 22–29. doi: 10.1016/j.cosust.2019.11.010

Jones, L., Champalle, C., Chesterman, S., Cramer, L., and Crane, T. A. (2017). Constraining and enabling factors to using long-term climate information in decision-making. *Clim. Policy* 17, 551–572. doi: 10.1080/14693062.2016.1191008

Jones, L., Harvey, B., Cochrane, L., Cantin, B., Conway, D., Cornforth, R. J., et al. (2018). Designing the next generation of climate adaptation research for development. *Regional Env. Change* 18, 297–304. doi: 10.1007/s10113-017-1254-x

Jones, L., Harvey, B., and Godfrey-Wood, R. (2016). *The Changing Role of NGOs in Supporting Climate Services*. Resilience Intel 4. Available online at: https://www.odi.org/publications/10560-changing-role-ngos-supporting-climate-services

Klerkx, L. (2012). "The role of innovation brokers in the agricultural innovation system," in *Improving Agricultural Knowledge and Innovation Systems: OECD Conference Proceedings* (Paris: OECD Publishing).

Koelle, B., Siame, G., Jones, R., and Jack, C. (2019). *City Learning Lab: For Dialogue and Decision Making*. Available online at: https://futureclimateafrica.org/news/webinar-invitation-city-learning-labs-for-dialogue-and-decision-making/

Lemos, M. C., Arnott, J. C., Ardoin, N. M., Baja, K., Bednarek, A. T., Dewulf, A., et al. (2018). To co-produce or not to co-produce. *Nat. Sustain.* 1, 722–724. doi: 10.1038/s41893-018-0191-0

Lemos, M. C., Kirchhoff, C. J., and Ramprasad, V. (2012). Narrowing the climate information usability gap. *Nat. Clim. Change* 2, 789–794. doi: 10.1038/nclimate1614

Mach, K. J., Lemos, M. C., Meadow, A. M., Wyborn, C., Klenk, N., Arnott, J. C., et al. (2020). Actionable knowledge and the art of engagement. *Curr. Opin. Env. Sus.* 42, 30–37. doi: 10.1016/j.cosust.2020.01.002

Mahon, R., Greene, C., Cox, S-A., Guido, Z., Gerlak, A. K., Petrie, J-A., et al. (2019). Fit for purpose? Transforming national meteorological and hydrological services into national climate service centers. *Clim. Serv.* 13, 14–23. doi: 10.1016/j.cliser.2019.01.002

Mauser, W., Klepper, G., Rice, M., Schmalzbauer, B. S., Hackmann, H., Leemans, R., et al. (2013). Transdisciplinary global change research: the co-creation of knowledge for sustainability. *Curr. Opin. Environ. Sustain.* 5, 420–431. doi: 10.1016/j.cosust.2013.07.001

McNie, E. C. (2012). Delivering climate services: organizational strategies and approaches for producing useful climate-science information. *Weather Clim. Soc.* 5, 14–26. doi: 10.1175/WCAS-D-11-00034.1

Meadow, A. M., Ferguson, D. B., Guido, Z., Horangic, A., Owen, G., and Wall, T. (2015). Moving toward the deliberate coproduction of climate science knowledge. *Weather Clim. Soc.* 7, 179–191. doi: 10.1175/WCAS-D-14-00050.1

Michaels, S. (2009). Matching knowledge brokering strategies to environmental policy problems and settings. *Env. Sci. Policy* 12, 994–1011. doi: 10.1016/j.envsci.2009.05.002

Mwalukanga, B., Siame, G., Koelle, B., and McClure, A. (2018). *FRACTAL Impact Case Study*. Internal Report (Unpublished).

Patt, A., and Gwata, C. (2002). Effective seasonal climate forecast applications: examining constraints for subsistence farmers in Zimbabwe. *Global Env. Change* 12, 185–195. doi: 10.1016/S0959-3780(02)00013-4

Phipps, D., Cummins, J., Pepler, D. J., Craig, W., and Cardinal, S. (2016). The co-produced pathway to impact describes knowledge mobilization processes. *J. Commun. Engage. Scholarship* 9:5.

Pohl, C., Rist, S., Zimmermann, A., Fry, P., Gurung, G. S., Schneider, F., and Hadorn, G. H. (2010). Researchers' roles in knowledge co-production: experience from sustainability research in Kenya, Switzerland, Bolivia and Nepal. *Sci. Public Policy* 37:267. doi: 10.3152/030234210X496628

Roncoli, C., Jost, C., Kirshen, P., Sanon, M., Ingram, K. T., Woodin, M., et al. (2009). From accessing to assessing forecasts: An end-to-end study of participatory climate forecast dissemination in Burkina Faso (West Africa). *Climatic Change* 92, 433–460. doi: 10.1007/s10584-008-9445-6

Shaxson, L., Bielak, A., Ahmed, I., Brien, D., Conant, B., Fisher, C., et al. (2012). *Expanding Our Understanding of K* (Kt, KE, Ktt, KMb, KB, KM, etc.): A Concept Paper Emerging From the K* Conference Held in Hamilton, Ontario, Canada, April 2012*. United Nations University.

Singh, C., Daron, J., Bazaz, A., Ziervogel, G., Spear, D., Krishnaswamy, J., et al. (2017). The utility of weather and climate information for adaptation decision-making: current uses and future prospects in Africa and India. *Clim. Dev.* 10, 389–405. doi: 10.1080/17565529.2017.1318744

SSHRC (2019). *Guidelines for Effective Knowledge Moblization*. Social Sciences and Humanities Research Council. Available online at: https://www.sshrc-crsh.gc.ca/funding-financement/policies-politiques/knowledge_mobilisation-mobilisation_des_connaissances-eng.aspx

Star, S. L., and Griesemer, J. R. (1989). Institutional ecology, translations' and boundary objects: Amateurs and professionals in Berkeley's Museum of Vertebrate Zoology, 1907-39. *Soc. Stud. Sci.* 19, 387–420. doi: 10.1177/030631289019003001

Steynor, A., Lee, J., and Davison, A. (2020). Transdisciplinary co-production of climate services: a focus on process. *Soc. Dyn.* 46, 414–433. doi: 10.1080/02533952.2020.1853961

Turnhout, E., Stuiver, M., Klostermann, J., Harms, B., and Leeuwis, C. (2013). New roles of science in society: different repertoires of knowledge brokering. *Sci. Public Policy* 40, 354–365. doi: 10.1093/scipol/scs114

Vaughan, C., Buja, L., Kruczkiewicz, A., and Goddard, L. (2016). Identifying research priorities to advance climate services. *Clim. Serv.* 4, 65–74. doi: 10.1016/j.cliser.2016.11.004

Vaughan, C., and Dessai, S. (2014). Climate services for society: origins, institutional arrangements, and design elements for an evaluation framework'. *Wiley Interdiscipl. Rev. Clim. Change* 5, 587–603. doi: 10.1002/wcc.290

Vaughan, C., Hansen, J., Roudier, P., Watkiss, P., and Carr, E. (2019). Evaluating agricultural weather and climate services in Africa: evidence, methods, and a learning agenda. *Wiley Interdiscipl. Rev. Clim. Change* 10:e586. doi: 10.1002/wcc.586

Vincent, K., Archer, E., Henriksson, R., Pardoe, J., and Mittal, N. (2020a). Reflections on a key component of co-producing climate services: defining climate metrics from user needs. *Clim. Serv.* 20:100204. doi: 10.1016/j.cliser.2020.100204

Vincent, K., Conway, D., Dougill, A. J., Pardoe, J., Archer, E., Bhave, A. G., et al. (2020b). Re-balancing climate services to inform climate-resilient planning – a conceptual framework and illustrations from sub-Saharan Africa. *Clim. Risk Man.* 29:100242. doi: 10.1016/j.crm.2020.100242

Vincent, K., Daly, M., Scannell, C., and Leathes, B. (2018). What can climate services learn from theory and practice of co-production? *Clim. Serv.* 12, 48–58. doi: 10.1016/j.cliser.2018.11.001

Vincent, K., Dougill, A. J., Dixon, J. L., Stringer, L. C., and Cull, T. (2017). Identifying climate services needs for national planning: insights from Malawi. *Clim. Policy* 17, 189–202. doi: 10.1080/14693062.2015.1075374

Vogel, C., and O'Brien, K. (2006). Who can eat Information? Examining the effectiveness of seasonal climate forecasts and regional climate-risk management strategies. *Clim. Res.* 33, 111–122 doi: 10.3354/cr033111

Ward, V., House, A., and Hamer, S. (2009). Knowledge brokering: the missing link in the evidence to action chain?. *Evidence Policy* 5, 267–279. doi: 10.1332/174426409X463811

Watkiss, P., and Cimato, F. (2015). *FCFA Applied Research Fund: Economics, Political Economy and Behavioural Science of Accounting for Long-term Climate in Decision Making Today*. Available online at: https://futureclimateafrica.org/wp-content/uploads/2018/02/ragl-0004c-deliverable-3-literature-review-draft_for-web-upload.pdf

Webber, S. (2019). Putting climate services in contexts: advancing multi-disciplinary understandings: introduction to the special issue. *Clim. Change* 157, 1–8. doi: 10.1007/s10584-019-02600-9

Webber, S., and Donner, S. D. (2017). Climate service warnings: cautions about commercializing climate science for adaptation in the developing world. *WIREs Clim. Change* 2017, 8:e424. doi: 10.1002/wcc.424

Zuber-Skerritt, O. (2002). The concept of action learning. *Learning Org.* 9, 114–124. doi: 10.1108/09696470210428831

Conflict of Interest: KV was employed by the company Kulima Integrated Development Solutions (Pty) Ltd. Funds for this research were provided through SouthSouthNorth, where JA was employed at the time of the study.

The remaining authors declare that the research was conducted in the absence of any commercial or financial relationships that could be construed as a potential conflict of interest.

Advantages of publishing in Frontiers

OPEN ACCESS
Articles are free to read for greatest visibility and readership

FAST PUBLICATION
Around 90 days from submission to decision

HIGH QUALITY PEER-REVIEW
Rigorous, collaborative, and constructive peer-review

TRANSPARENT PEER-REVIEW
Editors and reviewers acknowledged by name on published articles

Frontiers
Avenue du Tribunal-Fédéral 34
1005 Lausanne | Switzerland

Visit us: www.frontiersin.org
Contact us: frontiersin.org/about/contact

REPRODUCIBILITY OF RESEARCH
Support open data and methods to enhance research reproducibility

DIGITAL PUBLISHING
Articles designed for optimal readership across devices

FOLLOW US
@frontiersin

IMPACT METRICS
Advanced article metrics track visibility across digital media

EXTENSIVE PROMOTION
Marketing and promotion of impactful research

LOOP RESEARCH NETWORK
Our network increases your article's readership